Achievements with the Euroball spectrometer

1997-2003

W. Korten and S. Lunardi Eds.
on behalf of
Euroball Coordination Committee

Achievements with the

EUROBALL spectrometer

Scientific and Technical

Activity Report

1997-2003

W. Korten and S. Lunardi (Eds.)

on behalf of the

EUROBALL Coordination Committee

October 2003

Euroball Collaboration

Denmark

Niels Bohr Institute, Copenhagen

France

Institut de Recherches Subatomiques, Strasbourg
Centre d'études nucléaires, Bordeaux-Gradignan
Laboratoire de Physique Subatomique et de Cosmologie, Grenoble
Institut de Physique Nucléaire, Lyon
Centre de Spectrométrie Nucléaire et de Spectrométrie de Masse, Orsay
Institut de Physique Nucléaire, Orsay
Commissariat à l'Energie Atomique, DAPNIA, Saclay

Germany

Hahn-Meitner-Institut Berlin
Institut für Strahlen- und Kernphysik der Universität Bonn
Institute of Nuclear and Hadron Physics, Forschungszentrum Rossendorf
II. Physikalisches Institut, Georg-August-Universität, Göttingen
Gesellschaft für Schwerinonenforschung, Darmstadt
Forschungszentrum Jülich (KFA-IKP)
Institut für Kernphysik der Universität zu Köln
Max-Planck Institut für Kernphysik, Heidelberg

Italy

Laboratori Nazionali di Legnaro dell'INFN
INFN, Sezione di Perugia e Dipartimento di Matematica e Fisica, Università di Camerino
INFN, Sezione di Firenze e Dipartimento di Fisica, Università di Firenze
INFN, Sezione di Genova e Dipartimento di Fisica, Università di Genova
INFN, Sezione di Milano e Dipartimento di Fisica, Università di Milano
INFN, Sezione di Napoli e Dipartimento di Scienze Fisiche, Università di Napoli "Federico II"
INFN, Sezione di Padova e Dipartimento di Fisica, Università di Padova

Sweden

The Royal Institute of Technology, KTH,Stockholm
Lund University
Chalmers University of Technology, Göteborg
Uppsala University

United Kingdom

CCLRC Daresbury Laboratory
Department of Physics, University of Liverpool
Department of Physics, University of Manchester
Department of Physics, University of Surrey
Department of Physics, University of York

Euroball Project Management

Sites Euroball Project Managers

C. Rossi Alvarez (LNL), F.A. Beck (IReS) and D. Curien (IReS)

Euroball Joint Management Committee

N. Alamanos, P. von Brentano, J. Durell, H. Flocard, L. Gildefeldt, D. Guerreau, B. Haas, O. Hansen,

F. Karlsson, D. Kidd, K.P. Lieb, J. Martino, J. Mougey, D. Müller, P.J. Nolan, G. Pappalardo,

M. Pignanelli, H.G. Price, H. Schunck, P.J. Twin, S. Ward, D. Watson

Euroball Coordination Committee

F.A. Beck, A. Bracco, P. von Brentano, R. Broglia, D. Curien, G. de Angelis, F. Doenau, J. Eberth,

C. Fahlander, S.J. Freeman, J. Gerl, B. Herskind, A. Johnson, W. Korten, K.P. Lieb, R. Lieder

J.C. Lisle, S. Lunardi, D.R. Napoli, P.J. Nolan, J. Nyberg, N. Redon, C. Rossi Alvarez, D. Schwalm,

H. Sergolle, G. Sletten, P.J. Twin

Euroball Infrastructure Group

D. Bazzacco, D. Cullen, D. Curien, J. Eberth, C. Fahlander, R. Lieder, D.R. Napoli,

J. Simpson, G. Sletten

Electronics and Data Acquisition Group chairpersons

F.A. Beck, J.C. Lisle, N. Karkour, I. Lazarus, G. Maron, V. Pucknell, Ch. Ring

Data Analysis Group chairperson

B. Herskind

Euroball Ancillary Detectors Group chairpersons

O. Skeppstedt, H. Grawe, A. Gadea

Contents

7. Studies of *N~Z* nuclei beyond ⁵⁶Ni

8. Nuclei on the neutron-rich side of stability

9. Magnetic rotation

10. The technical merits of Euroball

11. Additional detectors for EUROBALL

Annex: EUROBALL experiments and publications

References

Executive Summary

W. Korten and S. Lunardi

Executive summary

The continuous development of high-resolution gamma-ray detector systems has been of vital importance to nuclear structure physics. It has steadily expanded the limits of what can be observed and many new phenomena have been discovered, leading to unexpected insights into the nature of the atomic nucleus. Several germanium arrays have been built in the last decade and these have significantly contributed to such progress: the most efficient and sensitive being EUROBALL in Europe and GAMMASPHERE in the USA. The EUROBALL [1] array was initially operated at the Laboratori Nazionali di Legnaro, Italy (1997-98) and later at the Institut de Recherches Subatomiques, Strasbourg, France (1999-2003). During this period more than 110 experiments were performed involving ~400 scientists representing 24 countries and ~75 institutes.

EUROBALL was designed with the principle aim of carrying out studies of nuclei at very high angular momentum, close to the fission limit. During the Strasbourg phase of operation (i.e. EUROBALL IV[a]) a Bismuth Germanate (BGO) calorimeter ("inner ball") was added to the array to assist with the investigation of these physics goals. The phenomenon of superdeformation, with its many fascinating properties, has been one of the major successes of this work. With the improved sensitivity of the new arrays it has been possible to study, in detail, the collective modes built on states at large deformation and to extend the concept of superdeformation to very light nuclei, where the elongated shapes are found to decay by both gamma ray and charged particle emission. The study of high spin states has also led to the discovery of new collective modes (wobbling motion) and of new symmetries (chirality) in nuclei, both of which are closely linked to a stable triaxial shape of the nuclear mean field.

EUROBALL has also been coupled to powerful "ancillary" detector systems, which have proved to be excellent instruments for exploring the properties of very exotic nuclei far from beta-stability. The ancillary detectors utilised include devices for the detection of light charged particles (ISIS [4], EUCLIDES [5] and DIAMANT [6]), neutrons (Neutron Wall [7]), evaporation residues (RFD) [8], fission fragments (SAPhIR) [9], binary reactions products (BRS) [10] and high-energy γ-rays (HECTOR) [11]. A large fraction of the most recent EUROBALL experiments has exploited the isospin degree of freedom by studying both proton-rich and neutron-rich nuclei populated with very low cross-sections (down to a few hundred nb). These studies have allowed new facets of the nuclear effective force to be investigated.

The contruction of the EUROBALL array required important technical developments in Germanium detector technology to be pursued. The Ge CLOVER detector, first used in the EUROGAM II array, was the first example of a *composite detector,* where several Ge crystals are operated in the same cryostat. For the EUROBALL CLUSTER detector a new technology to *encapsulate the Germanium crystals* in a sealed aluminium can had to be developed. This technology is currently being utilised for Ge detectors on European space missions. The EUROBALL collaboration has subsequently designed the first *segmented Ge detectors*, which are now operated in the EXOGAM and MINIBALL spectrometers. In 1999, these developments led to the initiation of a further development programme for gamma-ray tracking detectors in Europe.

---

[a] The official name of the array has been EUROBALL III during the Legnaro phase and EUROBALL IV for the one in Strasbourg. This to stress the fact that EUROBALL is a development of previously existing devices and that it was continuously improved. The first phase of EUROBALL were the GASP spectrometer [2] in Legnaro and EUROGAM phase I in Daresbury [3], while the second phase of EUROBALL corresponds to EUROGAM phase II in Strasbourg [3].

In this report the results obtained with EUROBALL are presented in a comprehensive way, together with an assessment of the technical merits of the array and reports on the ancillary detectors that were built for use with EUROBALL. Since many of the recently performed experiments are not yet fully analysed this document can only give a preliminary report on the achievements to date. In an annex information on the performed experiments, publications, and PhD thesis work is documented.

Superdeformation and other exotic shapes

The study of nuclear superdeformation has been one of the major successes of nuclear structure research in the last 15 years, since the discovery of the first superdeformed (SD) rotational band at high spin in ^{152}Dy. In this period more than 200 bands have been studied in many different regions of the Segrè chart (A~30, 60, 80, 130, 150, 160, 190 and 240). The large amount of experimental data collected, which began with the previous generation γ-arrays, have provided a continuous challenge to mean field theories aiming to explain the properties of nuclei in these very elongated shapes. Unexpected and sometimes surprising properties of superdeformed nuclei were found, but many open questions remained to be answered. The results obtained from EUROBALL will be discussed in detail in Section 1 ("Nuclei at very elongated shapes").

EUROBALL with its high resolving power, large efficiency and innovative additional detectors, especially the INNER BALL calorimeter, has brought new information on some of the most surprising phenomena observed in superdeformed nuclei, e.g. the observation of "identical bands" and very small regular oscillations in the moments of inertia ("ΔI=4 staggering"). Other highlights are the final proof of the existence of octupole vibrations, an elementary excitation mode built on the superdeformed shape and the extraction of the neutron pairing gap in the second well of the Nd isotopes. The results on the octupole vibration in the second minimum were obtained by utilising the EUROBALL Clover detectors as Compton polarimeters in order to measure the linear polarisation of gamma rays, and hence their electric or magnetic character.

One of the main achievements in this field has been the discovery of a new region of super-deformed nuclei with stable triaxial deformation in the Lu and Hf isotopes around mass A=170 (cf. Section 2, "Strongly deformed triaxial nuclei"). These results have provided the first experimental proof for the existence of the "wobbling mode", a collective motion charac-teristic of a triaxial shape, which was predicted more than 25 years ago. It has also been shown in ^{154}Er, for example, that superdeformed structures with both prolate and triaxial shapes can coexist at high spin. This observation has allowed the resolution of long-standing difficulties in the theoretical interpretation of superdeformation in the A=150 mass region.

Large efforts have also gone into the search for hyperdeformed nuclear shapes, but undeniable evidence for such very strongly prolate deformed nuclei with an axis ratio of 3:1 remains elusive. On the other hand we have siginficantly improved our understanding of the experimental conditions needed in order to populate nuclei at extreme spin values, well in excess of $70\hbar$, where hyperdeformed nuclei are expected to be formed. A successful search for hyperdeformation may well be one of the prime examples, for which we will have to wait for the next generation of gamma-ray tracking spectrometers such as AGATA.

Rotational motion at finite temperature

The study of the rotational motion at finite temperature plays a crucial role in the under-standing of the properties of the nuclear system beyond the mean-field description, providing relevant information on the two-body residual interaction responsible for the band mixing process. Many different studies related to the question of rotational motion at higher temperatures were performed with EUROBALL. These include the feeding and decay of superdeformed bands (cf. Section 3, "Population and decay from superdeformed states"), the investigation of the superdeformed quasi-continuum and the search for the Giant Dipole Resonance built on highly deformed nuclei (cf. Section 4, "Rotational motion in thermally excited nuclei").

The study of high lying excited states within a superdeformed well provides opportunities to investigate many intriguing nuclear structure aspects such as: the transition from ordered motion along the superdeformed yrast line to chaotic motion above it, perhaps through an ergodic regime; the robustness of collectivity with increasing excitation energy and spin and the largely-unexplored feeding mechanism of superdeformed bands. A very extensive study of superdeformed excited states has been carried out in ^{143}Eu and a clear picture of the feeding process in this nucleus is emerging. Concerning the decay-out, most bands are still not connected to the low-lying levels, because experiments are at the very limits of what present arrays can do. Here, the development of future gamma-ray tracking spectrometers will be vital. In the few cases where quantum numbers have been measured for superdeformed states, information on binding energies and pairing in the second minimum has been extracted as well as values for the interaction strength between superdeformed and normal-deformed states.

From experimental studies of the quasi-continuum we know at present that, in medium mass nuclei, already a few hundred keV in excitation energy above the yrast line rotational bands are close enough in energy to interact by residual interactions. In recent years, the study of rotational damping, i.e. the spreading of the electric quadrupole decay from a single state at spin I over a spectrum of final states all at spin I-2, has been focused on the dependence on nuclear mass and deformation. Several high-statistics EUROBALL experiments on normal-deformed nuclei in the mass region A~110 and of superdeformed nuclei in mass regions A~140 and 160 were performed and analysed using the fluctuation technique. The number of paths obtained by this analysis and their mass dependence is well reproduced by simulation calculations.

High spin physics and new modes of rotational motion

In the high-spin domain the phenomenon of terminating rotational bands is attracting much attention, since it relates the collective and single-particle properties of the nucleus. With the earlier arrays band termination had been extensively studied in the spin range 30-40$\hbar$, limiting the experiments to nuclei with a rather small number of valence nucleons. With EUROBALL it became possible to extend these studies to much higher spins as discussed in Section 5 ("Pairing correlations and band termination at the highest spins").

Detailed spectroscopy in the spin range 50-60$\hbar$ has been performed for several Er isotopes. These studies have provided the first firm evidence for the demise of both proton and neutron static pairing correlations at ultra high spins. In addition, they have allowed important studies of abrupt band termination to be carried out in nuclei around the original classic band termi-

nating nucleus ^{158}Er. Investigations of nuclei with A ~ 70 and 130 have also revealed new regions of "smoothly" terminating rotational bands, as well as providing the first hints of such behaviour in a highly deformed band of ^{132}Ce.

EUROBALL has also played an important role in disentangling the phenomenon of "magnetic rotation" (cf. Section 9), a new mode of nuclear excitation manifesting itself in regular bands in near-spherical nuclei where magnetic dipole transitions dominate the electric quadrupole decay. This phenomenon has now been established in several mass regions of near-spherical nuclei where high-spin orbitals are close to the Fermi surface. Magnetic rotation occurs when the symmetry of the nuclear system is broken by the current distributions of a few high-spin particles and holes outside a spherical or near-spherical core. If these currents lead to a large component of the magnetic moment vector perpendicular to the total angular momentum they generate strongly enhanced M1 radiation. In many cases data obtained with EUROBALL have allowed precise assignments to be made of the coupling of the relevant single-particle orbitals; lifetime measurements have also clearly proven a decrease of the M1 strength along the bands as expected from theoretical calculations.

The spectrometer has also been utilised to investigate chirality in nuclei. This phenomenon has been predicted in nuclei which have a stable deformed triaxial core and a few (1-2) valence nucleons occupying high spin particle and hole-like orbitals. Recent EUROBALL work, as well as studies in the USA, has revealed that odd-odd nuclei in the Rh region around mass 104 exhibit some of the nicest examples to date of chiral rotation in nuclei.

Physics near the *N=Z* line

The latest generation of large γ-ray spectrometers has boosted the exploration of nuclei under extreme conditions. Not only the limits of angular momentum and higher excitation energies have been approached, but the coupling of these instruments to selective ancillary devices has allowed for more and more refined investigations of the third important degree of freedom in contemporary nuclear structure studies, isospin. Near and along the line of nuclei with equal numbers of protons and neutrons (*N=Z*), a reinforcement of shell structures occurs, since the neutrons and protons are filling identical orbitals and as a consequence their wave functions have a large spatial overlap. Spectroscopic studies of these nuclei enable the investigation of isospin $T = 0$ or $T = 1$ neutron-proton pairing correlations and their consequences. In particular, the knowledge of high-spin levels gives important information on a new superfluid phase of nuclear matter. In addition, the greatly improved or new experimental techniques have initiated a renaissance of interest in questions related to the isospin symmetry.

EUROBALL provided a breakthrough in the study of high spin states in *N=Z* nuclei. Here, the meaning of "high spin" is of course different to nuclei lying closer to the valley of stability, where spins in excess of $60\hbar$ can be reached in discrete spectroscopy. Because of the severe experimental difficulties encountered when studying heavy *N~Z* nuclei, states with spins of the order of $10\hbar$ are often considered as being "high spin". A comprehensive summary of in-beam studies of exotic neutron-deficient nuclei in the vicinity of the *N=Z* line between ^{40}Ca and ^{100}Sn using the EUROBALL array is given in the Sections 6 and 7 of this report ("Symmetries in medium-light nuclei: at and beyond the *N=Z* line" and "Studies of *N~Z* nuclei beyond ^{56}Ni"). Highlights from these studies are new results on the isospin symmetry breaking in several *N=Z* nuclei, new or extended studies of mirror nuclei, shape changes in heavy *N~Z* nuclei and the approach to ^{100}Sn.

Nuclei on the neutron rich side of the valley of stability

Nuclei with an increased excess of neutrons as compared to the stable isotopes are even more difficult to access experimentally. Although often regarded as prime examples for the need of radioactive beam facilities, production methods with low-energy stable beams are available in limited form as spontaneous fission, fusion-fission or deep-inelastic reactions. These three classes of reactions have very different characteristics; both in the nuclei produced and in the angular momentum distribution achieved before γ-decay competes with neutron evaporation. They do, however, share some of the same practical difficulties, namely that in each event there are generally two product nuclei, and, that there are many possible products from any given choice of reaction or spontaneously-fissioning source.

In fission reactions there is an especially wide range of possible products - typical yields for a given isotope are of the order of 1% of the total - but tend to be much lower for the more exotic species. For this reason, the identification of data with a particular fragment requires exceptional selectivity, either through the use of high-fold γ data as available with EUROBALL, where it is a set of energies of coincident γ rays that uniquely identifies the product, or by the direct measurement of Z and A of one or both of the reaction products. In spite of these difficulties great progress has been made in the study of neutron-rich nuclei since the introduction of large arrays of Compton-suppressed Ge detectors as summarised in Section 8 of this report ("Nuclei on the neutron-rich side of stability"). New excited states in many isotopes have been identified and spectacular progress has been made in the techniques to measure spins, parities, lifetimes and even g-factors. As an example, new results obtained for several odd-proton isotopic chains, i.e. Tc, Rh, and In, has led to a better understanding of the properties of the proton single particle structure far from stability.

The powerful EUROBALL array is also a perfectly suited tool to unfold very complex gamma coincidence spectra arising from many nuclei produced in deep-inelastic heavy-ion reactions. The available quality and statistics of the gamma coincidence data makes it possible to reach products with very small production cross-sections and thereby to access a more neutron-rich region of isotopes. For example, an investigation of excited states in some nuclei around ^{48}Ca was possible despite very low production yields for the nuclei of interest.

Future perspectives

The EUROBALL coordination committee took the decision to stop the operation of the spectrometer in its current form in April 2003, once the campaign at IReS Strasbourg has been completed. In future, the resources from the EUROBALL array will be made available to the European Nuclear Physics community for dedicated campaigns at accelerator laboratories offering unique new physics opportunities. This programme, which should serve the needs of the community for the near future, will be coordinated by a network pooling the European resources for γ-ray spectroscopy. The EUROBALL campaigns have clearly shown that, besides a powerful gamma-ray spectrometer, efficient and dedicated particle detectors or spectrometers are the decisive ingredients if information from weakly populated nuclei is to be investigated. In fact, for a few years to come, until radioactive ion beams from the emerging new facilities reach appropriate intensities, gamma-ray spectrometers operated at a high intensity stable beam facility will be competitive for many of these studies.

For the first two years (2003/2004) campaigns at three different accelerator laboratories are being planned. They will employ different parts of the EUROBALL spectrometer and can hence

be performed in parallel. At the cyclotron laboratory of the University of Jyväskylä (Finland) 45 large-volume Ge detectors will be coupled to the gas-filled separator RITU to perform experiments on heavy exotic nuclei with an emphasis on the study of very heavy nuclei beyond Z=100. At the Legnaro National Laboratory (Italy) the EUROBALL Clover detectors will be coupled to the new PRISMA spectrometer in order to study neutron rich nuclei by means of multi-nucleon transfer and deep-inelastic reactions. The EUROBALL Cluster detectors will be used for the "Rare Isotope Investigations at GSI" (RISING), i.e. spectroscopic studies of relativistic energy beams provided by the SIS-FRS facility. On a longer timescale it is planned to construct more powerful arrays by integrating other resources such as the MINIBALL and EXOGAM spectrometers for experiments at GSI and GANIL/SPIRAL.

Although EUROBALL has enabled the studies of very rare nuclear phenomena to be carried out, i.e. at the level of ~10^{-5} of the production cross-section in a heavy-ion reaction, the development of a new generation of even more powerful gamma-ray spectrometers is vital to make future progress as has been illustrated by this report. Further progress, beyond the capabilities of EUROBALL, however, requires a completely new detection concept. For this purpose all interactions of each γ ray must be characterised in order to perform a full "*gamma-ray tracking*". Utilising this concept will allow the construction of a *complete Germanium shell*, which will have unprecedented qualities in terms of sensitivity and efficiency. Gamma-ray tracking is based on highly segmented, position sensitive Ge detectors and digital pulse processing electronics. Today we are at a stage where a new collaboration is emerging in order to develop the Advanced Gamma Tracking Array (AGATA). This array will open a broad range of new physics opportunities in connection with the (existing and future) radioactive and intense stable beam accelerators.

Acknowledgements

Nuclei at very elongated shapes

O. Stézowski and J.Wilson

1. Nuclei at very elongated shapes[*]

1.1. Superdeformation: a brief survey

Long cascades of equally spaced γ-rays were initially observed in ^{132}Ce [12] and ^{152}Dy [13] using the TESSA family of spectrometers at Daresbury. The close energy spacing of these transitions implied a larger moment of inertia than the low-spin ground-state bands and was interpreted in terms of the rotation of a superdeformed nuclear shape based on a secondary minimum in the nuclear potential energy surface at large deformation. These very elongated superdeformed shapes are stabilised by fast collective rotation and thus can be produced experimentally in fusion-evaporation reactions only at high spin and with very small cross sections (at most a few percent of the fusion-evaporation reaction channel). To observe them it is absolutely indispensable to have the largest possible γ-ray detection efficiency and a very high resolving power.

Taking advantage of new developments in Ge detector technology, several generations of γ-ray spectrometers were built since this time (cf. Section 10) in order to investigate the phenomenon of superdeformation more precisely. With modern multi-detector Germanium arrays superdeformed rotational bands have been found in many new regions of the Segrè chart. With the EUROGAM spectrometer [3], for example, many yrast and excited super-deformed bands were found in the heavier nuclei (A~130, 150, 190) and more recently also around A~170. An exhaustive review can be found in the "Table of Superdeformed Nuclear Bands and Fission Isomers" [14]. Several unexpected features were observed, like the identical superdeformed bands [15] and the "staggering effect" leading to $\Delta I = 4$ structures [16], most of which are still not completely understood. Thanks to the increased sensitivity, discrete linking transitions between the second and the first well were established for several superdeformed nuclei (cf. Section 3) giving an unambiguous assignment of the spin and the parity of some superdeformed rotational bands [17].

In Figure 1.1 a representation of all nuclei is given, in which at least one superdeformed rotational band has been found. The data are taken from [14] and represent about seventy known superdeformed nuclei. In this figure, the new triaxial superdeformed bands (cf. Section 2) and also some light superdeformed nuclei are not yet indicated. Superdeformed nuclei of different mass regions often give access to different nuclear properties, i.e. single-particle vs. collective excitations and the disappearance of pairing at the highest spins or for extreme values of the rotational frequency. Superdeformation has been found to be present in many nuclei, but it is still a challenge to find new superdeformed bands either residing far from the known superdeformed magic numbers or involving deeply-bound orbitals, both effects leading to highly excited superdeformed states.

Using a rather simple (axially symmetric) anisotropic harmonic oscillator potential, Bohr and Mottelson [18] predicted, quite accurately, the superdeformed magic numbers. In fact, theory predicts even more mass regions than what has actually been observed (see dashed lines in Figure 1.1). However more advanced theoretical calculations, often going beyond the mean-field approach, are needed in order to understand the structure of superdeformed nuclei in detail. These models have shown that the behaviour of the (dynamic) moment of inertia ($\Im^{(2)}$) for superdeformed rotational bands, is generally governed by the number of intruder orbitals occupied (see, e.g. [19], for results based on the macroscopic-microscopic approach). In this

---

[*] Contribution by O. Stézowski and J. Wilson

Figure 1.1: *Superdeformation and the associated "magic" numbers (dashed lines) as given by Bohr and Mottelson [18] and compared to the actual mass regions where Superdeformation has been observed (shown in red). Stable nuclei are indicated in blue, while all nuclei known to exist are marked in grey.*
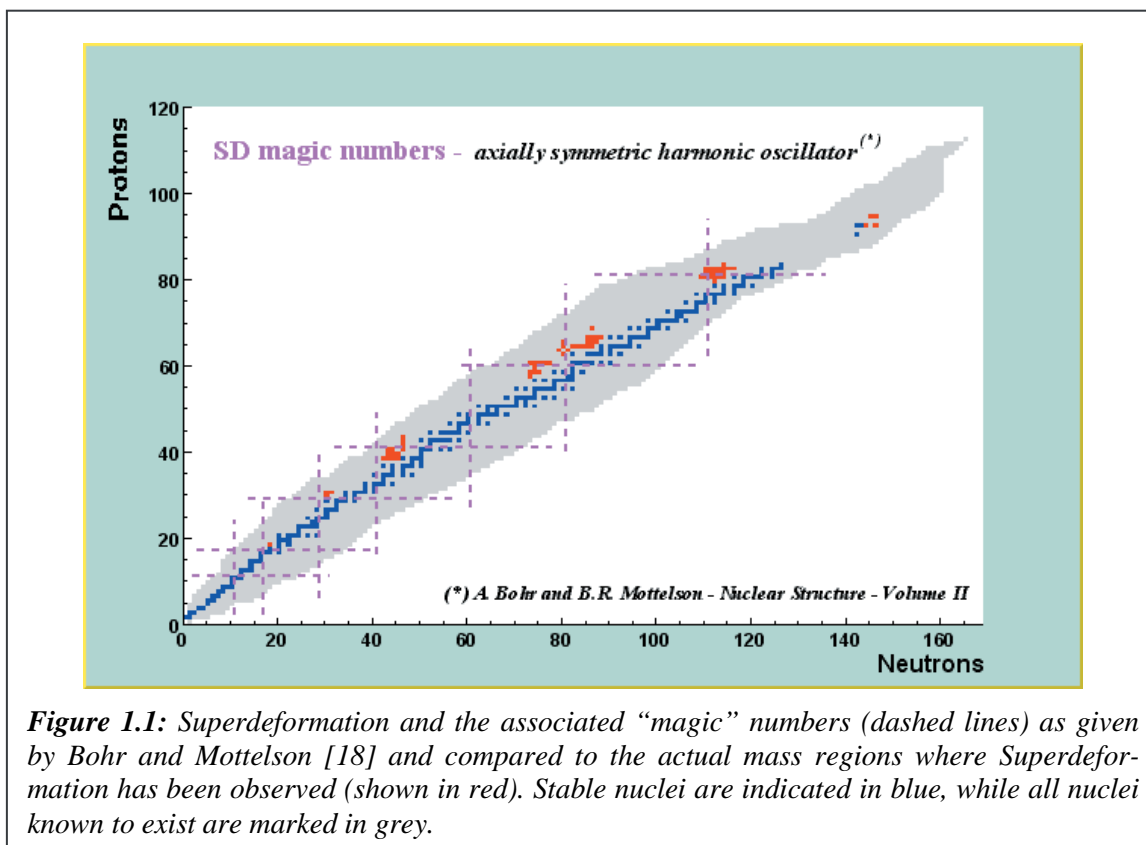
way the configuration of most of the superdeformed bands has been interpreted as based on single-particle (or quasi-particle) excitations obtained in a pure axially symmetric quadrupole type mean field. This represents a reasonable first order approximation, but in some cases other degrees of freedom need to be taken into account for a realistic description of the second well. Thus, some experimental findings can only be interpreted by the occurrence of stable triaxial superdeformed minima (cf. Section 2) like, for instance, in the A~170 mass region, in ^{154}Er [20] or in ^{86}Zr [21]. In some cases, especially in the A~190 mass region, also indications for an octupole vibrational character of the excited superdeformed states were obtained.

With EUROBALL, a broad and extensive study of the second well has been realised and, in particular, single-particle or quasi-particle excitations, collective vibrational states and shape coexistence have been investigated. With its high resolving power, large efficiency and dedicated additional detectors (i.e. the INNER BALL calorimeter to measure the total gamma-ray sum energy and multiplicity) it has been possible to find many excited superdeformed bands populated with very small cross sections. In particular, the strongly deformed triaxial nuclei observed in the A~170 mass region have been thoroughly investigated (cf. Section 2). The high sensitivity of EUROBALL has also allowed known superdeformed rotational bands to be investigated in more detail. New information was also obtained for discrete linking transitions between the second and the first well (cf. Section 3). The knowledge of these transitions is crucial to determine the spin, parity and excitation energy of superdeformed states. Magnetic and collective properties can be established by investigating transitions connecting different superdeformed rotational bands. In the following sections some of the main results that EUROBALL has brought concerning the phenomenon of superdeformation will be emphasised. A more exhaustive review on the influence of microscopic structures on the rotational motion of superdeformed nuclei can be found in [22].

1.2.   New results related to superdeformed rotational bands

Identical Bands

The search for new superdeformed rotational bands has revealed one of the most striking and unexpected results: the phenomenon of identical bands. It was first discovered in the nucleus ^{151}Tb [15], for which the γ-ray transitions of the first excited superdeformed band were found to be within 2 keV of the transitions in the yrast superdeformed band of ^{152}Dy. The associated dynamical moments of inertia $\mathfrak{I}^{(2)}$ are then identical. The $\mathfrak{I}^{(2)}$ moment depends on several contributions, like the mass, the deformation, the strength of the pairing field, the individual contribution of each valence orbital etc.. Considering two neighbouring nuclei, differing by one neutron, the simplest way to explain identical dynamical moments of inertia is to assume some kind of cancellation effect between these contributions [23], but its origin is not yet fully understood.

In a typical fusion-evaporation experiment, many nuclei are produced and one could expect identical bands in several of those nuclei. In order to separate them, a high resolving power is needed. As illustrated in Figure 1.2, two almost identical superdeformed rotational bands belonging even to the same nucleus (^{143}Eu) have been identified with EUROBALL [24]. From this result, the mass (or nucleon number) appears not to be a relevant degree of freedom in the description of identical bands. For two superdeformed bands in ^{194}Hg spins, parities and excitation energies have been established. Based on these results, a mechanism involving both pairing and particle alignment has been proposed to explain the identical band phenomenon [25]. In the A~150 mass region, on the other hand, where pairing correlations are supposed to be very weak, lifetime measurements indicate that alignment effects and deformation changes tend to compensate in identical bands [26]. A very similar phenomenon, called "shifted identical bands", has been discovered more recently in deformed neutron-rich nuclei [27]. It appears that identical bands are probably not a unique property of the second well, but seem to indicate a more general aspect of nuclear structure.
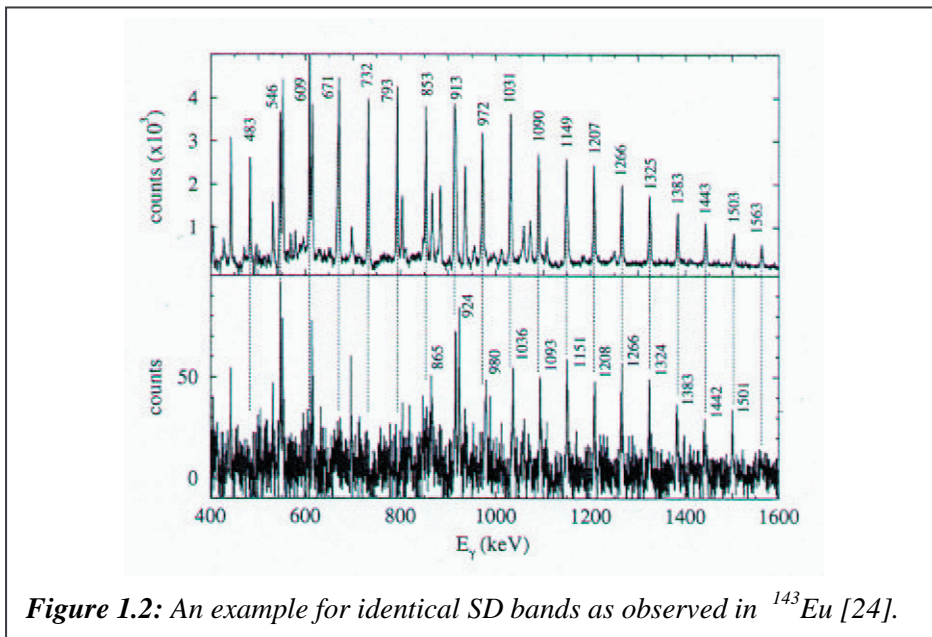
Figure 1.2: *An example for identical SD bands as observed in ^{143}Eu [24].*

Figure 1.3: *Summary of known SD bands showing a ΔI=4 bifurcation and compared to a prediction by Hamamoto and Mottelson [29] (courtesy of J.P. Vivien).*
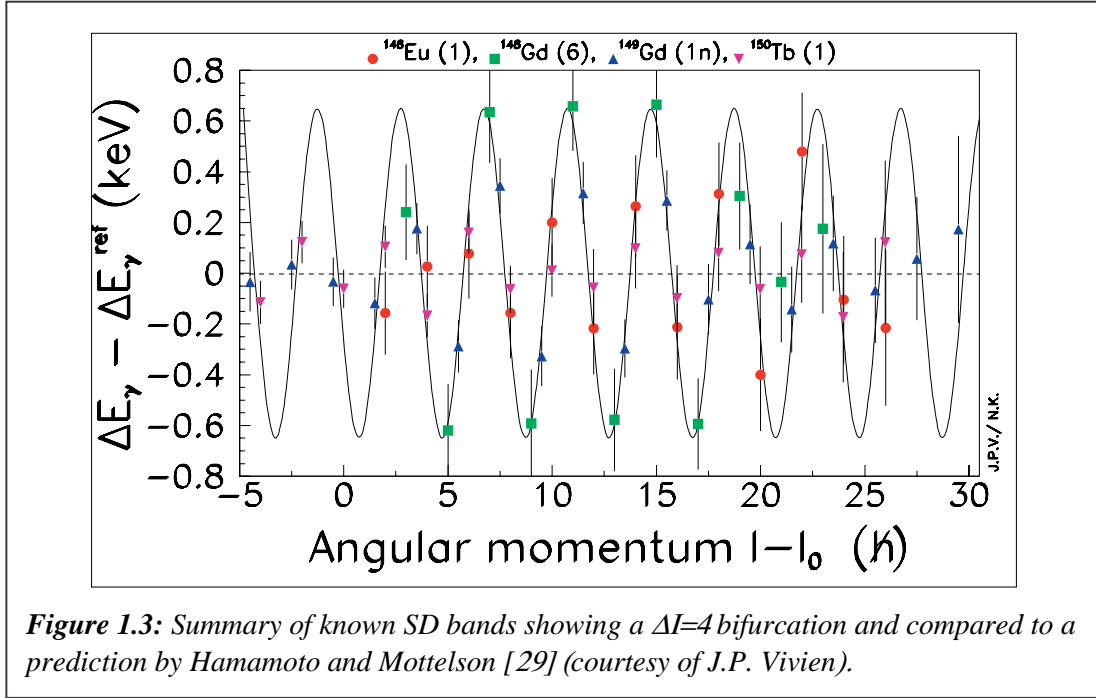
Staggering effects

The observation of $\Delta I = 4$ bifurcation (also called $\Delta I = 2$ staggering) in the yrast super-deformed band of ^{149}Gd was another exciting development for nuclear structure studies. It has been suggested that staggering effects are due to the presence of a hexadecapole perturbation of the prolate superdeformed shape [16]. The $\Delta I = 2$ rotational band is then split into two $\Delta I = 4$ sequences, perturbed by about 120 eV relative to one another. This represents a tiny effect on the γ-ray energies which must be measured experimentally with a very high precision of about 0.1 keV. Thus, it is necessary to have a high-statistics spectrum of the superdeformed band without any contamination. This can only be achieved with a combination of very high resolving power and large efficiency. Up to now, staggering patterns, persisting over a large spin region, have been found in four superdeformed rotational bands using three different detectors EUROGAM, GAMMASPHERE and recently EUROBALL for ^{150}Tb [28]. Hamamoto and Mottelson [29] have shown that, under some conditions, the magnitude of the staggering effects in two nuclei may be related. As shown in Figure 1.3, this theoretical interpretation fits well with the experimental data. In order to firmly establish the occurrence of such a staggering effect and to determine its microscopic origin the search for $\Delta I = 4$ bifurcation must be extended to superdeformed nuclei in other mass regions.

Coexistence of axial and triaxial superdeformed shapes

The possibility of prolate-triaxial shape coexistence in the second well has been highlighted by a EUROBALL experiment on ^{154}Er. Several types of model calculations have predicted the lowest-lying superdeformed band in ^{154}Er to be similar to the "doubly magic" yrast super-deformed band in ^{152}Dy, which is based on the vacuum configuration in the pronounced prolate *Z=66, N=86* shell gap. At *Z=68*, the additional two protons should occupy "spectator" orbits with low single-particle quadrupole moments. However, the first experimental observation of superdeformation in ^{154}Er at GAMMASPHERE [30] revealed a superdeformed band with quite different characteristics. Primarily, the $\mathfrak{J}^{(2)}$ moment of inertia for this band

Figure 1.4: *Moment of inertia plots for the two SD bands in ^{154}Er as a function of rotational frequency: (**a**) kinematic moments $\Im^{(1)}$ and (**b**) dynamic moments $\Im^{(2)}$. Open squares and open circles mark the theoretically predicted values for band 1 and 2, respectively, and filled squares and filled circles show the experimental values for bands 1 and 2. The inset shows theoretical excitation energies as a function of angular momentum for bands 1 and 2, as well as for the first excited prolate SD band (crosses). In the $\Im^{(2)}$ plot, the yrast superdeformed band in ^{152}Dy (stars) is also included. The rise in the calculated $\Im^{(1)}$ moment of inertia at $\hbar\omega \sim 0.65$ is due to rotational alignment of a pair of high-j particles.*

was significantly lower than the predictions. It was later suggested [31] that this superdeformed band might be the result of the nucleus having a triaxial shape. Recently, a second, weaker, superdeformed band was found in the analysis of EUROBALL data [20].

As can be seen in Figure 1.4 (b), the $\Im^{(2)}$ moment of inertia of this band closely follows the predicted values for the lowest-lying prolate superdeformed band in ^{154}Er, as well as the experimental values for the yrast superdeformed band in ^{152}Dy. In the figure is also shown the $\Im^{(2)}$ moment of inertia for the previously known band, together with the values predicted by Total Routhian Surface (TRS) calculations [20] for a triaxial superdeformed band. In Figure 1.4 (a) the $\Im^{(1)}$ moments of inertia of the bands is compared to theoretical predictions. Here, a bandhead spin of 24 $\hbar$ and 26$\hbar$ is assumed for the triaxial and prolate superdeformed bands, respectively. The inset of the figure shows theoretical excitation energies as a function of angular momentum for the lowest-lying and first excited prolate superdeformed bands, together with the predictions for the triaxial superdeformed band. The calculations not only agree with the rotational characteristics of the observed bands, but they are also consistent with the triaxial superdeformed band being more strongly populated than the prolate superdeformed band, i.e. in the angular momentum regime where the bands are fed in the experiment (45-55 $\hbar$) the prolate superdeformed band lies around 1 MeV higher than the other band.

1.3.   Octupole softness and vibrations in superdeformed nuclei

In the A~190 mass region, octupole softness of the second well has been predicted by several theoretical models. This is illustrated in Figure 1.5 where the potential energy surface for ^{194}Pb is plotted as a function of the quadrupole and octupole deformation parameters [32]. The second superdeformed well clearly appears to be much softer against the octupole degree of freedom than the first (spherical) well. Recent EUROBALL results have produced strong evidence that the lowest excited superdeformed states are, at least in some nuclei in the A~190 region, indeed based on octupole vibrational structures. To interpret the properties of excited superdeformed bands in ^{197}Pb some octupole softness is needed in the quasi-particle description. These aspects will be discussed in more detail in the following sections.

Octupole-vibrational superdeformed bands

Two EUROBALL experiments have been performed for ^{190}Hg [33] and ^{196}Pb [34,35] to establish the nature of γ-ray transitions connecting an excited superdeformed band with the yrast superdeformed band. In both cases, those transitions were intense enough to determine branching ratios for the inter-band and in-band decays, to measure angular distributions and to perform a linear polarisation analysis. Linear polarisation measurements are possible with EUROBALL since the Clover Ge detectors can be used as Compton polarimeters. The advantage of EUROBALL for this type of measurement is actually two fold: Firstly, clean (i.e. multi-gated) spectra can be obtained with sufficient statistics in the connecting transitions and secondly, the large detection efficiency of the Clover detectors allows the measurement of an accurate value of the polarisation. In the experiment on ^{190}Hg, shown as an example in Figure 1.6, $1.7 \cdot 10^9$ events were collected and about 12% of these were Compton-scattered events, which were used for the polarisation measurements.

Both experiments firmly establish the electric-dipole character of the inter-band transitions with a B(E1) strength of $\sim 2 \cdot 10^{-3}$ Wu and $\sim 10^{-4}$ W.u. for ^{190}Hg and ^{196}Pb, respectively. These

Figure 1.5: *Potential energy surface for ^{194}Pb as function of the quadrupole and octupole deformation parameters (β_2 and β_3) showing the pronounced octupole softness in the second (SD) well (courtesy of J. Meyer).*
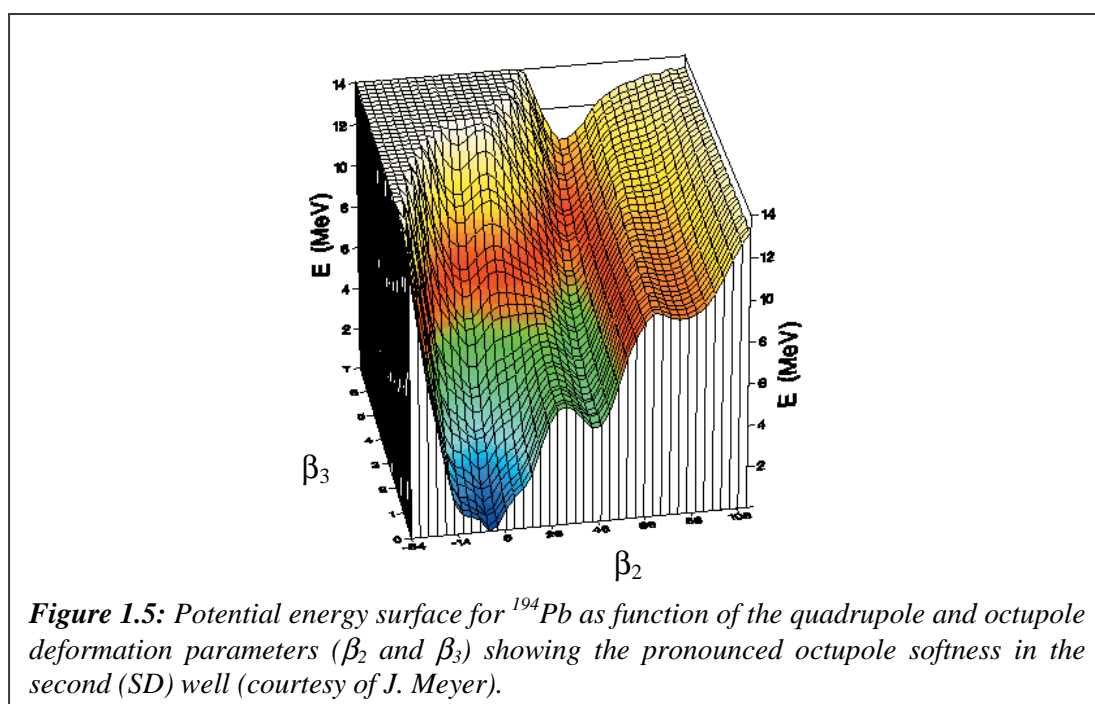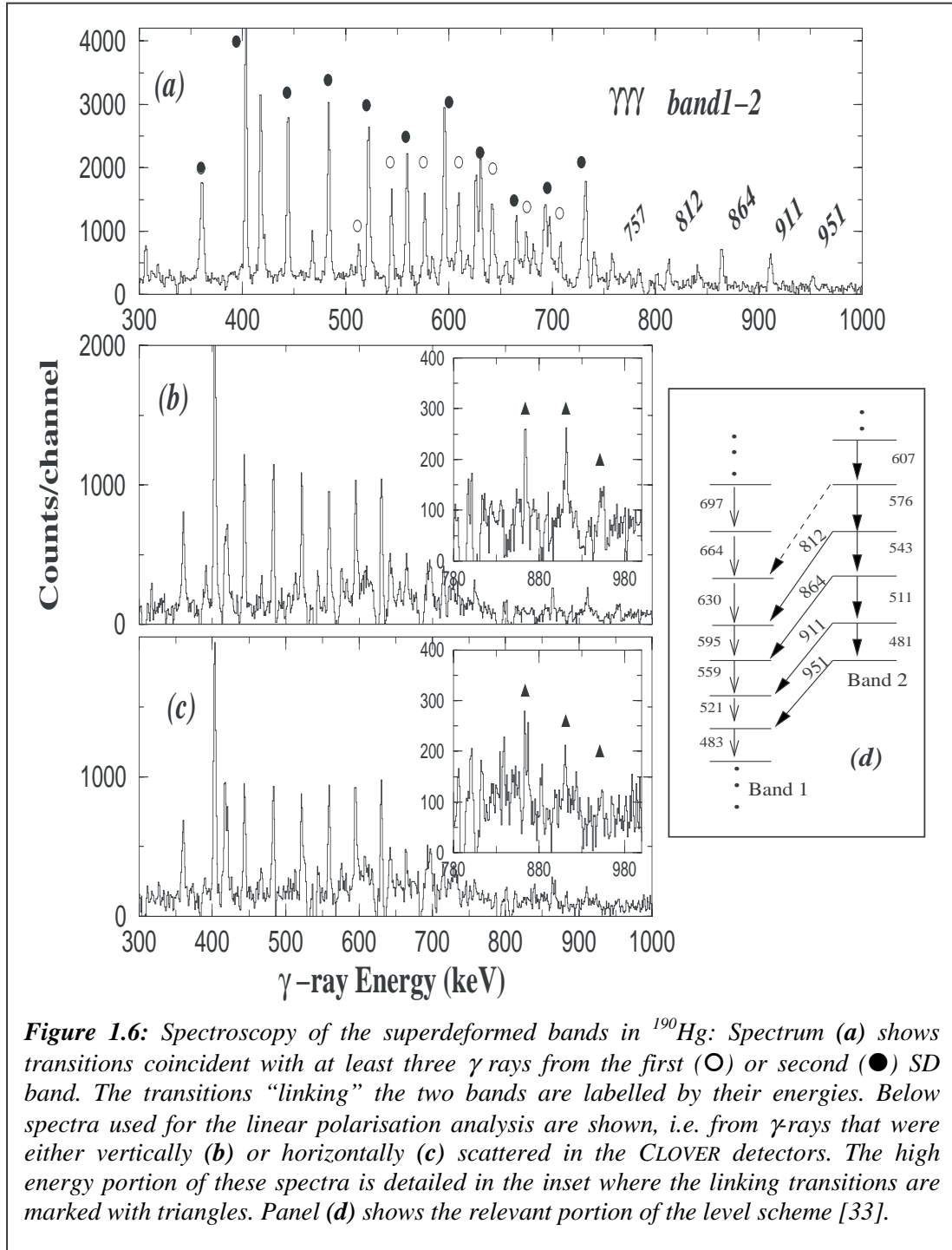
Figure 1.6: *Spectroscopy of the superdeformed bands in ^{190}Hg: Spectrum (a) shows transitions coincident with at least three γ rays from the first ($\bigcirc$) or second ($\bullet$) SD band. The transitions "linking" the two bands are labelled by their energies. Below spectra used for the linear polarisation analysis are shown, i.e. from γ-rays that were either vertically (b) or horizontally (c) scattered in the CLOVER detectors. The high energy portion of these spectra is detailed in the inset where the linking transitions are marked with triangles. Panel (d) shows the relevant portion of the level scheme [33].*

values are much larger than the E1 transition strength observed between excited quasi-particle states, but they are similar to those found in normal-deformed nuclei, where octupole deformation (or vibration) is known to play an important role. To confirm this interpretation, lifetime measurements have been performed in ^{196}Pb for both the yrast superdeformed band and the one based on the presumed octupole vibration [34]. The quadrupole moments deduced for the two superdeformed bands agree within the experimental uncertainties. All these results provide strong evidence that at least some of the low-lying excited superdeformed bands in the A~190 mass region are of octupole-vibrational character.

Influence of octupole softness in ^{197}Pb and ^{198}Pb

In another recent EUROBALL experiment six new excited superdeformed rotational bands have been discovered in $^{197\text{-}198}$Pb [36]. The yrast superdeformed band in ^{197}Pb (^{198}Pb) represents only 0.2% (0.5%) of the corresponding reaction channel. This population is much weaker than in lighter lead nuclei and presumably related to the high excitation energy of the super-deformed states relative to the yrast line. Another difficulty in studying superdeformation in these heavy nuclei is the strong fission channel. Here, the INNER BALL calorimeter was decisive in order to reduce the strong fission background by selecting very long cascades. The new superdeformed bands have been interpreted in the framework of cranked HFB calculations with approximate projection on the particle number by means of the Lipkin-Nogami method [37]. In this way quasi-particle excitations have been assigned to all bands. However, in order to explain their rather large intensity (relative to the yrast superdeformed band), it was suggested that some excitations might be lowered in energy by the coupling with a residual octupole interaction of a non-axial Y_{32} type.

1.4. Magnetic properties in the superdeformed minimum

The EUROBALL data from the experiments described above also revealed the presence of "cross-talk" transitions between two superdeformed signature-partner bands in ^{197}Pb [38]. Despite the very low intensities, i.e. the production cross section of the lowest excited super-deformed rotational band was estimated to ~0.5 mb, directional correlations from oriented states (DCO) measurements were possible. The DCO ratios confirm the $\Delta I=1$ character of the cross-talk transitions, but due to their low energy the (electric or magnetic) character could not be established from a measurement of their linear polarisation.

Assuming that the two bands are indeed signature partners, as indicated by the transition energies, the cross-talk transitions must have M1 multipolarity. Then B(M1)/B(E2) ratios can be determined experimentally for several states of the two bands. This ratio is proportional to $(g_K - g_R) K / Q_0$, g_K and g_R being the single-particle and collective gyromagnetic ratio, respectively, and Q_0 the intrinsic quadrupole moment. The collective g-factor can be estimated in the Inglis cranking approximation using microscopic HF+BCS calculations with the effective interaction SkM* [39]. This approach is preferred since the g_R value found for superdeformed states can be different from the rigid-body Z/A estimate. Direct measurements of g factors in three superdeformed bands of ^{194}Hg have confirmed the validity of this approach. If Q_0 is known, for example from lifetime measurements, it is possible to experimentally determine the g_K value, which depends on the orbitals occupied by the valence particles. With this method precise quasi-particle configurations could be assigned to several superdeformed bands in nuclei around A~190 [22]. In addition, the effective spin-gyromagnetic factor g_s^{eff} can be derived from the g_K value, which appears to be close to the theoretical value for a free neutron (g_s^{free}) indicating a unexpected lack of quenching for the neutron orbitals at super-deformed shapes [38]. More precise data on the B(M1)/B(E2) ratios are still needed to fully understand the underlying reasons for this apparent lack of quenching.

1.5. Structure of superdeformed bands in ^{131,132}Ce

The two superdeformed bands in ^{131}Ce and the three superdeformed bands in ^{132}Ce have been extended to higher spin with recent EUROBALL IV data. While none of the five bands have been connected into the normally deformed states, the two bands in ^{131}Ce have been linked to each other by three transitions. Angular correlation results indicate a $\Delta I=1$ M1/E2 character with a substantial E2/M1 mixing ratio ($\delta \sim +1$). It has also been possible, for the first time, to measure angular correlation ratios for the in-band transitions in all five SD bands.

The relative alignments of the SD bands are shown in Figure 1.7, with the yrast SD1 band of ^{132}Ce used as the reference. The important ingredient of the latter band is the $(\pi g_{9/2})^{-2}(v i_{13/2})^2$ configuration. The excited SD2 band in ^{131}Ce (with zero relative alignment) must also involve this structure, while the yrast SD1 band in ^{131}Ce (with less alignment) loses one of the $i_{13/2}$ neutrons. The excited SD2 and SD3 bands in ^{132}Ce are interpreted in terms of signature partner bands built on the $(\pi g_{9/2})^{-1}(v i_{13/2})^2$ configuration (cf. the SD bands in ^{133}Pr [40]). It can be seen that SD3 gains alignment above a transition energy of 1.6 MeV (i.e., $\omega \sim 0.8$ MeV/$\hbar$) which is attributed to a crossing between the high-Ω $\pi g_{9/2}$ orbital and the first low-Ω $\pi i_{13/2}$ intruder orbital. The structure of SD3 at high spin is then $(\pi g_{9/2})^{-2}(\pi i_{13/2})^1(v i_{13/2})^2$. This crossing provides the first evidence for the $i_{13/2}$ *proton* intruder in the cerium nuclei (Z=58); this orbital is usually only observed in superdeformed structures in nuclei with Z$\geq$63.

Figure 1.7: *Alignment plot for the superdeformed bands in ^{131,132}C relative to the yrast superdeformed band in ^{132}Ce.*
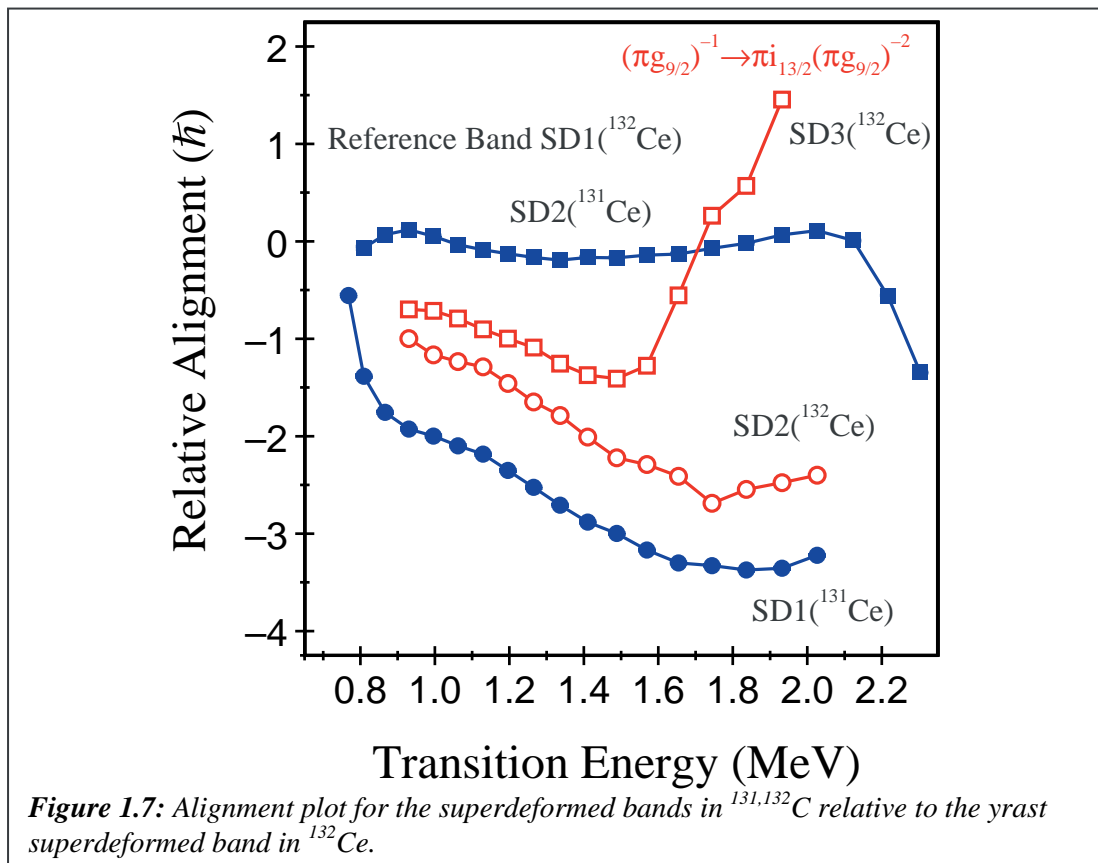
1.6. Search for Hyperdeformation

One of the main goals of nuclear structure research has been to observe hyperdeformed (HD) nuclear states at extremes of angular momentum. Such states are theoretically predicted in various regions of the nuclear chart and will become yrast at very high values of spin, typically above $80\hbar$ [41-45]. These states have very large prolate deformations with major to minor axis ratios of approximately 3:1. The discovery of hyperdeformed states at high angular momentum would be a very important test of nuclear models, and therefore the search for hyperdeformed states was an important part of the justification for constructing the EUROBALL array.

Many searches have been carried out for signals of HD nuclear shapes [46-51], however, as yet no compelling evidence for the existence of discrete hyperdeformed states at high spin exists. One of these searches has been performed in one of the first experiments with EUROBALL [52]. But many searches have been carried out without any prior experimental information about how much angular momentum these candidate nuclei can support before undergoing fission. Therefore, the non-observation of these states may be a direct consequence of fission or high evaporated-particle multiplicities imposing a limit on the angular momentum in the residual nucleus of study.

At such extremes of angular momentum and deformation it is not clear what parameterisations will allow the prediction of the correct sequence of single particle levels to create the shell gaps necessary to stabilize these deformations. Therefore, it may also be possible that hyperdeformed states have not yet been observed because of the failure of current models under such extremes of spin, and these models are predicting hyperdeformed minima to occur in the wrong nuclei.

Candidate nuclei

It is also interesting to note that gamma-ray spectra of superdeformed bands obtained with the latest generation of spectrometers (EUROBALL and GAMMASPHERE) only show, at best, 2-3 new transitions (on top of previously known bands), despite the spectra having 2-3 orders of magnitude more counts, and the arrays having two orders of magnitude better resolving power than the previous generation. This implies that something other than advances in detector technology is placing a limit on the ability to study states at the extremes of nuclear spin. We suggest this limit is primarily due to fission and/or excessive particle evaporation, and that too little attention has been paid to the reaction and reaction conditions necessary to populate HD states. Therefore, the system to be studied must be chosen very carefully. From recent experiments the following criteria for choosing the reaction to be studied could be extracted:

1) Compound nuclei must be in the mass A ~ 100-170 range, since this is the only region in which fission limits may be high enough to allow the population of very high spin states [53].

2) Since the fissility of the compound system increases with Z^2/A, the isotope under study must be as neutron rich as possible for a given element. In fact, intense neutron-rich radioactive ion beams are the best choice in order to maximise the angular momentum input into the compound nucleus.

3) Symmetric reactions are highly preferable since their Q-values are usually much lower than those of asymmetric ones allowing colder formation of the compound system. Furthermore, some experiments show that high spin states are more strongly favoured with such reactions (e.g the superdeformed band in ^{148}Gd is enhanced 4.6 times with symmetric reactions rather than asymmetric ones [54]). Neutron multiplicities will also be lower, therefore less angular momentum will be removed from the compound system.

4) Reactions involving beam/target combinations which are near magic, magic or doubly magic are also desirable, since the shell effects lower the Q-value of the reaction (e.g. when populating heavy elements [55] magic beam-target combinations are essential for these nuclei to be produced with as little fission as possible).

5) Suggestions have also been made [47,48] that detection of a proton in coincidence with gamma rays may enhance the probability of observing hyperdeformed structures. This may help for two reasons: Firstly, the peak to background ratio improves considerably because unwanted reaction channels and fission are rejected. Secondly, emission of protons from the hyperdeformed compound system might be enhanced due a lower Coulomb barrier at the "tips" of an extremely deformed shape where the charge is concentrating.

6) Exit channels with the lowest number of particles emitted have the best chance of being populated at the highest spins necessary to populate hyperdeformed shapes. Of particular interest are reaction channels such as *2n*, *3n* or *p2n*. These can be enhanced using the high-fold data from the inner BGO ball, and/or techniques such as γ-ray filtering [56].

Hyperdeformed minima are predicted in a wide range of nuclei between masses 130 and 170 [41-45]. It is interesting to note that in previous studies of rotational bands based on superdeformed shapes, the occurrence of second minima in the nuclear potential energy is a widespread phenomenon. Since many more energy levels intrude and cross over from shells above at even higher deformations it is expected that hyperdeformed shell gaps will be even more abundant than superdeformed shell gaps. What is not clear is whether it is possible to generate sufficient angular momentum, without inducing fission, to populate these minima in any of the nuclei accessible with stable beams and targets in this region. Furthermore, it is not clear how low in spin these minima persist. For long rotational superdeformed bands it has been observed empirically that it is possible to study structures as weak as 10^{-5} of a reaction channel. Provided that a hyperdeformed cascade is long (greater than 5 transitions), this observationally limit can be reached. However, the resolving power of EUROBALL may still not be sufficient for observation of such structures.

Recent EUROBALL Experiments

Four experiments fulfilling the criteria suggested in the introduction have been performed with the EUROBALL array, the latest being a very long experiment of ~4 weeks of beam time.

The reactions studied/to be studied are:

(i) ^{48}Ca + ^{82}Se   (June 2001 – Euroball)
(ii) ^{50}Ti + ^{124}Sn   (June 2001 – Euroball)

(iii) ^{48}Ca + ^{96}Zr   (June 2002 – Euroball)
(iv) ^{64}Ni + ^{64}Ni   (January 2002 & December 2002 – EUROBALL + DIAMANT)

The most promising results so far have come from the ^{48}Ca + ^{82}Se experiment producing isotopes of Xe. A candidate rotational structure with approximately 10 very weak evenly spaced transitions ($\Delta E_\gamma \sim 33$ keV) was found, however, the statistical significance of this structure ($\sigma = 2.31$) was not sufficient to confirm that the sequence was real and not a statistical aberration. Extensive work on analysis of these data is ongoing.

Future perspectives

EUROBALL, together with its counterpart GAMMASPHERE, has provided many new results on the superdeformed world of nuclei. But these results also show that many experiments are on the very limits of what can be done with present arrays. This is especially true for more information on spins, parities and excitation energies of superdeformed states and for the search for hyperdeformed nuclei. New data in these domains can only be provided by a new generation of γ-ray spectrometers built from γ-ray tracking detectors with a much increased efficiency and resolving power.

Acknowledgements

Triaxial Nuclei

G. Hagemann

2. Triaxial nuclei[*]

2.1. Introduction

Nuclei may acquire shapes with non-axial symmetry, but triaxiality is in general difficult to prove experimentally. Although signature effects are expected in energies as well as in electromagnetic properties, such effects may also arise as a result of the interplay of mechanisms not related to triaxiality. Unique, but substantially different effects of stable triaxiality are *chiral twin bands* and the *wobbling mode*.

The *chiral symmetry* relates to the orientation of the angular momentum vector relative to the three different intrinsic principal axes of the nucleus, and requires an orientation at variance with any of these. In such cases two solutions, with left- and right-handed orientation, respectively, may exist [57] leading to chiral twin bands. The *wobbling mode*, predicted more than 25 years ago [18] is uniquely related to a stable triaxial deformation, exploiting the rotational degree of freedom in a triaxial quantal system. For a triaxial body with different moments of inertia $\Im_i$ with respect to the principal axes (i.e. $\Im_x \gg \Im_y , \Im_z$) and in the high spin limit with most of the spin aligned along the x-axis, the wobbling mode introduces a sequence of bands with increasing number of wobbling quanta ($n_w = 0,1,2, \ldots$) and a competition between the inter-band and the in-band transitions.

Most of the efforts at EUROBALL to study triaxiality has gone into the investigation of nuclei with strongly deformed triaxial shapes, and, as a break through, provided the first evidence for the wobbling mode [58,59]. Consequently, the focus of this section will be concentrated in this area. In a recent EUROBALL experiment the wobbling mode was even developed to the 2nd phonon excitation [60]. The wobbling interpretation is based on comparison to particle-rotor calculations [61]. In parallel with the experiments carried out at EUROBALL data have also been obtained from the GAMMASPHERE and GASP arrays. A discussion of these data will be included in the present status report on strongly deformed triaxial nuclei.

Nuclei with *N~94* and *Z~71* constitute a new region of exotic shapes coexisting with normal prolate deformation [62,63]. They provide a unique possibility of studying strongly deformed shapes with a pronounced triaxiality. At the beginning of the first EUROBALL campaign at Legnaro two such cases were known in ^{163,165}Lu [64-66]. Large Q_t values, corresponding to $\varepsilon \sim 0.4$ with $\gamma \sim 18°$, were derived for the triaxial superdeformed (TSD) band in ^{163}Lu [65] from both Recoil Distance and Doppler Shift Attenuation Method measurements. This band was interpreted as most likely corresponding to the $\pi i_{13/2}$ configuration. Later, a band with transition energies, identical within 1-3 keV to those in ^{163}Lu, was found in ^{165}Lu, and, based on the similarity, also interpreted as a $\pi i_{13/2}$ excitation. Calculations with the Ultimate Cranker (UC) code [67,68] based on a modified harmonic oscillator potential have revealed that large deformation minima are actually expected for all combinations of parity, π, and signature, α, in a region of nuclei around ^{163,165}Lu [64,69]. As an example a potential energy surface for ^{163}Lu is shown in Figure 2.1.

The most favourable even-even nuclei in the region among Yb-, Hf- and W-isotopes for finding low-lying TSD structures are calculated [68,69] to be ^{164,166}Hf. It appears that in spite of various searches no examples of TSD band structures could be found in those isotopes,

---

[*] Contribution by G. Hagemann

Total Energy Surface, ^{163}Lu, I=53/2, $(\pi,\alpha) = (+,+1/2)$

Figure 2.1: *Potential energy surface for ^{163}Lu and for parity and signature $(\pi,\alpha) = (+,+\frac{1}{2})$ at spin I=53/2$\hbar$; besides the normal minimum at $\varepsilon \sim 0.2$ two triaxial minima are developing at $\varepsilon \approx 0.4$ and with $\gamma \approx \pm 20°$.*
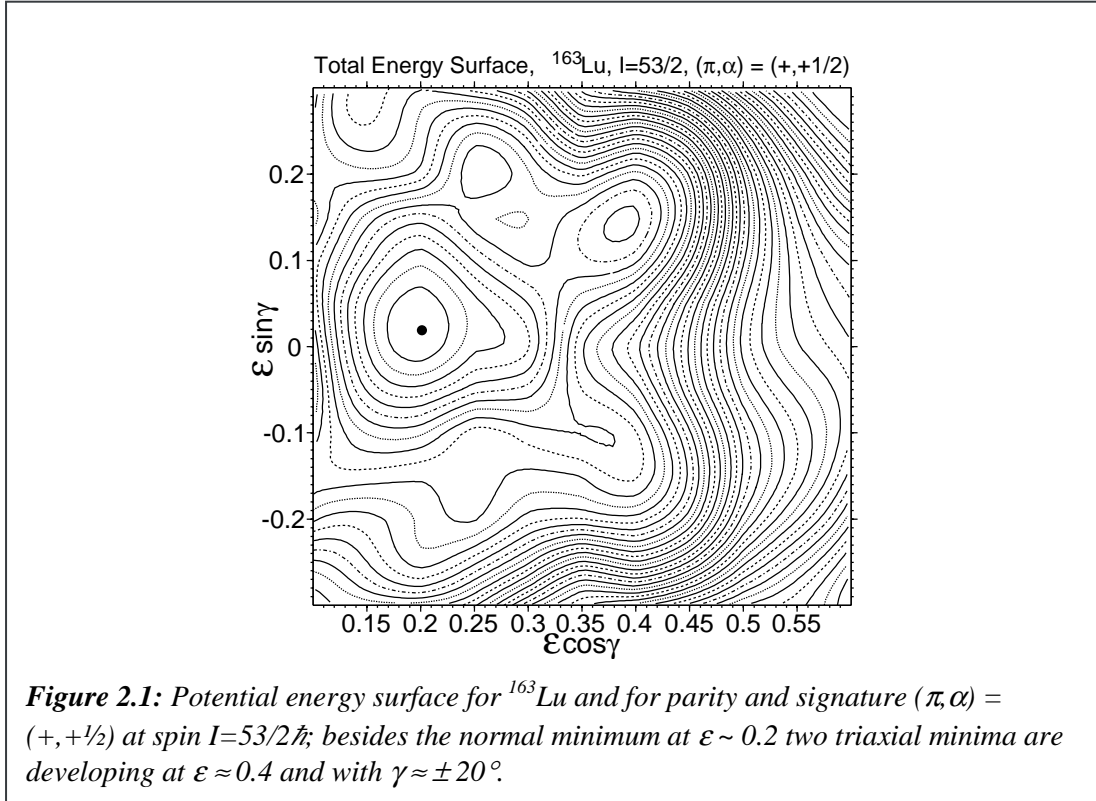
whereas there is new experimental evidence for three weakly populated TSD bands in ^{168}Hf, for which lifetime measurements have confirmed the large deformation [70]. It will be interesting to extend the search for TSD bands in the region to heavier Hf isotopes as well as to neighbouring Lu-isotopes. Lifetime measurements will also be required to substantiate the expected large deformations.

In addition to these investigations in the Lu-Hf region a recent EUROBALL experiment has revealed that a band in ^{154}Er, formerly interpreted as being superdeformed, but with properties resembling those found for TSD bands in the Lu-Hf region, should be reinterpreted as a TSD band (cf. Section 1). The expected superdeformed band with larger dynamic moment of inertia, $\Im^{(2)}$, and weaker population, was also established in this EUROBALL experiment [20]. The presumed triaxial structure in ^{154}Er most likely also has an $i_{13/2}$ proton involved in its configuration.

In this report on triaxial nuclei we will first concentrate on TSD bands in the Lu-Hf region; Sections 2.2 and 2.3 contain an overview of experiments and results and a presentation of the information on the spectroscopy of strongly deformed triaxial nuclei obtained primarily from EUROBALL measurements. The recent evidence for the 1st and 2nd phonon wobbling excitation Lu isotopes will be presented in section 2.4. New results on chirality in nuclei will be discussed in section 2.5 followed by some conclusions and perspectives.

2.2. General properties of strongly deformed triaxial nuclei

Figure 2.2 shows an overview of TSD bands found in Lu- and Hf-nuclei in the recent years. These data have come from the EUROBALL, GAMMASPHERE and GASP arrays. The very first TSD band in the region, TSD1 in ^{163}Lu, with a population of ~10% relative to the yrast strength in the reaction channel, was found with the OSIRIS array (12 Ge-detectors with an inner BGO ball) [65]. Lifetimes for that band were later measured with the NORDBALL array consisting of 20 Ge detectors with a BGO INNER BALL of 55 elements [66].

Figure 2.2: *Overview of searches and results for Lu and Hf nuclei. References for TSD band structures are: ^{161,162}Lu [71], ^{163}Lu [65,72,59], ^{164}Lu[73], ^{165}Lu [64,74], ^{167}Lu [75, 76], ^{168}Lu [77], ^{166}Hf [78], ^{168}Hf [70] and ^{170}Hf [79]. In addition, at the time of writing this report a new Euroball experiment with the aim of studying further the bands found in ^{161,162}Lu is being performed. References for lifetime measurements on TSD bands are: ^{163,164,165}Lu [66,80,81] and ^{168}Hf [70].*

It should be noted that the expected, most favourable nucleus for TSD structures, ^{164}Hf has been studied with NORDBALL, with negative results. Although NORDBALL was considerably less effective at discovering long cascades of γ-rays than the later arrays included in Figure 2.2, a TSD band of a strength comparable to those seen in ^{163}Lu and ^{165}Lu, should have shown up in the NORDBALL data. Furthermore, ^{165,166,167}Hf were studied with EUROBALL, but once again no TSD bands were found [78].

The identification of TSD bands in the Lu-Hf nuclei is in most cases based on the observation of large dynamic moments of inertia similar to the first observed TSD bands in ^{163}Lu and ^{165}Lu. A comparison of the values for odd-N and even-N Lu isotopes is shown in Figure 2.3.

For most of the bands quoted in Figure 2.2 it has not been possible to establish connections to known normal-deformed (ND) structures. Therefore, the excitation energy, spin and parity are unknown. However, with reasonable assumptions of alignments (comparable to what has been determined in ^{163,165}Lu and ^{164}Lu), the spins of the unconnected bands can be estimated within ~2ℏ. The relative population of the TSD bands compared to the yrast normal-deformed structures in the same nucleus must be related to the excitation energy of the local, triaxial
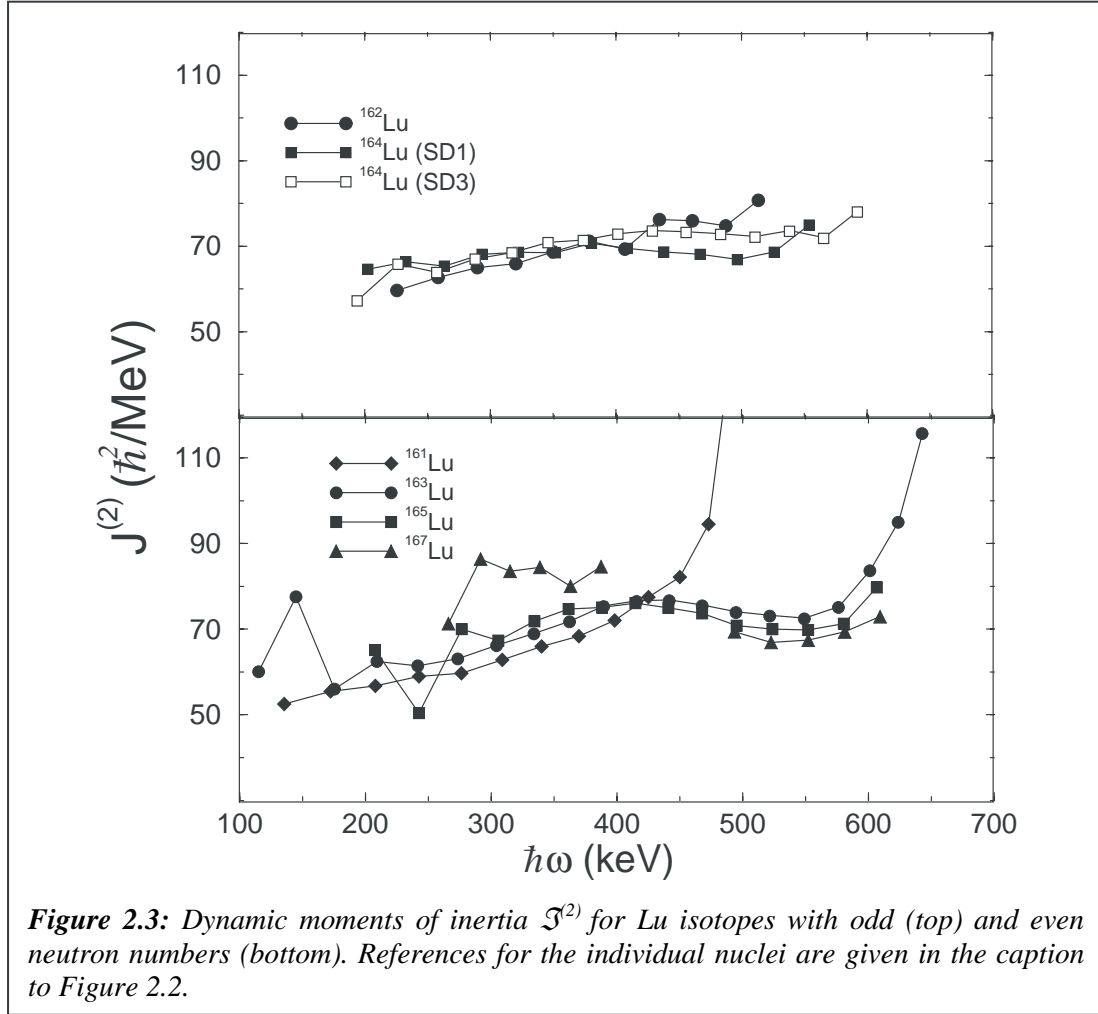
Figure 2.3: *Dynamic moments of inertia $\mathfrak{J}^{(2)}$ for Lu isotopes with odd (top) and even neutron numbers (bottom). References for the individual nuclei are given in the caption to Figure 2.2.*

superdeformed minimum relative to the global normal defomed minimum in the potential energy surface (see Figure 2.1.). From such a comparison one can conclude that among the lighter Lu isotopes, ^{163}Lu has the lowest TSD minimum. The population strength found in ^{161,162}Lu is considerably lower than in ^{163}Lu. The strength found in ^{165}Lu seems to stay constant (or even increase) towards the heavier isotopes, ^{167,168}Lu. For the two even-even Hf isotopes an increase by a factor of ~3.5 is measured in the population of the new TSD band in ^{170}Hf over the population of the strongest TSD band in ^{168}Hf, to which the one in ^{170}Hf has a pronounced resemblance.

In conclusion, it seems that the pattern of population does not match what should be expected from the properties of the local triaxial minima calculated by the cranked shell model [68,69] for the even-even nuclei in the region.

2.3. New results on TSD bands in the Lu-Hf region

In the first very successful EUROBALL experiment on triaxial structures eight TSD bands were established in the odd-odd isotope ^{164}Lu. Connections to the normal-deformed structures were found for two of the strongest populated TSD bands. In the same experiment the complete decay-out from the first TSD1 band in ^{163}Lu could be established, and the spin and parity assignment confirmed its interpretation as a $\pi\, i_{13/2}$ configuration. The two connected TSD bands in ^{164}Lu with firm spin and parity assignments could be interpreted as also based on an

$i_{13/2}$ proton, coupled to neutrons occupying the lowest positive and negative parity orbitals, respectively [73].

Partial level schemes of ^{164}Lu [73] and ^{163}Lu [60,72] are shown in Figures 2.4 and 2.5, respectively. These two nuclei represent the most comprehensive determination of different decay-out properties of states in a TSD well to the normal-deformed structures. The mechanism behind the decay-out from a potential well of a different shape to the normal-deformed well (cf. Section 3) will depend on its excitation energy and on the height of the barrier between the two minima.

Figure 2.4: *Partial level scheme of ^{164}Lu [73]*

Figure 2.5: Partial level scheme of ^{163}Lu showing the three TSD bands together with the connecting transitions to the ND-structures to which the TSD states decay [72,60].

Figure 2.6 (Top panels): *Excitation energy relative to a rigid-rotor reference of the TSD bands (filled circles) together with normal-deformed bands (open squares) in* ^{163}*Lu and* ^{164}*Lu.* ***(Bottom panels):*** *Excitation energy in the spin region where the decay-out of the TSD bands takes place for* ^{163}*Lu and* ^{164}*Lu. Only bands in connection with the TSD band decay are shown. The arrows represent the observed connecting transitions. The figure is taken from Ref. [82].*

Two different decay-out scenarios are demonstrated in Figure 2.6 [82]. The preferred decay of a particular TSD band will depend on the excitation energy, relative to normal-deformed structures with the potential of causing a mixing of the TSD and normal-deformed states at their closest distance, at the lowest spins. The decay-out observed in ^{164}Lu of TSD1 with (π,α) = (-,0) shown in the bottom-right part of Figure 2.6, comprises both stretched and unstretched E1 and E2 transitions, the strongest decay being the stretched $16^{-} \rightarrow 15^{+}$ E1-transition. For TSD3 with (π,α) = (+,1) only one stretched E1 transition was found. From the out-of-band to in-band branching ratios the strongest E1 decay-out transitions are estimated to be of the order of ~0.3·10^{-4} W.u., which is around 300 times faster than the E1 decay found for the (axially symmetric) superdeformed states in ^{194}Hg [25], and only ~5 times slower than octupole-enhanced E1 transitions between some of the normal-deformed structures in the same and neighbouring nuclei. This suggests that octupole enhancement may also play a role in the TSD to ND E1 decay. From a similar consideration the B(E2, TSD $\rightarrow$ ND) values are 10^{3} - 10^{4} times reduced compared to the TSD in-band B(E2)-values.

In contrast, the decay-out from TSD1 in ^{163}Lu at spins I = 23/2 and 21/2 $\hbar$ can be completely explained by mixing at spin I = 21/2 $\hbar$, with a rather large interaction strength (~22 keV). Since the band TSD1 comes considerably closer to the normal-deformed structures at higher spin with no observation of cross-band transitions one may conclude that the barrier separating the two minima is probably more efficient at higher spin values, which also agrees with calculations. The different branching ratios also contain information on the ratio of the

quadrupole moments, i.e. $Q_t(TSD)/Q_t(ND) \sim 2$, which confirms the larger deformation of TSD1. The weak E1 decay observed from the $17/2^+$ state resembles the E1-decays observed in ^{164}Lu.

In addition to the decay out properties of ^{163,164}Lu summarised in Figure 2.6, there are data from GAMMASPHERE under analysis on the decay-out in ^{167,168}Lu [76,77], and a very recent EUROBALL experiment has provided new data on ^{165}Lu [74]. In both of these even-N Lu-isotopes the decay-out of the yrast TSD band occurs through mixing with normal-deformed states as in ^{163}Lu, however in ^{167}Lu the TSD and normal-deformed bands cross and interact at intermediate as well as at low spin.

2.4.   The wobbling mode and the first and second phonon excitation

The most striking feature of the level scheme of ^{163}Lu shown in Figure 2.5 is that all decays of the excited TSD bands proceed through the yrast TSD1 band. In addition, all three bands have very similar dynamic moments of inertia and alignments over almost the entire observed frequency range. The multipolarity of the transitions from TSD2 and TSD3 to TSD1 and from TSD3 to TSD2 have been determined by the analysis of the Directional Correlation from Oriented states, angular distribution ratios and linear polarisation data of the strongest transitions. It has thereby been possible to assign firm spins and positive parity to this family of bands, and a pattern compatible with expectations from wobbling phonon excitations has emerged [58-61].

The wobbling degree of freedom in an odd, triaxial nucleus like ^{163}Lu with aligned particle angular momentum in addition to the collective angular momentum is different from the original picture presented for an even-even system [18]. Here the total angular momentum is tilted away from the axis of the largest moment of inertia by a "wobbling angle", which

Figure 2.7: *Calculated expectation values of the collective angular momentum and its projection on the x-axis for the lowest favoured (f1, f2) and unfavoured (u1) bands in ^{163}Lu; f1, u1 and f2 correspond to bands with $n_w = 0$, 1 and 2, respectively[61].*

Figure 2.8: *Experimental and theoretical values of B(E2)$_{out}$/B(E2)$_{in}$. TSD1, TSD2 and TSD3 are identified with n$_w$ = 0,1 and 2, respectively [60].*

increases with the phonon number n$_w$. The possible presence of the angular momentum coming from intrinsic motion can in many ways make the nuclear wobbling mode much richer. The presence of aligned particles favours a particular (triaxial) shape and produces a unique pattern of electromagnetic transitions between the bands. The decomposition of the collective angular momentum shown in Figure 2.7 has been calculated with a model in which the aligned particle is coupled to a triaxial rotor [61]. The lowest solution with positive parity and favoured signature (α=+½), *f1*, has the collective angular momentum fully aligned with the x-axis (of largest moment of inertia). This solution is identified with TSD1 in [163]Lu. The second lowest solutions, *f2*, obtained with (π,α)= (+,+½) has a considerably smaller expectation value of the component R$_x$ than *f1*. For the lowest solution with positive parity and unfavoured signature, (α=-½), *u1*, the expectation value of R$_x$ is intermediate between *f1* and *f2*, thus bearing out the expected increase in wobbling angle, here for the collective part of the angular momentum.

The most crucial information from the particle-rotor calculations in Ref. [61] is contained in the electro-magnetic transition matrix elements. In particular, in the spin-range covered by the experiment the B(E2, n$_w$ = 1 $\rightarrow$ n$_w$ = 0) values for the inter-band transitions are calculated to be around 22-30% of the collective in-band B(E2, n$_w$ = 1 $\rightarrow$ n$_w$ = 1) values, which is large compared to single-particle values. Furthermore, with a wobbling phonon description it is expected that B(E2, n$_w$ = 2 $\rightarrow$ n$_w$ = 1) ~ 2 · B(E2,n$_w$ = 1 $\rightarrow$ n$_w$ = 0). The values of B(E2, n$_w$ = 2 $\rightarrow$ n$_w$ = 0) are small and only nonzero due to anharmonicities in the quantal phonon description.

In Figure 2.8 the data obtained for [163]Lu are compared to calculations. The agreement illustrated in the figure, together with difficulties in alternative interpretations of the large B(E2) values for the TSD2 $\rightarrow$ TSD1 transitions and in particular the crucial TSD3 $\rightarrow$ TSD2 transition, provides the principal evidence for the wobbling excitation mode in [163]Lu with both the 1st and 2nd phonon modes being established. New data in [165,167]Lu [74,76] show

candidate bands with very similar properties to the TSD2 band, and for [165]Lu also the TSD3 band, in [163]Lu. In both nuclei the electromagnetic properties, when measurable, also resemble those found in [163]Lu. Very recent Euroball data on [161]Lu also indicate the existence of the 1st phonon wobbling excitation connected to the TSD band.

2.5. New Results on chirality in nuclei

The most likely candidates to show chiral twin bands are odd-odd triaxial nuclei in which the odd proton and neutron occupy orbitals with specific preference for two of the principal axes, while the collective rotation preferring the third axis ensures that the angular momentum is oriented out of any of the principal planes. Some cases are suggested in the region around [134]Pr [83,84], and data from a recent EUROBALL experiment may indicate the possibility for the existence of chiral twin bands in even-even [136]Nd, although the two candidate bands may also be interpreted differently [85]. Recently, experiments have been carried out on the odd-odd nuclei [130,132]Cs [86] using the EUROBALL IV array at Strasbourg. These are near-neighbours to [134]Pr, and potential chiral structures have been previously observed at low-spin in both nuclei [87]. The prime focus of the experiment on [130]Cs is to measure the lifetimes of the states and hence determine the in-band and inter-band B(E2), B(M1) transition rates. These data will be particularly important since B(M1)/B(E2) ratios deduced for the chiral bands in [134]Pr are proving to be difficult to understand in terms of the chiral picture.

Figure 2.9 : EUROBALL results on chirality in [106]Rh. The two upper panels show plots of the excitation energy vs. spin for the proposed chiral bands in [104,106]Rh and the bottom panels show the variation of $B(M1)/B(E2)$, $B(M1)_{in}/B(M1)_{out}$ and $S(I)$, respectively, with spin for [106]Rh (see text for further details).
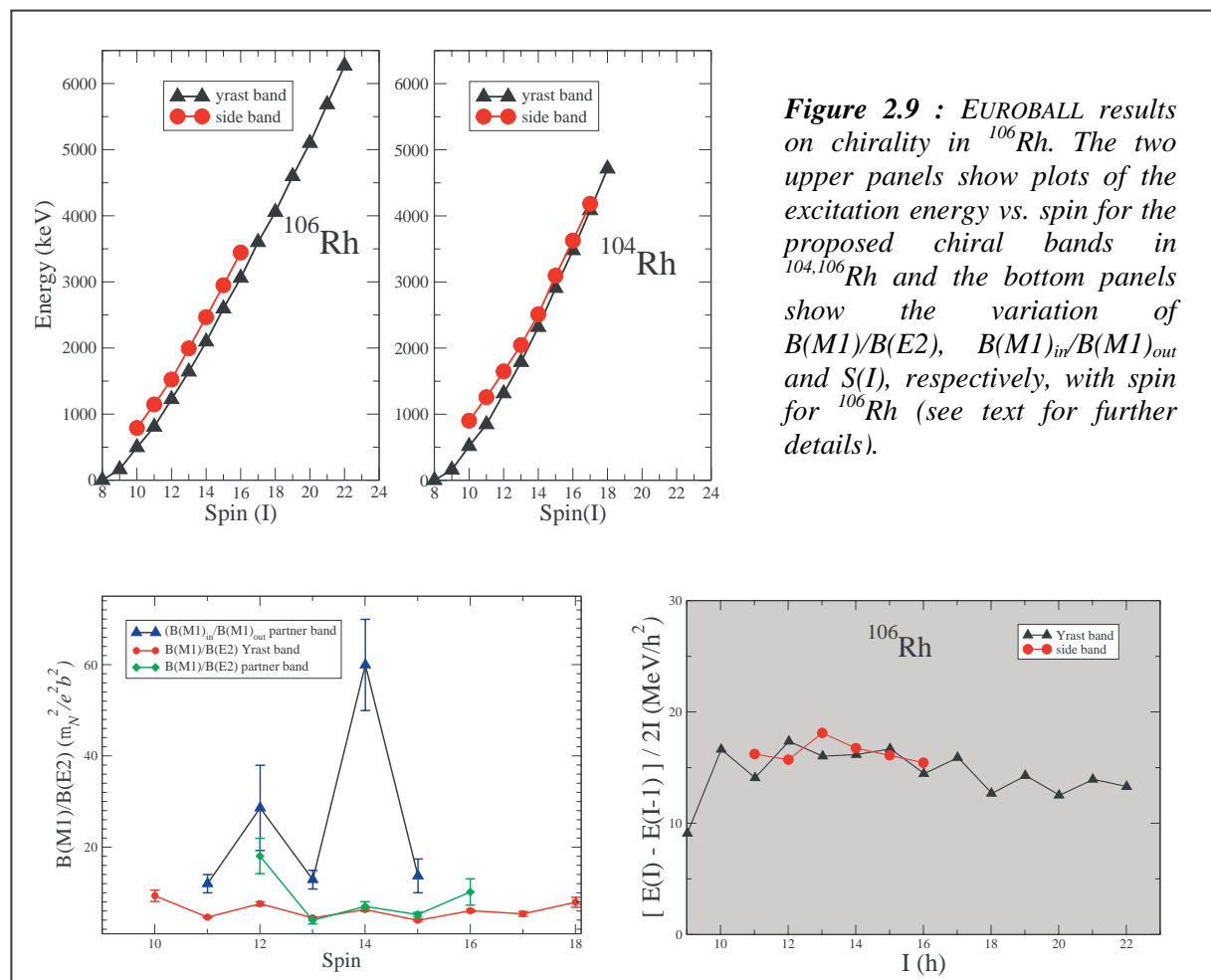
Recent studies have highlighted a new region of chiral structures in the neutron rich rhodium nuclei; the first case being identified in [104]Rh [88]. In this study the authors reported three fingerprints for the observation of chiral structures in nuclei. These may be summarised as follows: (1) the presence of near degenerate doublet $\Delta I=1$ bands over a range of spins; (2) the parameter $S(I) = [E(I) - E(I-1)] / 2I$ should be independent of spin and (3) there exists chiral symmetry restoration M1 and E2 selection rules as a function of spin. According to theoretical predictions the latter results in a staggering of the B(M1)/B(E2) ratios for in-band transitions and a similar staggering (with the same phase) for the ratio of the B(M1) in-band to B(M1) out of band transitions, $B(M1)_{in}/B(M1)_{out}$.

A recent experiment on neighbouring nuclei, carried out using EUROBALL, has revealed further evidence in support of this new region of chiral nuclei (see figure 2.9). The data for [106]Rh show good agreement with the above fingerprints, and consequently provides further evidence for the existence of chiral structures in this mass region. One clear difference between [106]Rh and [104]Rh, which can be seen in Figure 2.9, is that the chiral partner bands do not become degenerate in [106]Rh. Instead, they appear to have a near constant separation of ~350 keV. This is reminiscent of observations for nuclei neighbouring [134]Pr in the A=130 region, where the effect was attributed to the existence of chiral vibrations rather than chiral rotation [84]. The present experiment has also revealed the first evidence for chiral structures in an odd mass nucleus in this mass region, [105]Rh [89]. The properties of the observed structure suggest that this is the best example of chirality in an odd mass nucleus observed to date in any mass region.

2.6. Conclusions and perspectives

A new and very interesting region of nuclei presenting strongly deformed triaxial shapes has been revealed, by experiments carried out primarily with the EUROBALL array. Triaxiality provides the possibility of studying coexistence not only between different shapes, but also between the normal cranking solution in the strongly deformed triaxial well and the wobbling-phonon excitation, which represents a different manifestation of the rotational degree of freedom, that is realised in a triaxial nuclear quantal system.

Firm evidence for stable triaxiality is obtained from the presence of both the 1st and 2nd phonon wobbling excitations in [163]Lu. Wobbling excitations are present in the neighbouring nuclei [165,167]Lu and possibly also in [161]Lu, which confirms wobbling as a general phenomenon of triaxially deformed nuclei. It remains a challenge to establish a wobbling excitation in an even-even nucleus without having particle alignment in addition to the collective angular momentum. Other regions of nuclei may be found with a favourable potential for local triaxial minima as shown for example by the case of [154]Er [20] and possibly its neighbours (cf. Section 1).

Different decay-out mechanisms from a strongly deformed (local) triaxial minimum have been identified. The size of mixing matrix elements is related to the barrier between TSD and normal-deformed minima. Pure statistical decay-out is found when levels do not come sufficiently close to the normal-deformed states. The decay-out transitions of E1 character may be octupole enhanced. Further support for the coexistence of minima of different shapes comes from a fluctuation analysis of the number of bands in the different wells (cf. Section 4), showing that a large number of triaxial bands exist before damping of the rotational strength sets in [90].

The present variance between predictions from the cranked shell model and the experimental results concerning the most favourable location and relative excitation energy of the triaxial minima presents a challenge to nuclear structure theory. With spectroscopy in the triaxial well further developed a better understanding of the exact location of the shape-driving orbitals underlying the triaxial shapes can be obtained. In addition to the particle-rotor calculations, which provide the basis for our evidence for the observation of wobbling-phonon excitations, alternative theoretical formulations, for example using the cranked shell model plus random phase approximation [91] now exist. Other attempts from nuclear structure theory are underway.

Finally, there is also a growing body of evidence in support of the existence of the phenomenon of chirality in nuclei. At the present time the mass 130 region has received most attention, both theoretically and experimentally. Here there is evidence for chiral rotation in ^{134}Pr, with an island of odd-odd nuclei surrounding this nucleus, which have structures that have been interpreted in terms of chiral vibrations [83]. Chiral rotation may be expected to be found in nuclei which have a stable triaxial shape and valence protons and neutrons occupying high-j hole- and particle-like orbitals (or vice versa) respectively. Recent work suggests that nuclei in the Rh region around mass 100, where structures involving $g_{9/2}$ proton holes and $h_{11/2}$ neutron particles have been found, provide some of the best examples of chiral rotation and vibration observed to date. However, many other potential regions remain unexplored. It will be interesting to see if any of these can provide more than one example of chiral rotation, as seems to be the limit in the two regions explored so far.

Acknowledgements

Population and decay from superdeformed states

A. Lopez Martens

3. Population and decay from superdeformed states[*]

3.1. Introduction

Superdeformed states are generally populated at high spin in fusion evaporation reactions but, in spite of numerous examples for superdeformed nuclei, the mechanisms governing their population are still not fully understood. The open questions concern the entrance channel effects, the enhanced cooling of superdeformed nuclei compared to normal-deformed nuclei and the transition from thermally excited motion to ordered regular rotation within the superdeformed well. The other topic of investigation is the decay from superdeformed states, which occurs very suddenly, in the space of 1-2 transitions. In the process, the nucleus gains a certain amount of deformation energy and cools down by emitting a series of gamma rays and in some cases, light particles. The questions here are what are the decay pathways in order to establish the excitation energies, spins and parities of superdeformed states, how the shape change occurs and more particularly how do superdeformed and normal-deformed states interact and mix and does the nucleus undergo a transition from ordered to chaotic motion?

3.2. Population of superdeformed states

The E1 emission

The intensity of superdeformed yrast states is typically of the order of ~ 1% of the fusion-evaporation channel. Albeit being small this value is still very large compared to what is extrapolated from the intensities of yrast states [92] (see Figure 3.1). One of the mechanisms

Figure 3.1: Discrete line intensities (normalised to the $2^+ \rightarrow 0^+$ ground-state transition) vs. spin for some deformed nuclei and for superdeformed ^{152}Dy. The lines are simulation calculations tuned for ^{168}Yb using different values of the energy U_c below which all cascades are collected into the yrast band (from Reference [92]).

---
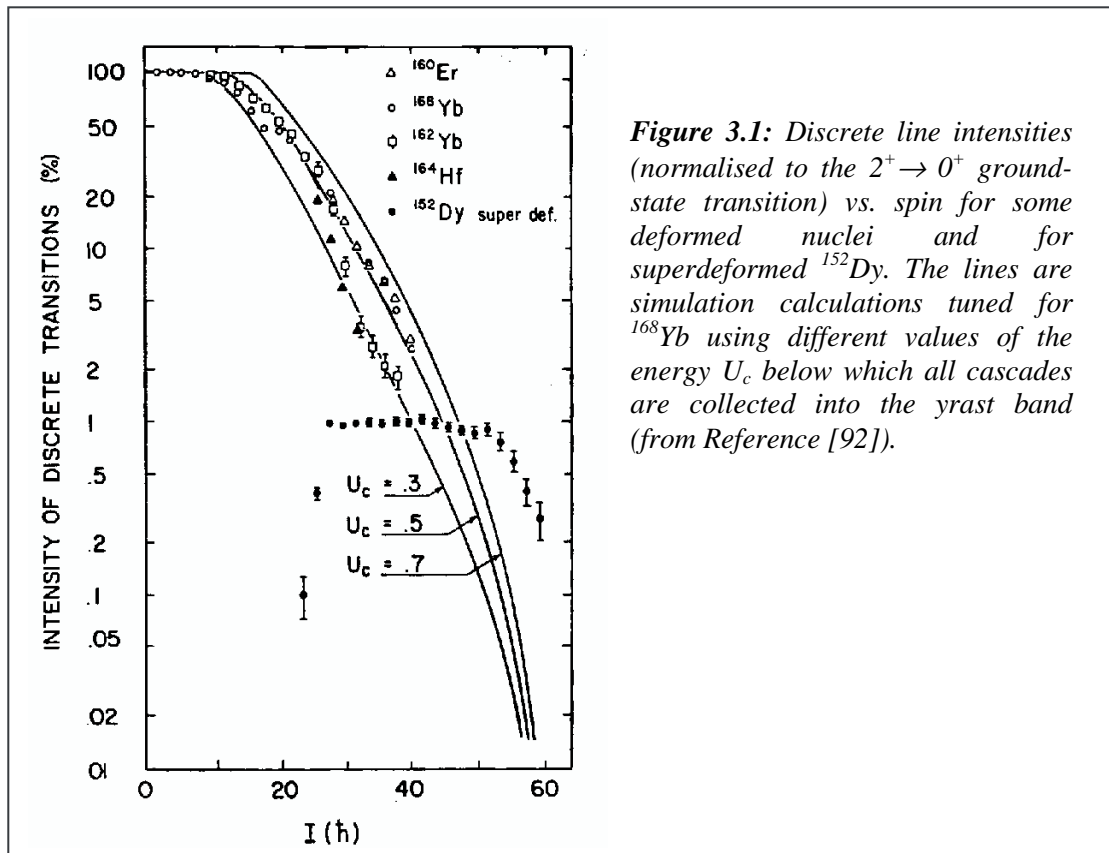
[*] Contribution by A. Lopez-Martens

invoked to explain this enhancement is the enhanced E1 emission from the superdeformed nucleus [93] (cf. Section 4). This is due to the combination of two effects: the lower level density of superdeformed states and the splitting of the GDR built on superdeformed states which gives E1 strength at lower energies. In nuclei where the particle binding energy lies between 8-11 MeV, gamma emission can therefore compete more effectively with particle evaporation in a superdeformed nucleus than in a spherical one.

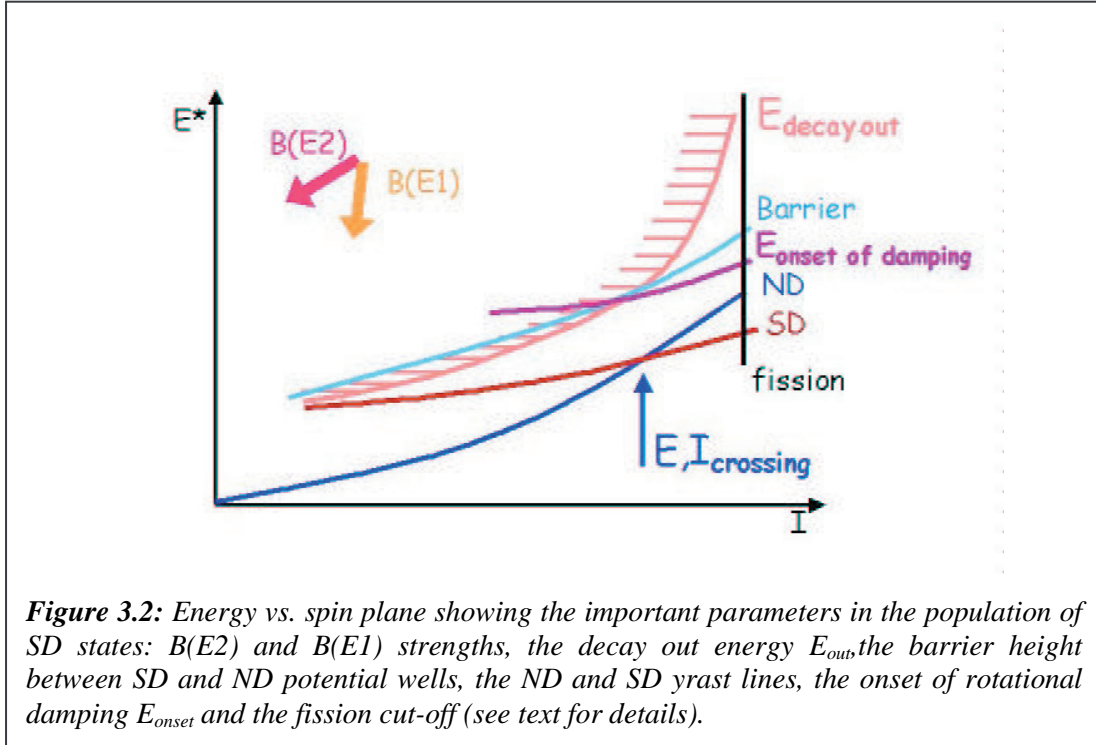A recent experiment using EUROBALL and the BaF_2 HECTOR array (cf. Section 4) shows evidence for an excess intensity in the high energy part of the spectrum of gamma-rays detected with HECTOR in coincidence with superdeformed states in ^{143}Eu. This excess strength is observed at ~11 MeV, where one expects the low-energy component of the GDR. Inversely, superdeformed structures are enhanced when high-energy γ-rays are required in coincidence. All these experimental observations support the fact that instead of emitting a neutron, the superdeformed nucleus ^{143}Eu can emit a GDR photon and that high-energy E1 cooling is the preferred way to feed superdeformed structures [94,95].

The question that still needs to be addressed is whether this is a general feature of the population of superdeformed states or particular to the ^{143}Eu nucleus. Part of the answer to this question should be known quite soon from a EUROBALL experiment to study this feature also in ^{196}Pb.

The E2 emission

As the nucleus cools down, E2 transitions start to compete with the E1 cooling and the question is where does the gamma flow go and what kind of superdeformed structures are sampled? The pattern of the regularly spaced E2 transitions of the yrast superdeformed structures is a very well known feature. Since the discovery of the first superdeformed rotational band in ^{152}Dy [13], more than 200 bands have been studied in nuclei of mass A~30, 60, 80, 130, 150, 160, 190 and the properties of the states which form the yrast superdeformed bands have shed light on many phenomena such as octupole vibrations, triaxial shapes and wobbling mode, C4 staggering, identical bands,... (cf. Sections 1 and 2). However, little is known about the E2 emission, which occurs at higher excitation energy. Only in one nucleus, ^{143}Eu, have these features been extensively studied. Two different E2 regimes have been identified [96] in this nucleus: (1) a very intense (~50%) "E2 bump", which is interpreted as being due to damped rotational transitions and (2) an intense ridge structure (~2%), which corresponds to the 2D correlation pattern from unresolved transitions that form excited discrete bands. Lifetime measurements at EUROBALL have firmly established their super-deformed nature [97]. A small damped continuum is seen in coincidence with the yrast super-deformed band, but no ridges are observed to feed the yrast superdeformed band. The number of discrete bands which contribute to the intensity of the ridges reflects the density of states at superdeformation, but it can also tell us something about the excitation energy at which rotational damping sets in and the magnitude of the rotational damping width. It was possible with EUROBALL to extract the number of discrete excited bands in ^{143}Eu and it was found that this number gradually decreases with spin [97] (cf. Section 4). This is well reproduced by theoretical calculations if the effect of mixing with normal-deformed states and subsequent decay-out is included in a broad spin and excitation energy range [98].
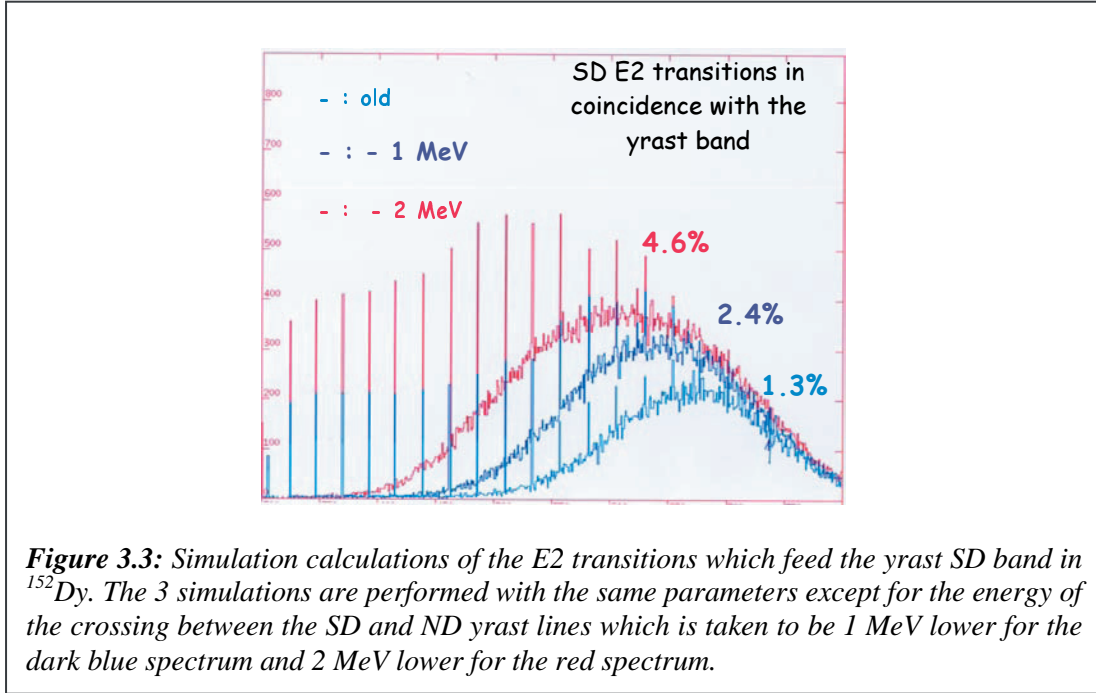
In other mass regions, there is little data available on this subject, but theoretical predictions exist and predict very different behaviours [99]. Because of the different shell structure involved in mass-190 superdeformed nuclei, the dispersion in frequency of the multi-particle

Figure 3.2: *Energy vs. spin plane showing the important parameters in the population of SD states: B(E2) and B(E1) strengths, the decay out energy E_{out}, the barrier height between SD and ND potential wells, the ND and SD yrast lines, the onset of rotational damping E_{onset} and the fission cut-off (see text for details).*

multi-hole states is considerably smaller when the spin changes by 2ℏ than in the mass-150 region. This is why a much smaller rotational damping width Γ_{rot} is predicted, with the consequence that the onset of damping, or the onset of the fragmentation of the E2 strength over many final states will occur at higher excitation energy than the configuration mixing itself. One should therefore expect to observe more discrete bands (discrete in the sense little or no spreading out of the E2 strength). In some cases, these bands may even be ergodic bands [100]: regular bands built on compound states. Theory also predicts that the number of bands should decrease at high spin because of the decrease in the height of the barrier separating superdeformed and normal-deformed states. There are preliminary GAMMASPHERE results on this subject, but only a high-statistics experiment (as was recently performed with EUROBALL to study ^{192}Hg) will allow a detailed investigation of the feeding properties of the superdeformed nucleus as a function of temperature and spin.

The properties of the gamma flow in the second well depend on the energy vs. spin (E,I) landscape, which is drawn schematically in Figure 3.2. E2 transitions associated with superdeformed states can only exist between the superdeformed yrast line and the decay-out energy (E_{out}). This region is further divided by the onset energy of damping (E_{onset}); below E_{onset}, superdeformed states form regular rotational bands and above it, states decay by E2 transitions characteristic of the superdeformed shape, but the strength is fragmented over many final states. Where the flow will go and how much of it actually feeds into the yrast line will depend on the initial (E,I) distribution of the compound nucleus, on the magnitude of the B(E2) and B(E1) strengths at super- and normal deformation and on the relative positions of all the lines drawn in Figure 3.2, especially the relative position of the superdeformed and normal-deformed yrast lines.

Recently, the yrast band in ^{152}Dy has been linked [101] into the rest of the level scheme of ^{152}Dy and it turns out that the crossing point between the normal-deformed and super-deformed yrast lines is 1 MeV and 10ℏ lower than previously thought. This has a dramatic influence on the simulation of the population of superdeformed (yrast and excited) and

Figure 3.3: *Simulation calculations of the E2 transitions which feed the yrast SD band in* ^{152}*Dy. The 3 simulations are performed with the same parameters except for the energy of the crossing between the SD and ND yrast lines which is taken to be 1 MeV lower for the dark blue spectrum and 2 MeV lower for the red spectrum.*
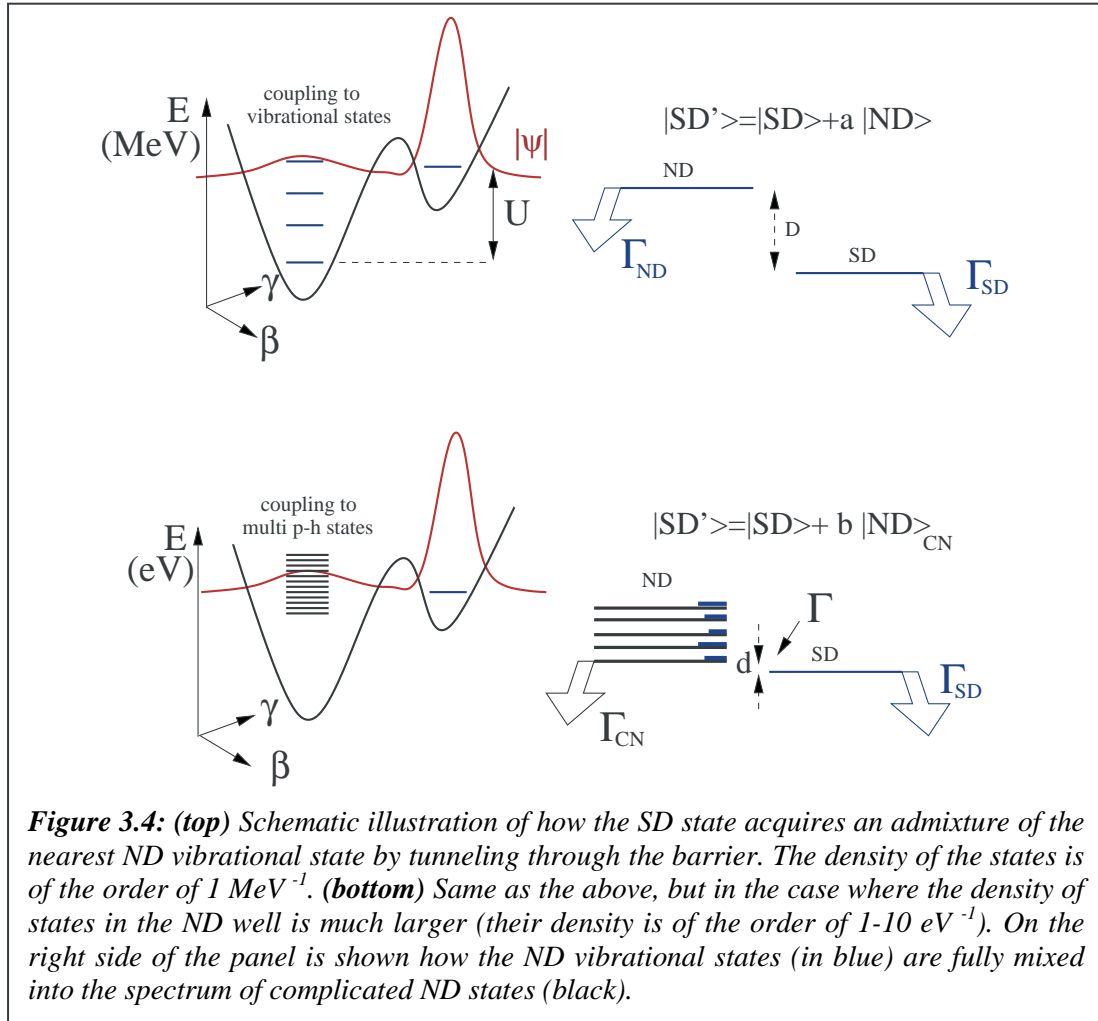
normal-deformed states. Indeed, as is shown in Figure 3.3, given a set of simulation parameters, if the superdeformed yrast line is lowered by 1 MeV, the population of the yrast superdeformed states increases from 1.3 to 2.4% and the superdeformed continuum (which is made up of damped transitions and the projection of the ridges) grows and is shifted to lower spin (the profile of the yrast band also moves down by 4 ħ). A similar increase in intensity and a shift to lower spin occur when the excitation energy of the crossing point is lowered by another 1 MeV.

Much has been learnt on the different stages of the feeding of superdeformed states using EUROBALL, but it is clear that in order to understand the important parameters of the population process, one must first have a better knowledge on the decay-out properties of the superdeformed yrast states.

3.3. Decay from superdeformed states

The decay out of superdeformed bands is due to the coupling between superdeformed and normal-deformed states. The coupling or tunneling occurs in collective coordinate space by quadrupole couplings between the different configurations along the path between the superdeformed and normal-deformed minima. If the excitation energy of the superdeformed state is low, it will couple to the closest lying collective normal-deformed state and acquire an admixture of such a normal-deformed state (see Figure 3.4, top panel). This can be calculated in a fully microscopic way going beyond the mean field in order to take into account correlations and fluctuations (GCM approach [102]). The resulting state has then a partial E2 width (Γ_{SD}) to decay to the next superdeformed state and a partial width (Γ_{ND}) to decay out of the band, down to low energy normal-deformed states.

If, on the other hand, the excitation energy is such that the collective states (often called doorway states) on the normal-deformed side are fully mixed into a dense sea of very complicated multi-particle multi-hole excitations, and if the coupling is weak, the
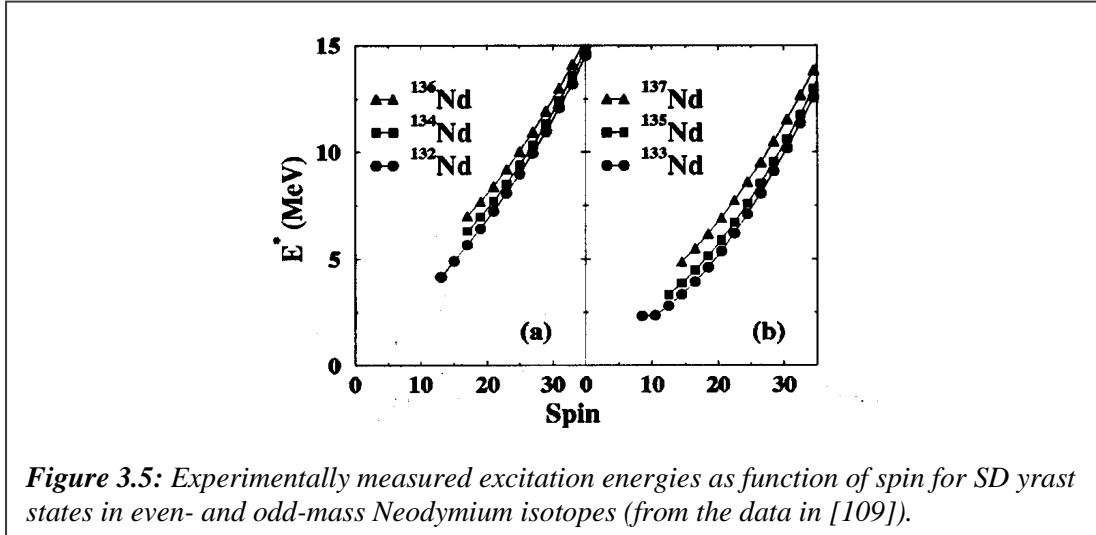
Figure 3.4: (top) *Schematic illustration of how the SD state acquires an admixture of the nearest ND vibrational state by tunneling through the barrier. The density of the states is of the order of 1 MeV^{-1}. (**bottom**) Same as the above, but in the case where the density of states in the ND well is much larger (their density is of the order of 1-10 eV^{-1}). On the right side of the panel is shown how the ND vibrational states (in blue) are fully mixed into the spectrum of complicated ND states (black).*

superdeformed state will couple to the closest compound state which has a statistical decay width (Γ_{CN}) to decay down to low energy normal-deformed states (see Figure 3.4, bottom panel). This other extreme decay-out scenario can be calculated using micro-macroscopic models combined with statistical approaches [103,98].

Excitation energy of superdeformed states

One can unambiguously determine the absolute energy, spin and parity of superdeformed states by identifying directly connecting pathways from the superdeformed state to known normal-deformed states. However, only a handful of superdeformed bands have been connected to the low-lying normal-deformed states. This is because in most of the cases, the density of final states for the decay is very large. The decay is consequently highly fragmented and the transitions, which directly connect superdeformed states to low-lying normal-deformed states, are high-energy γ-rays. It is therefore a difficult experimental task to observe these single-step links since their signal corresponds to ~10^{-4} of the reaction channel, not counting the reduced γ-ray efficiency at high energy and possible chaotic effects.

But in some cases nature is kind and the differences in configuration between superdeformed and normal-deformed states can be less pronounced and the excitation energy of super-deformed states smaller. This is the case of the Neodymium isotopes. The yrast super-deformed bands in $^{132-137}$Nd have all been connected to the corresponding normal-deformed level scheme [104-108]; the most recent case, ^{136}Nd, was studied at EUROBALL [109]. As is

Figure 3.5: *Experimentally measured excitation energies as function of spin for SD yrast states in even- and odd-mass Neodymium isotopes (from the data in [109]).*

shown in Figure 3.5, the excitation energies of superdeformed states in six Nd isotopes are known as a function of spin. The value of the observed decay-out intensity is 100, 50 and 20% for ^{132}Nd, ^{134}Nd and ^{136}Nd and 100, 65 and 30% for ^{133}Nd, ^{135}Nd and ^{137}Nd, respectively. This decrease is related to the increase in the excitation energy of the superdeformed bands with neutron number: as N approaches 82, deformed structures are getting more costly in energy. Also, the excitation energy is systematically higher in the even systems than in the odd ones. This is related to the nature of the superdeformed configuration, which is two quasi-particle in the even cases and one quasi-particle in the odd cases.

From these data it was possible to extract the neutron pairing gap in the superdeformed well of Nd nuclei [109,110]: In the independent quasi-particle picture, and with some assumptions on the contribution of rotation to the excitation energy of the six superdeformed nuclei, one can relate the odd-even mass difference at spin I to an average neutron pairing gap Δ_n. The values of Δ_n plotted in Figure 3.6 for superdeformed matter are mean values extracted within the spin range of the bands. The error bars are large (~50%) due to the approximations made and the uncertainties in the mass values. It is expected that Δ_n should be reduced because of the blocking effect of the quasi-particles. This is estimated to be a 20% effect, but here the

Figure 3.6: *Experimental neutron pairing gaps Δ_n extracted from the odd-even mass difference of ND and SD Neodymium isotopes.*
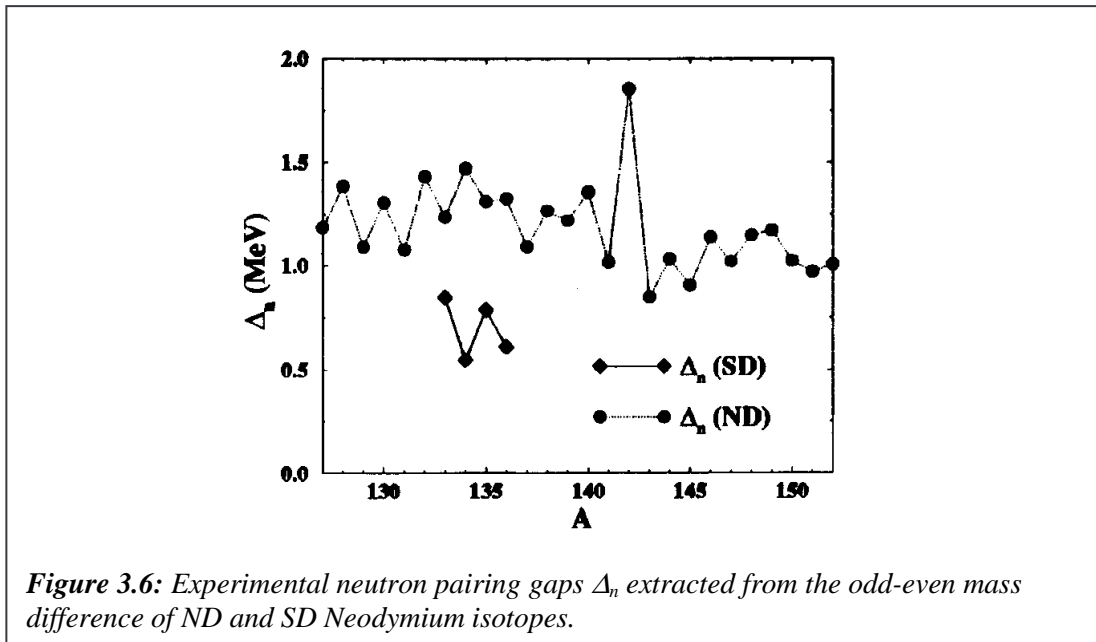
quenching is stronger. Pairing correlations are therefore reduced but the most important result is that they still exist in mass-130 superdeformed nuclei at relatively high spins.

Coupling between superdeformed and normal-deformed states

Another new result concerning the decay out comes from the triaxial superdeformed bands in ^{163}Lu. The yrast superdeformed states (band TSD1) to which the excited, so-called "wobbling" band [58] decays have been connected to the lower lying states [72]. In fact, there is a very strong interaction between the superdeformed state and a neighbouring normal-deformed state at spin $21/2\hbar$. The superdeformed $21/2^+$ state acquires a small admixture of the normal-deformed $21/2^+$ state and vice versa. As can be seen in Figure 2.5 (cf. Section 2), the superdeformed transition $25/2^+ \rightarrow 21/2^+$ is actually split into two transitions of 315 and 427 keV, respectively. The normal-deformed and superdeformed $21/2^+$ states will be fed from the $25/2^+$ superdeformed state proportionally to their squared superdeformed amplitudes, α^2 and $(1-\alpha^2)$ respectively. From the experimental intensity and B(E2) ratios, a value of ~ 4 % was extracted for α^2. This is of the order of what one obtains in the mass 190 and 150 regions assuming a statistical decay. The unperturbed energies of band TSD1 can then be derived and the dynamical moment of inertia recalculated.

Figure 3.7 shows the moments of inertia using the experimental energy differences between 2 consecutive transitions (filled circles) and the energy differences, which result when the level shift due to the mixing at spin $21/2\hbar$ is removed (open circles). As in the ^{133}Nd case, the irregularities of the moment of inertia disappear. The interaction strength between the superdeformed and normal-deformed states is large (22 keV). Similar values are found in the Nd isotopes. In mass 150 and 190 nuclei this interaction is estimated to be of the order of 1 to a few eV. This is because the difference between normal-deformed and superdeformed configurations is much larger and many more particles have to be rearranged to go from one configuration to the other.

This rearrangement of particles involved in the decay-out process is also nicely supported by the observations of "scaled" decay-out strengths in ^{58}Cu [111] (cf. Section 7). Indeed, the E2 strengths of the 830, 1519 and 4171 keV transitions depopulating the (11^+) second minimum state in ^{58}Cu scale as 0.1^N; N=0,2,4 being the number of particle-hole excitations which are to
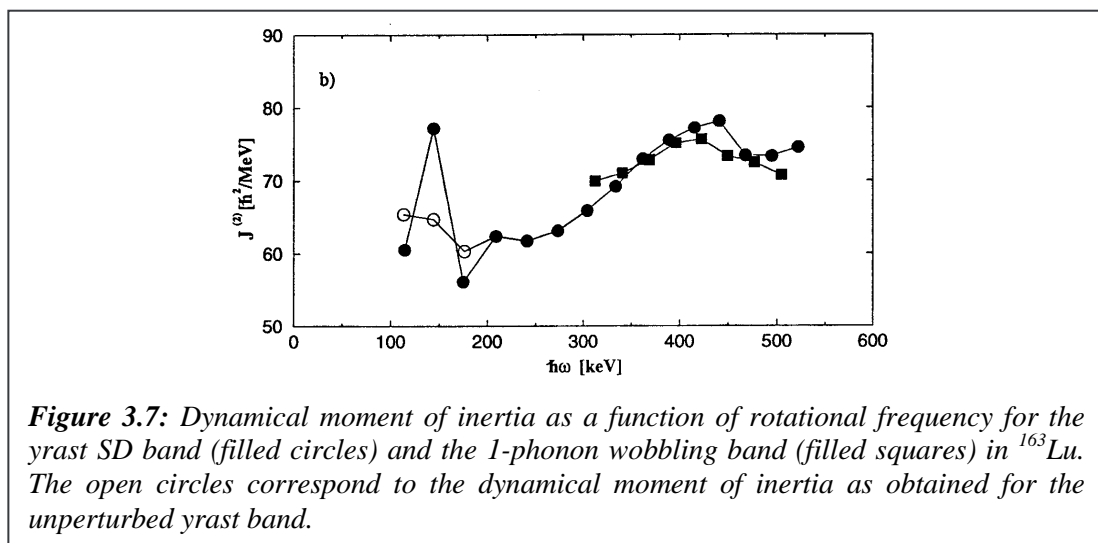
Figure 3.7: Dynamical moment of inertia as a function of rotational frequency for the yrast SD band (filled circles) and the 1-phonon wobbling band (filled squares) in ^{163}Lu. The open circles correspond to the dynamical moment of inertia as obtained for the unperturbed yrast band.
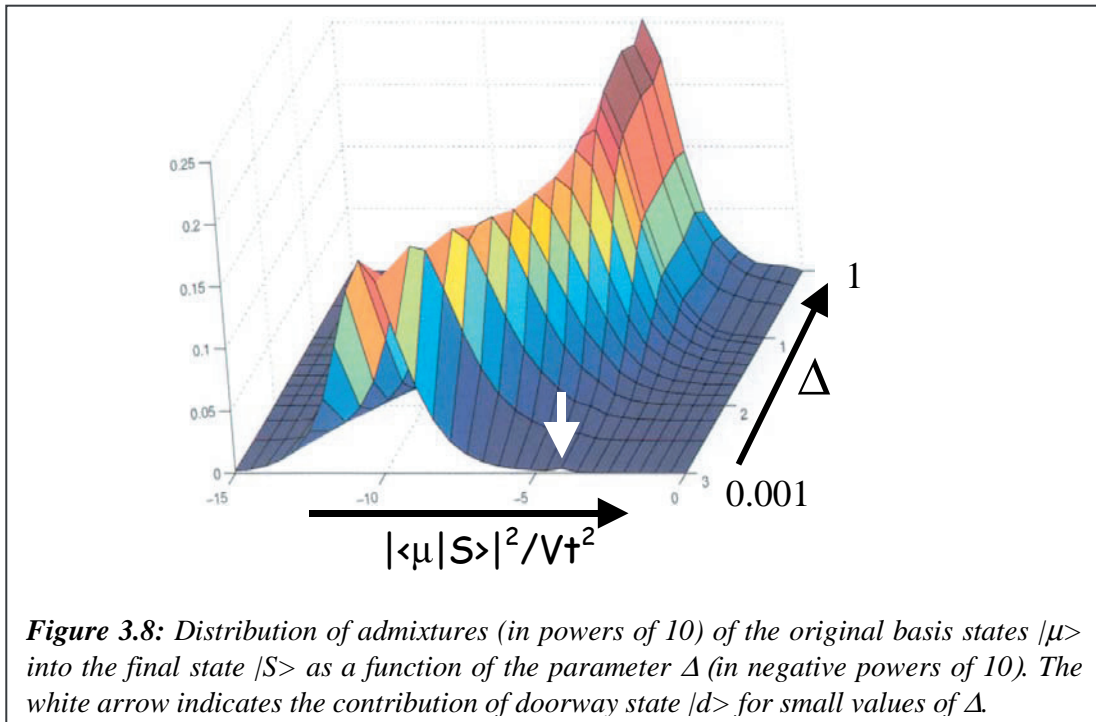
be reconfigured. The γ decay-out strengths are based on lifetime measurements of individual states, which were performed for the first time in the A=60 mass region using EUROBALL.
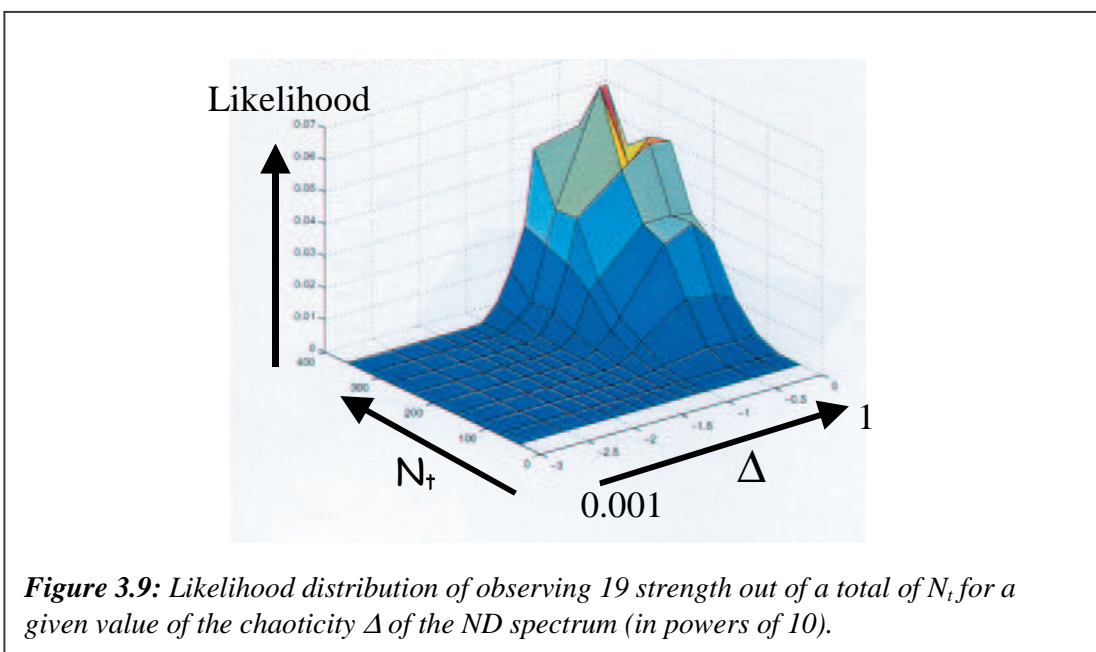
Primary decay-out strength distribution

In the cases where the excitation energy of the superdeformed nucleus and the density of normal-deformed states at the point of decay are very large, the superdeformed state couples to the nearest compound state and the decay-out should be typical of the decay of a hot compound state. It should be made up of a broad bump corresponding to the pileup of primary and secondary and may be tertiary transitions leading the nucleus down to the yrast states, the yrast transitions and the single-step links which sit close to the endpoint of the spectrum. As in the neutron resonance case [112], the primary transition strengths should follow a χ^2 distribution with $\nu=1$ degree of freedom, often called Porter-Thomas distribution [113]. This is a direct consequence of random matrix theory and more specifically, it reflects the properties of the Gaussian Orthogonal Ensemble of matrices (GOE). This gives rise to very strong strength fluctuations which could be the reason why single-step links are sometimes enhanced and can be observed experimentally. This is the case in ^{194}Hg, for which strong high-energy links have been identified [114,25] while in the neighbouring ^{192}Hg, studied with similar statistics, no such lines could be observed.

In order to verify that the enhancement of the strengths in ^{194}Hg is due to Porter-Thomas fluctuations, a study of the primary strength distribution was performed [115]. The aim was to determine which χ^2 distribution of ν degrees of freedom and average strength θ could best fit the experimental strengths ω_i above the experimental strength threshold ω_{low}. The result for the most likely χ^2 distribution is the following: $\nu=1$ and θ is found to be nearly 4 times smaller than the experimental strength threshold. The uncertainty on ν is very large because only the high-strength tail of the distribution is accessible experimentally and this is a strength domain for which there is not a pronounced difference between χ^2 distributions. In other words, only the strongest 19 strengths are observed, whereas a fluctuation analysis in the same energy range tells us there should be ~600 (primary) transitions.

In order to apply this method, more primary γ-rays need to be identified. This can be done in the cases where the phase space for the decay-out transitions is more favourable and the primary lines more intense. The problem, however, in dealing with χ^2-distributions is that only the $\nu=1$ distribution has a well-defined meaning. In order to overcome this problem, a formalism developed by Sven Åberg [116] was used. This method introduces a "chaoticity" parameter and since it is no longer analytical, it requires simulations. The spectrum of normal-deformed states is constructed from a GOE matrix of size N. One of the basis states $|\mu\rangle$ is special since it can couple to the superdeformed state. This state is named $|d\rangle$ for doorway. The off-diagonal elements of the matrix, which govern the mixing between the normal states, are scaled with a parameter Δ ($0 \leq \Delta \leq 1$). After a first diagonalisation procedure, the superdeformed state $|SD\rangle$ is included together with its coupling V_t to the doorway state and another diagonalisation is carried out. When the parameter Δ is 0, the ND states do not interact with each other and the superdeformed state can only acquire an admixture of the doorway state. When Δ is equal to 1, the normal-deformed spectrum is fully mixed, the doorway state has dissolved among all the normal-deformed states and since the coupling V_t is weak, one of the final states $|S\rangle$, which has a predominant superdeformed component, will include many small admixtures of the original normal-deformed states $|\mu\rangle$.

Figure 3.8: *Distribution of admixtures (in powers of 10) of the original basis states |μ> into the final state |S> as a function of the parameter Δ (in negative powers of 10). The white arrow indicates the contribution of doorway state |d> for small values of Δ.*

In the plot of the distribution of these admixtures into the final state $|S\rangle$ as a function of Δ (Figure 3.8), it is immediately clear what is meant by "chaos-assisted tunneling". At small Δ, the admixture into $|S\rangle$ is mostly due to the doorway state at an arbitrary value of 10^{-5}. At Δ = 1, all the N basis states will contribute on average with one admixture of that order: the admixture of normal-deformed states into the superdeformed state is ~N times larger in the chaotic limit than in the ordered limit. To proceed further, the conjecture is that admixtures can be viewed as strengths. N_s simulations are carried out. For each simulation, N_t strengths are randomly chosen. Out of these N_t strengths, the N_o strongest (o for observed as in the experiment) are selected.

Figure 3.9: *Likelihood distribution of observing 19 strength out of a total of N_t for a given value of the chaoticity Δ of the ND spectrum (in powers of 10).*

The smallest of these N_o strength is then equivalent to the experimental strength threshold and all the strengths are normalised to it. As in the χ^2 case, the likelihood that the 19 experimental strengths correspond to 19 strengths sampled from a total of N_t, given a value of Δ can be plotted. In Figure 3.9 the preliminary results for the ^{194}Hg nucleus are shown. Each point in the plot corresponds to the average of 500 different GOE matrices of size 400 and subsequent diagonalisations and the strength threshold is given by the observation of 19 strengths. The likelihood to observe 19 strengths is peaked when the total number of primary strengths is larger than 200 and when Δ is larger than 0.1. This is in agreement with the measurement of 600 primary lines in the transition energy range from 2.6 to 5 MeV and with the result of the most likely χ^2 distribution. It therefore appears highly probable that the decay-out in ^{194}Hg is a statistical process and that the normal-deformed states to which the superdeformed states couple to at 4.2 MeV above yrast are compound states.

3.4.   Conclusion

Excited states within a superdeformed well provide opportunities to investigate many intriguing nuclear structure aspects: a transition from ordered motion along the superdeformed yrast line to chaotic motion above, perhaps through an ergodic regime; the robustness of collectivity with increasing excitation energy and spin and the largely-unexplored feeding mechanism of superdeformed bands. A very extensive study of superdeformed excited states has been carried out in ^{143}Eu and a clear picture of the feeding process in this nucleus is emerging. Theoretical calculations predict different phenomena in other mass regions and experiments to study mass 190 and 150 nuclei have recently been performed and are still being analysed.

Concerning the decay-out, most bands are still not connected to the low-lying levels. This is because experiments are at the very limits of what present arrays can do. In the few cases where quantum numbers have been measured for superdeformed states, information on binding energies and pairing in the second minimum has been extracted as well as values for the interaction strength between superdeformed and normal-deformed states. The decay-out is also a tool to study the nature of normal-deformed states in a large (E,I) domain and methods have been developed to exploit this. Finally, and this was not mentioned, considerable effort has been done at EUROBALL to study the conversion-electron and possible E0 decay-out spectrum in ^{136}Nd and ^{194}Pb. However, these experiments are very difficult and no results could be obtained so far.

The near future of γ-ray spectroscopy in the superdeformed well and its future in general look rather bright. Indeed, several experiments recently performed with EUROBALL are still being analysed and will reveal new and exciting physics. On a longer time scale, the new generation of 4π γ-ray spectrometers such as AGATA, combined with intense stable and radioactive beams, will no doubt allow us to revisit superdeformation and discover more exotic nuclear shapes.

Rotational motion in thermally excited nuclei

S. Leoni and A. Bracco

4. Rotational motion in thermally excited nuclei[*]

4.1. Introduction

The study of the nucleus at the limits of excitation energy and angular momentum is one of the central topics addressed with EUROBALL γ-spectroscopy measurements. In particular, the study of the rotational motion at finite temperature plays a crucial role in the understanding of the properties of the nuclear system beyond the mean field description, providing relevant information on the two-body residual interaction responsible for the band-mixing process.

At present, we know that, in medium mass nuclei, already at few hundreds keV excitation energy above the yrast line, rotational bands are close enough in energy to interact by residual interactions. This implies that the shell-model states occurring at low excitation energy will mix strongly, leading to complicated stationary states that no longer correspond to any simple motion, as a part of the general order-to-chaos transition that the nucleus undertakes with increasing temperature. As a consequence, due to the different response of the intrinsic states to the Coriolis and centrifugal forces, the rotational motion becomes *damped*, namely the electric quadrupole decay from a single state at spin I will be distributed over a spectrum of final states all at spin I-2, with a strength function whose width at half maximum is called the *rotational damping width* Γ_{rot} [117]. This results in quasi-continuum ridge-valley structures in γ–coincidence spectra, which are not accessible by standard discrete spectroscopy techniques. The dependence of the rotational damping width on the mass number A, the nuclear shape deformation ε, the angular momentum I and the intrinsic excitation energy U of the nucleus has been originally predicted by a schematic model [117], and lately confirmed by more realistic calculations [118].

In the last two decades considerable experimental effort has been given to the study of the rotational motion at finite temperature. Focusing on nuclei of mass A~160 the gross features have been explored in a long series of pre-EUROBALL experiments, making use of smaller arrays such as NORDBALL, GASP, EUROGAM I and II. By making use of an ad-hoc technique based on a statistical analysis of γ–γ and higher fold coincidences, it was for the first time possible to extract quantitative information from the quasi-continuum distributions [119]. In fact, the very existence of a *finite* number of γ-decay paths, below the particle binding energy, leads to enhanced fluctuations in γ-coincidence spectra (at variance from a purely statistical spectrum), whose magnitude is fixed by the number of paths. In addition, the development of cranked shell model calculations, including a two-body residual interaction allowed for a proper direct comparison between data and theory [118].

The first basic result obtained with the fluctuation analysis technique has been the direct experimental evidence for the damping phenomenon [120], earlier studied via comparison of the spectrum landscape with simulation calculations of the γ-decaying cascades only [121]. In this context, the importance of the two-body residual interaction has also been established in the onset of the damping phenomenon and in the further transition to the compound nucleus regime at higher excitation energies. The basic features of the residual interaction, such as its intensity and its dependence on the various component of the two-body force, have also been established by a comparison with experimental data concerning the number of discrete unresolved bands [118,122]. The dependence of rotational damping on the intrinsic nuclear

---

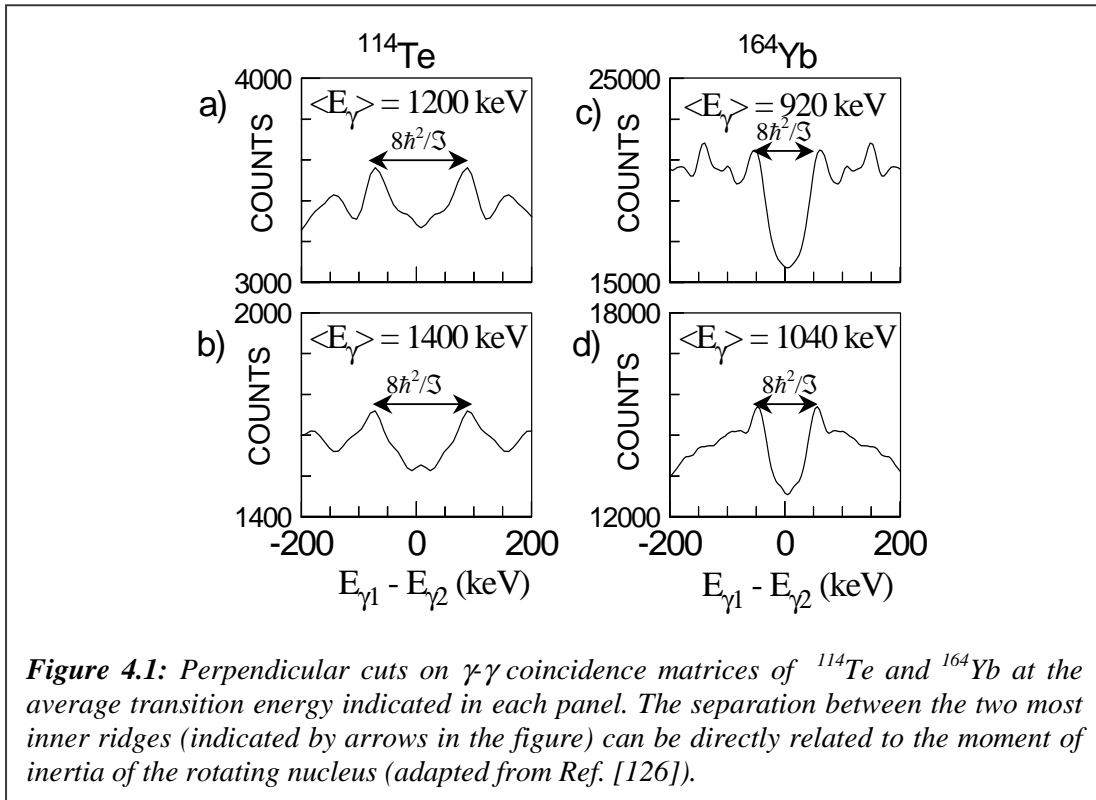[*] Contribution by S. Leoni and A. Bracco

configuration, corresponding for example to specific values of the K quantum number (e.g. high-K vs. low-K) has also been investigated to establish the degree of mixing of the various configuration in the gradual transition towards the compound nucleus regime [123]. A review of these achievements obtained in the field of warm rotation can be found in Ref. [124].

In more recent years, the study of rotational damping has been focused on the dependence on nuclear mass and deformation. This has been done making use of high statistics EUROBALL experiments concerning normal-deformed nuclei in the mass region A~110 and super-deformed nuclei in the mass regions A~140 and 160 as well as in connection with a search for the Giant Dipole Resonance built on highly deformed nuclei, as it will be discussed in the following sections.

From the discussion presented in the following it is clear that the extensive work made so far has indeed allowed to make a good progress in the understanding of the structure of warm nuclei. However, as discussed in the final section, there are still basic questions which are not fully solved, mainly related to the precise determination of the rotational and compound nucleus widths [125], and to the direct experimental observation of the GDR on superdeformed nuclei.

4.2. Mass dependence of rotational damping

One of the main achievements in the field of warm rotation, obtained with EUROBALL experiments, has been the study of the dependence of the damping phenomenon on the nuclear mass and deformation. As originally proposed in a schematic formulation of the damping model [117], the energy U_0 for the onset of rotational damping and the rotational damping width Γ_{rot} are expected to depend on the level density and on the strength of the

Figure 4.1: *Perpendicular cuts on γ-γ coincidence matrices of ^{114}Te and ^{164}Yb at the average transition energy indicated in each panel. The separation between the two most inner ridges (indicated by arrows in the figure) can be directly related to the moment of inertia of the rotating nucleus (adapted from Ref. [126]).*
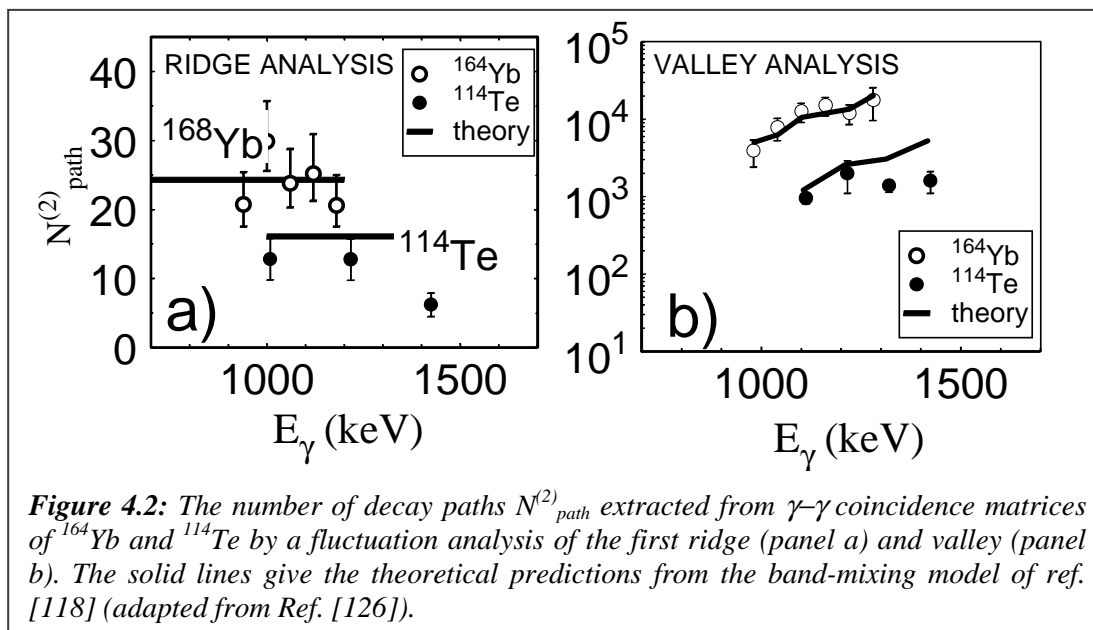
two-body residual interaction, leading to the dependences $U_0 \propto A^{-2/3}$ and $\Gamma_{rot} \propto I\, A^{-5/2}\, \varepsilon^{-1}$, with I and ε being the spin and the nuclear deformation, respectively.

The validity of the relations given above has been established by the study of nuclei with similar deformation ($\varepsilon \sim 0.25$), but with different masses, namely ^{164}Yb (A~160) and ^{114}Te (A~110). As discussed in Ref. [126], the analysis has been performed on quasi-continuum spectra, which in both cases are characterised by similar rotational pattern, forming ridge-valley structures in $\gamma-\gamma$ coincidence matrices, as shown in Figure 4.1. In particular, while the ridges are populated by unresolved discrete excited bands extending up to the onset of rotational damping, the valley region collects the contribution from the warmer region of damped rotation.

Figure 4.2 (a) shows the results obtained from the fluctuation analysis of the ridge structures observed in the $\gamma-\gamma$ coincidence spectra of ^{114}Te and ^{164}Yb, as reported in Ref. [126]. It is found that the number of paths is of the order of 25 for the typical rare earth nucleus ^{164}Yb, while it is smaller by approximately a factor of 2 in the ^{114}Te case, as it was also observed in the case of ^{112}Sn in the same mass region [127]. The solid lines in the figure represent the theoretical value for the number of discrete excited bands populating the ridge structures, as obtained from band-mixing calculations for the rare earth nucleus ^{168}Yb and for ^{114}Te [118]. It is found that the calculations, averaged over the spin interval 25-35$\hbar$, well reproduce the experimental data.

As shown in Figure 4.2 (b), the number of damped decay paths, obtained from the analysis of the valley region, is found to be much larger (of the order of 10^3-10^4), again with a significant difference between the ^{114}Te and ^{164}Yb data. The full drawn lines give the expected theoretical dependence obtained by applying the fluctuation analysis technique to numerically calculated spectra produced by the simulation code MONTESTELLA [128], which are based on calculated levels and transition probabilities for a specific nucleus, as obtained by the same band-mixing calculations used for the analysis of the ridge structures. As one sees from the figure, the calculations are found to reproduce both the ridge and the valley results quite well, giving a strong support to the band-mixing model in different regions of masses [118].

Figure 4.2: *The number of decay paths $N^{(2)}_{path}$ extracted from $\gamma-\gamma$ coincidence matrices of ^{164}Yb and ^{114}Te by a fluctuation analysis of the first ridge (panel a) and valley (panel b). The solid lines give the theoretical predictions from the band-mixing model of ref. [118] (adapted from Ref. [126]).*

The quantitative agreement between calculations and experiment, seen in Figure 4.2, strongly supports the scaling with mass number of the residual interaction and of the level density. According to the present band-mixing calculations, damping should set in around a heat energy of $U_0 \sim 0.9$-1.0 MeV in ^{114}Te, compared with $U_0 \sim 0.7$-0.8 MeV in ^{168}Yb, in rather good agreement with the scaling $U_0 \propto A^{-2/3}$, originally proposed in Ref. [117].
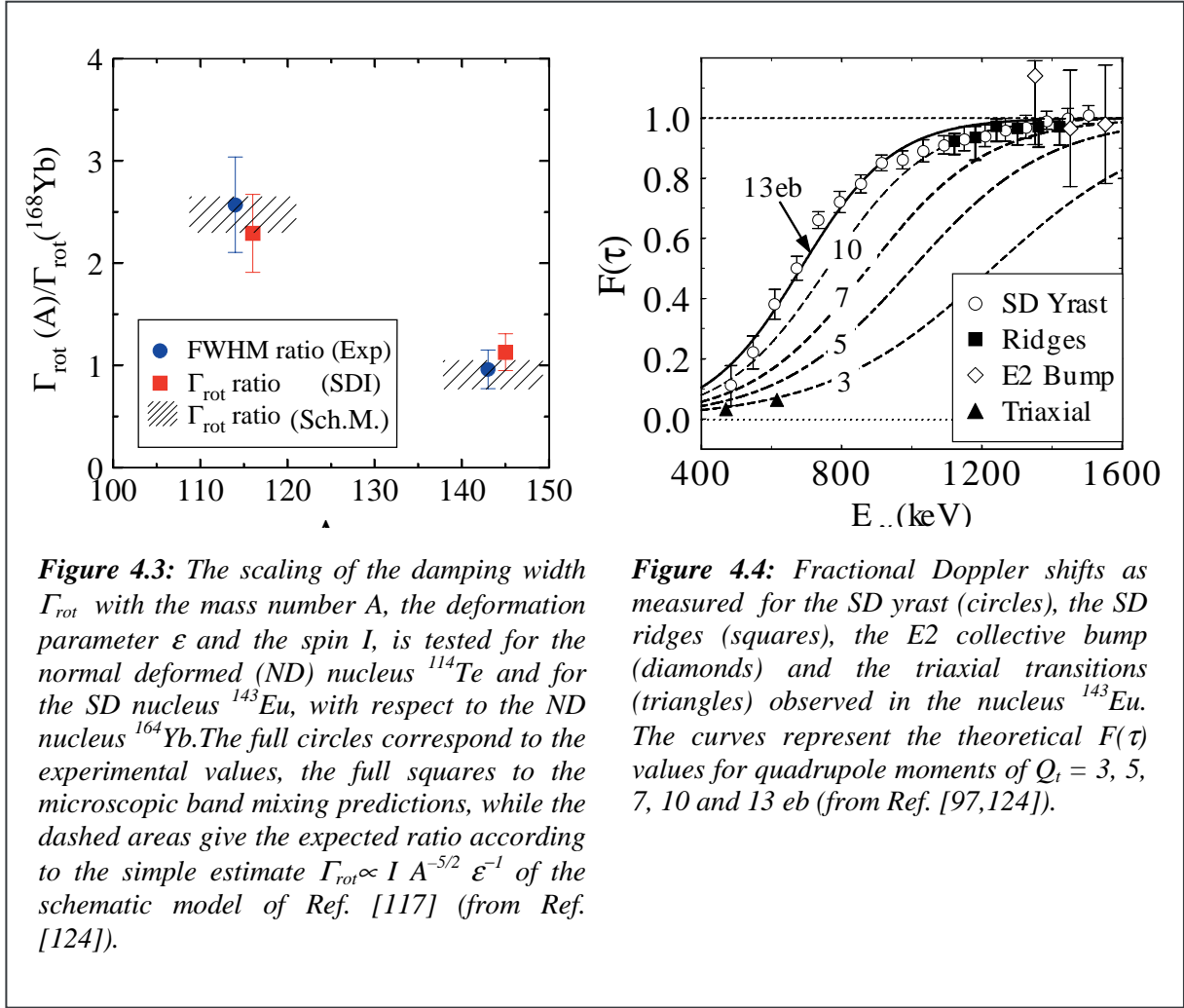
An experimental estimate of the upper limit of the rotational damping width Γ_{rot} can be inferred by measuring the width of the E2 bump constructed as a difference between single spectra at consecutive bombarding energies, as discussed in Ref. [126,127]. In such cases, since all the decays from the entry distribution contribute to the difference spectrum, and not only E2 transitions corresponding to a given $I \rightarrow I$-2 decay, the widths of the difference spectra can only be taken as an upper limit for the rotational damping width. The results obtained from such an analysis are given in Figure 4.3, where the damping width Γ_{rot} measured in the normal-deformed nuclues ^{114}Te and in the superdeformed nucleus ^{143}Eu is given relative to the corresponding value in ^{164}Yb [124]. As can be seen from the figure, consistency is found among all evaluations, supporting the dependence of the rotational damping width Γ_{rot} on the mass A, nuclear shape deformation ε and spin I, as originally predicted [117]. However, only the scaling of Γ_{rot} has been measured, but not yet the absolute value of the rotational damping width. One may conclude that the dependence of the damping mechanism on the mass and deformation can be closely tested by studying the shapes and fluctuations carried by γ-coincidence spectra produced by excited rotating nuclei.

4.3.   Superdeformation at finite temperature

In recent years, weakly populated structures of superdeformed nature, corresponding to highly elongated prolate nuclear shapes with an approximate axis ratio of 2:1, have been found in many different mass regions [14] (cf. Section 1). This has motivated many theoretical and experimental investigations, mainly aiming at the understanding of the mechanisms which allow to observe these peculiar configurations over a wide spin interval, from the fission limit down to the angular momentum region where the superdeformed yrast band rather suddenly decays into the normal-deformed states. We now know that this is due to the presence of different nuclear shapes (normal and superdeformed), which can coexist over a wide spin range, being well separated by a potential energy barrier in the deformation space. The tunneling through the potential energy barrier allows the decay-out of the superdeformed states into the normal-deformed states (cf. Section 3).

This scenario has been extensively investigated in the case of the superdeformed yrast and of the first few superdeformed excited bands experimentally observed, while much less information is available on the thermally excited rotational motion in the superdeformed well. This is because it requires not only the experimental analysis of quasi-continuum spectra connected with the superdeformed structures, but also the comparison with calculations describing both the thermally excited rotational motion and the barrier penetration effect.

The superdeformed quasi-continuum has been extensively studied in the nucleus ^{143}Eu, during a series of pre-EUROBALL and EUROBALL experiments [96,97,129]. In this case, ridge structures with a spacing corresponding to the moment of inertia of the superdeformed yrast line have been observed in the high transition energy region of γ–γ coincidence matrices, and for the first time a lifetime analysis based on the measurement of the fractional Doppler shift of the ridges has been performed [97]. As shown in Figure 4.4, the fractional Doppler shift

Figure 4.3: *The scaling of the damping width Γ_{rot} with the mass number A, the deformation parameter ε and the spin I, is tested for the normal deformed (ND) nucleus ^{114}Te and for the SD nucleus ^{143}Eu, with respect to the ND nucleus ^{164}Yb. The full circles correspond to the experimental values, the full squares to the microscopic band mixing predictions, while the dashed areas give the expected ratio according to the simple estimate $\Gamma_{rot} \propto I\ A^{-5/2}\ \varepsilon^{-1}$ of the schematic model of Ref. [117] (from Ref. [124]).*

Figure 4.4: *Fractional Doppler shifts as measured for the SD yrast (circles), the SD ridges (squares), the E2 collective bump (diamonds) and the triaxial transitions (triangles) observed in the nucleus ^{143}Eu. The curves represent the theoretical $F(\tau)$ values for quadrupole moments of $Q_t = 3, 5, 7, 10$ and 13 eb (from Ref. [97,124]).*

$F(\tau)$ measured for the ridge structures (squares) is consistent with a quadrupole moment of 10-13 eb, as obtained from the analysis of the superdeformed yrast band of ^{143}Eu, giving further support to the superdeformed nature of the unresolved discrete excited bands populating the ridges.

The superdeformed ridge structures observed in the γ–γ coincidence matrices of ^{143}Eu have been further investigated by the statistical analysis of the counts fluctuations [119,97]. This has allowed to estimate the total number of discrete (excited) superdeformed rotational bands, which can not be resolved individually due to their extremely weak population. As shown in Figure 4.5, it is found that the number of superdeformed excited discrete bands depends very strongly on the transition energy, reaching a constant value of ~30 at the highest energies, where the superdeformed ridge structure is populated. In contrast, at lower transition energies the number of superdeformed bands is found to decrease continuously, while the intensity of the ridge structure is still observed to increase. The experimental results have been compared with microscopic cranked shell model (CSM) calculation plus a two-body residual interaction for the specific nucleus ^{143}Eu [130,99]. It is found that the predicted number of discrete excited superdeformed bands reproduces the experimental data at the maximum of the distribution, while it deviates strongly at lower transition energies. This is generally expected for the lower part of the ridge structure, as a consequence of the barrier penetration into the first well.
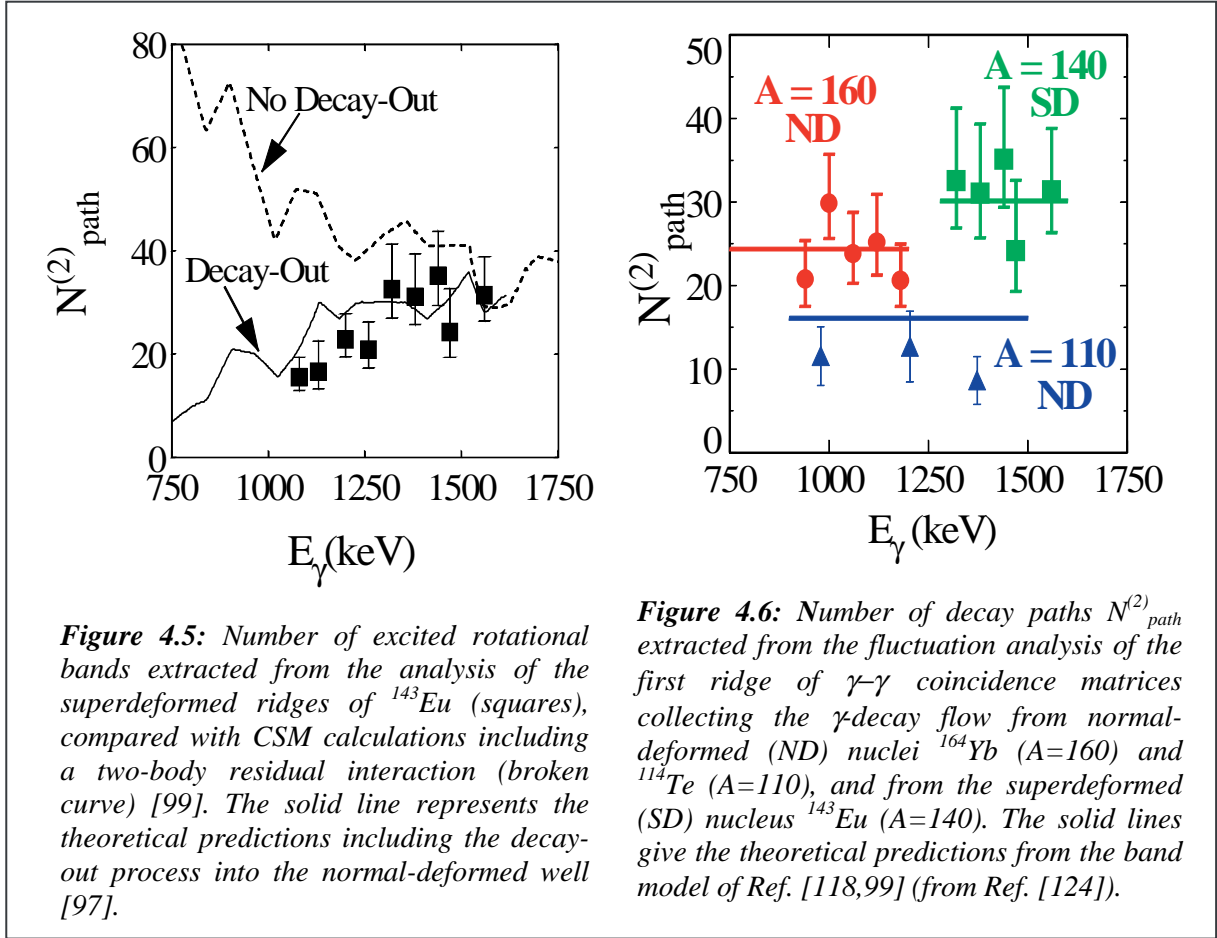
Figure 4.5: *Number of excited rotational bands extracted from the analysis of the superdeformed ridges of ^{143}Eu (squares), compared with CSM calculations including a two-body residual interaction (broken curve) [99]. The solid line represents the theoretical predictions including the decay-out process into the normal-deformed well [97].*

Figure 4.6: *Number of decay paths $N^{(2)}_{path}$ extracted from the fluctuation analysis of the first ridge of γ–γ coincidence matrices collecting the γ-decay flow from normal-deformed (ND) nuclei ^{164}Yb (A=160) and ^{114}Te (A=110), and from the superdeformed (SD) nucleus ^{143}Eu (A=140). The solid lines give the theoretical predictions from the band model of Ref. [118,99] (from Ref. [124]).*

The reduction in the measured number of excited superdeformed bands can be reproduced by the model, when the decay-out mechanism of the excited states is taken into account (solid line) [98,131]. In the model, the superdeformed states obtained by cranking calculations are coupled to normal-deformed compound states which lie energetically near, following a prescription similar to the one used in the case of the decay-out of the superdeformed yrast band. In this way, the decay-out of the excited superdeformed states is described in terms of a quantum tunneling through the potential energy barrier in the deformation space, leading some components of the normal-deformed states to be mixed into the superdeformed state. Since the normal-deformed states also have an associated electromagnetic transition probability, the superdeformed state thus mixed will have the possibility of decaying not only with rotational E2 transitions within the superdeformed well, but also with γ rays feeding to the normal states, thereby giving rise to the decay-out into the normal-deformed well.

One can then conclude that the satisfactory agreement between the data and the number of superdeformed bands predicted by the microscopic calculations, including also the decay-out mechanism, not only provides a clear evidence for the tunneling process in the thermally excited nucleus, but also gives a further support to the validity of the band-mixing model, which is found to properly describe the thermally excited rotational motion in different regions of mass and deformation. This is clearly illustrated in Figure 4.6 where the number of superdeformed bands of ^{143}Eu, measured in the transition energy region not affected by the decay-out process (e.g. 1300 keV < E_γ < 1600 keV) is compared with the band-mixing model predictions, together with similar results for normal-deformed nuclei of mass A~110 and 160.
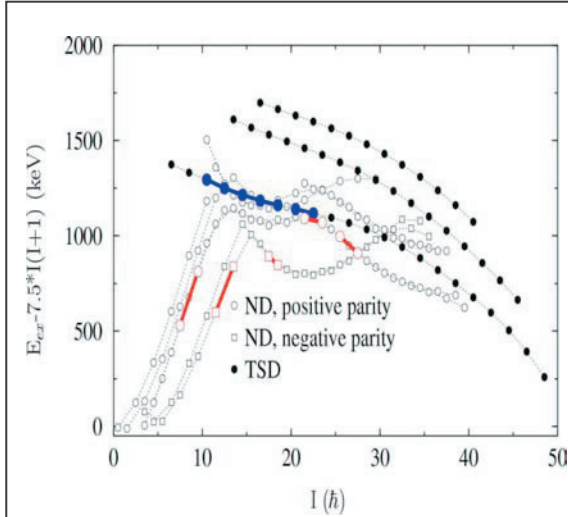
Figure 4.7: *Excitation energy relative to a rigid rotor for selected normal deformed (ND) and triaxial superdeformed (TSD) bands in [163]Lu. The transitions used for creating the gated matrices are marked by a solid line together with larger symbols for the initial and final states [90].*
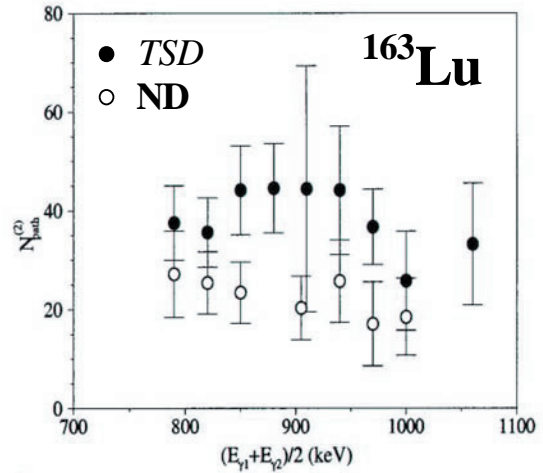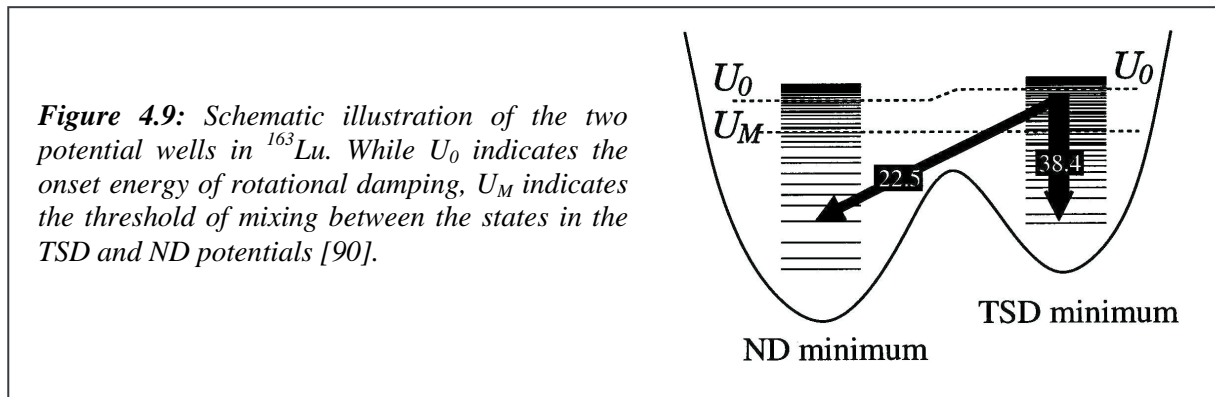
Figure 4.8: *Number of two-step paths along the TSD ridge of [163]Lu, as obtained from the fluctuation analysis of the TSD gated matrix (filled circles) and ND gated matrix (open circles) [90].*

The triaxial superdeformed nucleus [163]Lu has also offered the possibility to study the excited rotational motion in a strongly deformed well. According to theoretical predictions based on the modified oscillator potential, local minima in the potential energy surface are expected at deformation $\varepsilon \sim 0.4$, with a triaxiality parameter $\gamma \sim \pm 20^o$. These predictions have been recently confirmed in a series of EUROBALL experiments (cf. Section 2), by the observation of one and two-phonon excitations, which are the first firm experimental evidence for a stable triaxial deformation in nuclei [58,60].

The properties of this nucleus at excitation energies above the energies of the resolved triaxial superdeformed discrete bands have been investigated by a fluctuation analysis [90]. In order to study the onset of damping in this triaxial superdeformed nucleus and to learn more about the mixing mechanisms between excited triaxial superdeformed states and normal-deformed states, γ–γ coincidence matrices gated by normal-deformed (ND) and TSD yrast transitions have been constructed. In particular, as shown in Figure 4.7, the transitions used as ND gates have been carefully selected in order to avoid any contaminants from the strongly populated TSD band, which is observed to decay-out into the normal-deformed well at lower spins as compared to the ND gates.

It is found that a similar ridge structure, with a spacing corresponding to the moment of inertia of the TSD yrast band, is present in both γ–γ coincidence matrices gated by ND and TSD configurations, although no sign of the strongly populated TSD yrast is observed in the ND gated matrix. Figure 4.8 shows the number of discrete unresolved bands populating the TSD ridge, obtained by the fluctuation analysis of the TSD and ND gated matrices. While for the TSD ridge the average number of bands is ≈ 40, the number of paths extracted from the ND gated matrix is almost a factor of 2 lower.

In order to explain these experimental findings, it has been suggested that about fifty percent of the TSD paths feed into the normal-deformed potential well, due to a mixing between the unresolved states in the two minima at excitation energies right below the onset of damping, but still above a certain energy U_M, where mixing sets in and induces a cross-talk between the potential wells. As schematically illustrated in Figure 4.9, at lower excitation energy, the potential barrier is most probably too large, and the bands closer to the TSD yrast states stay in the TSD well. Therefore, when they finally decay into the normal-deformed well it happens at such a lower angular momentum that the decay cascades bypass the ND gates used. Alternatively, the observed types of decay-paths may not originate from the same states, and this possibility could be investigated by a covariance analysis on experimental data with a better statistics [132].

Figure 4.9: *Schematic illustration of the two potential wells in ^{163}Lu. While U_0 indicates the onset energy of rotational damping, U_M indicates the threshold of mixing between the states in the TSD and ND potentials [90].*
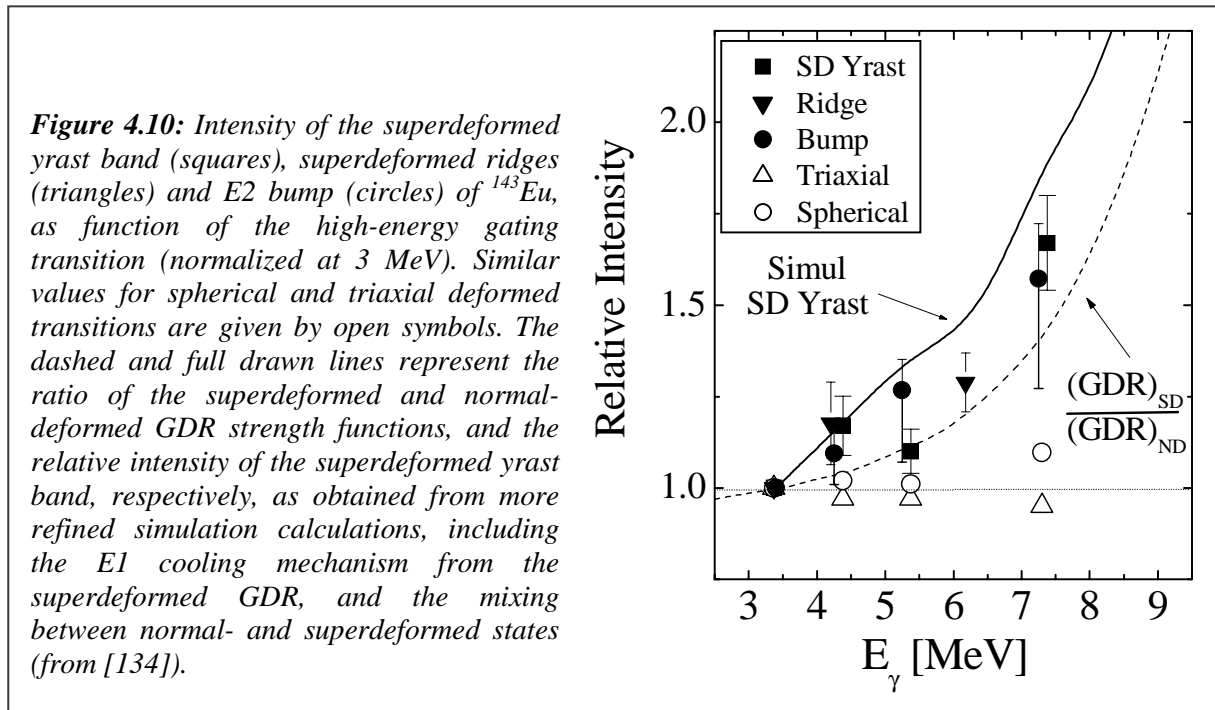
In conclusion, the study of the excited rotational motion in the superdeformed well is found to provide valuable information on the mixing between normal and superdeformed states, leading to the tunnelling process through the potential energy barrier between the two minima. However, several open questions concerning the coupling between the different configurations still remain, calling for better statistics experiments with the next generation of Ge detector arrays.

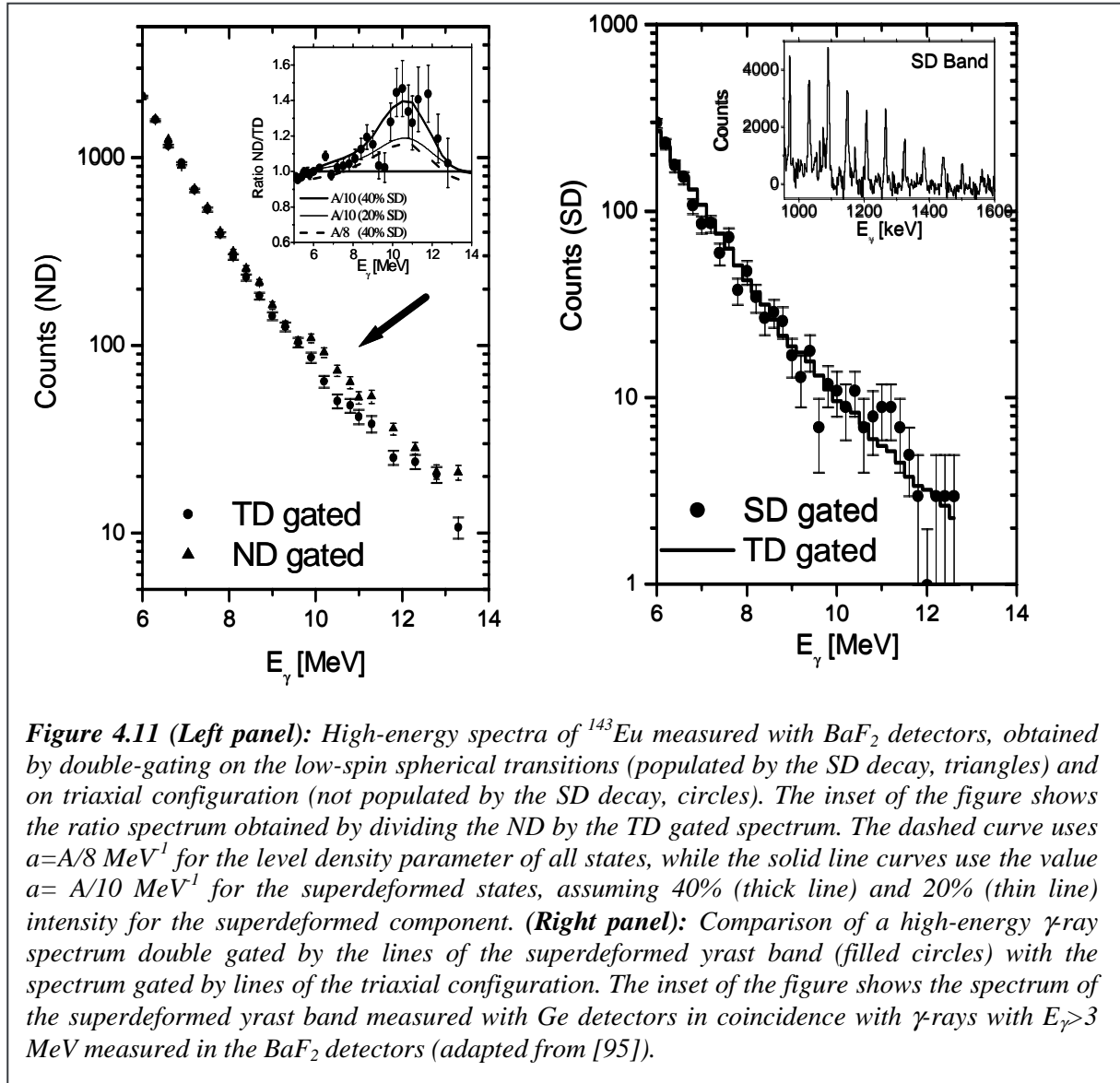## 4.4. Role of E1 feeding in the population of the superdeformed states

The study of the quasi-continuum in the superdeformed nucleus ^{143}Eu has also been an essential tool for the understanding of the feeding mechanism of superdeformed states. In fact, one of the outstanding problems in superdeformation is the understanding of the population of such structures (in particularly the yrast one) which, at the highest spins, are found to be one order of magnitude larger than in normal-deformed nuclei. To explain this finding it has been proposed that the cooling of the residual nucleus by statistical E1 transitions could be an important mechanism leading to the population of the superdeformed states [93]. This is due to both the shape of the giant dipole resonance (GDR) built on a superdeformed configuration (which is expected to display a low-energy component around 8-10 MeV excitation energy above yrast) and to the lower level density of the superdeformed states [133]. Although several attempts have been made in the last decade to find experimental evidence for the E1 feeding of superdeformed states, no conclusive answer could be given to the problem, mainly due to the experimental limitations.

In the ^{143}Eu experiment, previously discussed in connection with the analysis of the rotational quasi-continuum, the EUROBALL array was combined with 8 large-volume BaF$_2$ scintillation

detectors from the HECTOR array, for the measurement of high-energy γ–rays [95]. This made it possible to investigate the effect of the E1 population of the superdeformed states through the γ-decay of the GDR built on a superdeformed nucleus, by measuring the relative intensity of the superdeformed band, of the ridge structure and of the E2 bump at different values of the gating high-energy γ rays. As shown in Figure 4.10, the relative intensities of the super-deformed yrast band (squares), of the superdeformed ridges (triangles) and of the E2 bump (circles) are found to rapidly increase with the high-energy gating transition, following the ratio between the superdeformed GDR strength function and the spherical one (dashed line). This is also consistent with the expected behaviour from simulation calculations of the γ–ray cascades, including the E1 cooling mechanism from the GDR built on a superdeformed nucleus and the mixing process with the normal-deformed states (full drawn line). In contrast, the relative intensities of less-deformed configurations also observed in [143]Eu (represented by the open symbols) do not show any sensitivity to the high-energy condition. One may conclude that the enhanced feeding of the superdeformed structures consistently shows the important role played by the E1 emission from the GDR built on superdeformed states in the population of such highly deformed shapes.

Figure 4.10: *Intensity of the superdeformed yrast band (squares), superdeformed ridges (triangles) and E2 bump (circles) of [143]Eu, as function of the high-energy gating transition (normalized at 3 MeV). Similar values for spherical and triaxial deformed transitions are given by open symbols. The dashed and full drawn lines represent the ratio of the superdeformed and normal-deformed GDR strength functions, and the relative intensity of the superdeformed yrast band, respectively, as obtained from more refined simulation calculations, including the E1 cooling mechanism from the superdeformed GDR, and the mixing between normal- and superdeformed states (from [134]).*

In the same EUROBALL experiment it was also attempted to measure directly the GDR built on the superdeformed configuration. The nucleus [143]Eu represents a favourable case in this respect since it shows particular features, which should make the search for the γ-decay of the GDR built on a superdeformed shape more favourable by selecting cascades that populate yrast and excited superdeformed states. In fact, it was found that both the superdeformed yrast band and the excited superdeformed states of the E2 continuum follow decay routes leading to the population of spherical low-spin states only [96]. This is a consequence of the higher potential energy barrier between the superdeformed and the triaxial minimum. This feature of the superdeformed structures of [143]Eu can be exploited to search for the γ-decay of the GDR built on superdeformed nuclei in spectra gated by spherical low-spin transitions. In fact, since these transitions collect a large fraction of the entire superdeformed flux (and not

Figure 4.11 (Left panel): *High-energy spectra of ^{143}Eu measured with BaF$_2$ detectors, obtained by double-gating on the low-spin spherical transitions (populated by the SD decay, triangles) and on triaxial configuration (not populated by the SD decay, circles). The inset of the figure shows the ratio spectrum obtained by dividing the ND by the TD gated spectrum. The dashed curve uses a=A/8 MeV^{-1} for the level density parameter of all states, while the solid line curves use the value a= A/10 MeV^{-1} for the superdeformed states, assuming 40% (thick line) and 20% (thin line) intensity for the superdeformed component. (Right panel): Comparison of a high-energy γ-ray spectrum double gated by the lines of the superdeformed yrast band (filled circles) with the spectrum gated by lines of the triaxial configuration. The inset of the figure shows the spectrum of the superdeformed yrast band measured with Ge detectors in coincidence with γ-rays with E$_\gamma$>3 MeV measured in the BaF$_2$ detectors (adapted from [95]).*

only from the yrast band), the high energy γ-ray spectrum gated by these lines should provide a stronger signal than in the spectrum gated by the superdeformed yrast band only.

The left panel of Figure 4.11 shows high-energy spectra measured in the BaF$_2$ detectors requiring either double gates on spherical (ND) low-spin transitions (populated by the super-deformed flux, triangles) or double gates on triaxial (TD) configurations (*not* populated by the superdeformed states, circles). As shown by the arrow, an excess yield is observed in the ND-gated spectrum in the region 9 – 12 MeV, where one expects to find the low-energy component of the superdeformed Giant Dipole Resonance. This excess can be better seen in the ratio spectrum between the ND- and TD-gated spectra, as shown in the inset of the figure. The intensity excess is found to be rather small (being in average 20%) in agreement with simple statistical model calculations based on a modified version of the CASCADE code (see figure caption for more details).

In the right panel of Figure 4.11 is also shown an attempt to measure the GDR strength function directly gating on the superdeformed yrast band (shown in the inset). As one can see from the figure, in spite of the rather poor statistics of the SD-gated spectrum, one cannot rule out the presence of an excess yield in the same region as observed in the left part of Figure

4.11. Further experimental confirmations are however necessary in other regions of mass, aiming also at a direct gate on superdeformed yrast lines, which will benefit from more powerful Ge detector arrays such as AGATA.

4.5. The double giant resonance in fusion-evaporation reactions

The interest in the study of the double giant resonance state is related to the search of the phonon-phonon interaction and anharmonic effects in nuclear collective modes. A relevant aspect to be investigated is the possible dependence of the anharmonicity on the nuclear temperature and its correlation with the parameters characterizing the double giant dipole resonance (DGDR) state.

The available experimental data about the DGDR are related to the resonance built on the ground state. A way to study temperature effects on this two phonon state is to use fusion-evaporation reactions. However, the first step in this search is a characterisation of the DGDR events which requires the measurement of two coincident high energy γ-rays (with $E_\gamma > 8$ MeV). The emission of two coincident energetic γ-rays has been observed in the reaction ^{37}Cl $+ ^{120}$Sn at the bombarding energy of 187 MeV and using the EUROBALL array [135]. It has been found that the shape of the γ-ray spectrum obtained by requiring a coincidence with a second photon having energy in the range $E_\gamma = 6\text{-}20$ MeV is roughly accounted by statistical model predictions.

The attribution of events from the decay of the double giant dipole resonance state relies on the fact that the multiplicity of these events is larger than the estimated upper limits for the emission of two uncorrelated photons in the same deexcitation cascade. From these indications obtained with the EUROBALL experiment it is clear that any further investigation on the temperature effects in multi-phonon states requires the use of a detector system with better high-energy response and suppression of neutron events. In addition, an implementation in the statistical model codes of the excitation and decay of the DGDR is necessary for the interpretation of the data.

4.6. Future Perspectives

Important progress has been made in the understanding of the structure of warm nuclei. But in spite of the extensive work carried out in the field of rotational motion at finite temperature, as here discussed in connection with recent EUROBALL experiments, several questions still remain to be addressed. Among them, there is the direct measurement of the spreading width of the B(E2) strength, namely the rotational damping width Γ_{rot}. As discussed in Section 4.1, this quantity appears not easily accessible, since it is experimentally difficult to isolate excited rotational transitions corresponding to a given I $\rightarrow$ I-2 decay. However, according to recent theoretical studies based on microscopic band-mixing calculations [125], information on the rotational damping width Γ_{rot}, and also on a much more fundamental quantity such as the compound nucleus width Γ_μ, are expected to be obtained from the analysis of the spectral shape of double and higher fold γ-coincidence spectra. Such kind of studies requires large statistics EUROBALL-type experiments, allowing to select specific intrinsic nuclear configurations.

In connection with superdeformation, a further study of quasi-continuum spectra, based on larger statistics experiment than presently available, is expected to give additional crucial information on the mixing mechanism between excited normal-deformed and superdeformed states, leading to the quantum tunnelling through the potential energy barrier in the deformation space. This is also expected to shed light on the gradual transition from order to chaos undertaken by the nuclear system with increasing temperature.

Moreover, in order to obtain a full understanding of the feeding mechanism of the super-deformed structures from the Giant Dipole Resonance one needs additional work in other mass regions than presently investigated (^{143}Eu), also in connection with particle feeding mechanisms.

Pairing correlations and band termination at the highest spin

E. Paul, J. Simpson and R. Wadsworth

5. Pairing correlations and band termination at the highest spins[*]

5.1.   Introduction

The evolution of the superfluid properties of the nucleus with increasing angular momentum is of considerable interest. At low spins, the nucleus displays well-established superfluid properties with nucleons teaming up in time-reversed orbits, or Cooper pairs. But collective rotation of the nucleus tries to break these correlated fermions apart, the Coriolis anti-pairing effect. With increasing rotational frequency and particle alignments it was thought that a transition out of the superfluid paired phase may occur, in an analogous manner to the quenching of superconductivity by a sufficiently high magnetic field (the Meissner effect). However, while it now seems that the occurrence of such a phase change is somewhat more complex in nuclei than at first thought, "the question of how does rotation affect the pairing correlations at very high spin is still an important and unfinished business" (Nobel Laureate, Ben Mottelson, NBI, September 1997).

One test for the existence of static pairing correlations at large angular momentum is through the study of band crossings. In regions of spin where pairing is significant, band crossings are expected to occur at a similar rotational frequency in all rotational bands where the associated alignment is not blocked. In the absence of pairing, a rotational band based on a particular single-particle configuration can be crossed by another rotational band based on a different but more energetically favourable configuration. The rotational frequencies at which such rearrangements occur are specific and highly dependent on the details of the single-particle spectrum of states. Thus, one characteristic of the decline of static pairing correlations would be the observation at high angular momentum of band crossings not correlated in rotational frequency.

5.2.   High spin spectroscopy

Nuclei in the mass $A \sim 160$ region present the best opportunity to observe and investigate the very highest nuclear spins possible in a chain of isotopes or isotones. They are the best cases to probe the ultimate angular-momentum limit for discrete nuclear states, beyond which the huge rotational forces cause the nucleus to fission. EUROBALL is the ideal instrument to perform this ultra high spin spectroscopy.

Using EUROBALL, very high spin states ($I = 50$-$60\hbar$) have been observed in the transitional nuclei ^{159}Er – ^{162}Er [136]. The positive parity, even spin (+, 0), the negative parity, odd spin (–,1) and even spin (–,0) bands in ^{160}Er were established up to $I^{\pi} = 54^{+}$, 51^{-} and 54^{-}, respectively. In ^{161}Er, three bands are observed well above spin $50\hbar$. In the positive parity, positive signature (+,+½) band a discontinuity in the regular rotational behaviour occurs at $109/2^{+}$ and a splitting into two branches occurs at $97/2^{-}$ in the negative parity, positive signature (–,+½) band. The (–,–½) band continues in a regular fashion to $115/2^{-}$, tentatively ($119/2^{-}$). In ^{162}Er the (+,0) yrast band is observed to continue smoothly up to 60^{+} (see Figure 5.1) and the (–,0) and (–,1) bands have been extended from 30^{-} to 34^{-} and from 31^{-} to 49^{-} , respectively.

---

[*] Contribution by E. Paul, J. Simpson, and R. Wadsworth

Figure 5.1: *EUROBALL spectrum showing the yrast band in ^{162}Er up to spin 60ℏ.*
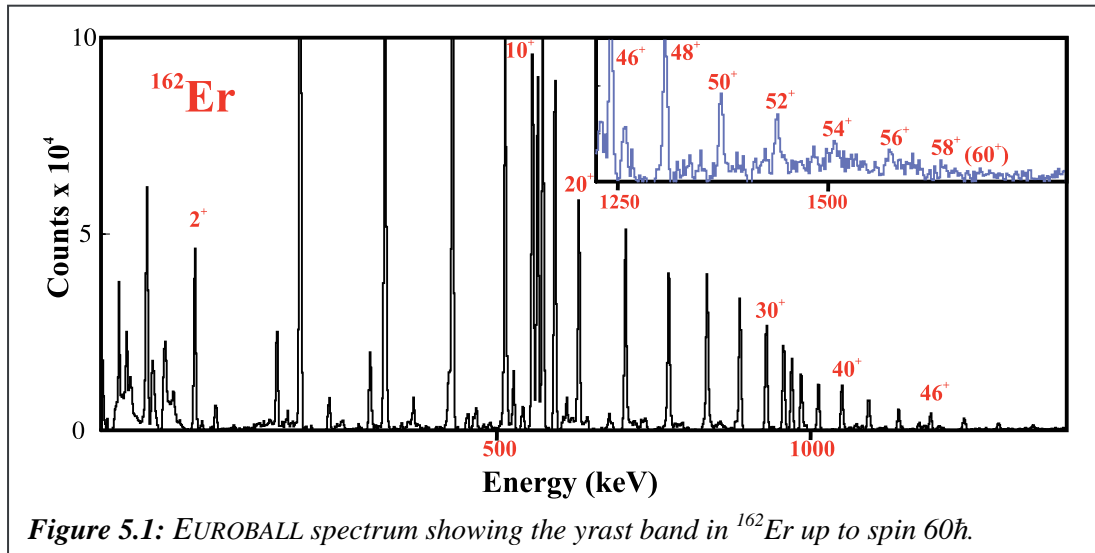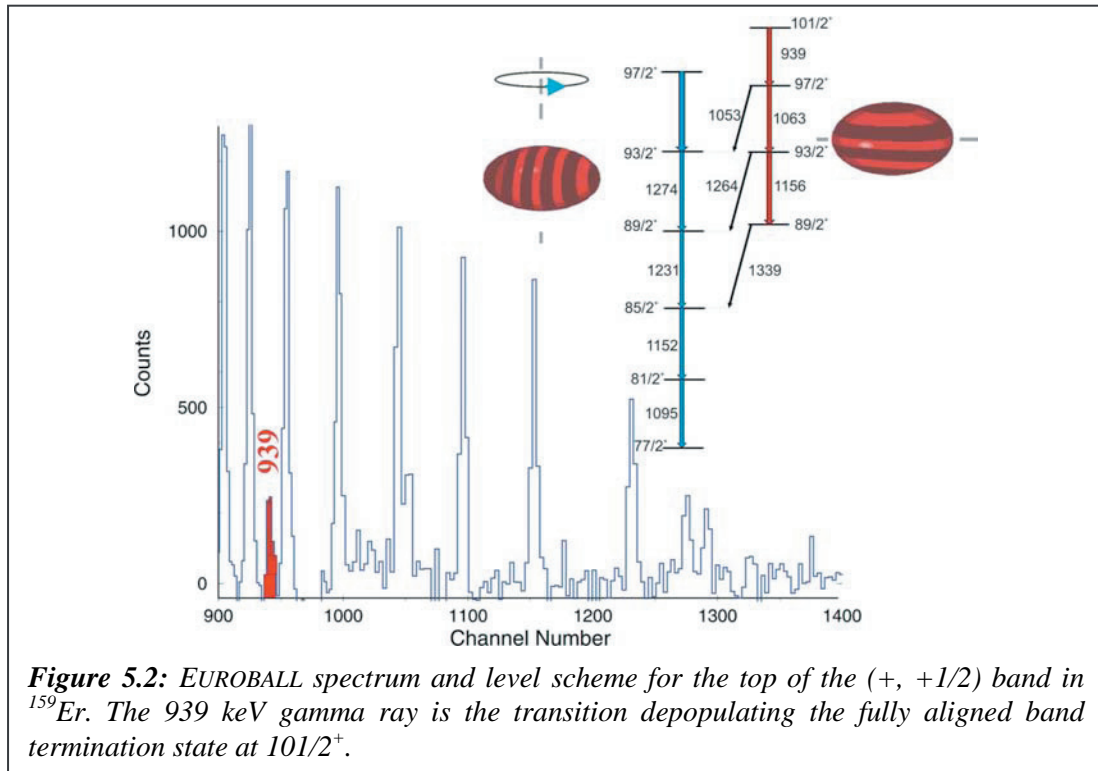
The high spin experimental spectra were compared with both a simple model involving the occupation of specific single neutron states in the absence of neutron pair correlations and with more detailed cranked Nilsson-Strutinsky calculations in which both proton and neutron pairing correlations are neglected. The very high spin domain was found to comprise a series of unpaired rotational bands. Excellent agreement between the experiment and theory for the relative energy of the bands at high rotational frequency and for the observation and interpretation of the band crossings in the (+,+½) and (–,+½) sequences in ^{161}Er was obtained. This work provided, for the first time, strong evidence for the demise of both proton and neutron static pairing correlations at these ultra high spins. It is also worth noting that the nucleus ^{159}Er was the first one to establish an unpaired band crossing in the (–,+½) sequence, i.e. at $\hbar\omega \sim 0.55$ MeV [137]. The simple model predicts another such crossing in the (–,–½) sequence at higher rotational frequency and indeed the Euroball data shows good evidence for this crossing at $\hbar\omega \sim 0.62$ MeV.

5.3. Termination of rotational bands

Two types of band termination have been observed to occur in nuclei. The first involves the crossing, in terms of excitation energy, of deformed collective rotational states and oblate non-collective single-particle states, the latter becoming favoured at high-spins. This is often called "abrupt" band termination. The second type, which has been called "smooth" or "soft" band termination, results when, for a given configuration, a deformed collectively rotating nucleus gradually changes its shape from a near-prolate to a non-collective oblate shape at termination. Detailed discussions of band termination can be found in the review article by Afanasjev et al. [138]. Experiments have been carried out to study both of these phenomena at EUROBALL.

The transitional erbium isotopes exhibit perhaps the classic examples of the angular momentum induced abrupt prolate-collective to oblate non-collective shape change at high spin in heavy nuclei [138,139]. This band termination effect, which is a consequence of the finite number of valence particles outside the $Z = 64$ and the $N = 82$ core has been traced in a range of Er isotopes using EUROBALL.

Figure 5.2: *EUROBALL spectrum and level scheme for the top of the (+, +1/2) band in ^{159}Er. The 939 keV gamma ray is the transition depopulating the fully aligned band termination state at 101/2$^+$.*

In ^{159}Er there is clear evidence for the first time of the fully aligned band terminating state in the (+,+½) sequence at 101/2$^+$ (see Figure 5.2). This state corresponds to a fully aligned $[\pi(_{h11/2})^4]_{16^+} \otimes [\nu (i_{13/2})^3 (h_{11/2}, f_{7/2})^6]_{69/2^+}$ configuration and is formed by adding one extra favoured $i_{13/2}$ (9/2$^+$) neutron to the classic favoured band terminating state at spin 46$\hbar$ in ^{158}Er [140]. In the heavier isotopes these non-collective states are predicted to move to higher excitation energy with respect to the yrast line, which is consistent with the experimental observations.

Some of the best examples of smoothly terminating bands have been found in the *A~110* mass region [138]. In the Sn nuclei these structures are mainly based on two-particle-two-hole (2p-2h) proton excitations across the *Z=50* shell gap. Examples have also been found in Sb, Te, I and Xe nuclei where the configurations involve 3p-2h, 4p-2h, 5p-2h and 6p-2h proton excitations respectively.

Using EUROBALL, evidence has been found in ^{73}Br and the odd-*A* Lanthanum isotopes for smoothly terminating bands which do not involve proton particle-hole excitations. In ^{73}Br [141] a negative parity band was observed up to its terminating spin of 63/2$\hbar$. This was the first terminating band to be identified in the *A~70* mass region. Following comparison with unpaired cranked Nilsson-Strutinsky calculations the band was assigned a *[43,73]* configuration relative to a ^{56}Ni core. The notation used is *[p_1,p_2,n_1n_2]* where *$p_1(n_1)$* is the number of protons (neutrons) in the *$p_{3/2},f_{5/2}$* orbitals and *$p_2(n_2)$* represents the number of protons (neutrons) in the *$g_{9/2}$* orbitals.

The existence of smoothly terminating structures in the highly-deformed bands in *A~130* nuclei was predicted some time ago by Afanasjev and Ragnarsson using cranked Nilsson-Strutinsky calculations [142]. However, because the terminating spins were expected to be very high (e.g. >70$\hbar$ in ^{132}Ce) it was believed that it would be too difficult to observe such states. Recent EUROBALL studies have revealed the first hint for smooth band termination
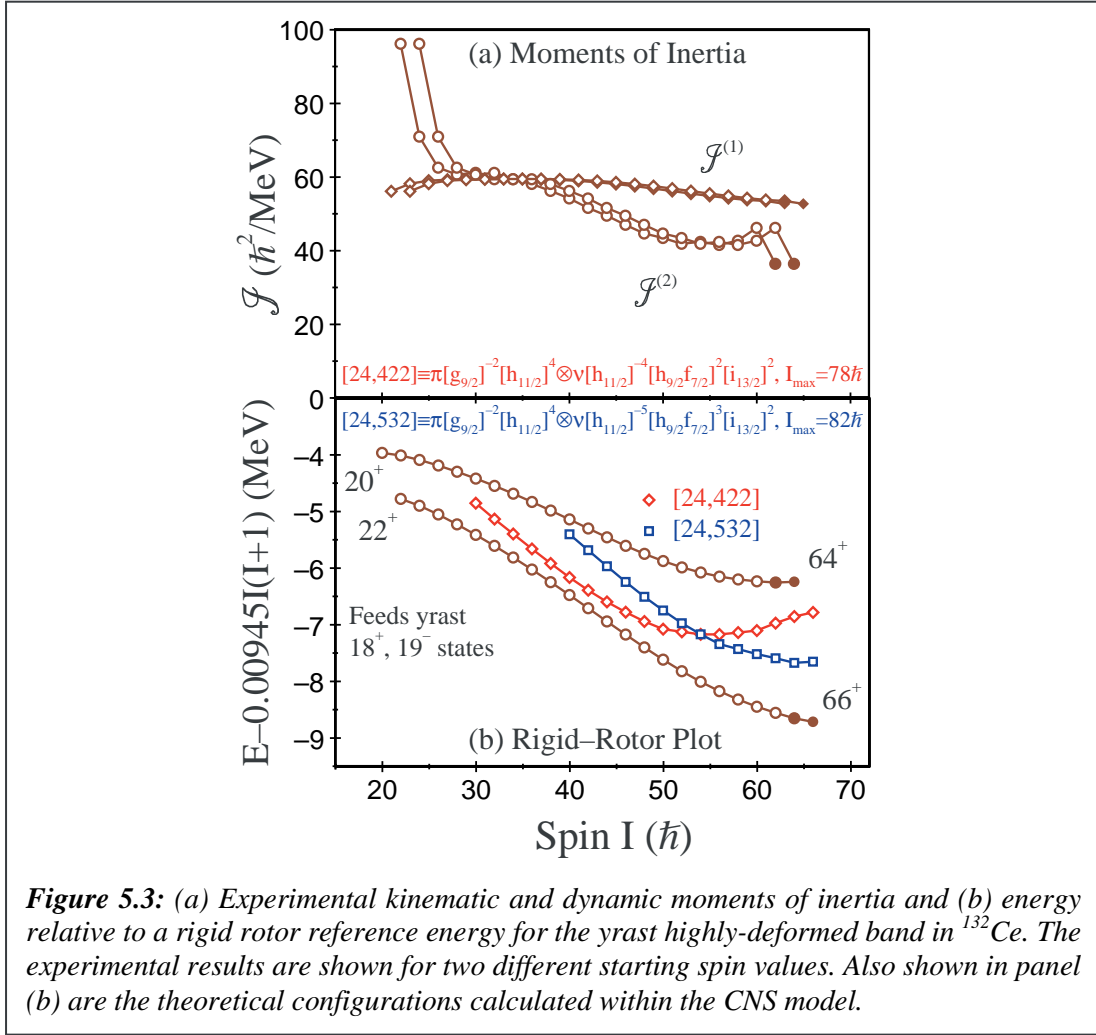
Figure 5.3: *(a) Experimental kinematic and dynamic moments of inertia and (b) energy relative to a rigid rotor reference energy for the yrast highly-deformed band in* ^{132}*Ce. The experimental results are shown for two different starting spin values. Also shown in panel (b) are the theoretical configurations calculated within the CNS model.*

behaviour in the yrast highly deformed band in ^{132}Ce [143]. Figure 5.3 shows the experimental results for this along with the results of unpaired cranked Nilsson-Strutinsky (CNS) calculations. Experimentally, two starting spin values are shown since the decay to the normal-deformed yrast states has not yet been established. Below spin $60\hbar$ the band has been assigned a *[24,422] =* $\pi[g_{9/2}^{-2}h_{11/2}^{4}]\otimes\nu[h_{11/2}^{-4}(h_{9/2}f_{7/2})^{2}i_{13/2}^{2}]$ configuration relative to a ^{132}Sn core, whilst above this spin calculations suggest that an $h_{11/2}$ neutron is promoted into an $h_{9/2}/f_{7/2}$ orbital, which raises the termination spin for the resulting $\pi[g_{9/2}^{-2}h_{11/2}^{4}]\otimes\nu[h_{11/2}^{-5}(h_{9/2}f_{7/2})^{3}i_{13/2}^{2}]$ configuration from $78\hbar$ to $82\hbar$. Although the present calculations reveal some discrepancies with the data, such as the crossing point for the two structures discussed above, the behaviour of the kinematic and dynamic moments of inertia (panel a) and the rigid rotor plot (panel b) suggests that the experimental band is approaching termination. These results reveal important insight into the microscopic structure of highly-deformed collective bands in this region.

In the odd mass La isotopes with *A=127,129,131* the normal-deformed structures ($\varepsilon_2{\sim}0.2$) have been extended to very high spins ($\sim$37-44$\hbar$) using EUROBALL and found to have the characteristics of smoothly-terminating bands [144,145]. This provided the first evidence for such behaviour in normal-deformed bands in this mass region. In these nuclei, however, the structures were found not to involve $g_{9/2}$ holes, which are observed to play an important part in the A$\sim$110 mass region and in the highly-deformed bands in the Ce isotopes. They are

based on protons and neutrons in the $d_{5/2}, g_{7/2}$, $h_{11/2}$ valence orbitals with additional neutrons in the $s_{1/2}$ and $d_{3/2}$ orbitals.

5.4.   Summary

Experiments with EUROBALL have allowed, for the first time, detailed spectroscopy to be carried out in the spin $50\hbar$ to $60\hbar$ regime in a range of Er isotopes. This has enabled us to gain some insight into the behaviour of the atomic nucleus in the absence of static pairing correlations and to investigate shape competition at the very highest excitation energy and angular momentum. Further experiments in this area will be required since it is important to investigate band crossing frequencies in a range of nuclei. It will be exciting to continue the experimental quest to even higher spins ($\sim$60-70$\hbar$) in this region of nuclei where many aligned oblate states and numerous unpaired crossings are predicted to occur. It is also of fundamental interest to find the actual limit of discrete nuclear states before the large rotational forces cause the nucleus to fission.

Abrupt band termination is now a well established phenomenon in a few nuclei in various mass regions. One of the best areas to study this phenomenon is in the A$\sim$160 region, where it has been possible to establish evidence for single-particle states and their configuration at high spin ($\sim$40$\hbar$) and high excitation energy ($\sim$40 MeV). Such work is vital for fixing the location of the single-particle orbitals. One interesting question that remains in this area is; what lies beyond band termination? In other words, what structures feed these special terminating states. At the present time studies are continuing in the Er nuclei to investigate whether such structures involve a breaking of the [146]Gd core or if they are fed from a semi-continuum of states based on proton and neutron particle-hole excitations.

EUROBALL has provided evidence for smooth band termination in new regions (A$\sim$70 and 130) of the Segrè chart. These results, along with those from other arrays such as GAMMA-SPHERE, have helped to establish that this phenomenon is observed when a well defined configuration is followed to very high-spin, and is a natural consequence of the alignment of all the valence nucleon spin vectors within the configuration with the initial axis of rotation. The properties of such bands can be well reproduced by unpaired cranked Nilsson-Strutinsky calculations. Comparison of such calculations with the available data suggests that for structures that involve particle-hole (p-h) excitations the states within the smoothly terminating bands have rather pure wavefunctions. However, in [73]Br and the odd-mass La isotopes, where the configurations do not involve particle-hole excitations, the structures do not seem to evolve as smoothly. This may reflect the fact that the wavefunctions of the states in these bands are less pure than those resulting from the 2p-nh bands in the mass 110 region, for example. The EUROBALL spectrometer has also provided the first hints that smooth band termination may also occur at the highest spins in the yrast highly deformed band in [132]Ce. Further work will, however, be required to establish whether termination is achieved.

Symmetries in medium-light nuclei at and beyond the N = Z line

S. M. Lenzi and P.G. Bizzeti

6. Symmetries in medium-light nuclei: at and beyond the *N=Z* line[*]

6.1. Introduction

Symmetry is normally associated to the concept of beauty. In physics, symmetries help to better understand the world around us and, in nuclear physics, they play a key role in the understanding of the behaviour of matter. Isospin symmetry is a consequence of the (approximate) charge invariance of nucleon-nucleon forces. Although the symmetry is already broken, to some extent, at the level of strong interaction and - to a much larger extent - by electromagnetic forces, the isospin formalism remains a very powerful tool to relate the properties of corresponding levels in different nuclei, from which complementary information can be derived on the structure of the nuclear wave function. The most important component of the symmetry breaking interaction, i.e., the Coulomb force between protons, is certainly the best known part of the Hamiltonian, and its effects can be calculated as a perturbation series if the structure of unperturbed charge-symmetric states is assumed to be known.

Due to the Coulomb forces (and other non charge-invariant effects) the isospin is not - strictly speaking - a good quantum number. Every nuclear state is expected to contain, in addition to the main component of isospin T, minor components of different isospin. Although this is not the only effect of symmetry breaking forces (and perhaps not even the most important one) the square of the isospin mixing amplitude can be taken as an indicator of the size of the symmetry violation. The amount of isospin mixing in the ground state of even-even nuclei has been calculated by Colò and collaborators [146] by assuming a dominant role of the Giant Monopole Resonance. For *N=Z* nuclei, similar results have been obtained by Dobaczewski and Hamamoto with a self-consistent Hartree-Fock calculation (not restricted to a spherical shape) [147]. The mixing is found to increase rapidly with *A* and, for a given *A*, is maximum for *N=Z*.

Isospin mixing is by no means the only effect of symmetry breaking forces. At the lowest order of perturbation, the degeneracy in energy of the different members of a multiplet is broken, and, also in the absence of isospin mixing, Coulomb energy terms are different for nuclei of a given isospin multiplet. The resulting failure of isospin symmetry is relevant for transitions leading, within a multiplet, from one nucleus to another, as in the case of beta decay. This fact has a large potential interest for the evaluation of the Fermi coupling constant and, therefore, for the apparent lack of unitarity of the Cabibbo-Kobayashi-Maskawa quark mixing matrix [148]. It is therefore important to develop appropriate models to evaluate the necessary corrections for the nuclear matrix element of the Fermi transitions. The reliability of the models can be tested with other experimental observables related to the symmetry breaking, preferably in several nuclei and in the region where the effects are larger, i.e., on the heavier available nuclei with almost equal values of *N* and *Z*.

A large amount of theoretical and experimental work has been devoted to the investigation of isospin symmetry and symmetry breaking effects [149] in two different regions of the chart of nuclides: in the region of light nuclei with *N* close to *Z*, where members of low lying isospin multiplets are observed as bound states or very narrow resonances, and in heavier nuclei with fairly large neutron excess, where the isobaric analog states are observed as resonances in proton scattering and (p,n) reactions.

---

[*] Contribution by S.M. Lenzi and P.G. Bizzeti

The present contribution will discuss the region of heavier nuclei with approximately equal proton and neutron number, from the $f_{7/2}$ shell up to the limit of the proton drip line. The experimental work in this area is just at the beginning, and will profit from the intense radio-active ion beams provided by future facilities. The available results are, however, sufficient to take a glance over this varied landscape, where, in comparison to lighter symmetric nuclei, one should meet larger Coulomb effects and also qualitatively new aspects, as those related to the onset of nuclear deformation.

In Section 6.2 we discuss the experimental signatures of isospin symmetry breaking (ISB). The experimental results obtained with EUROBALL are presented in Section 6.3. Finally, conclusions and perspectives are given in Section 6.4.

6.2. Isospin symmetry breaking

Coulomb energy differences and isospin mixing

If the Coulomb interaction (and other symmetry breaking forces) is assumed to take place between pairs of nucleons (excluding three-body and n-body forces), its expansion in irreducible tensors with respect to rotations in isospin space contains only three terms, with isoscalar, isovector and isotensor (of rank 2) character, respectively. The isoscalar term has the same effect on every member of a given multiplet, and can be included in the isospin conserving part of the Hamiltonian. The other two terms are responsible for the symmetry breaking. In the first order, the total energy of the different levels of a multiplet - or their excitation energy over the ground state - are related by the equation $E(i,T_z) = a_i + b_i\, T_z + c_i\, T_z^2$ where a_i, b_i and c_i are constant for a given multiplet i. This relation can be experimentally verified if at least four levels of a multiplet (with T greater or equal to 3/2) are known.

Moreover, it can be shown [150] that a large part of the isovector term is proportional to the third component of the isospin, and is therefore diagonal in the isospin representation, its only effect being a constant contribution to the Coulomb energy of every nuclide. The residual non-diagonal part of the isovector term is entirely responsible for the mixing between $T = 0$ and $T = 1$ states in self-conjugate nuclei, as well as for the (symmetry-breaking) mixing between $T = 1/2$ states in nuclei with $N = Z \pm 1$. In all other cases, both the isovector and isotensor terms contribute; their corresponding matrix element have equal magnitude in mirror nuclei, while the relative sign of the isovector and isotensor terms is opposite.

Experimental signatures of the symmetry breaking.

Every single-nucleon operator (as, e.g., those responsible for γ or β transitions) contains, at most, an isoscalar and an isovector part. Some of them are purely isovector: The $E1$ transition operator (whose isoscalar part would only involve the center-of-mass coordinates, and would only be relevant for the Thomson scattering of photons on the nucleus) and the nuclear part of the beta transition operators.

A number of selection or symmetry rules can be derived as a consequence of the tensor character of the operator in the isospin space:

1) $E1$ transitions between states of equal isospin are strictly forbidden in *N=Z* nuclei.
2a)   Beta transitions between two $I^{\pi}=0^+$ states (pure Fermi transitions) are only allowed between states belonging to the same isobaric multiplet,

2b) and, in particular, are strictly forbidden between states having different isospin *T*.

3) *E*1 transitions between corresponding states of mirror nuclei should have equal reduced strength.

4) Mirror β decays (e.g. transitions between two corresponding *T = 1* states of mirror nuclei and a common state of the *N=Z* isobar) should have equal reduced strength.

5) Mirror γ transitions of any multipolarity with *ΔT = 1* should have equal reduced strength.

6) The transition amplitudes of γ analog transitions of any multipolarity between corresponding states of two given isobaric multiplets should depend linearly on T_z and, therefore, on *Z*.

These rules are strictly valid only if the isospin symmetry holds. Any failure of them implies a failure of the isospin symmetry (although not necessarily an isospin mixing, that is only implied by a failure of rules 1 and 2b). In addition, some approximate selection rules hold for γ transitions of magnetic-multipole character:

7) *M1* transitions between states of equal isospin are hindered in self-conjugate nuclei.

8) On the average, magnetic multipole transitions of any order are somewhat hindered in self-conjugate nuclei.

9) *M1* transitions between corresponding states in mirror nuclei should have similar strength.

10) On the average, *ML* transitions of any *L* between corresponding states in mirror nuclei should have similar strengths.

Rules 7-10 follow from the fact that the proton and neutron contributions nearly cancel each other in the non-diagonal part of the isoscalar magnetic moment. In the case of higher magnetic multipoles they also depend on additional approximations. Their utility for the investigation of isospin symmetry is therefore limited, while the investigation of analog magnetic transitions (also in connection with the analog Gamow-Teller transitions) can be relevant for other aspects of nuclear spectroscopy. Other selection rules can be derived for the alpha decay (transitions with isospin change are forbidden) or proton decay (transitions with isospin change greater than 1/2 are forbidden); however, this subject will not be treated here.

Finally, we must notice that the failure of any one of the above-mentioned rules is not necessarily related in a simple way to the parameters describing the symmetry breaking. For example, in the case of rule 1, a non vanishing amplitude of the forbidden *E*1 transition certainly implies an isospin mixing either in the initial or in the final state (or, very probably, in both of them). However, supposing that only one of the two levels is subject to isospin mixing, the amplitude of the forbidden transition takes the form

$$< a \mid M(E1) \mid b > = \sum_i \alpha_i < a, T = 0 \mid M(E1) \mid i, T = 1 >,$$

$$\alpha_i = \frac{< i, T = 1 \mid V_C^{(1)} \mid b, T = 0 >}{E_b - E_i}, \tag{1}$$

where $V_C^{(1)}$ is the isovector part of the isospin-violating interaction and we have assumed that the level *a* has pure isospin *T = 0*, while in level *b* some mixing occurs with levels *i* having *T = 1*. If the sum is extended to more than one level, the squared amplitude of the transition is not related in a simple way to the overall isospin mixing $\alpha^2 = \Sigma\alpha_i^2$ of the level *b*: The mixing with levels *i* having a negligible *E*1 transition amplitude to the level *a* contribute to the isospin mixing but not to the transition amplitude, while if many terms $\alpha_i <a,T=0|M(E1)|i,T=1>$ from
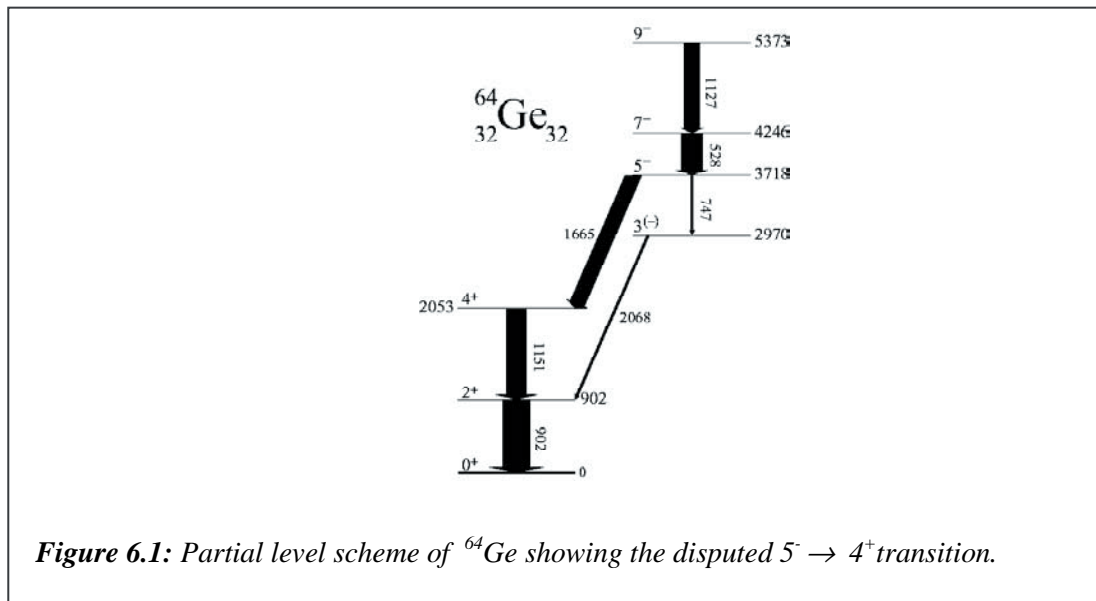
different levels *i* contribute coherently to the sum, the transition amplitude might be comparatively large while the isospin mixing α^2 remains comparatively small. Therefore, we cannot expect that a single measurement (e.g. of a forbidden *E*1 strength), even if it is a carefully selected case, will be sufficient to verify the reliability of a model which can be used to calculate corrections for a different observable (e.g. Fermi matrix element). Several independent measurements, preferably on different observables, will be necessary for this purpose.
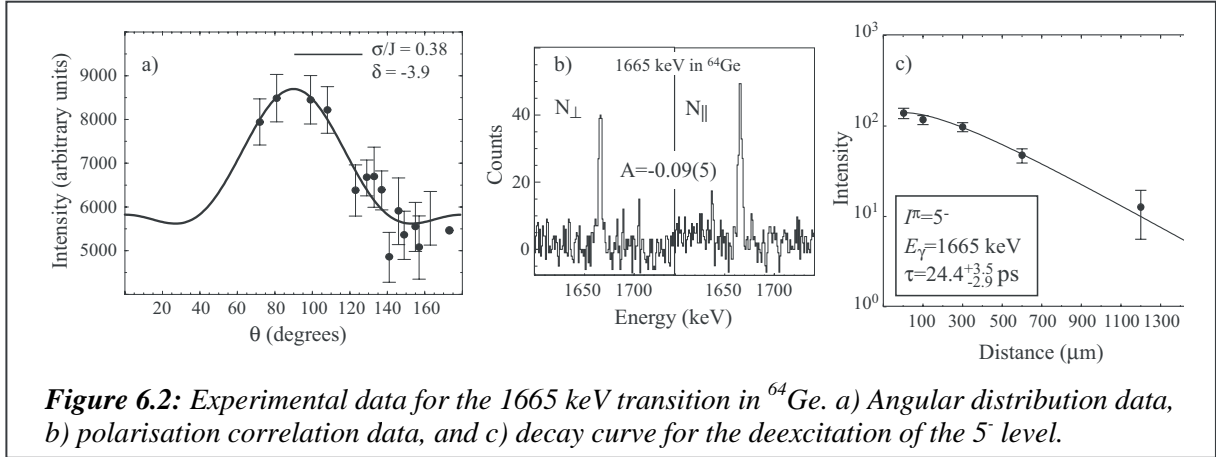
In this work we will concentrate on the isospin symmetry studies performed by means of γ-ray spectroscopy with EUROBALL. These investigations cover a wide spectrum of experiments where self-conjugate nuclei and isobaric multiplets have been populated in fusion-evaporation reactions between heavy ions.

6.3. Isospin symmetry breaking studies with EUROBALL

Observation of forbidden *E*1 transitions in *N=Z* nuclei

In the long-wavelength limit, the matrix elements of the nuclear *E*1 operator vanish when both the initial and final states have equal isospin T and $T_z = 0$ [151]. However, the Coulomb interaction induces the admixture between these low-lying $T = 0$ states and higher-lying $T = 1$ states of the same configuration having the same spin and parity. Electric dipole transitions are thus allowed between the $T = 0$ ($T = 1$) component of the initial state and the $T = 1$ ($T = 0$) component of the final one. The observed *E*1 strength is therefore a signature of the isospin mixing. Actually, the systematics of *E*1 transitions observed in light nuclei shows that the strength of isospin forbidden transitions between low-lying states is significantly smaller than those in $N \neq Z$ nuclei. With increasing *Z,* the amount of isospin symmetry violation is expected to increase.


Figure 6.1: *Partial level scheme of ^{64}Ge showing the disputed 5⁻ → 4⁺ transition.*

Figure 6.2: *Experimental data for the 1665 keV transition in ^{64}Ge. a) Angular distribution data, b) polarisation correlation data, and c) decay curve for the deexcitation of the 5$^-$ level.*

In the $N = Z = 32$ nucleus ^{64}Ge, an intense transition of 1665 keV deexciting the yrast 5$^-$ level to the 4$^+$ level was already observed by P.J. Ennis and co-workers [152]. In that experiment, it was not possible to determine the multipole mixing ratio δ of the 1665 keV transition and a stretched electric dipole character was assigned on the basis of systematics arguments. In a recent investigation performed at EUROBALL, E. Farnea and collaborators [153] have measured the multipole mixing ratio δ, the linear polarisation of the 1665 keV line, and the lifetime of the 5$^-$ level. These measurements have enabled the electric dipole strength to be extracted and hence for the first time, the amount of isospin mixing to be investigated.

In a first experiment performed at the Laboratori Nazionali di Legnaro using EUROBALL coupled to the ISIS Si-ball [4] and to the Neutron Wall [7], ^{64}Ge was populated via the ^{40}Ca (^{32}S, 2α)^{64}Ge reaction at 125 MeV beam energy, using a 1 mg/cm^2 thick ^{40}Ca target evaporated on a 12 mg/cm^2 thick gold backing. A partial level scheme of ^{64}Ge is shown in Figure 6.1. The values for δ and σ/*J* were determined from an angular distribution analysis. A polarisation correlation from oriented states analysis was performed using the EUROBALL Clover detectors as Compton polarimeters [154]. The asymmetry parameter *A*, defined as *A* = (N$_\perp$-N$_\parallel$)/(N$_\perp$ + N$_\parallel$), was determined, where N$_\perp$ and N$_\parallel$ stand for the number of coincidences between two sectors of the Clover in a direction perpendicular and parallel to the plane containing the detector and the beam direction, respectively. The value of the polarisation sensitivity *Q*, relating the measured asymmetry to the linear polarisation *P*, was obtained through a Monte Carlo simulation using GEANT III subroutines modified to include the effect of the linear polarisation [155,156].

The results of the angular distribution and polarisation correlation analyses, shown in Figure 6.2, confirm a 5$^-$ → 4$^+$ transition, but with a much larger multipole mixing ratio than the tentative assignment of Ennis and co-workers [152]. In the analysis of the angular distribution data for the 1665 keV transition, a large multipole mixing ratio $\delta = -3.9^{+0.7}_{-0.4}$ was obtained. With such a large value of δ for the 1665 keV transition, one would tend to assume a mixed *E*2/*M*1 character, in contrast with the systematics of the light even germanium isotopes. The results from the linear polarisation analysis support the systematics argument favouring a parity-changing transition, since the measured asymmetry for the 1665 keV γ-ray, *A*=-0.09(5), turns out to be in agreement with a parity-changing transition with large negative δ (while it would imply no parity change in the case δ ≈ 0). Therefore, the conclusion is that the 1665 keV γ-ray has a mixed *M*2/*E*1 character with a large negative multipole mixing ratio, corresponding to a quadrupole content of about 93%.

The lifetime of the 5⁻ state was measured in a second experiment performed at the IReS Strasbourg, using the EUROBALL IV array coupled to the Köln plunger device [157], which is especially designed for coincidence measurements. The same reaction (^{32}S + ^{40}Ca) was employed as in the Legnaro experiment, but in this case the beam energy was increased to E=137 MeV, in the attempt to favour the production of ^{64}Ge. A lifetime of $\tau = 24.2^{+3.5}_{-2.9}$ ps was obtained and reduced transitions strengths $B(E1) = 2.47^{+0.91}_{-0.57} \cdot 10^{-7}$ W.u. and $B(M2) = 6.06^{+0.91}_{-1.13}$ W.u. were deduced. For comparison, in the case of ^{66}Ge the deduced strengths for the corresponding $5^- \rightarrow 4^+$ transition of 1510 keV are $B(E1)=3.7(6)\cdot10^{-6}$ W.u. and $B(M2)=0.39(7)\cdot10^{-2}$ W.u.. The resulting $B(M2)$ strength in ^{64}Ge is large compared to the corresponding transition in ^{66}Ge, but is not far from the corresponding transition in ^{68}Ge, which has $B(M2) = 0.71(11)$ W.u. [158]. This suggests that there is an accidental cancellation of the isoscalar and the isovector components of the *M2* transition amplitude in ^{66}Ge, which does not occur in ^{64}Ge and ^{68}Ge. To estimate the amount of isospin mixing α^2 implied by the presence of a forbidden *E1* transition between $T = 0$ states, a very schematic calculation has been done in Ref. [153] and the obtained value is consistent with those predicted in Refs. [146,147].

Another interesting case is the nucleus ^{48}Cr (*N=Z=24*) which presents a rotational ground state band that terminates at I$^\pi$=16$^+$. At low spin the deformation parameter is β=0.3. As shown in Figure 6.3 this nucleus presents also a side band which decays to the 4$^+$ state in the g.s. band. The spin and parity assignments to the bandhead of the side band at an excitation energy of 3532 keV have been changed several times during the last twenty years (I$^\pi$ = 5$^-$, 5$^+$, 6$^-$, 6$^+$ [159]). In Ref. [160] I$^\pi$ = 4$^-$ was suggested and recently confirmed in an EUROBALL experiment performed at LNL. The nucleus ^{48}Cr was populated in the reaction ^{28}Si(^{28}Si,2α) at 110 MeV. The target consisted of 0.85 mg/cm^2 of ^{28}Si (enriched to 99.9%) with a 15 mg/cm^2 gold backing. Gamma rays were detected with EUROBALL and charged particles with the ISIS

Figure 6.3: *Level scheme and polarisation data for ^{48}Cr.*
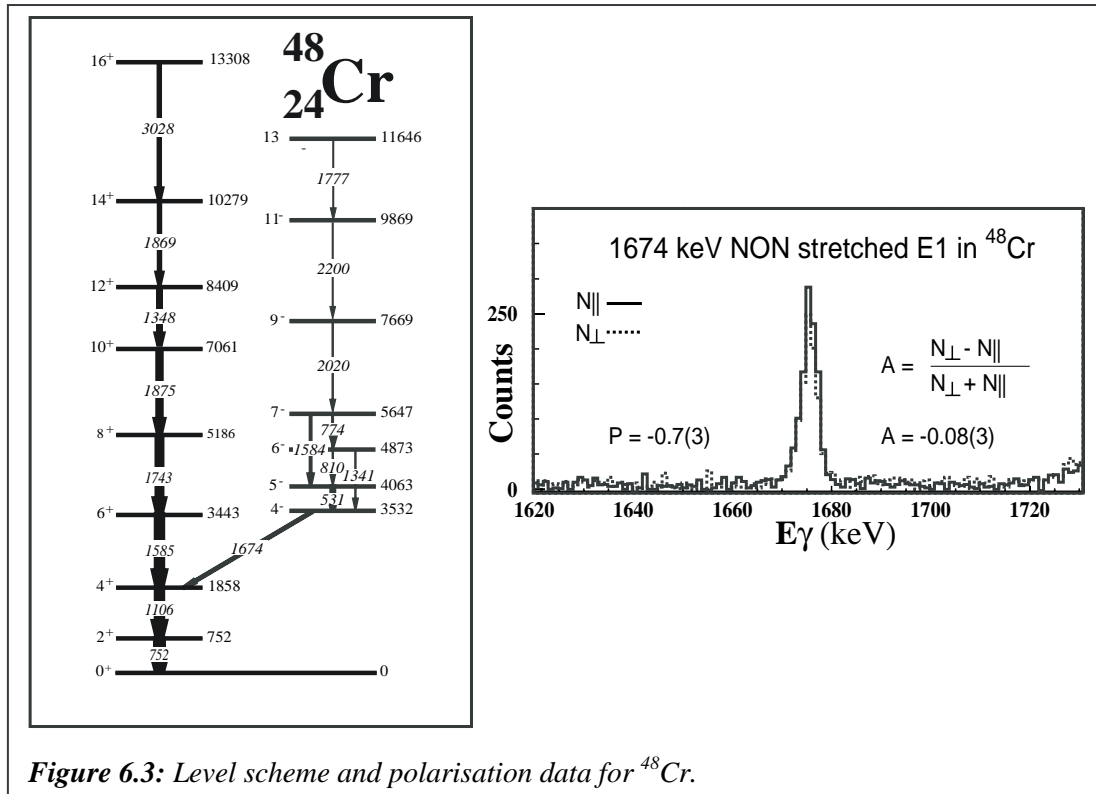
array [4]. The angular distribution of the 1674 keV transition to the 4^+ state is compatible with a stretched quadrupole transition or with an $I \rightarrow I$ dipole transition. Using the Clover detectors as polarimeters, an asymmetry A = -0.08 (3) was measured which means a polarizarion P = -0.7(3). These results not only confirm the suggested $I^\pi = 4^-$ assignment to the state at 3532 keV but also indicate a pure non-stretched $E1$ character of the 1674 keV transition. In this case, the deduced $B(E1)$ value is about two orders of magnitude smaller than the corresponding one in ^{50}Cr. The analysis of other experimental data for forbidden transitions in this mass region is presently in progress.

It is interesting to note that isospin-mixing values obtained in recent β-decay experiments (see for instance the study of ^{52}Mn [161]) are approximately two orders of magnitude lower than the theoretical expectations. The point is that the Fermi transition is even more selective than the $E1$ γ decay, probing just the isospin impurity related to the mixing with one particular state (the analog of the daughter state).

Analog *E2* transitions in mirror nuclei

Nuclei in the middle of the $f_{7/2}$-shell are well known to be deformed and to display rotational bands. Here the number of active nucleons and the number of orbitals in the model space is large enough to make coherent phenomena important, and collective excitations having a simple geometrical meaning naturally emerge from the large scale shell model description. The success of large scale shell model calculations in describing rotational motion in this mass region is already well established [162,163]. Calculated energy levels and reduced transition probabilities are in very good agreement with the experimental findings.

The Coulomb energy differences (CED) along rotational bands in mirror nuclei have been investigated in the last few years in the $f_{7/2}$ shell. The first experiments on CED in this mass region were performed at Daresbury by J. Cameron and collaborators [164]. In later experimental studies by M.A. Bentley, C.D. O'Leary and co-workers the CED have been extended up to the band termination states and interpreted as evidence of nucleon alignment and shape changes [165,166]. In spite of the fact that coincidence with neutrons and/or charged-particles has been required to enhance the relative yield of neutron deficient channels, the statistics obtained was not sufficient to allow the measurement of lifetimes to better establish the changes in structure as a function of spin.

It is with the advent of EUROBALL that these measurements have become feasible. In an experiment done at LNL using EUROBALL combined with ISIS and the Neutron Wall the lifetimes in the $E2$ cascades of the mirror nuclei ^{47}Cr-^{47}V were measure by D. Tonev and collaborators [167]. This is the first determination of lifetimes of high-spin states in mirror nuclei of the $1f_{7/2}$ shell. The reaction was the same as that described above for ^{48}Cr. The ^{47}Cr nucleus was populated after the evaporation of two alpha particles plus one neutron, with a relative yield of 0.5%, while for the exit channel ^{47}V+2αp a yield of 8% was obtained. Lifetimes were determined using the Doppler Shift Attenuation Method (DSAM). In Figure 6.4 the level schemes and measured lifetimes are reported. The lifetime values in ^{47}V are in agreement with data from earlier measurements. In ^{47}Cr the lifetimes are determined for the first time. It should be noted that the derivation of lifetimes in ^{47}Cr and ^{47}V in the same experiment makes the determination of the ratios of the corresponding transition strengths very precise since uncertainties related to the stopping powers nearly cancel.

Figure 6.4: *Level schemes of the T=1/2, A= 47 mirror nuclei.*
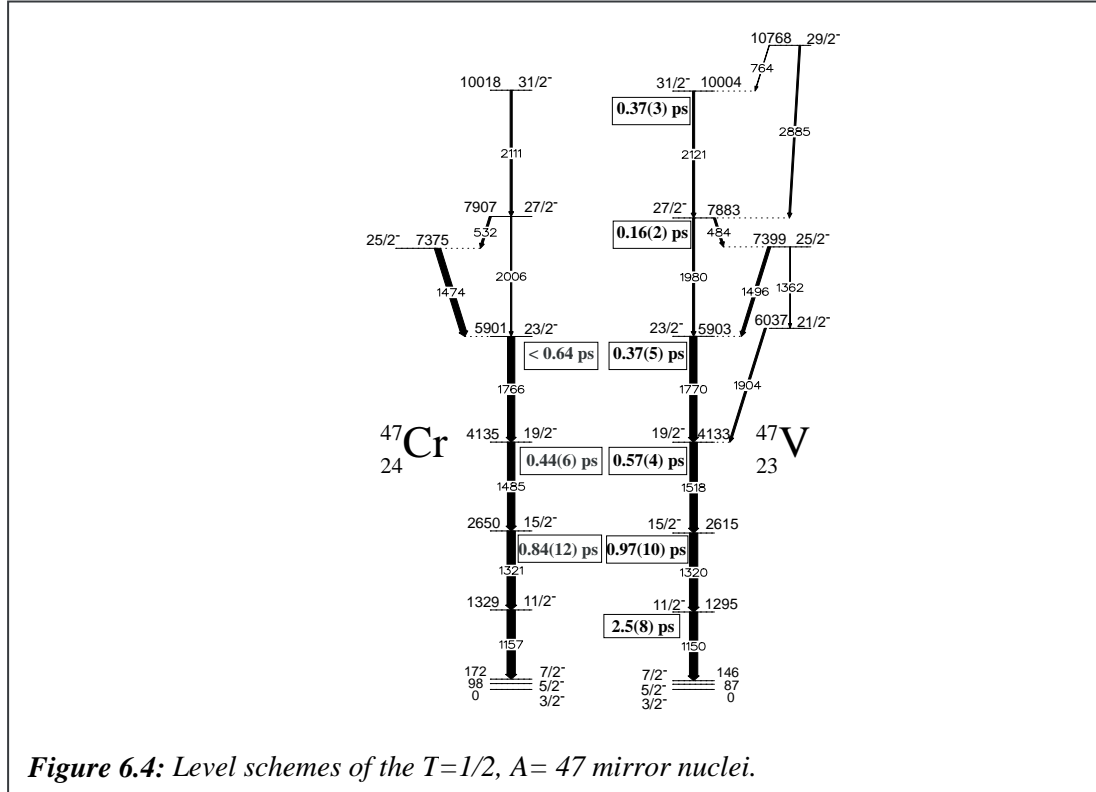
In the rotational model [18], the *B(E2)* values can be related to the transition quadrupole moments:

$$B(E2, I \rightarrow I - 2) = \frac{5}{16\pi} < IK 20 \mid I - 2 \; K >^2 \; (Q_t)^2 \qquad (2)$$

In the case of the ground state bands in the mirror nuclei $A = 47$, the Q_t values obtained in this way correspond to the intrinsic quadrupole moment Q_0 of the rotational model for a band with $K = 3/2$. This can also be related to the deformation parameter β:

$$Q_0 = \frac{3}{\sqrt{5\pi}} ZeR_0^2 \beta(1 + \tfrac{1}{8}\sqrt{\tfrac{5}{\pi}}\beta) \qquad (3)$$

The Q_t values for the mirror nuclei ^{47}Cr and ^{47}V are shown in Figure 6.5 together with the deduced deformation parameter β as a function of spin. The experimental data are compared with the results of a full *pf* shell model (SM) calculation performed with the code ANTOINE using the KB3 interaction [168]. The Q_t's show a systematic decrease with increasing spin in good agreement with SM calculations. At $I^\pi = 19/2^-$ the change of the experimental Q_t's is smoother than that of the theoretical values. The insert to Figure 6.5 at the left bottom side shows the CED's between the levels of the g.s. bands in ^{47}Cr and ^{47}V. The abrupt decrease of the CED at $I^\pi = 19/2^-$ has been interpreted by Bentley *et al.* [165] as evidence for particle alignment in both nuclei. Due to the blocking effect of the unpaired nucleon, a pair of protons aligns first in ^{47}V and a pair of neutrons aligns at the same spin in ^{47}Cr; when a pair of protons aligns the Coulomb repulsion decreases which gives rise to an additional compression of the levels in ^{47}V. The reduction of the Q_t values starting at the 19/2$^-$ state confirms a change of regime in both mirror nuclei which reduces the deformation with increasing spin. The alignment of nucleons becomes energetically favored with respect to the collective rotation at high angular momentum in these rather light nuclei. The bands terminate when the angular momentum reaches the maximum value ($I^\pi = 31/2^-$) that can be obtained in the $(f_{7/2})^7$ configuration.
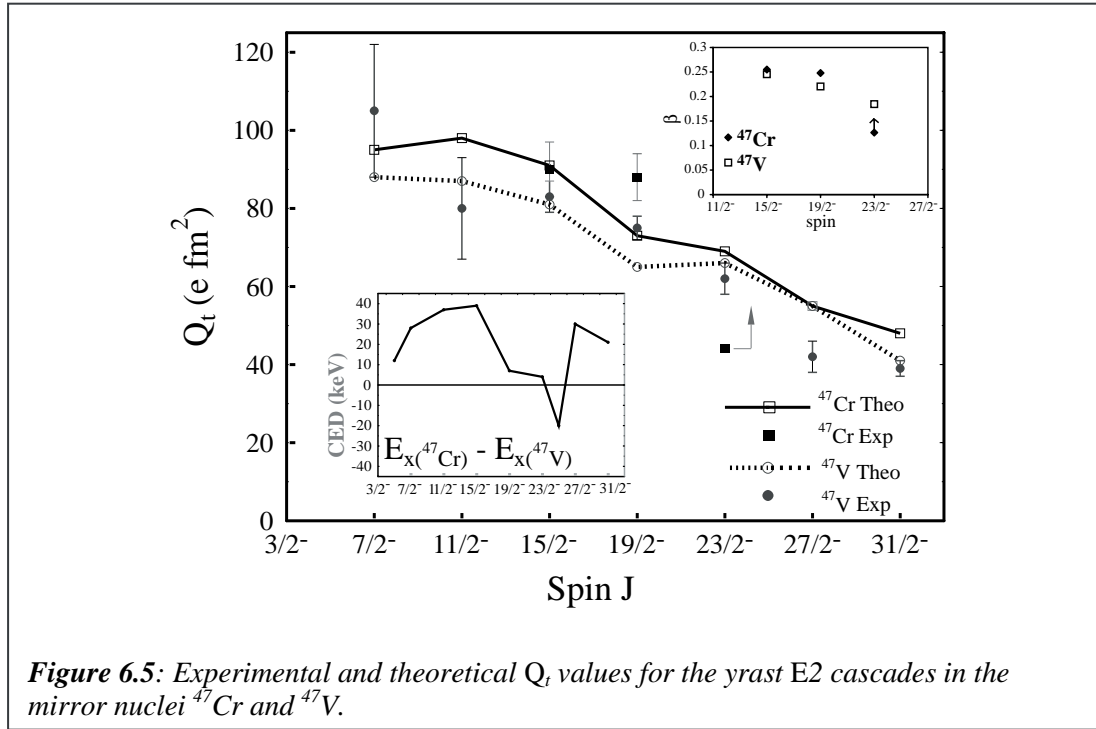
Figure 6.5: *Experimental and theoretical* Q_t *values for the yrast* E2 *cascades in the mirror nuclei* ^{47}*Cr and* ^{47}*V.*
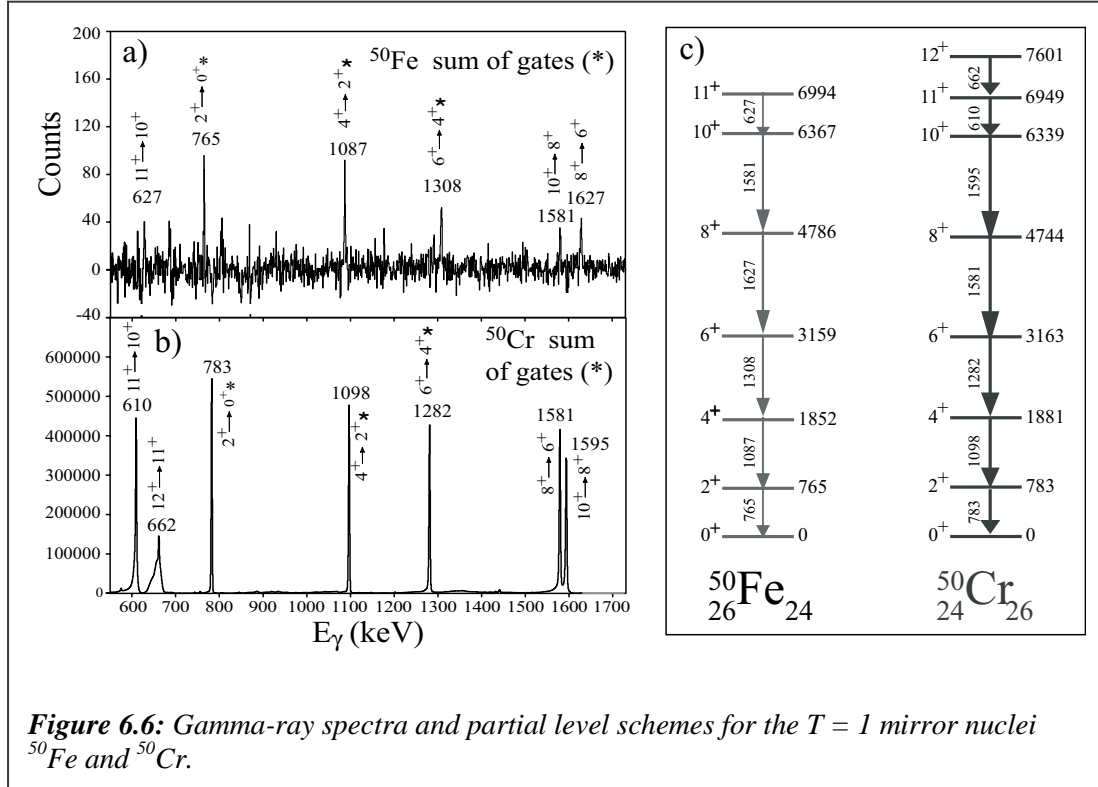
It is important to note that the ratios of the mirror *E*2 strengths are close to those of the square of the total charges, as one would expect for two geometrically identical and uniformly charged rotors.

Coulomb energy differences

Isospin symmetry is revealed experimentally as nearly identical spectra in pairs of mirror nuclei. The Coulomb contribution to the bulk energy in a nucleus, which is proportional to Z^2, can be of the order of hundreds of MeV. The displacement energies (CDE) between analog ground states, which vary as *Z,* can be as large as tens of MeV. When we come to Coulomb energy differences between *excited* analog states in mirror nuclei, the effects become so small (10-100 keV) that they can be treated in first order perturbation theory, i.e., by taking the expectation value of the Coulomb potential between nuclear wave functions of good isospin. Given that large effects have been eliminated in the CED, and that the wave functions remain essentially unperturbed, the Coulomb field becomes a delicate probe of *nuclear* structure.

In particular, as stated in the previous section, the alignment of pairs of nucleons in the backbending region can be inferred from CED's between mirror nuclei. These studies were so far limited to odd-mass (*T* = 1/2) nuclei and their extension to even-mass nuclei (*T* = 1) became feasible only with EUROBALL.

One of the best rotors in the $f_{7/2}$ shell is the nucleus ^{50}Cr [163] (β = 0.25) which presents a backbending at I^{π}=10$^+$. No γ rays were known in its mirror (*N* = *Z* - 2, T_Z = -1) nucleus ^{50}Fe. An experiment was done in LNL using EUROBALL to investigate the high spin structure in ^{50}Fe. Together with ^{50}Cr it constitutes the heaviest *T* = 1 mirror pair studied using γ-ray spectroscopy techniques and it is the first case in which *T* = 1 rotational bands can be investigated at the backbending region. The nucleus ^{50}Fe was produced in the reaction ^{28}Si+ ^{28}Si at 110 MeV bombarding energy, after the evaporation of one α-particle and two neutrons

Figure 6.6: *Gamma-ray spectra and partial level schemes for the T = 1 mirror nuclei* ^{50}*Fe and* ^{50}*Cr.*

[169]. The target consisted of 0.85 mg/cm^2 of ^{28}Si (enriched to 99.9%) with a 15 mg/cm^2 gold backing. Gamma rays were detected with the EUROBALL array where the forward 1π solid angle was covered by the Neutron Wall. Charged particles were detected with the ISIS array.

In Figure 6.6(a) a spectrum corresponding to a sum of gates on the lowest three transitions assigned to ^{50}Fe is shown. It was obtained from a matrix constructed by adding a γ-γ matrix in coincidence with neutrons and one α-particle plus another matrix coincident only with neutrons (with a veto for any charged particle). The latter matrix takes into account those α-particles not detected due to the low efficiency detection. For comparison, the spectrum for ^{50}Cr (α2p reaction channel) is shown in Figure 6.6(b). It was obtained as a sum of spectra gated on the first three analog transitions in ^{50}Cr in a γ-γ matrix in coincidence with one proton. Due to the different trigger conditions in the two cases, it is difficult to give a precise relative cross section. An estimated ratio of the cross sections is $\sigma(^{50}\text{Cr})/\sigma(^{50}\text{Fe}) \approx 10^4$.

Both level schemes are shown in Figure 6.6(c) where the backbending above $I^\pi=8^+$ can be seen. Different interpretations have been given to this backbending in terms of band crossing with a high *K* band or with an oblate band. Shell model calculations indicate that the rotational behaviour changes at $I^\pi=10^+$ to a weakly deformed regime. This is consistent with the sharp decrease of quadrupole collectivity observed in lifetime measurements at the 10_1^+ state [160]. Above this spin the extracted *B(E2)* values suggest that the ground state band continues in the yrare 10_2^+ and 12_2^+ states [160,163].

By resorting to the CED, the effect of nucleon alignment can be inferred. The role of the Coulomb force is clear: Repulsion is weakest for aligned protons, because the overlap of wave functions is smallest. Hence, we expect a jump in CED at backbending, whose sign will depend on which fluid (neutrons or protons) aligns first. While in odd-mass nuclei the blocking effect in the odd fluid favours alignment in the even one [165,170], in even-even nuclei the choice is not *a priori* evident. Experimental and shell model CED's for the *A* = 50
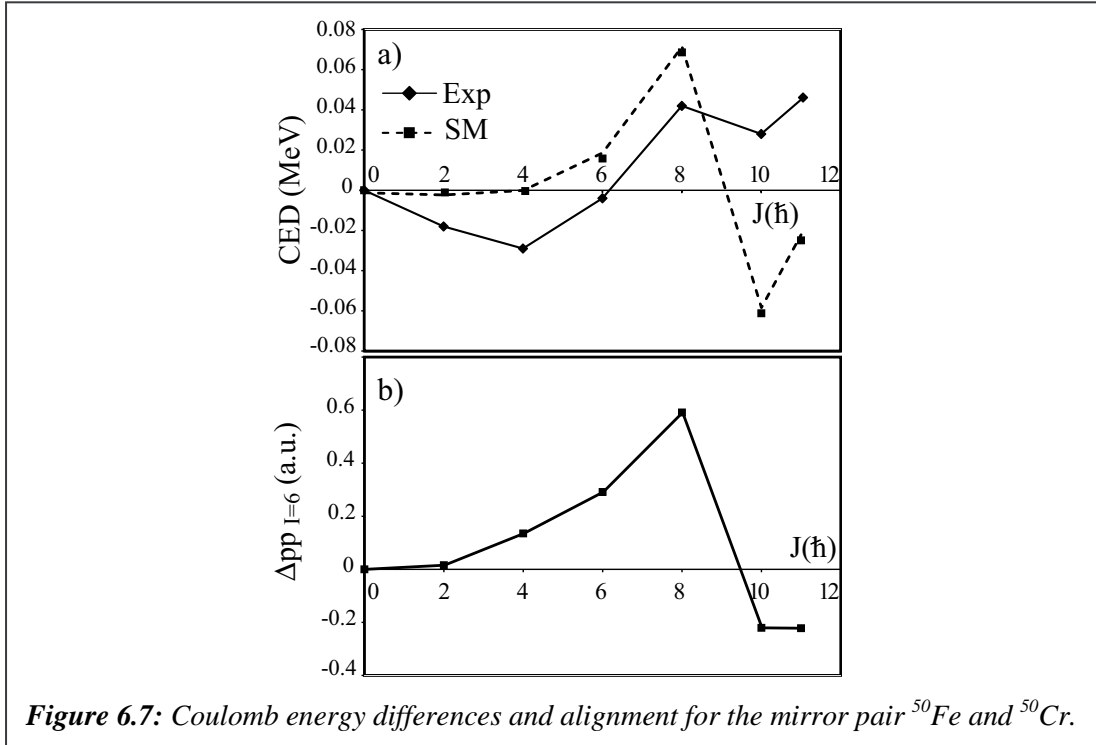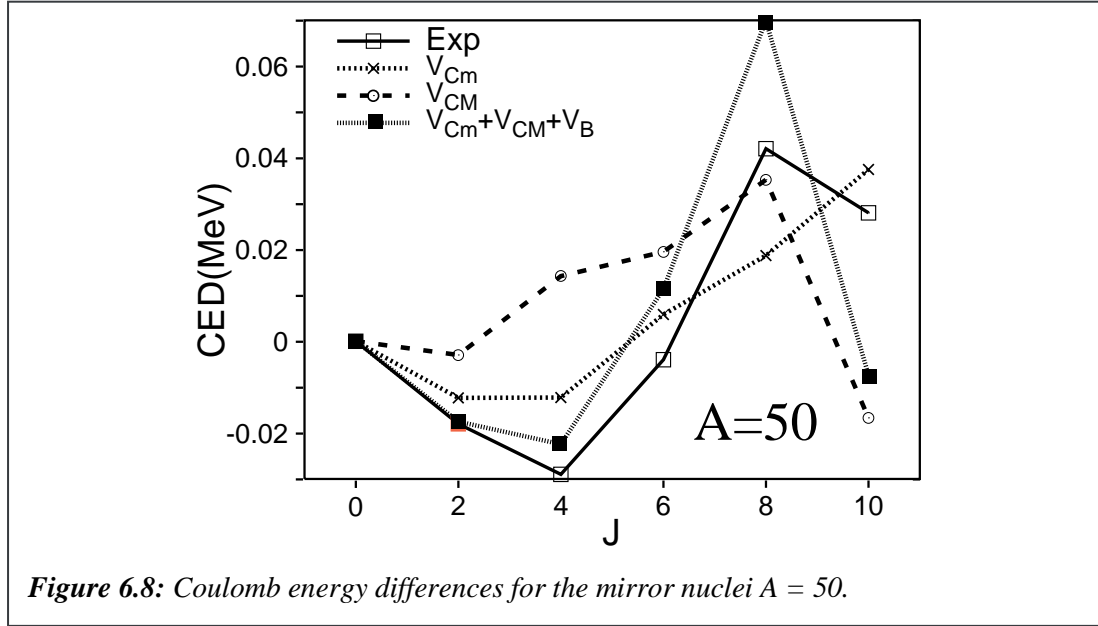
Figure 6.7: *Coulomb energy differences and alignment for the mirror pair ^{50}Fe and ^{50}Cr.*

mirrors are reported in Figure 6.7(a). A rapid increase is observed at $I = 8$ followed by a decrease at $I = 10$. The trend is reproduced but grossly emphasized by shell model calculations in the full *pf* shell (dashed line). The interaction is KB3 with Coulomb matrix elements in the harmonic oscillator basis, except for those involving only the $f_{7/2}$ orbits, which are extracted from the CED of the ^{42}Ti-^{42}Ca mirror nuclei. In Figure 6.7(b) we report the difference in the expectation value of the operator $A = [(a^+a^+)^{J=6} (aa)^{J=6}]^0$ which "counts" the number of maximally aligned pairs in the $f_{7/2}$ shell [171]. In this plot, the difference is between the number of aligned protons minus the number of aligned neutrons in ^{50}Cr (the opposite happens in ^{50}Fe). The similarity of the curves in the Figures 6.7(a) and (b) suggests the connection between backbending and alignment. One can thus deduce that a pair of protons in ^{50}Cr (neutrons in ^{50}Fe) aligns first, and pairs in the other fluid later, at higher angular momentum. This agrees with the predictions done in the framework of cranked shell model calculations [172].

To have a better quantitative description of the experimental data in CED's, in Ref. [169] one has to consider the change in radii along the yrast bands. In the *pf* shell they originate in differences between the 1*f* and 2*p* orbits. The latter have a larger radial extension, which leads to the Thomas-Ehrmann shift in ^{41}Sc where the excitation energy of the $p_{3/2}$ level is 200 keV below its analog in ^{41}Ca. The deformed yrast states have large $p_{3/2}$ admixtures, and hence larger radius and smaller Coulomb energies than their aligned counterparts. Within the shell model, orbital occupancies are translated into changes in radii. This is a residue of the mono-pole Coulomb contribution and taking it into account the theoretical description improves.

However, this is not enough to reproduce satisfactorily the data and in Ref. [169] the need for a renormalization of the multipole component of the Coulomb contribution was suggested. This gave a good quantitative agreement for the CED's not only in the case of $A = 50$ but also for the $T = 1/2$ mirror pairs measured in the $f_{7/2}$ shell ($A = 47$, 49 and 51) [173].

Figure 6.8: *Coulomb energy differences for the mirror nuclei A = 50.*

Only very recently, when data for $T = 1$ bands in the $N = Z$ odd-odd members of the multiplets were available, it became clear that the Coulomb effects were not the only thing responsible for the isospin symmetry breaking. The experimental triplet energy differences [174] cannot be reproduced with the renormalisation suggested in Ref. [169]. Data indicate that the role of isospin non conserving *nuclear* forces could be as important as the one of the Coulomb field in the observed CED's between mirror nuclei and among the members of the triplets [174].

Following the notation of Ref. [174], the CED's at spin *I* for a mirror pair can be obtained theoretically as:

$$CED_I = E_I^*(Z > N) - E_I^*(Z < N) = < V_{Cm} >_I + < V_{CM} >_I + < V_B >_I \tag{4}$$

where V_{Cm} is the monopole component of the Coulomb field that accounts for the changes in nuclear radii. V_{CM} is the multipole Coulomb component calculated using harmonic oscillator matrix elements in the *pf* shell; and V_B is the "nuclear" isospin non conserving term. This latter term is deduced from the A=42 data, thus allowing for a parameter free description of the CED data for the heavier mirrors in the $f_{7/2}$ shell. The calculated CED for the mirror nuclei ^{50}Fe-^{50}Cr is shown in Figure 6.8 (taken from Ref. [174]).

Very good fits are also obtained for the CED of the other mirror nuclei in this mass region. When the *N=Z* odd-odd member [175] of the T=1 A=50 triplet is taken into account in calculating the triplet energy differences, the agreement with the experimental data is excellent [174].

In an experiment performed on April 2003 with EUROBALL, EUCLIDES and the Neutron wall, the ground-state band of the extremely neutron-deficient nucleus ^{54}Ni was observed up to $I^\pi = 6^+$ by A. Gadea and collaborators. The measured CED with its mirror ^{54}Fe gives almost the same absolute values as obtained for the cross-conjugate pair in the $f_{7/2}$ shell ^{42}Ca-^{42}Ti and as expected from the particle-hole symmetry. In particular, an increase of the CED at $I = 2$ is observed in these two pairs, which cannot be explained by considering only the Coulomb interaction and constitutes the basic ingredient in the "nuclear" isospin non-conserving term.
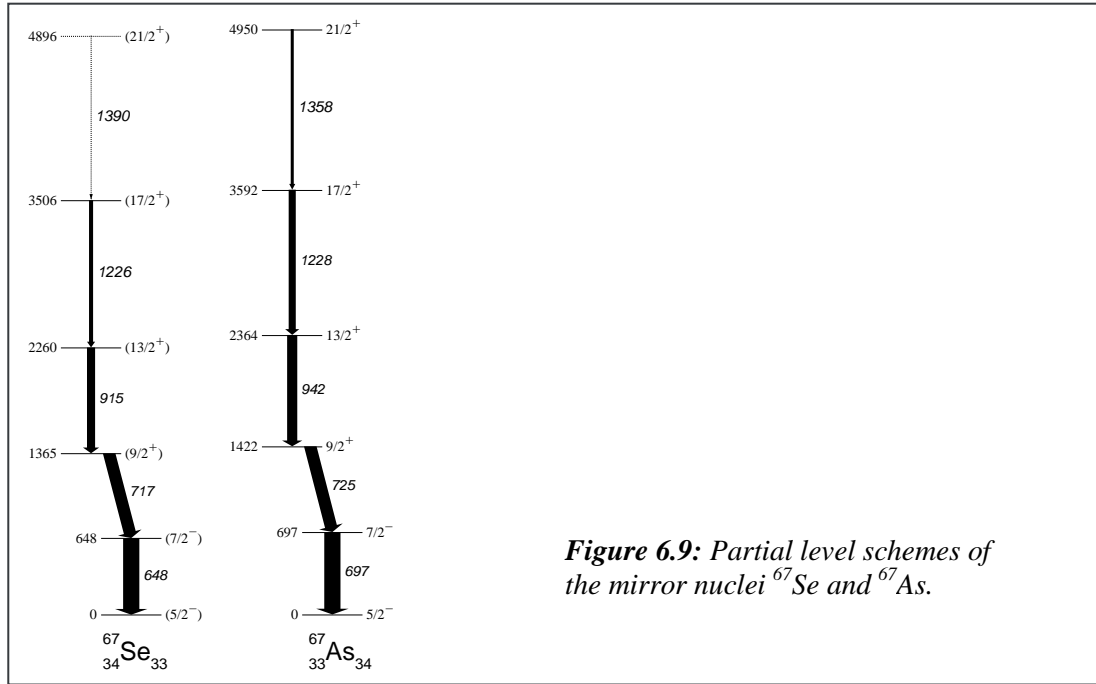
***Figure 6.9:** Partial level schemes of the mirror nuclei ^{67}Se and ^{67}As.*

The extension of these investigations to other mass regions is in progress. In particular, new data from EUROBALL has been obtained recently for the mirror nuclei *A*=67 with the reaction ^{32}S on ^{40}Ca at 90 MeV bombarding energy. The mirrors ^{67}Se and ^{67}As were studied at IReS Strasbourg with EUROBALL IV combined with the charged-particle array EUCLIDES and the Neutron Wall. The level schemes shown in Figure 6.9 are taken from Ref. [176]. In this case an unexpected behaviour is observed for the CED's which awaits for new detailed theoretical calculations.

6.4.   Conclusions and perspectives

In the last few years, we have explored new aspects of the isospin symmetry in nuclei at high angular momentum with EUROBALL. These investigations have been possible thanks to the high efficiency for detecting gamma rays and to the high sensitivity achieved with ancillary detectors such as the charged-particle arrays ISIS and EUCLIDES, the Neutron Wall, and the Köln plunger.

The measurement of forbidden *E*1 transitions in *N=Z* nuclei has enabled an estimate of their degree of isospin mixing. A great amount of information has also been obtained from mirror nuclei. The measurement of the lifetimes in *E2* cascades (A=47) probes the nuclear structure and shape changes at the backbending region in rotational bands.

Comparisons of the excitation energies in mirror nuclei have revealed the nature and the mechanism of backbending in rotating nuclei. Moreover, they also give information on the evolution of radii along the yrast bands and provide direct evidence for charge symmetry breaking of the nuclear field.

In the future the availability of high intensity stable beams and radioactive proton rich beams will enable these studies to be extended to analog yrast or quasi-yrast bands up to the limit of nuclear stability. In particular, it will be interesting to explore isobaric multiplets with T > 1

and heavier mirror nuclei, where the effects of isospin symmetry breaking are expected to be stronger.

Acknowledgements

Studies of N = Z nuclei beyond ^{56}Ni

D. Rudolph

7. Studies of *N~Z* nuclei beyond ⁵⁶Ni[*]

7.1. Introduction

The study of nuclei far from stability at the extreme values of *N/Z* is one of the major incentives of the existing and projected radioactive ion-beam facilities around the world. By investigating such exotic species certain terms of the nuclear Hamiltonian can be viewed under a magnifying glass, which are otherwise difficult to access. The region of interest of the nuclidic chart, namely *N~Z* nuclei between ^{40}Ca and ^{100}Sn is shown in Figure 7.1 together with some of the physics issues that have been addressed by EUROBALL studies. The horizontal and vertical lines in this figure mark the magic and semi-magic numbers 20, 28, 40, and 50, and the red squares represent the compound nuclei formed in the fusion-evaporation reactions used in the experiments. The size of these squares scales with the number of experiments, i.e., the larger the square the more studies employed a given compound nucleus.

In a typical fusion-evaporation experiment aimed at the spectroscopy of *N~Z* nuclei, 20 to 30 different residual nuclei are populated with relative cross sections ranging from fractions of a percent up to more than 30%. Since the nuclei of interest are often those with tiny cross-sections, involving one or even multiple neutron evaporation, the coincident detection of γ rays and evaporated neutrons is of vital importance. Despite their significant contribution to the aspect of reaction channel selection, the charged-particle detection arrays surrounding the target serve yet another issue. The exclusive measurement of energies and momenta of the evaporated neutrons, protons, and especially α-particles has enabled an event-by-event determination of the velocity vector of the recoiling nuclei. Depending on the mass region and the nucleus of interest, this kinematical correction procedure may improve the γ-ray energy
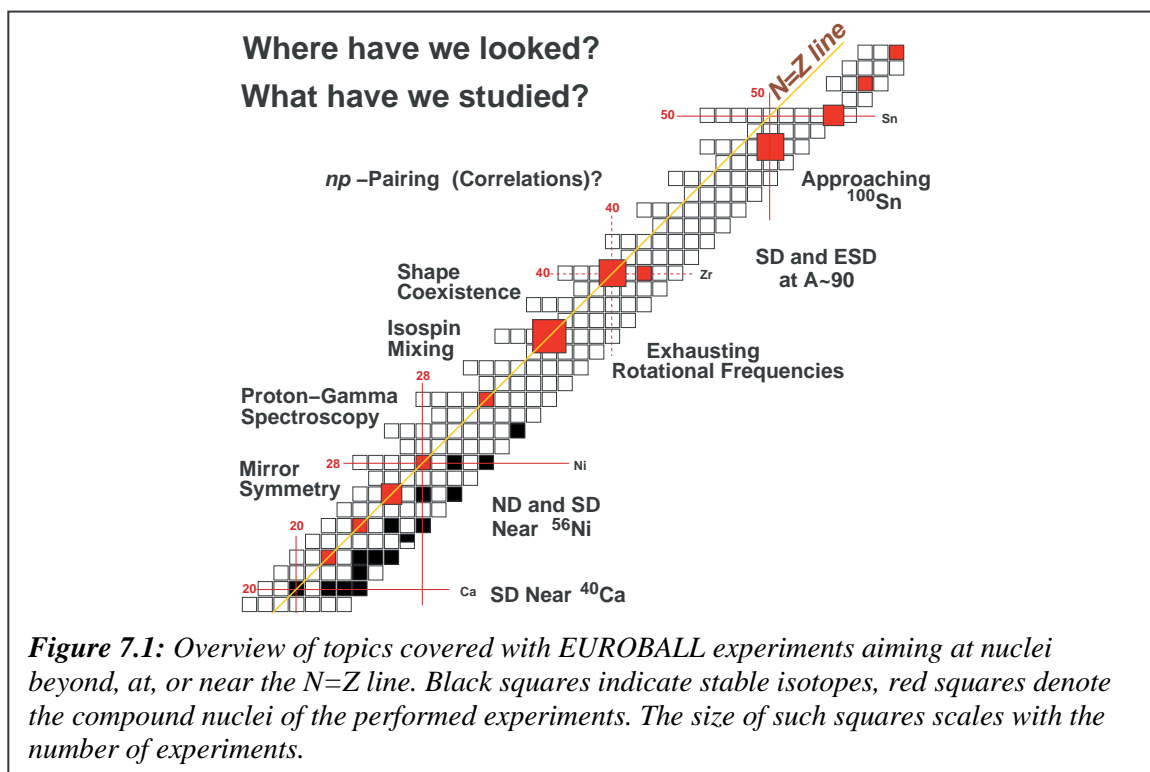
Figure 7.1: *Overview of topics covered with EUROBALL experiments aiming at nuclei beyond, at, or near the N=Z line. Black squares indicate stable isotopes, red squares denote the compound nuclei of the performed experiments. The size of such squares scales with the number of experiments.*

---

[*] Contribution by D. Rudolph

resolution by a factor of two to three, which in turn increases the sensitivity of the experimental set-up by almost the same magnitude.

It is important to note that up to ^{40}Ca the line of stability coincides with the $N{=}Z$ line, which is marked by the yellow diagonal line in Figure 7.1. Beyond ^{56}Ni, however, the line of stability bends more and more towards more neutron-rich nuclei, such that ^{100}Sn is twelve neutrons away from the most neutron-deficient, stable Sn isotope ^{112}Sn. ^{100}Sn is the last particle bound $N{=}Z$ nucleus, while the proton drip line more or less equals the $N{=}Z$ line starting from mass $A{\sim}70$ for the odd-Z nuclei.
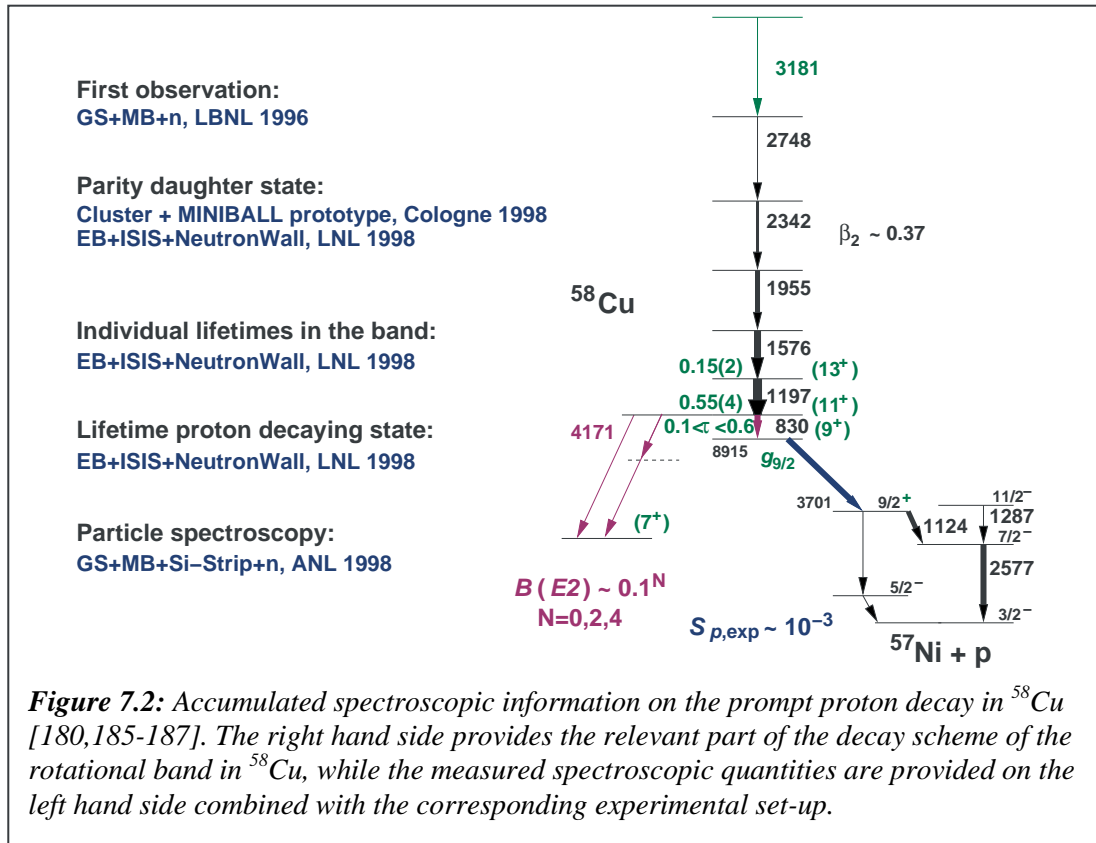
Medium heavy nuclei on the neutron deficient side of the valley of stability can be produced using a combination of stable beams and targets. But the increasing difference between the stable isotopes and the $N{=}Z$ line puts severe constraints on the present-day experimental possibilities: ^{80}Zr marks the heaviest $N{=}Z$ compound nucleus, which can be formed with stable beams and targets, namely via the reaction ^{40}Ca$+^{40}$Ca. This implies that up to ^{72}Kr even-even $N{=}Z$ nuclei can be studied via 2α-evaporation. Starting from ^{76}Sr and up to ^{96}Cd the possible reaction channels involve two-neutron evaporation, while the population of excited states in ^{100}Sn would imply the evaporation of four neutrons. This scheme is reflected by the compound nuclei chosen for the EUROBALL experiments (cf. red squares in Figure 7.1). Similarly, odd-odd $N{=}Z$ nuclei up to ^{78}Y can be reached via 1p1n- or 1α1p1n reactions, while the study of heavier odd-odd $N{=}Z$ nuclei requires the population via three neutron evaporation.

It is important to recall that the evaporation of any additional neutron typically reduces the relative cross section by a factor of fifty to hundred, on top of the general decrease of the cross section with increasing mass, i.e., ~2 mb for ^{56}Ni down to ~1 μb in the case of ^{96}Cd. In-beam studies with present-day techniques and available stable beam-target combinations can probe cross section down into the few μb regime. However, it is not only the absolute but also the relative cross section which is of importance. Depending on the efficiency and quality of the channel selection, tiny components ($< 0.1\%$) of heavier, more neutron-rich isotopes of the target species or common problems with oxygen and/or carbon contaminations of the target material may inhibit a clear identification of exotic reaction channels. It appears that studies of $N{=}Z$ nuclei beyond ^{96}Cd and ^{78}Y, respectively, have to await more efficient future spectrometers in conjunction with intense radioactive beams.

7.2. Exotic decays

For nuclei above mass $A = 40$ the $N = Z$ line drifts more and more away from the line of stability with increasing mass of the nuclei. Together with a rather small Coulomb barrier this gives rise to an intriguing facet of the heavier $N \sim Z$ nuclei, namely that proton, α-, or even cluster emission may play a role in the decay of their excited states. For a more general recent review of in-beam and decay work of $N{\sim}Z$ nuclei we refer to [177]. Another related facet of medium-mass $N{\sim}Z$ nuclei is the astrophysical rapid proton capture process, which is thought to follow them from about mass $A{\sim}60$ up to ^{100}Sn. A number of nuclear structure features of specific $N{=}Z$ nuclei provide important input into the respective modelling of stellar evolution scenarios (see, e.g., Ref. [178]).

Soon after the mass $A \sim 60$ regime had been marked as a region of superdeformed nuclear shapes [179], some of the rotational bands associated with the second minimum of the nuclear

Figure 7.2: *Accumulated spectroscopic information on the prompt proton decay in ^{58}Cu [180,185-187]. The right hand side provides the relevant part of the decay scheme of the rotational band in ^{58}Cu, while the measured spectroscopic quantities are provided on the left hand side combined with the corresponding experimental set-up.*

potential were found to decay via mono-energetic prompt proton- or α-particle emission [180-184]. This new particle decay mode, which was first established in ^{58}Cu [180] competes with in-band and γ-ray linking transitions between the well- (or super-) deformed states and the spherical states in the first minimum of the potential energy surface. In ^{58}Cu the prompt proton decay connects the lowest observed state in the rotational band with the spherical neutron $g_{9/2}$ single-particle state in ^{57}Ni [185].

The relevant part of the decay scheme of ^{58}Cu is provided in Figure 7.2. The left hand side of Figure 7.2 describes the progress in terms of spectroscopic information regarding the ^{58}Cu case starting from the first observation of the new decay in 1998 [180] until 2002. Within this period, the spin and parity of the daughter state in ^{57}Ni was determined [185], spins and parities were tentatively assigned to the band members, lifetimes of the low lying states in the band were measured [111], and last but not least the lifetime of the proton-decaying state could be limited to 0.1 ps $< \tau <$ 0.6 ps [186].

The latter two results were obtained from an experiment performed with EUROBALL coupled to the 4π ΔE-E Si-array ISIS [2] and the Neutron Wall [5]. The use of a backed target allows the Doppler Shift Attenuation Method (DSAM) to be used to determine lifetimes. The 830 keV line, which depopulates the 9745 keV state and feeds the proton-decaying level at 8915 keV, reveals both a stopped and a shifted component in its lineshape observed in the backward-angle Cluster section of EUROBALL. Therefore, energy correlations between the 830 keV γ ray measured in the Cluster detectors and the 2.3 MeV proton peak in the most forward detector elements of ISIS have been studied successfully, and it was possible to derive the above mentioned lifetime limits for the proton decaying state [186]. This experiment was the first attempt to perform in-beam high-resolution particle-γ coincidence spectroscopy.
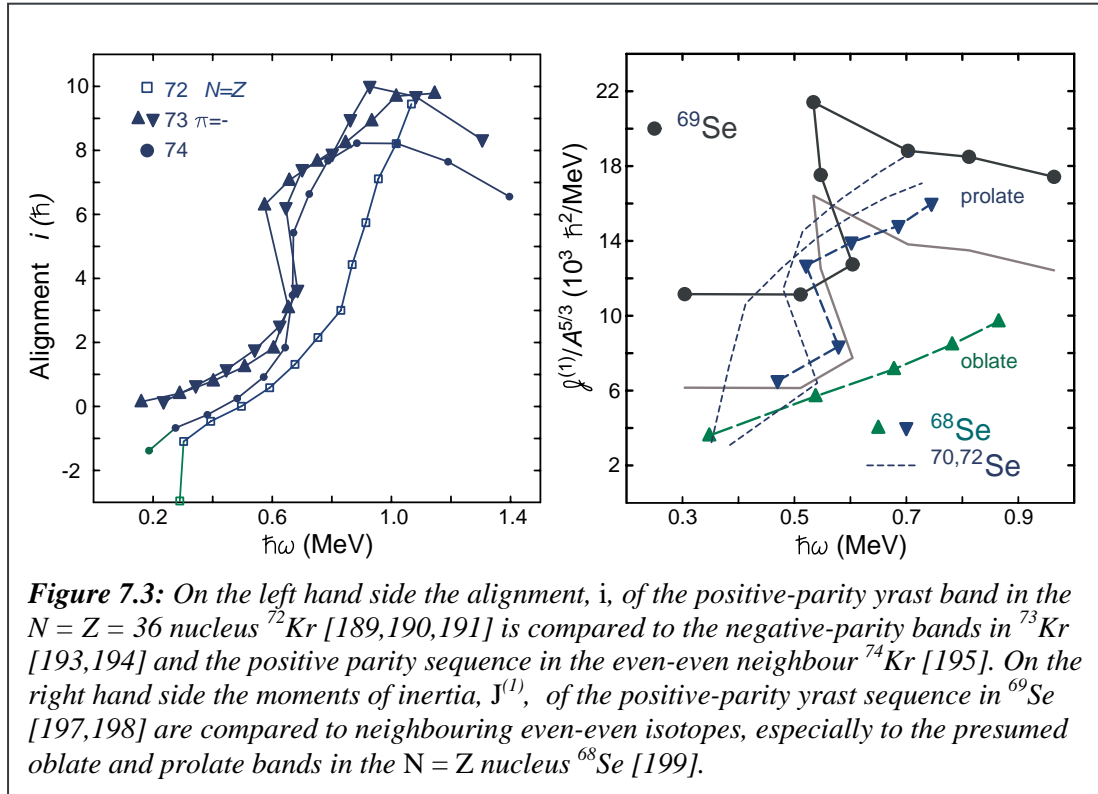
Lifetime measurements of the γ- and proton-decaying states suggest a similar hindrance for the single-step 4171 keV γ-ray transition and the $g_{9/2}$ proton decay. In fact, the proton decay appears to be somewhat less hindered (~10^{-3}) than the single-step γ decay (~10^{-4}). One possible explanation is that the emission of the $g_{9/2}$ proton naturally helps in reducing the deformation of the system, because it is moving in the shape driving orbit located more towards the surface of the deformed ^{58}Cu nucleus. It is also interesting to note that the deformation of the rotational band in ^{58}Cu increases towards the bottom of the band - more than expected employing contemporary mean-field calculations [111]. Similar to ^{60}Zn [188], there is evidence in ^{58}Cu that the decay-out from the second minimum in *N = Z* nuclei in the mass *A* ~ 60 region is rather selective - a scenario which is supported by the suppression of isoscalar dipole transitions in such nuclei, the low level density, and the small number of particles which need to be rearranged in the decay process.

7.3.   The mass *A* ~ 70 - 80 region

One possible indicator for the enhancement of neutron-proton pair correlations in *N = Z* nuclei is a delay of the alignment frequency of high-*j* orbits. In the mass *A* ~ 70 - 80 region all even-even *N = Z* nuclei between ^{72}Kr and ^{88}Ru exhibit such a delay of alignment of $g_{9/2}$ particles with respect to rotational bands in odd-*A* and *N = Z* + 2 even-even neighbours [189-192]. However, this mass region is also well known for sudden and drastic shape changes as a function of nucleon number and excitation energy, which clearly affect the band crossing phenomena. Therefore, it is equally important to study the nearest neighbours and check carefully, whether or not their structure can be explained with nuclear structure models that do not specifically include neutron-proton pair correlations. If the same models subsequently fail to reproduce the excitation pattern of the *N = Z* nuclei, then the presence of such pairing modes could be evidenced.

On the left hand side of Figure 7.3 recent results on a negative-parity band in ^{73}Kr obtained from both EUROBALL [193] and GAMMASPHERE [194] data are compared to the course of the alignment of the even-even nuclei ^{72}Kr [189-191] and ^{74}Kr [195]. Clearly, the crossing frequency for ^{72}Kr ($\hbar\omega$ ~ 0.9 MeV) found in these experiments is different from the one observed for ^{73,74}Kr ($\hbar\omega$ ~ 0.6 MeV). However, more recent results in ^{72}Kr indicate that the delay in alignment is less pronounced [196]. In all three cases the spin amount associated with the alignment indicates a simultaneous neutron and proton $g_{9/2}$ alignment. On the right hand side of Figure 7.3 the kinematic moments of inertia of several light Se isotopes are plotted. Recent results on the *N = Z* + 1 isotope ^{69}Se [197,198] are compared to heavier even-even Se isotopes (thin dashed lines) and the *N = Z* nucleus ^{68}Se, in which coexisting bands of oblate and prolate shape have been identified [199]. The positive-parity yrast band of the rather complex and irregular excitation scheme of ^{69}Se is a nice example of prolate-oblate shape coexistence. If one accounts for the polarisation effect of the odd neutron, the moment of inertia of this sequence (grey solid line) seems to evolve from an oblate shape in the beginning to a prolate shape after the first band crossing and possibly back to oblate shape at high spin again.

The advent of the latest generation of 4π Ge-detector arrays has not only enabled the identification of a few excited states of rare isotopes far from stability, it has also enabled us to observe somewhat less exotic nuclear species up to very high angular momenta, and in particular the termination of rotational bands, i.e., the evolution of a given configuration from collective rotation towards a state of single-particle character, for which the individual

Figure 7.3: *On the left hand side the alignment,* i, *of the positive-parity yrast band in the N = Z = 36 nucleus [72]Kr [189,190,191] is compared to the negative-parity bands in [73]Kr [193,194] and the positive parity sequence in the even-even neighbour [74]Kr [195]. On the right hand side the moments of inertia, J[(1)], of the positive-parity yrast sequence in [69]Se [197,198] are compared to neighbouring even-even isotopes, especially to the presumed oblate and prolate bands in the N = Z nucleus [68]Se [199].*
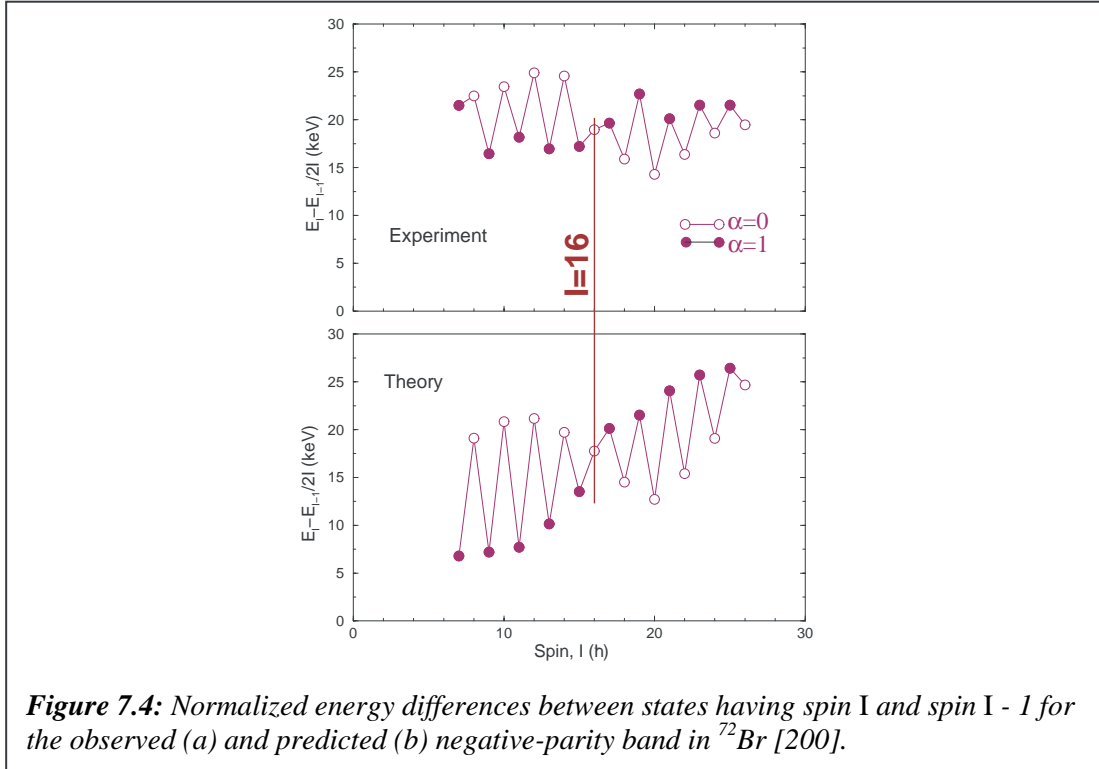
angular momenta of the participating nucleons are fully aligned along one axis (cf. Section 5). Based on EUROBALL data it was possible to derive the first case of band termination in the *A* ~ 70 - 80 region, namely in [73]Br [141]. The highest states observed lie at about twice the excitation energy (E_{max} ~ 25 MeV) than known from spectrometers of the previous generation, the spin exceeds 30$\hbar$, and the γ-ray energies at the top of the bands (up to E_γ ~ 3.7 MeV) mark the fastest rotating systems ever observed, along with the superdeformed bands in the *A* ~ 60 region (see above).

The second topic related to high-spin phenomena is the observation of a signature inversion in a pair of negative-parity bands in [72]Br [200]. The signature splitting and eventual inversion can best be seen when the energy differences of subsequent states are plotted as a function of spin (see Figure 7.4). In both experiment (top) and calculation (bottom) the signature α = +1 odd-spin states are favoured energetically at low spin, while the inversion occurs at spin *I* = 16$\hbar$. This is very different from other odd-odd nuclei in the mass region, which often reveal signature inversions in positive-parity bands at relatively low spin *I* = 9$\hbar$, which is the maximum value of an aligned neutron and proton moving in orbitals of the $g_{9/2}$ shell.

In general, signature inversion is viewed as a fingerprint for triaxiality in nuclei [cf. Section 2]. The only explanation of the high-spin signature inversion in [72]Br is the evolution from a triaxial shape rotating around the intermediate axis to a triaxial shape with rotation around the smallest axis [200]. The detailed interpretation of the data reveals the importance of the low-*j* orbitals of the *fp* shell.

Another significant part of the studies with EUROBALL has been devoted to odd-odd *N* = *Z* nuclei. Two issues seem to be important for all such nuclei - the features of rotational bands, which evolve at high angular momentum, and the determination of the *T* = 1 isobaric analog states, which are difficult to access due to their energetic location relatively high above the
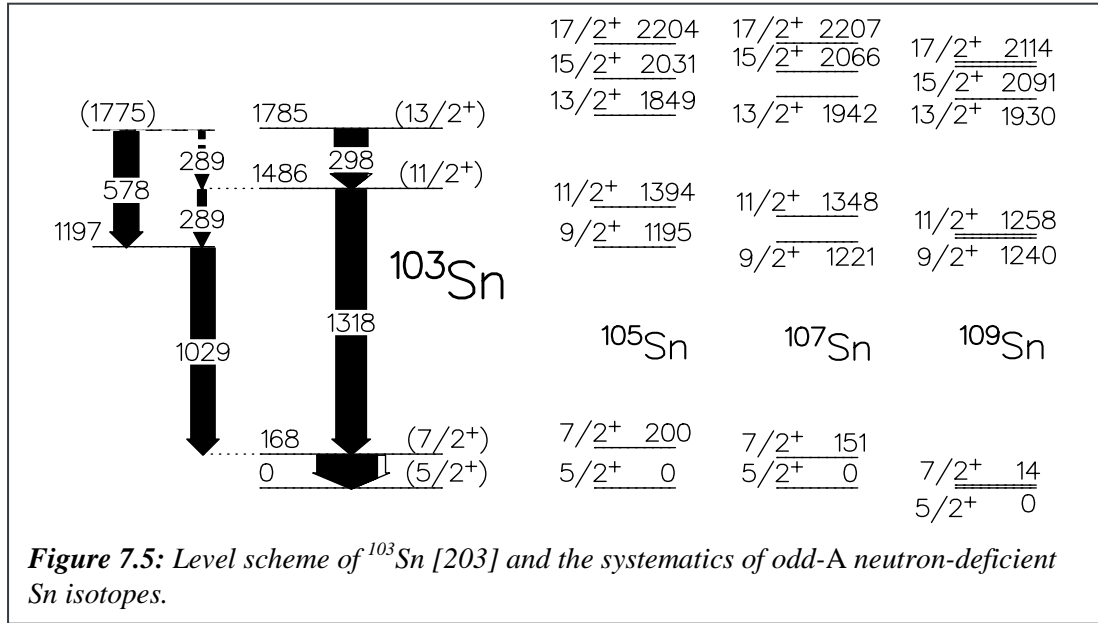
Figure 7.4: *Normalized energy differences between states having spin* I *and spin* I *- 1 for the observed (a) and predicted (b) negative-parity band in* ^{72}Br *[200].*

yrast line. For the former, new results in ^{66}As indicate the existence of a prolate deformed band in the spin regime ~ $13 \leq I \leq$ ~ 23. Interestingly, this band has an unsually large moment of inertia. The analysis is still in progress [201]. Excited states in ^{70}Br were identified for the first time, including $T = 1$ isobaric analog states up to spin $I = 8$ [202]. The surprising result is that the energy differences $E_x(^{70}\text{Br})$-$E_x(^{70}\text{Se})$ take negative values for the four known states, while corresponding numbers for other pairs of nuclei (^{50}Mn-^{50}Cr, ..., ^{74}Rb-^{74}Kr) are basically all positive. In principle one would expect no difference between neutron-proton and neutron-neutron interactions if the states were pure seniority $\nu = 2$ excitations. A positive energy difference implies that more proton pairs have to be aligned in the even-even $T_z = 1$ nucleus compared to its $T_z = 0$ odd-odd $N = Z$ neighbour. This can be understood because protons may be bound in neutron-proton pairs in these nuclei. The negative energy difference for the $A = 70$ pair is probably due its close proximinity to the proton dripline: An increased proton radius due to weak binding leads (*i*) to a reduction of the Coulomb repulsion (Thomas-Ehrman shift) and (*ii*) reduces neutron-proton two-body matrix-elements of in particular low-*j* orbitals, thus leading to a less bound 0^+ state [202].

7.4.   Approaching ^{100}Sn

^{100}Sn is the heaviest particle-bound nucleus having the same number of neutrons and protons, $N = Z = 50$. It is expected to reveal all the expected characteristics of a doubly magic nucleus lying far from the line of stability. Since doubly magic nuclei can be considered as bench marks within the chart of nuclides, this explains the experimental and theoretical efforts put into the study of nuclei in the vicinity of ^{100}Sn.
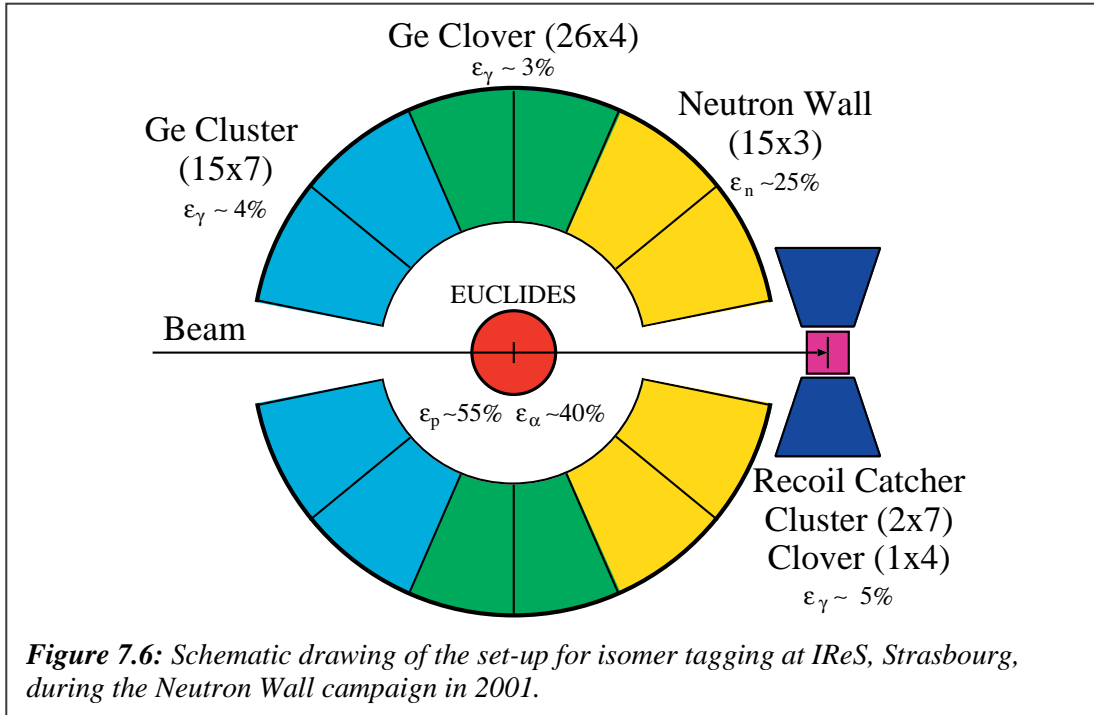
A number of experiments at EUROBALL have been devoted to specific aspects of the ^{100}Sn region, namely to study the shell structure by means of investigations of single-particle

Figure 7.5: *Level scheme of ^{103}Sn [203] and the systematics of odd-*A *neutron-deficient Sn isotopes.*

energies and the two-body (neutron-proton) residual interactions, and core polarizations of various kinds. Of course, the neutron single-particle energies could be derived best from excited states in ^{101}Sn. However, at present this extremely neutron deficient nucleus does not seem accessible for in-beam studies. Therefore, the single-particle energies have to be estimated from known excited states in more remote neighbours of ^{101}Sn by comparing them to predictions of shell-model calculations using an appropriately comprehensive model space as well as a realistic interaction. However, the further away one moves from the doubly magic core the more hampered such estimates become because of uncertain two-body interactions and/or restrictions in the tractable model space.

Currently, the best possible information on neutron single-particle energies comes from new information in ^{103}Sn [203]. Together with ^{97}Ag, which was the focus of another EUROBALL experiment, ^{103}Sn marks the closest approach to ^{100}Sn in terms of odd-*A* nuclei, the knowledge of which is vital for the experimental determination of the single-particle energies. These in turn provide stringent test of the mean-field models. Figure 7.5 shows on the left hand side the previously unknown excitation scheme of ^{103}Sn, which is compared to heavier odd-*A* Sn isotopes on the right hand side. The energy difference of 168 keV between the $5/2^+$ and $7/2^+$ states yields the most accurate result to date for the relative energies of the neutron $d_{5/2}$ and $g_{7/2}$ orbitals with respect to ^{100}Sn. Using an interaction based on the Bonn-A potential an energy difference of 110(40) keV can be derived. The error reflects uncertainties related to variations of the effective interaction [203].
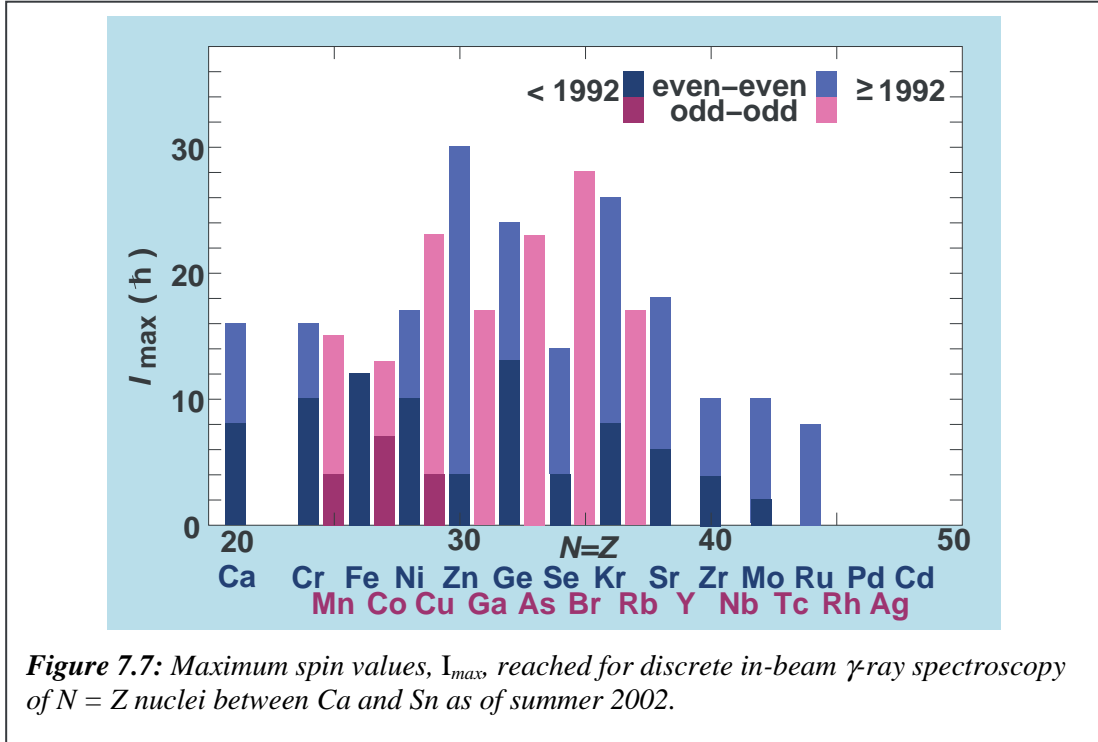
The identification of excited states in ^{103}Sn shows that scarce data in exotic nuclei is often more valuable than ample information on nuclei closer to the line of stability. Evidence for excited states in ^{95}Ag has been presented recently [204]. Another key isotope is ^{100}In, which has one neutron and one proton hole relative to the ^{100}Sn core. The identification of excited states in ^{100}In will provide important information on neutron-proton two-body matrix elements. An experiment has recently been performed at EUROBALL to achieve this goal. Presently, excited states in ^{98}Ag, ^{102}In, and ^{106}Sb provide the best grounds for studying the neutron-proton interaction near ^{100}Sn. In particular, resent results in ^{102}In, which include core-excited states, reveal new information on neutron-proton matrix elements, namely on the $\nu(h_{11/2}) \otimes \pi(g_{9/2})^{-1}$ multiplet [205,206].

Figure 7.6: *Schematic drawing of the set-up for isomer tagging at IReS, Strasbourg, during the Neutron Wall campaign in 2001.*

The knowledge of excited states in the two $T_z = 1$ nuclei ^{98}Cd [207] and ^{102}Sn [208] yields the closest approach to ^{100}Sn to date. In both even-even neighbours, µs-isomers have been observed in a series of pre-EUROBALL experiments (PEX) at the NBI Tandem Accelerator Laboratory. The isomeric states correspond to fully aligned $\pi(g_{9/2})^{-2}_8$ and $\nu(g_{7/2})^2_6$ or $[\nu(g_{7/2})\otimes\nu(d_{5/2})]_6$ configurations, respectively. The comparison between the predicted and measured $B(E2;6^+\rightarrow4^+)$ transition strength in ^{102}Sn yields a relatively large polarizability induced by the two extra neutrons. However, the derived effective neutron charge, $e_\nu \sim 2.0$, is model dependent, because the wave functions of both the initial and final state, which are mixtures of mainly $d_{5/2}$ and $g_{7/2}$ components, rather strongly depend on the shell-model parameters used. In turn, the wave function of the 8^+ state in ^{98}Cd turns out to be rather insensitive to the parametrisations, while the originally measured half-life of the 8^+ isomer calls for an unexpectedly low effective proton charge of $e_\pi \sim 0.9$ [207].

The presence of a second, higher-lying isomer would be a possible solution to increase the effective proton charge to values in excess of unity. Indeed, an isomer study of neutron deficient nuclei near ^{100}Sn using a fragmentation reaction and subsequent in-flight separation techniques reported a shorter half-life for the 8^+ state in ^{98}Cd, which can be attributed to the on average lower angular momentum input of fragmentation reactions, i.e., the second, higher-lying isomer has not been populated.

The similarities between the shell structure of the ^{56}Ni and ^{100}Sn regions shall not remain unmentioned (see, e.g., Ref. [209] for a recent review). For example, polarisation effects or $E2$ and $M1$ correlations across the double shell closure should be present in both cases. In this respect it is interesting to note that (*i*) there is a well-known 10^+ high-spin isomer in ^{54}Fe, which is the two proton-hole nucleus relative to ^{56}Ni, and (*ii*) that the 2668 keV $6^+\rightarrow4^+$ core excitation transition in ^{58}Ni is nearly identical to the 2701 keV 2^+ energy in ^{56}Ni. Therefore, the identification of the corresponding core excited states in the ^{100}Sn region was the focus of two recent EUROBALL experiments aiming at ^{98}Cd and ^{102}Sn. Their dedicated set-up is

Figure 7.7: *Maximum spin values, I$_{max}$, reached for discrete in-beam γ-ray spectroscopy of N = Z nuclei between Ca and Sn as of summer 2002.*

sketched in Figure 7.6 and is a close resemblance of the original set-up used at NBI: The prompt evaporated particles are detected in EUCLIDES [5] and the Neutron Wall [7] and correlated with delayed γ-rays detected in two Cluster and one Clover Ge detector surrounding the recoil catcher. The combined information of these detector systems is then used to tag prompt γ radiation measured with the standard Cluster and Clover sections of EUROBALL. The analysis of these two experiments is in progress.

7.5. Perspectives

The combination of powerful ancillary devices and the EUROBALL spectrometer has led to a significant increase in knowledge concerning *N ~ Z* nuclei over the past few years. This is summarized schematically in Figure 7.7, which provides the maximum spin values reached for discrete in-beam γ-ray spectroscopy of *N = Z* nuclei before (dark histograms) and after 1992 (light histograms), i.e., with the advent of the latest generation of 4π Ge-detector arrays.

The limit of spectroscopy has been pushed into the Zr region, while the observation of a few states up to [96]Cd appears feasible with present day technology and techniques. The study of excited states in odd-odd *N = Z* nuclei seems to be limited to [78]Y, because starting from [82]Nb their production via stable beam-target combination involves the evaporation of at least three neutrons. Thus the next major breakthrough, for example, the identification of the 2[+] state in [100]Sn, will have to wait for the currently projected 4π gamma-tracking arrays (AGATA and GRETA), improved ancillary detectors, and possibly involve the use of (re-accelerated) unstable ions.

Until then, further evidence for the influence of neutron-proton pair correlations on high-spin properties might be gathered from either very high spin states in e.g., [48]Cr, or by deducing more detailed spectroscopic information for the heavier even-even *N = Z* systems such as

^{72}Kr, ^{74}Rb, ^{76}Sr, or possibly ^{80}Zr via lifetime measurements. Similarly, the quest for excited states in rare isotopes will continue - experiments have been performed at EUROBALL to hunt for ^{78}Y, ^{96}Cd, and ^{100}In.

Another direction could be more elaborate studies of particle-γ correlations, including the evaporated (charged) particles from the compound systems. Eventually hyperdeformed structures at very high angular momentum in more strongly populated nuclei near the *N ~ Z* line may become tractable.

Finally, other in-beam techniques are going to be exploited in the near future. For example, there are going to be attempts to further tighten the limits of the shell model parameters around ^{100}Sn by measuring the $B(E2;2^+\rightarrow0^+)$ values for several $N = 50$ isotones and light Sn isotopes via relativistic Coulomb excitation of secondary beams in the framework of the RISING campaign at GSI Darmstadt employing EUROBALL Cluster detectors. Further, new or updated techniques with respect to these fast radioactive secondary beams are currently being considered to derive static electric or magnetic moments of specific states or structures along the *N = Z* line.

Acknowledgements

Nuclei on the neutron–rich side of stability

A.G. Smith and M.-G. Porquet

8. Nuclei on the neutron-rich side of stability[*]

8.1. Introduction

The study of nuclei on the neutron-rich side of the valley of stability is an area of research in which great progress has been made since the introduction of large arrays of Compton-suppressed Ge detectors. For such nuclei, production methods at (low-energy) stable beam facilities are limited to deep inelastic, fusion-fission and spontaneous fission. These three classes of reactions have very different characteristics, both in the nuclei produced and in the angular momentum distribution achieved before γ-decay competes with neutron evaporation. Deep-inelastic reactions with heavy ion beams achieve high angular momentum, but are limited to the study of nuclei close to a stable target or beam. These reactions are the primary way to access neutron-rich nuclei with atomic numbers (Z) greater than around 65. Spontaneous fission provides the best available method to produce neutron-rich nuclei for *36 $\leq Z \leq$ 46* and *50 $\leq Z \leq$ 64*, albeit with rather low angular momentum. The fusion-fission reactions lead to the production of a compound system, which already has an appreciable angular momentum, and which due to a reduced barrier fission readily produces fragments with $I \lesssim 20$ $\hbar$. The enhanced excitation energy and angular momentum of the compound system washes out the shell effects that are responsible for asymmetric spontaneous fission and leads to a single-humped yield distribution centered on an atomic number roughly half that of the compound system, thereby filling in the gap in Z between the heavy and the light fragments distributions of spontaneous fission. In addition, the higher excitation energy and angular momentum of the fragments of fusion-fission reactions promotes neutron evaporation leading to products which are generally closer to stability than those observed following spontaneous fission. The three classes of reactions are clearly complementary, but not exhaustive in the ranges of spin and isospin of the nuclear states produced.

Experiments involving these three reaction mechanisms do share some of the same practical difficulties, namely that in each event there are generally two product nuclei, and, that there are many possible products from any given choice of reaction or spontaneously-fissioning source. In fission reactions there is an especially wide range of possible products - typical yields for a given isotope are of the order of 1% of the total. For this reason, the identification of data with a particular fragment requires exceptional selectivity, either through the use of high-fold γ data, where it is a set of energies of coincident γ rays that uniquely identifies the product, or by the direct measurement of Z and A of one or both of the products.

8.2. Gamma rays from fission fragments

Over the last decade there has been a dramatic increase in the available spectroscopic information relating to neutron-rich nuclei populated in spontaneous and heavy-ion induced fission. This renaissance in fission-fragment spectroscopy has been due primarily to the much increased resolving power of large arrays of germanium detectors. Through improved detection efficiency and high granularity, these arrays have made it possible to obtain reasonable rates for the detection of three coincident γ-rays out of the cascades of multiplicity ten that are typically produced in the decay of the secondary fission fragments (i.e. after neutron emission). In addition to the determination of the energies of excited levels, developments in spectroscopic techniques have allowed for information to be deduced
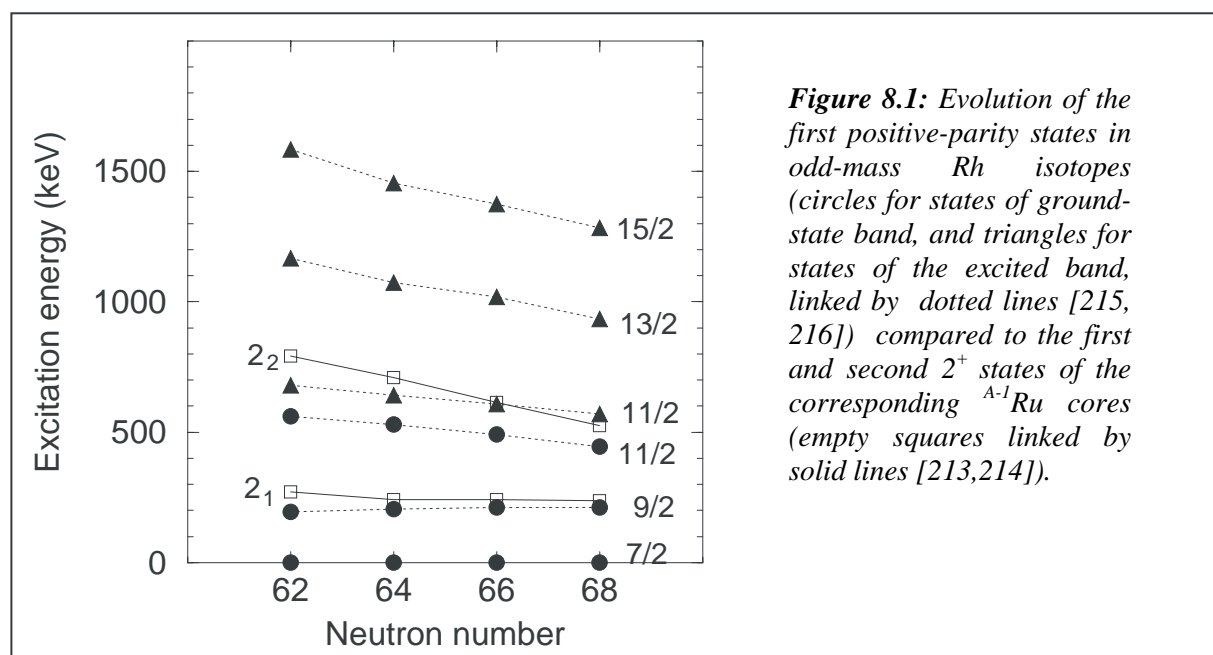

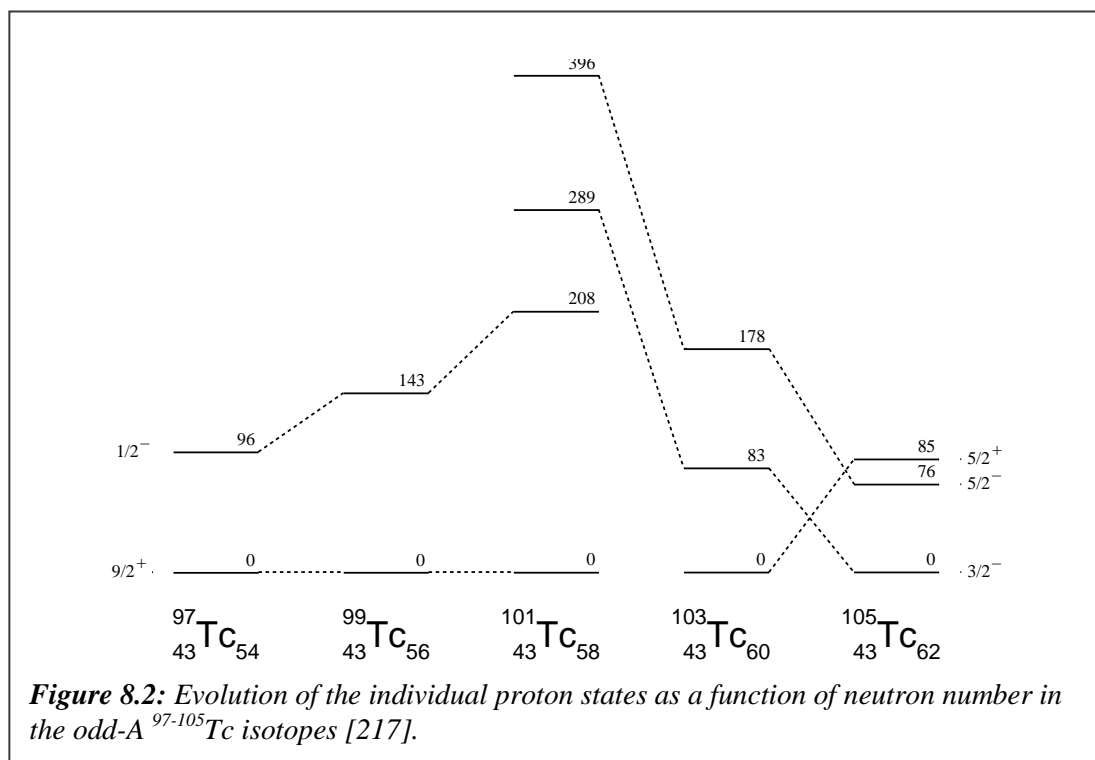[*] Contribution by A.G. Smith and M.-G. Porquet

regarding the spins and parities [210] and lifetimes [211] of such states of extreme isospin. EUROBALL has facilitated the continued investigation of the decay properties of fission fragments using established techniques but has also fostered the development of new methods for the measurement of *g*-factors and state lifetimes.

8.3.   Identification of new excited states in fission products

It is a testament to the richness of fission data and to the resolving power of the large Ge-detector arrays that a steady stream of publications containing new level schemes deduced from EUROGAM II experiments continues to complement the more recent work using EUROBALL. These large data sets, typically containing several times 10^9 events of γ–rays emitted from many tens of different fragments, encompass a microcosm of nuclear structure, including collective rotation and vibration, single particle motion, triaxiality and octupole deformation. In this section we take a brief tour of the recent highlights, putting them in the context of work carried out with the earlier phases of the EUROBALL device.
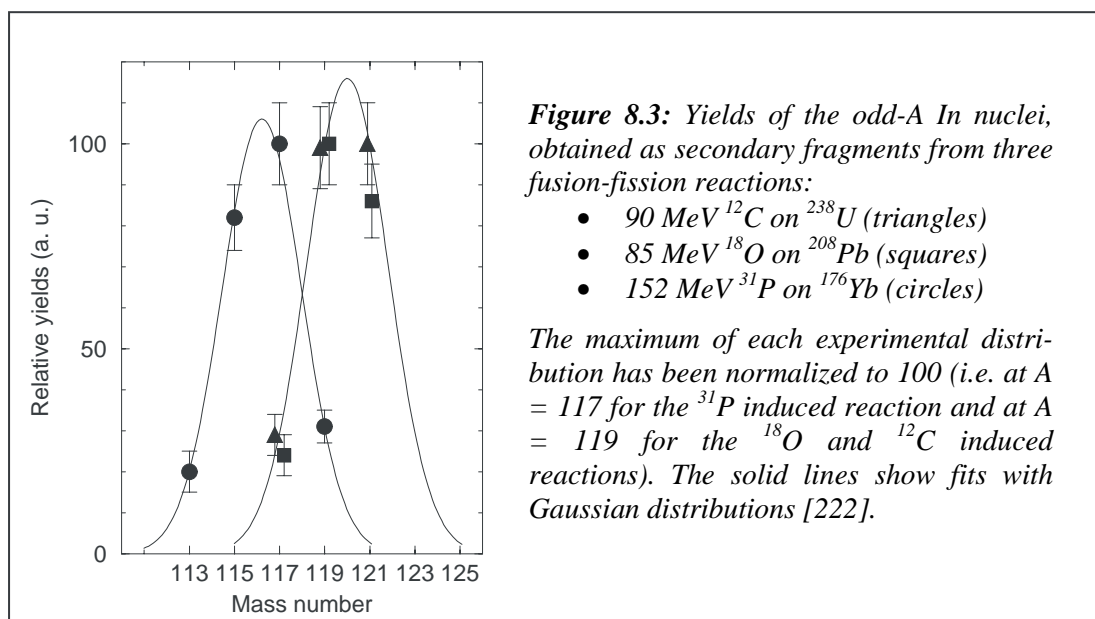
It has been established that, as the neutron number is increased from the valley of stability near *Z=40*, the onset of quadrupole deformation occurs. The transition from a spherical to a deformed ground-state shape is sudden for Sr and Zr isotopes, but is gradual for higher Z nuclei. Furthermore, increasing proton number from *Z=40* has the effect of softening the nuclear energy surface to triaxiality. This is evidenced firstly by EUROGAM II measurements that have demonstrated the existence in ^{106}Mo of a two-phonon vibrational state [212], which shows that ^{106}Mo is soft to triaxial deformation; and secondly by the energy levels of the neutron-rich ^{108,110,112}Ru [213] isotopes, which suggest the presence of a more rigid triaxial shape. Heavy-ion induced fission has been used to populate ruthenium nuclei closer to stability, and evidence for triaxial structures has also been observed in ^{104,106,108}Ru [214]. In addition, work on the *Z=45* ^{107,109}Rh nuclei [215] populated following fusion/fission of ^{28}Si + ^{176}Yb has revealed several new rotational structures, two of which can be interpreted within the framework of a particle-triaxial-rotor model. Using yet another fusion reaction ^{18}O+^{208}Pb, which populates heavier isotopes, high spin states of the very neutron rich ^{111,113}Rh have been recently identified [216]; they exhibit the same behaviour as shown in Figure 8.1.

Figure 8.1: *Evolution of the first positive-parity states in odd-mass Rh isotopes (circles for states of ground-state band, and triangles for states of the excited band, linked by dotted lines [215, 216]) compared to the first and second 2⁺ states of the corresponding $^{A-1}$Ru cores (empty squares linked by solid lines [213,214]).*

Figure 8.2: *Evolution of the individual proton states as a function of neutron number in the odd-A $^{97-105}$Tc isotopes [217].*
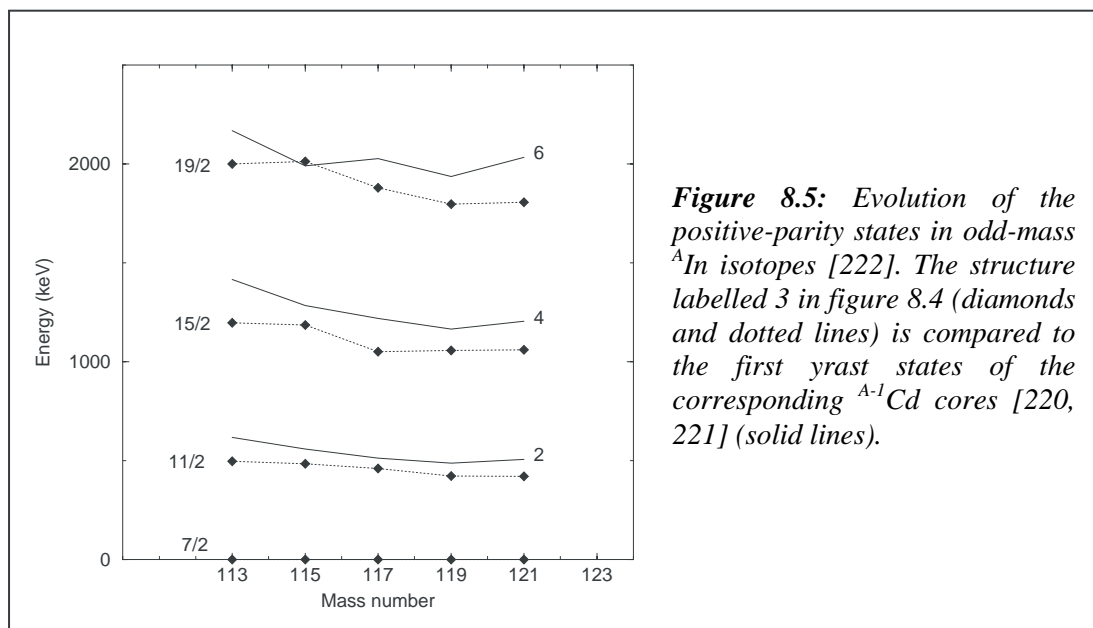
EUROBALL data on fission fragments following the reaction of ^{37}Cl on ^{176}Yb has been used to identify high spin states in ^{103}Tc for the first time [217], and to allow a systematic analysis of the important single particle orbitals as deformation is increased with increasing neutron number (see Figure 8.2). As Z increases, the triaxial rotation gives way to a quasi-rotational character in the neutron-rich ^{109,111,112,113,115,118}Pd nuclei, which have been studied in heavy-ion induced fission using EUROBALL (^{12}C + ^{238}U [218]) and earlier with EUROGAM II (^{28}Si + ^{176}Yb [219]). The band structures that are observed in these nuclei show no sign of the sudden shape change that occurs with increasing neutron number in the Zr and Sr isotopes.

The Cd isotopes near stability have long been regarded as good examples of spherical vibrators. Since spontaneous fission gives poor yield for the heavy Cd isotopes, heavy ion

Figure 8.3: *Yields of the odd-A In nuclei, obtained as secondary fragments from three fusion-fission reactions:*
- *90 MeV ^{12}C on ^{238}U (triangles)*
- *85 MeV ^{18}O on ^{208}Pb (squares)*
- *152 MeV ^{31}P on ^{176}Yb (circles)*

The maximum of each experimental distribution has been normalized to 100 (i.e. at A = 117 for the ^{31}P induced reaction and at A = 119 for the ^{18}O and ^{12}C induced reactions). The solid lines show fits with Gaussian distributions [222].

induced fission has been used to establish structures based on weakly deformed configurations in $^{113-116}$Cd [220] and ^{120,122}Cd [221].

Three different reactions have been used to do a detailed investigation of the Indium isotopes ^{115,117,119,121}In [222]). The relative yields of In nuclei in these reactions have been deduced from the number of γ-rays populating their ground states (see Figure 8.3). While the ^{12}C and ^{18}O induced reactions give similar results, the maximum of the distribution obtained in the ^{31}P induced reaction is shifted to lower mass number. The use of three different reactions to produce the various In isotopes has turned out to be very efficient to disentangle the coincidence relationships which are often complicated by the existence of many doublets or triplets of transitions very close in energy.

To identify new isomeric states in fission fragments, experiments have also been performed using a fission fragment detector to trigger the EUROBALL array and isolate the delayed γ-ray cascades. The heavy-ion detector, SAPHIR, is made from photovoltaic cells, which can be arranged in several geometries [9]. In the present work [218], it consisted of 32 photovoltaic modules laying in four rings around the target. Fragments escaping from the thin target are stopped in the photovoltaic cells of SAPHIR. The detection of the two fragments in coincidence provides a clean signature of fission events. The EUROBALL time window was 1μs, allowing detection of delayed γ-rays emitted during the de-excitation of isomeric states. Time spectra between fragments and γ-rays have been analysed in order to measure the half-life of isomeric levels. The FWHM of the time distribution for prompt γ-rays was around 15 ns. In this experiment, new isomeric states have been found in ^{119,121}In nuclei. As an example the level scheme of ^{119}In and the decay curve of the 152 keV transition depopulating the new 25/2^{+} isomer is shown in Figure 8.4.

Figure 8.4: *Level scheme for ^{119}In [222] and decay time spectrum of the 152 keV transition depopulating the new 25/2^{+} isomer. The fitted line corresponds to a half life of 240 ns.*

***Figure 8.5:*** *Evolution of the positive-parity states in odd-mass ^{A}In isotopes [222]. The structure labelled 3 in figure 8.4 (diamonds and dotted lines) is compared to the first yrast states of the corresponding $^{A-1}$Cd cores [220, 221] (solid lines).*

Most of the excited states observed in $^{115-121}$In can be interpreted in terms of a proton $g_{9/2}$ hole coupled to the Sn core excitations. In addition, intruder bands based on an orbital from the $\pi[g_{9/2},d_{7/2}]$ sub shells have been extended up to spin 19/2 $\hbar$. They behave like the ground state bands of neighbouring Cd isotopes (see Figure 8.5), showing that the shape coexistence phenomenon, well known at low spin in In isotopes, survives at least up to this spin.

Spontaneous fission is an excellent method of populating structures near ^{132}Sn [223,224], which give important information on the single particle orbitals far from stability. These nuclei delimit the edge of the heavy-fragment bump in the asymmetric yield distribution for spontaneous fission, the peak of which lies near the octupole deformed ^{144}Ba and which includes the transitional Xenon nuclei [225], and the strongly quadrupole-deformed neutron-rich Ce and Nd isotopes.

8.4. Angular correlations, magnetic moments and spin alignment properties

Until very recently, there have been no measurements of the *g*-factors of excited states populated in the decay of the secondary fission fragments, although there have been for some time experiments that measure *g*-factors of excited states populated in the β-decay of mass–separated fission products. The advantage of being able to use the secondary-fragment γ–rays, as opposed to those emitted following β decay is two fold. Using the secondary-fragment γ–ray cascades allows access to yrast states up to intermediate spin (I ~ 8-16 $\hbar$) whereas β-delayed γ–rays are generally emitted from states whose spin is close to that of the parent nucleus. In addition, the use of secondary-fragment γ–ray cascades may allow access to more neutron-rich species with shorter β-decay lifetimes. During the EUROBALL III phase, a pioneering experiment [226] was performed to test the possibility of measuring *g*-factors of excited states using a spontaneous fission source in conjunction with a large array of Ge detectors. The method involves the direct implantation of the fission fragments into a ferromagnetic host (Gd or Fe) in the form of a thin foil.
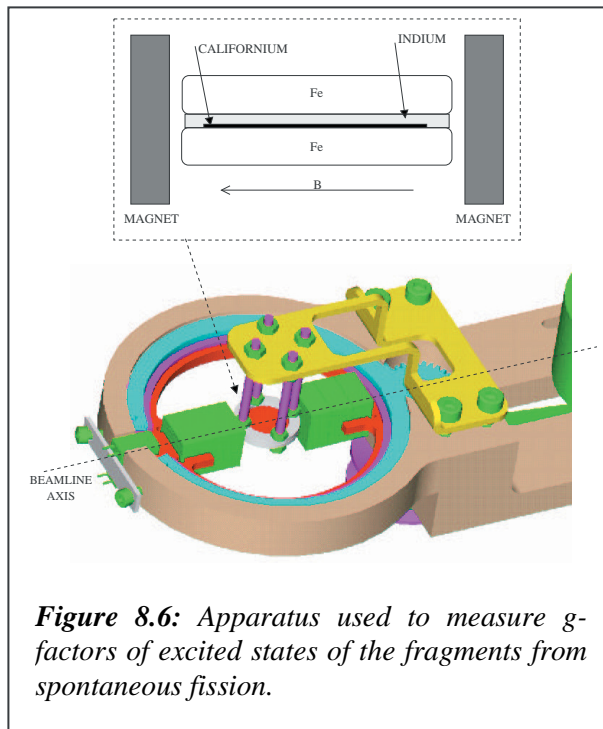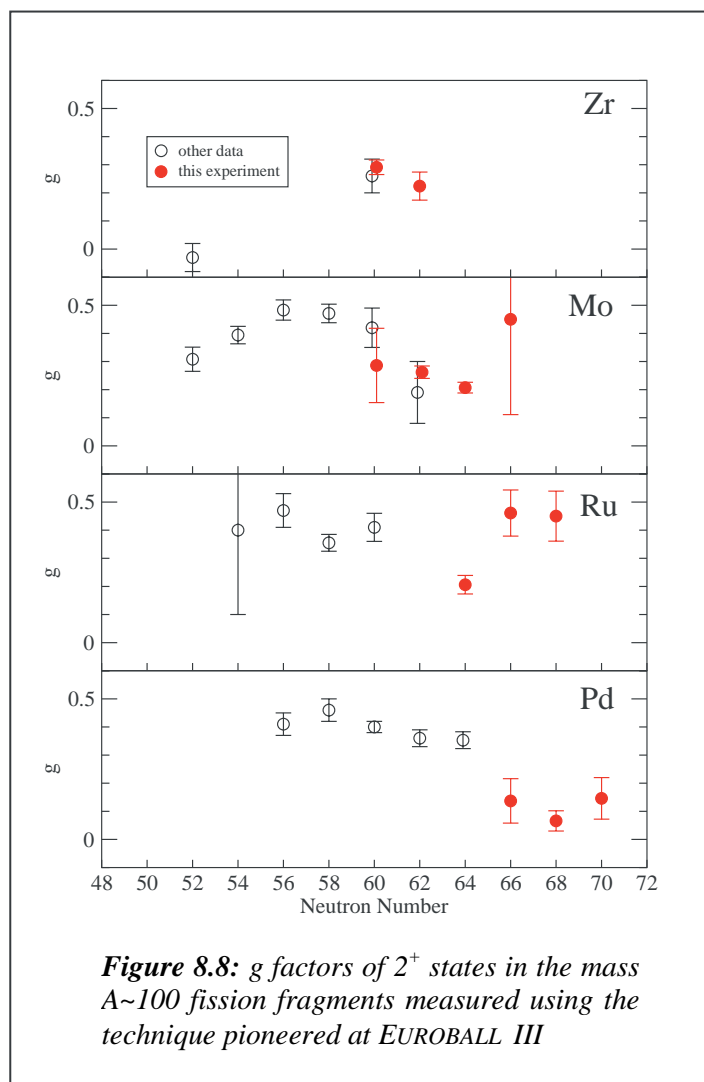
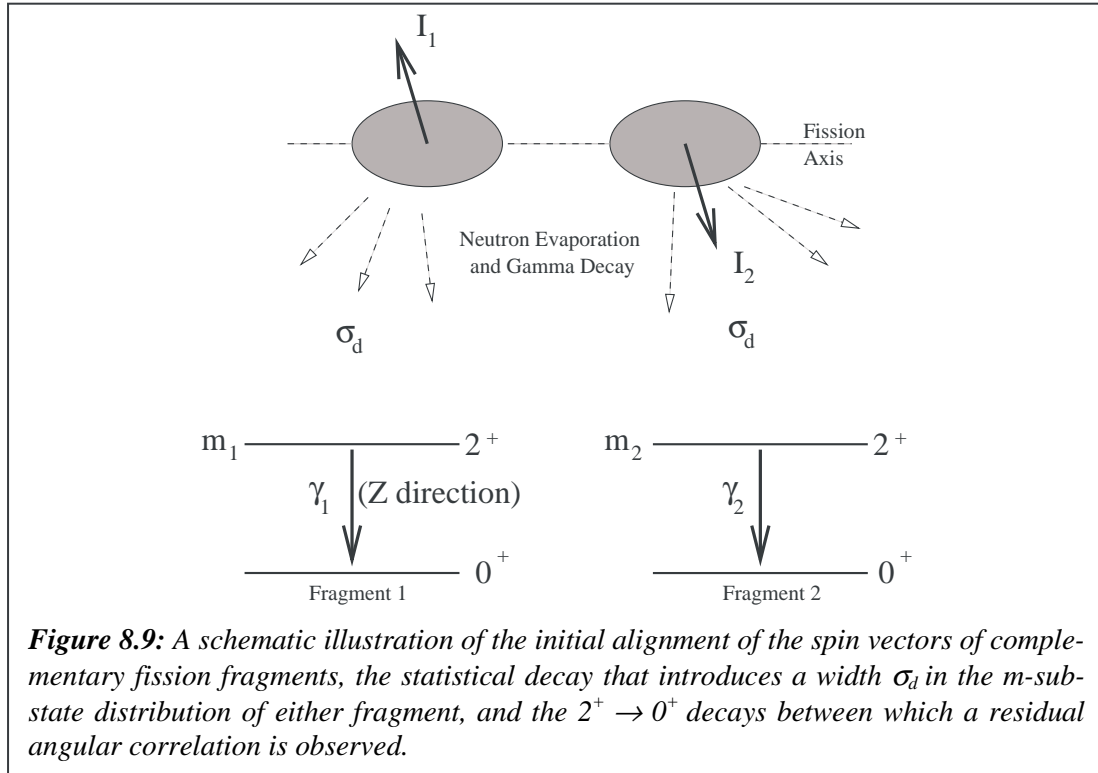**Figure 8.6:** *Apparatus used to measure g-factors of excited states of the fragments from spontaneous fission.*

Figure 8.7: (a) *Perturbed E2-E2 γ–ray angular correlation (i.e. $4^+ \to 2^+$ and $2^+ \to 0^+$ cascade in ^{104}Mo) as a function of cos(θ), the angle between the γ-rays.* **(b)** *Measurement of the Larmor precession angle achieved through the use of double-ratios to which uncertainties in the detector efficiencies do not contribute.*

As shown in Figure 8.6, the foil is magnetised by a pair of small permanent magnets which can be rotated through 180º. The fission fragments stop in the ferromagnetic host and are exposed to impurity hyperfine fields, which are generally two to three orders of magnitude greater than the applied field of 0.1 Tesla. The impurity hyperfine field causes a Larmor precession of the nuclear magnetic moment, and in so doing cause a perturbation to the *m*-substate distributions of any aligned nuclear states. Since in this experiment the fragment direction is not measured, the Larmor precession angle is determined through a careful measurement of perturbed γ–γ angular correlations. An example of such a measurement, for the first 2^+ state in ^{104}Mo is shown in Figure 8.7. This technique has enabled a survey of *g*-factors of 2^+ states to be made in the A~100 region (see Figure 8.8).

Figure 8.8: *g factors of 2^+ states in the mass A~100 fission fragments measured using the technique pioneered at EUROBALL III*

Figure 8.9: *A schematic illustration of the initial alignment of the spin vectors of comple-mentary fission fragments, the statistical decay that introduces a width σ_d in the m-sub-state distribution of either fragment, and the $2^+ \rightarrow 0^+$ decays between which a residual angular correlation is observed.*
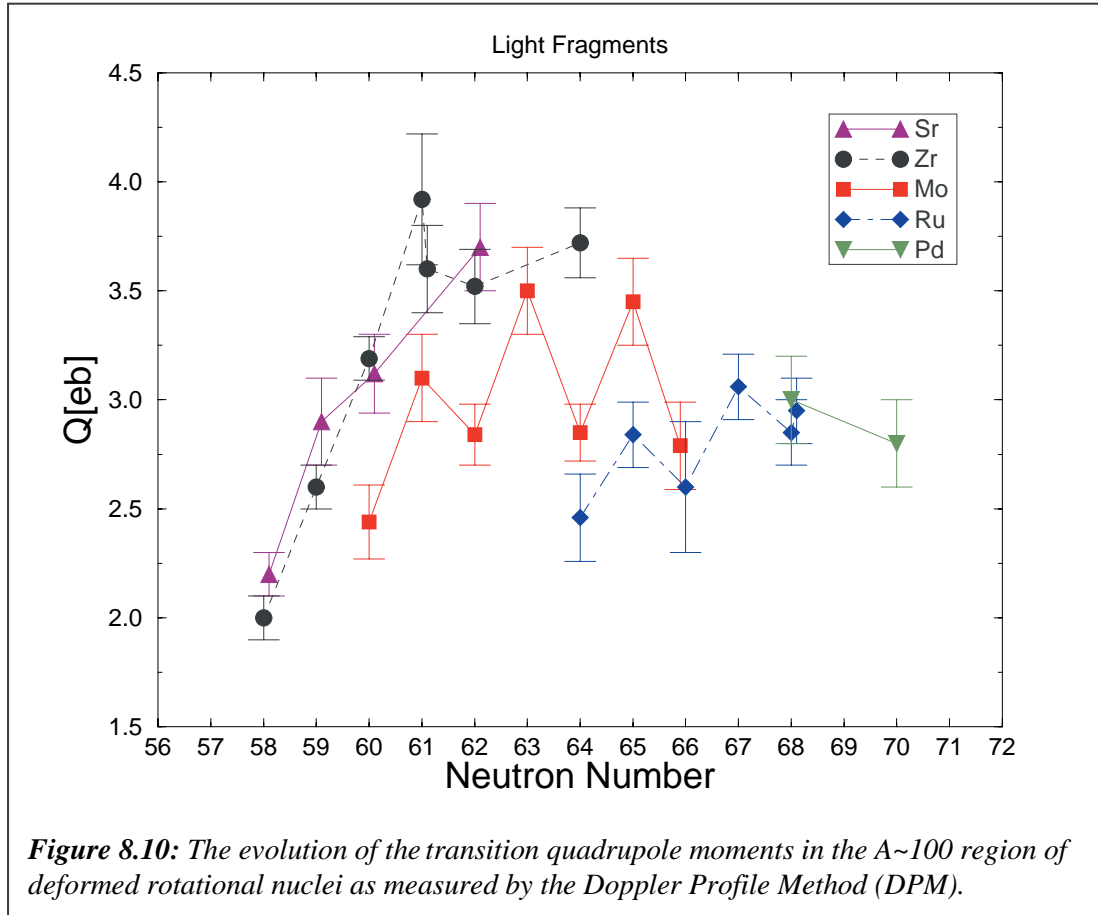
The internal angular momentum of the fragments has its origin in dynamical processes that occur in the fissioning system, the so-called bending and wriggling modes as well as in Coulomb torque immediately following scission. For many years it has been known that the spin of a fragment from spontaneous fission tends to be aligned in a plane perpendicular to the fragment direction, suggesting that twisting modes about the fission axis play at most a minor role in the generation of fission-fragment spins. This conclusion has been drawn from measurements of the angular correlation between the fission axis and the direction of γ-rays emitted in the prompt decay of the excited fragment. Such experiments have been performed with NaI detectors [227] as well as germanium detectors [228].

Recently, a study of the γ-ray decay of low-lying excited states in fragments produced in the spontaneous fission of ^{252}Cf has revealed a significant correlation between the angles of emission of the $2^+ \rightarrow 0^+$ transitions of complementary fragment pairs. Calculations of the amount of dealignment that is needed to reproduce the measured a_2 values, and comparison with the results of previous fragment-γ angular distribution measurements, suggest that at scission there may be significant population of $m \neq 0$ substates associated with the projection of the fragment spin vector on the fission axis (Figure 8.9). Fragments from the spontaneous fission of ^{248}Cm emit $2^+ \rightarrow 0^+$ γ rays that show markedly reduced inter-fragment correlations, suggesting that either a larger role is played by the relative angular momentum of the fragments, or that the dealignment introduced by the neutron emission and statistical γ decay to the 2^+ state is larger in ^{248}Cm than ^{252}Cf fission.

8.5. Lifetime measurements in fission fragments
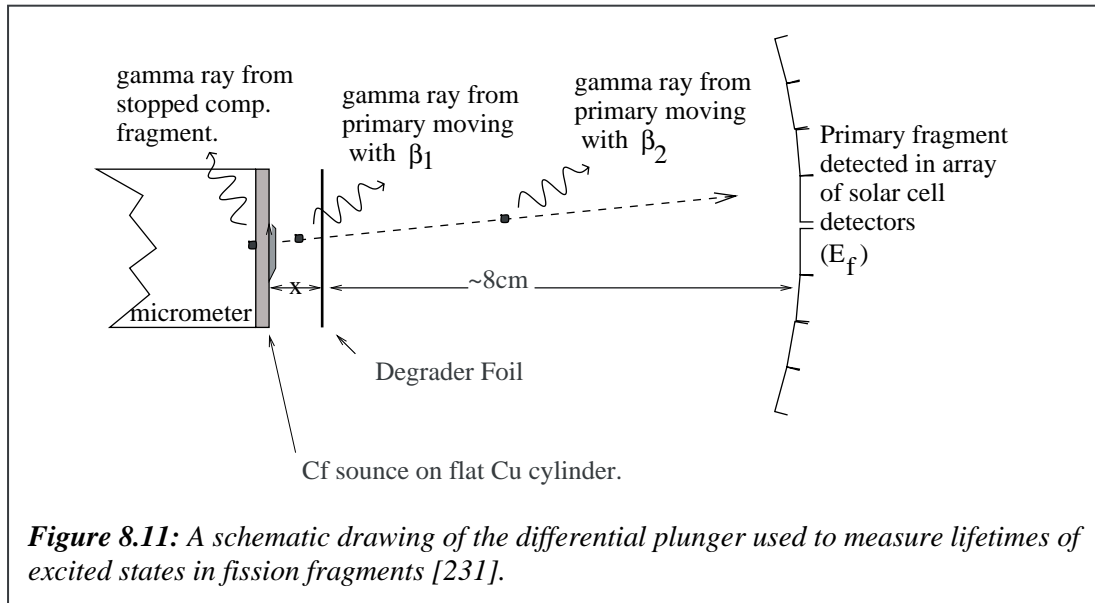
At spins of I~10$\hbar$, symmetrically Doppler-broadened lineshapes are observed in the γ-ray energy spectra of many of the light fission fragments from ^{248}Cm embedded in KCl. The broad lineshapes correspond to decays from states that have lifetimes comparable to (or faster

Figure 8.10: *The evolution of the transition quadrupole moments in the A~100 region of deformed rotational nuclei as measured by the Doppler Profile Method (DPM).*

than) the stopping time (~1-2 ps) of the fission fragments in the source pellet, the broadening being due to the variable Doppler-shift that is observed for the time distribution of decays from such states. The Doppler-profile method (DPM) [211,229] combines a simulation of the stopping of the isotropically-directed fission fragment with a simulation of the electro-magnetic decay to generate a lineshape that can be compared directly with the data and thereby extract state lifetimes.

Figure 8.10 shows the quadrupole moments deduced from lifetime measurements for the light fission-fragments at I~10$\hbar$. The onset of deformation in the Sr and Zr isotopes is clearly seen to be smooth for these excited states [230], as is the trend to lower quadrupole moments with increasing Z. The quadrupole moments of the even Mo isotopes are lower than expected, when compared to either predicted ground-state quadrupole moments, or to those deduced from measurements of lifetimes for the first 2^+ states. This difference between the quadrupole moments at low and intermediate spin has previously been interpreted in terms of a change in the triaxiality due to $h_{11/2}$ neutron alignment [229].

In the data presented here, it appears that the quadrupole moments of the odd Mo isotopes show greater stability with increasing spin, having values similar to the Zr isotopes at I~10$\hbar$. All of the measurements made in the odd Mo and Ru nuclei correspond to bands of $h_{11/2}$ character and it may be that the occupation of the moderately prolate-driving $h_{11/2}$ orbitals by the odd neutron is sufficient to stabilise the axial symmetry. In order to further explore the influence of nuclear rotation on deformation in this region the EUROBALL Fission Fragment Plunger has been constructed [231].
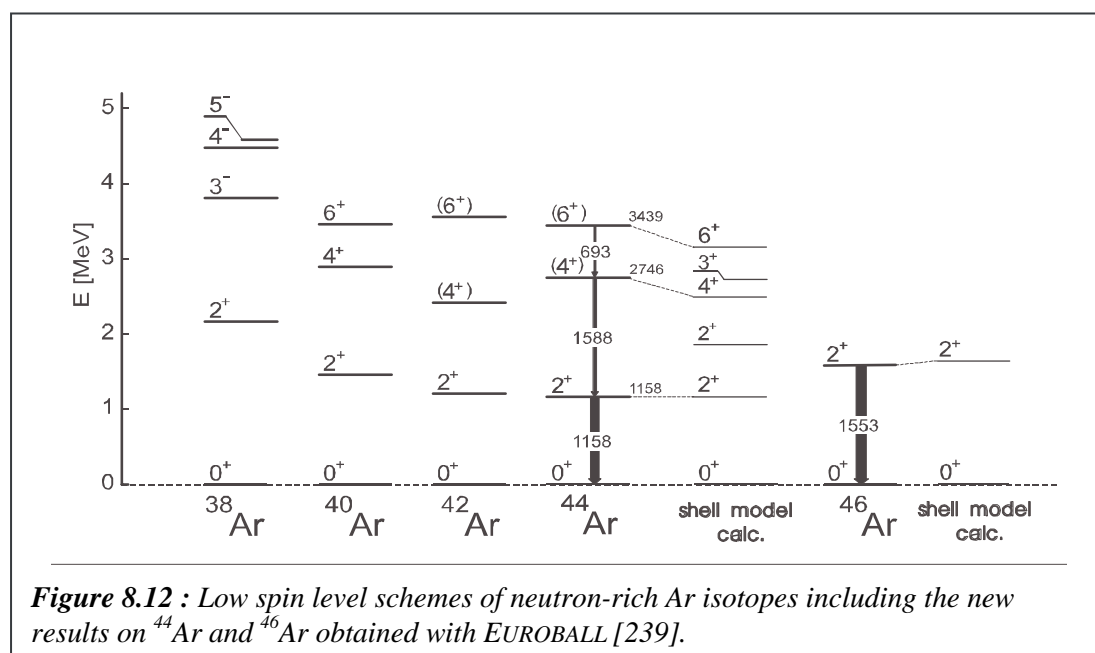
Figure 8.11: *A schematic drawing of the differential plunger used to measure lifetimes of excited states in fission fragments [231].*

This device, depicted schematically in Figure 8.11 comprises a ^{252}Cf source on a flat backing, which is mounted on the end of a micrometer. At the centre of EUROBALL IV, a large stretched foil is used to degrade the kinetic energy of fragments emanating from the source. The slowed fragments are then detected in a special configuration of the SAPHIR array [9] of solar cell detectors. Detection of the in-flight fragment in SAPHIR allows γ-ray energies to be Doppler corrected, either using the full fragment velocity (emission before the foil) or the partial velocity (emission after the foil). Lifetime measurements are made through a comparison of count rates in the fully-shifted and partially-shifted spectral peaks as a function of the source-foil distance. This technique has been proven to have the capability for measurement of life-times ranging from a nanosecond to less than a picosecond, and has been used to confirm the decrease with spin of the quadrupole moment of the yrast band of ^{104}Mo, that was suggested by the DPM data [229].

8.6. Gamma spectroscopy with deep inelastic heavy-ion reactions

The excellent resolving power of large Ge detector arrays opened the way to unfold very complex gamma coincidence spectra arising from many nuclei produced in deep-inelastic heavy ion reactions. As a consequence, one can use such processes for the study of yrast structures in nuclei that were hitherto inaccessible in standard fusion evaporation reactions with stable beams. The strong tendency to equalize the *N/Z* ratio between the two nuclei colliding at energies significantly above the Coulomb barrier, by appropriate direction of the proton and neutron flow taking place during the collision, gives rise to the production of many nuclei located at the neutron-rich edge of the beta stability line and far beyond it. It has been numerously demonstrated [e.g. 232-234] that, using such reactions, spectroscopy studies could be performed in many neutron-rich nuclei by simple thick target gamma coincidence experiments. Although in such experiments the Doppler broadening might exclude the observation of few gamma rays emitted in flight from short-lived states of recoiling nuclei, the vast majority of important yrast transitions can be detected as discrete gamma lines, since in the populated excitation energy and spin ranges the state life-times and/or feeding times are usually much longer than the stopping time of nuclear products.

The data analysis involves close inspection of gamma coincidence spectra, where, among many families of known transitions arising from the well studied nuclei, one is able to discover new gamma transitions yielding information on yrast structures in nuclei that were previously very poorly known, or even completely unknown. In the latter case special identification procedures are performed by the analysis of gamma cross-coincidences, in which new gamma rays arising from unknown product nucleus are identified by the observation of coincidences with the well known gamma transitions emitted simultaneously from the partner nuclei present in the binary reaction exit channel. In the last decade a number of successful spectroscopic studies of neutron-rich nuclei have been performed, involving also high-spin state studies in the shell model doubly-magic nuclei and their closest neighbourhood. As example one may recall the study of neutron-rich Ni isotopes [235] and observation of subshell closure in the ^{68}Ni [236], as well as the high-spin state study of the ^{208}Pb doubly magic nucleus [237], where recent experiments extended the information to states exceeding the *I=26* spin value [238].

Figure 8.12 : *Low spin level schemes of neutron-rich Ar isotopes including the new results on* ^{44}*Ar and* ^{46}*Ar obtained with* EUROBALL *[239].*
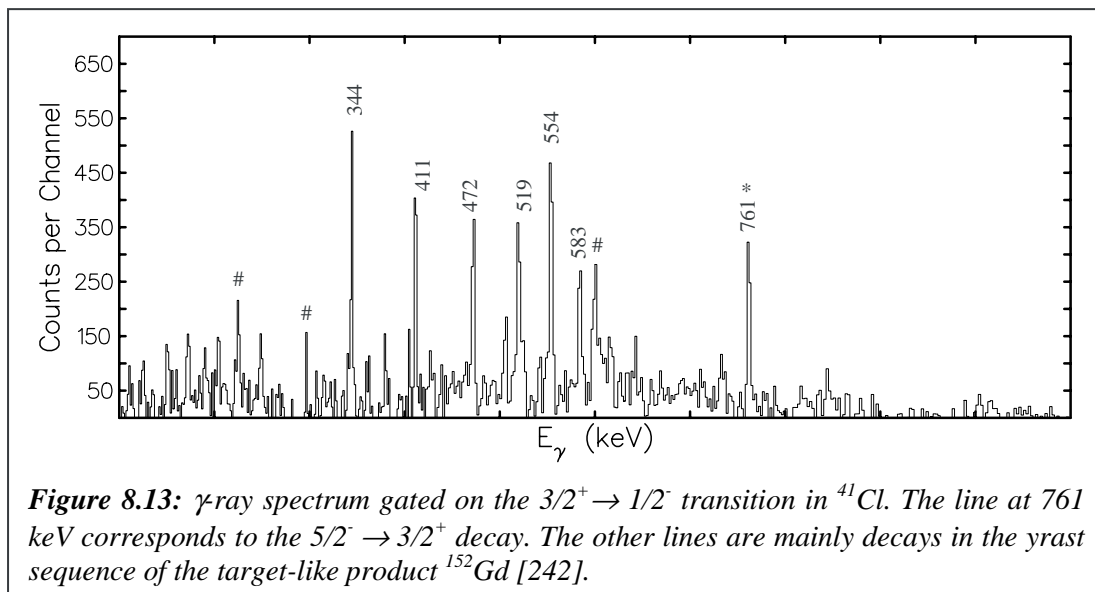
The powerful EUROBALL array is a perfectly suited tool for this type of experiments since the available quality and statistics of the gamma coincidence data allows to reach products with very small production cross sections and thereby to access more neutron-rich region of isotopes. However, installation of EUROBALL at accelerators with rather restricted range of energy and mass of available heavy-ion beams, resulted in somewhat limited number of experiments that were devoted to spectroscopic studies with the use of deep-inelastic heavy-ion reactions. Nevertheless, a successful experiment was performed to study neutron-rich nuclei in the region of ^{48}Ca. A beam of 140 MeV ^{48}Ca ions from the Tandem accelerator of the Laboratori Nazionali di Legnaro was used to bombard a target of 0.74 mg/cm^2 ^{48}Ca (backed by 40 mg/cm^2 of evaporated ^{208}Pb). The gamma-gamma coincidences were collected with the Euroball array. Fusion-evaporation was a main reaction channel, whereas multi-nucleon transfer processes, leading to nuclei from the vicinity of ^{48}Ca, accounted for less than 1% of the total reaction cross section. Despite this very low production yield, investigation of excited states in some of nuclei around ^{48}Ca was possible [239]. By examining the cross coincidence relationship between complementary Ar and Ti reaction products one was able to identify in ^{44}Ar a cascade of gamma rays with energies 1158, 1588 and 693 keV deexciting

the yrast states 2^+, 4^+ and 6^+, respectively. Also a gamma ray from the first excited state 2^+ to the ground state in ^{46}Ar, was found at 1553 keV.

These new data on yrast excitations in ^{44}Ar offer a more stringent test of the large-scale shell model calculations and interactions used. Such calculations were performed for the ^{44}Ar and ^{46}Ar nuclei and their results are compared with the experimental findings in Figure 8.12. The agreement is very good for the 2^+ states and satisfactory for higher lying yrast levels. In ^{46}Ar, our data confirm the increase of excitation energy of the first 2^+ level, which is in line with the persistence of magicity at N=28. Such phenomenon is indeed predicted by the calculations.

Another example of such a deep inelastic reaction used for spectroscopy with Euroball involved the use of a 234 MeV ^{37}Cl beam on backed ^{160}Gd target. States in the target-like species ^{159,160,161,162}Dy [240] have been observed up to spins in excess of $20\hbar$ and the data interpreted within the framework of cranked shell model and projected shell model calculations. The quasi-neutron $(\nu i_{13/2})^2$ crossing in the yrast sequence of ^{162}Dy is not identified in this work despite being predicted to lie within the observed range of rotational frequencies, and may indicate a larger than expected quadrupole deformation parameter. Spectroscopy has also been performed on the projectile-like species ^{36}S [241] and ^{41}Cl [242] (see Figure 8.13). For the first time excited yrast states have been identified in ^{41}Cl and these have been interpreted as shell model states using an *sdfp* space.

Figure 8.13: *γ-ray spectrum gated on the $3/2^+ \rightarrow 1/2^-$ transition in ^{41}Cl. The line at 761 keV corresponds to the $5/2^- \rightarrow 3/2^+$ decay. The other lines are mainly decays in the yrast sequence of the target-like product ^{152}Gd [242].*

Acknowledgements

Magnetic rotation

H. Hübel

9. Magnetic rotation[*]

9.1. Introduction

The first experimental evidence for sequences of strongly enhanced magnetic dipole (M1) transitions in Pb isotopes that follow a rotational I(I+1) dependence was found about ten years ago [243-245]. The measurements were performed using the OSIRIS and TESSA3 spectrometers in Germany and the United Kingdom, respectively. These bands had surprising features: The M1 transitions were strong, and no, or only extremely weak, E2 crossover transitions were found. The resulting B(M1)/B(E2) ratios led to the conclusion that the deformation is very small. However, for near-spherical states the occurrence of regular band structures, similar to the bands of strongly enhanced E2 transitions in well-deformed nuclei, could not be understood.

Almost all the M1 bands that were discovered at that time were not connected to lower-lying states [243-251] and their excitation energy, spin and parity were not determined experimentally. From the decay pattern it was concluded that they are built on high-spin states, most likely on high-spin proton excitations coupled to the high-spin neutron states that were well known in the Pb isotopes [251]. It was noted, however, that the M1 bands are not built on these proton or neutron states directly.

The M1 bands are nowadays well understood in terms of a new mode of nuclear excitation which has been called "magnetic rotation" (MR) [252,253]. It is also established in other mass regions [254] of near-spherical nuclei where high-spin orbitals are close to the Fermi surface. Magnetic rotation occurs when the symmetry of the nuclear system is broken by the current distributions of a few high-spin particles and holes outside a spherical or near-spherical core. If these currents lead to a large component of the magnetic moment vector perpendicular to the total angular momentum, they generate the enhanced M1 radiation as illustrated schematically in Figure 9.1.
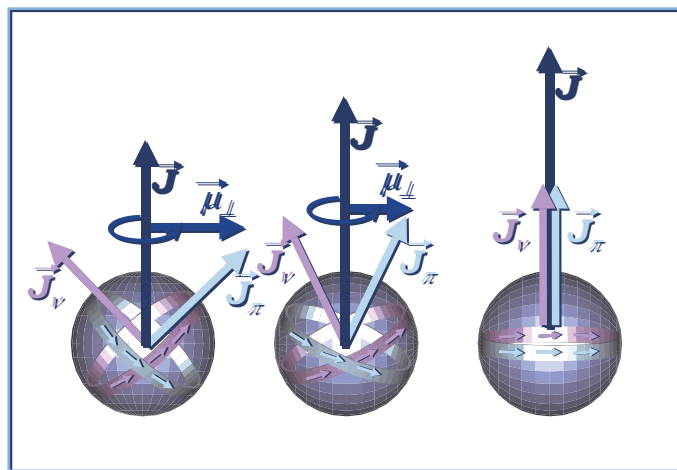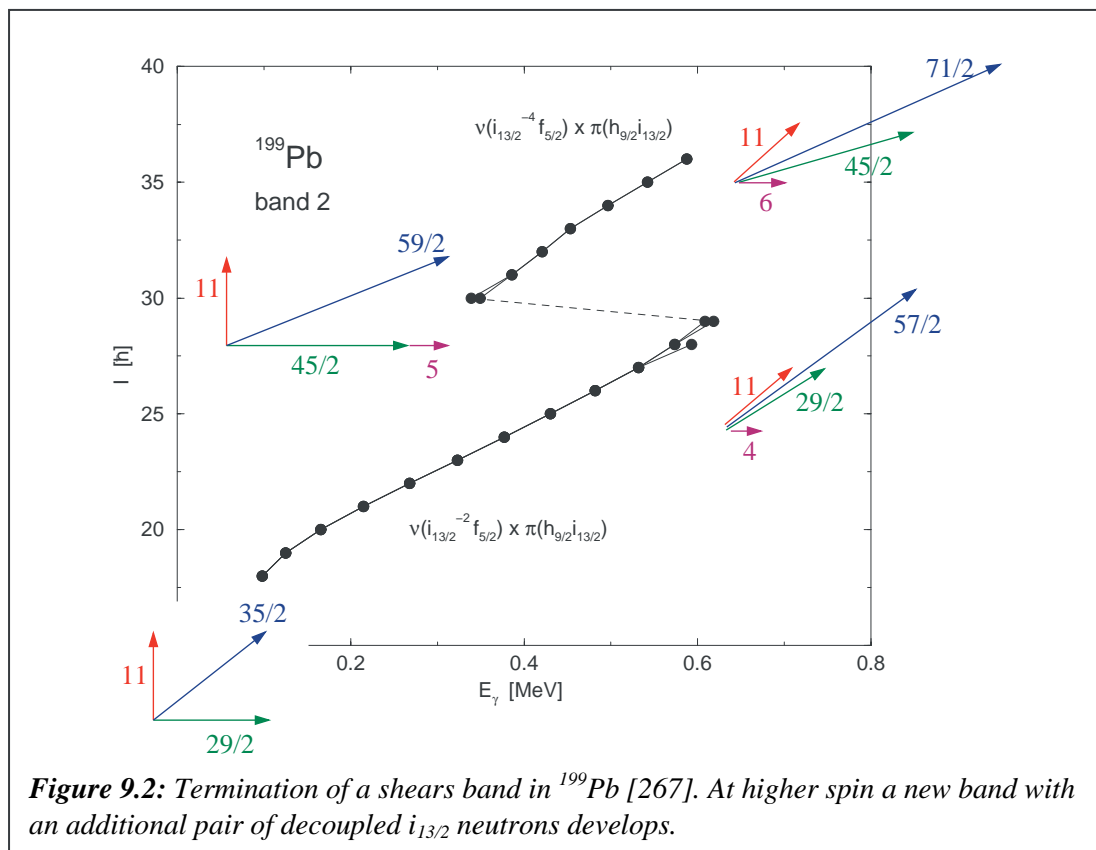

Figure 9.1: *Schematic illustration of the shears effect in magnetic rotation bands [256].*

---

[*] Contribution by H. Hübel

Asymmetric currents result from the coupling of particle- to hole-type of excitations. The particle-hole interaction is repulsive and favours a perpendicular orientation of the current distributions and, hence, of their angular momenta. The left-hand panel of Figure 9.1 shows the perpendicular coupling as it is realised near the band head of the MR bands. It has actually been verified experimentally by a measurement of the g factor of the band head of a MR band in ^{193}Pb [255]. The two other panels illustrate how angular momentum is generated within the bands by a step-by-step alignment of the particle and hole spins into the direction of the total spin. Since this resembles the closing of the blades of a pair of shears, the MR bands have also been called "shears bands" [256]. Consequences of the shears effect are that the total angular momentum J remains almost fixed in direction in the intrinsic system and that the perpendicular component of the magnetic dipole moment decreases with increasing J. As this component is responsible for the M1 radiation strength, the B(M1) values are expected to decrease in a characteristic way with increasing spin within the bands. This effect has been verified by lifetime measurements [257-266].

The right-hand panel of Figure 9.1 illustrates the full alignment of the particle and hole spins with the total angular momentum J. This is the maximum angular momentum that can be generated by the shears effect (a small contribution is added from the low-spin orbitals) and at this point the MR band terminates. A clear example of such a band termination is shown in Figure 9.2 where the angular momentum is plotted as a function of the transition energy for MR band 2 in ^{199}Pb [267]. Termination is reached for the configuration of this band at spin 57/2. At higher spins, an additional pair of $i_{13/2}$ neutrons is broken and this neutron-hole pair is coupled to the proton excitation causing the shears to open again. In that way a new band head is formed and a new shears band develops at higher spins.

Figure 9.2: *Termination of a shears band in ^{199}Pb [267]. At higher spin a new band with an additional pair of decoupled $i_{13/2}$ neutrons develops.*

As mentioned above, before the multi-detector spectrometers EUROBALL (with its pre-decessors EUROGAM I and II) and GAMMASPHERE came into operation, most of the MR bands remained unconnected to lower-lying known levels. As band-head spins, parities and excitation energies were unknown, comparison to model calculations, like the tilted-axis cranking (TAC) [252,253,268] or the semi-classical calculations [269], remained largely speculative. With these powerful spectrometers existing bands could be linked to known states and extended to higher spins. In several cases E2 crossover transitions were discovered for the first time and the ordering of the M1 transitions was corrected. Furthermore, many new MR bands were found and new regions of magnetic rotation were established. For several bands precision lifetime measurements were performed which were needed to establish the shears effect. In the following sections the results on magnetic rotation obtained in recent EUROBALL experiments will be summarised.

9.2. Investigation of magnetic rotation with EUROBALL

Magnetic rotation in the A=130 mass region

In the A = 130 mass region sequences of M1 transitions have been observed in several nuclei [254]. However, in most of these cases the quadrupole deformation parameters are rather large, around 0.2. Therefore, it is not clear if these structures are MR bands or if they can be explained in terms of conventional high-K bands. The question may be answered by the behaviour of the B(M1) values as a function of spin.

For ^{124}Xe, where an M1 band has been known from previous work [270], a recoil-distance method (RDM) lifetime measurement was performed with the EUROBALL spectrometer array [271]. The Köln plunger was used for a precise variation of the target-stopper distances. High-spin states in ^{124}Xe were populated in the reaction ^{110}Pd(^{18}O,4n) at a beam energy of 86 MeV. Lifetimes of states in the ground-state band as well as in the M1 band were determined from gamma-ray coincidence spectra. By gating above the levels of interest, uncertainties due to the feeding of the levels could be avoided.

The B(M1) values of transitions in the M1 band deduced from the lifetimes are displayed in Figure 9.3. As can be seen, they show a modest decrease with increasing spin. This is in


Figure 9.3: *Reduced M1 transition probabilities, B(M1), for states in the M1 band in ^{124}Xe [271]. In the calculation a high-K four quasi-particle configuration was assumed.*
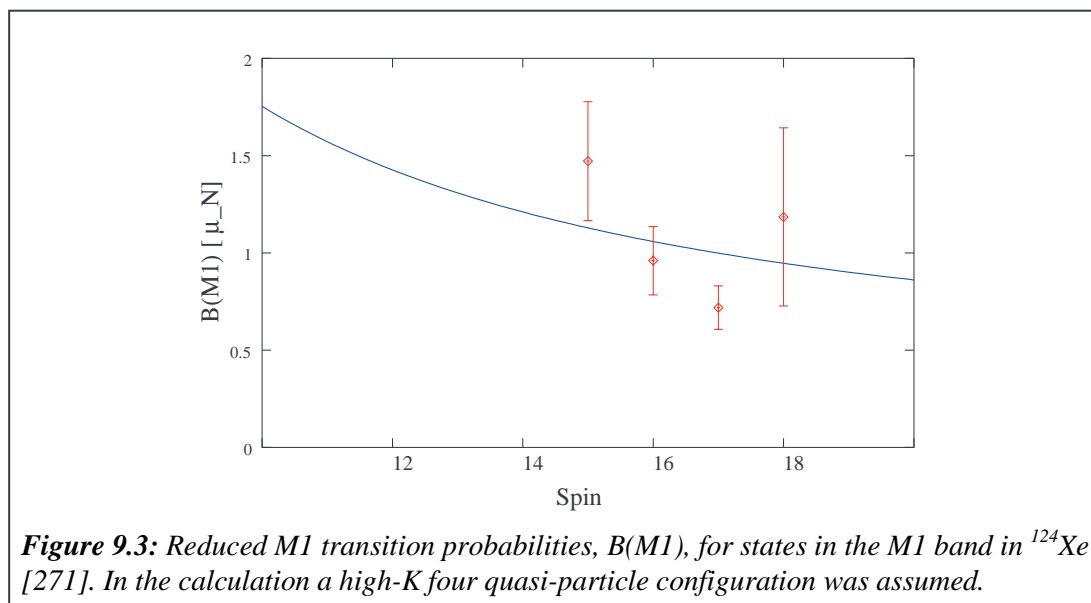
contrast to the corresponding band in ^{128}Ba which shows increasing B(M1) values [272]. The calculated curve in Figure 9.3 was obtained assuming a four quasi-particle structure with high K. For the configuration of two $h_{11/2}$ protons coupled to a $h_{11/2}g_{7/2}$ neutron excitation the semi-classical approach of DÖNAU and FRAUENDORF [273] describes the observed behaviour rather well. Thus, the EUROBALL experiment shows that the M1 band in ^{124}Xe is probably not pre-dominantly of magnetic rotation character.

Magnetic rotation around ^{142}Gd

In a search for magnetic-dipole bands around ^{142}Gd, high-spin states were populated in the reaction ^{99}Ru(^{48}Ti,xnyp) at a beam energy of 240 MeV at the Legnaro National Laboratory. The spectroscopic investigation with EUROBALL revealed four M1 bands in ^{142}Gd and ^{143}Gd. In ^{141}Eu three M1 bands and in ^{144}Gd two irregular dipole sequences were found. The level scheme of ^{142}Gd with the four M1 bands discovered in that nucleus is shown in Figure 9.4. From the intensity branching ratios the B(M1)/B(E2) ratios displayed in Figure 9.5 were obtained. They are exceptionally large and show the decrease expected for shears bands when compared to TAC calculations [274].

The M1 bands in ^{142}Gd can be associated with the minima seen in the calculated total routhian surfaces at small oblate deformation in the frequency range between 0.2 and 0.5 MeV. For this deformation the $h_{11/2}$ neutron-hole and $g_{7/2}$ proton-hole states with small K values and the $h_{11/2}$ proton states with large K values contribute to the configurations of the bands. A neutron $h_{11/2}$

*Figure 9.4: Partial level scheme of ^{142}Gd [274].*
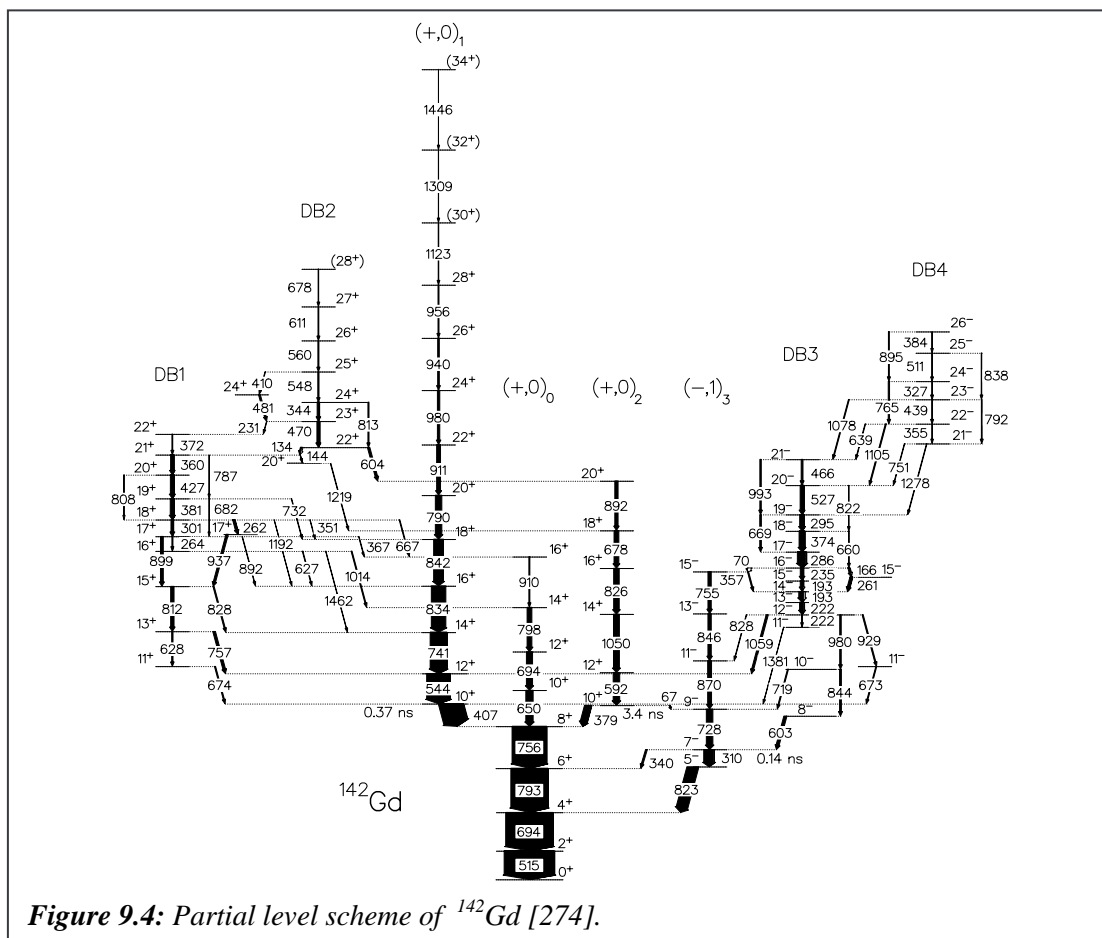
two-hole excitation coupled to a proton $h_{11/2}$ two-particle configuration may be assigned to dipole band 1. The same neutron $h_{11/2}$ two-hole excitation coupled to a proton $h_{11/2}g_{7/2}$ particle configuration may be responsible for band 3. Bands 2 and 4 most likely result from the breakup of an additional $h_{11/2}$ neutron-hole pair. Considering an alignment of the spins of the hole states along the rotation axis and those of the particle states along the symmetry axis, these configurations could give rise to MR bands. However, for a final confirmation, we have to wait for the results of a lifetime measurement performed recently with EUROBALL.

The angular momenta of two of the dipole bands in ^{141}Eu and ^{143}Gd, respectively, have similar frequency dependencies as bands 1 and 2 in ^{142}Gd, but the angular momenta are smaller. This indicates that their configurations result from those of ^{142}Gd by subtraction of a proton and a neutron hole, respectively. In this case the band crossings may result from the breakup of a second $h_{11/2}$ neutron-hole pair [275].

Figure 9.5: *Ratios of reduced transition probabilities B(M1)/B(E2) for the M1 bands in* ^{142}*Gd [274]. The dashed lines were obtained by TAC model calculations.*
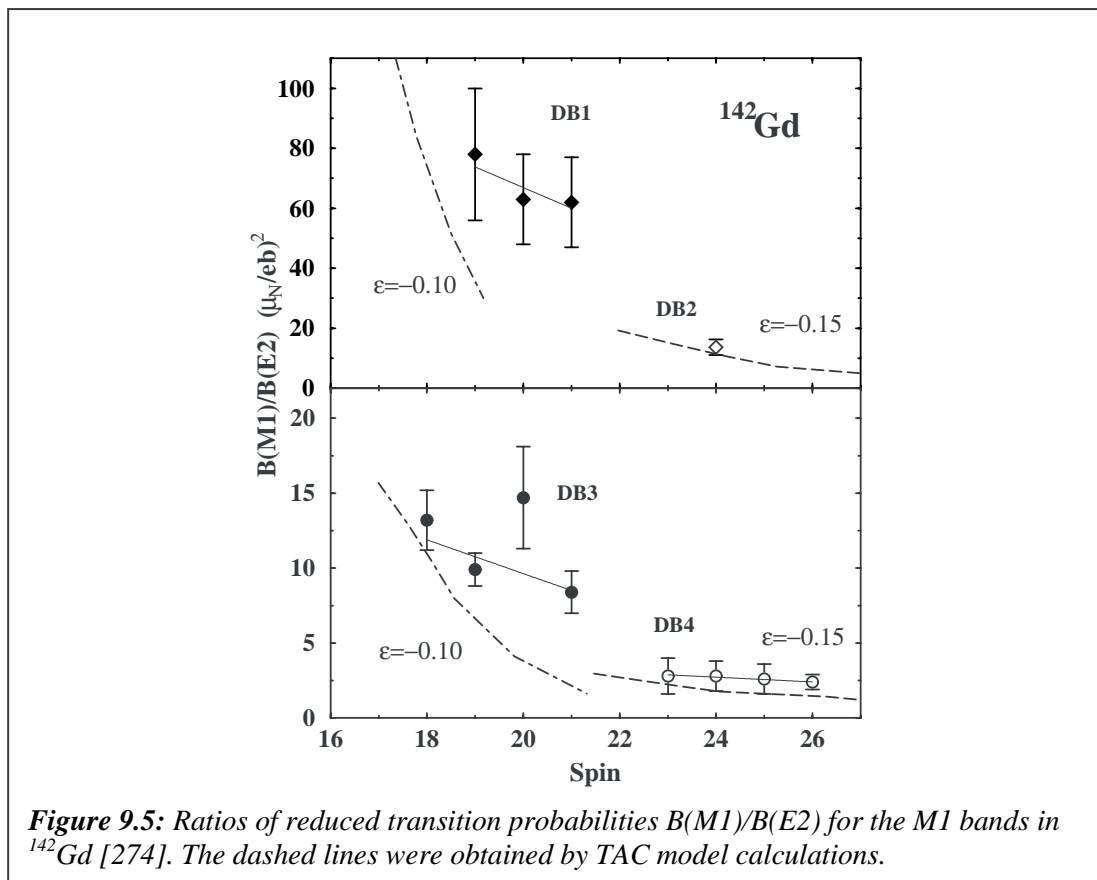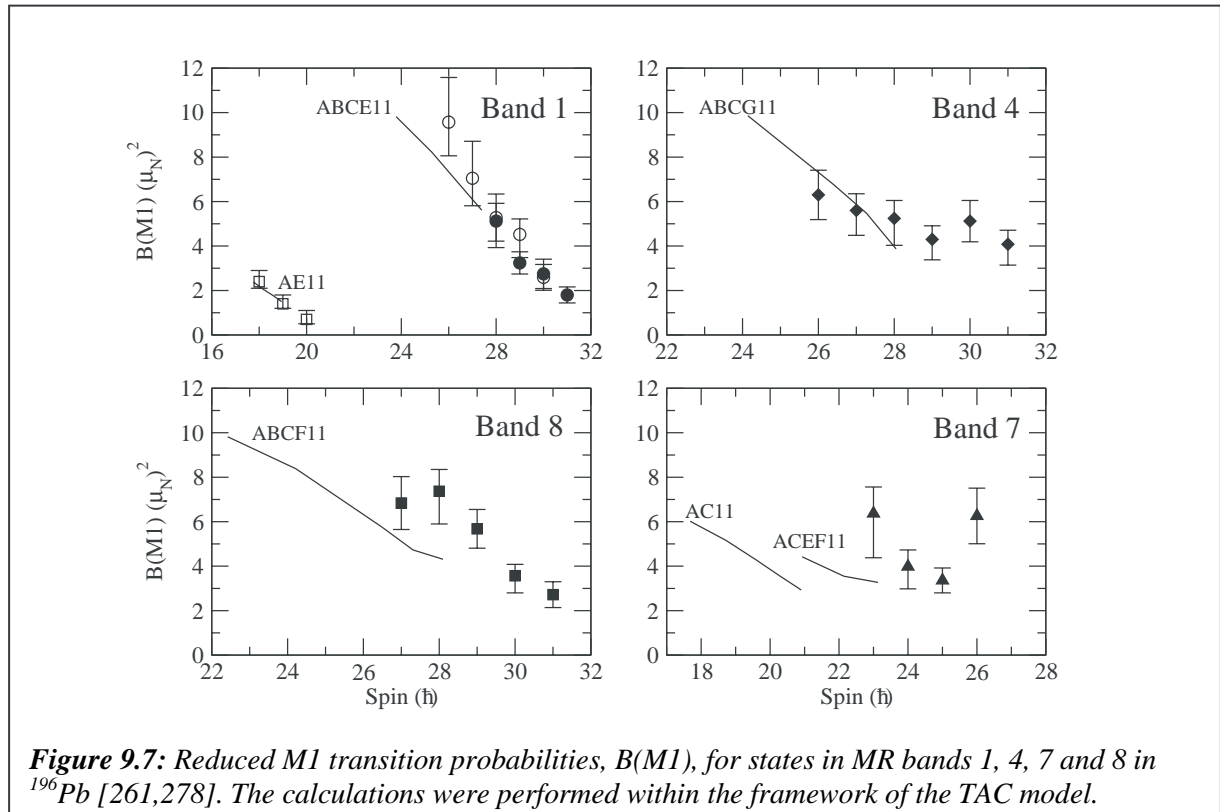
Detailed study of magnetic rotation in ^{196}Pb

An experiment to study magnetic rotation in ^{197}Pb and ^{198}Pb using the EUROGAM II spectrometer [276] showed a significant improvement in the quality of the data compared to previous studies. In both nuclei, new MR bands were found and the known ones were partly reordered and extended to higher spins. In most cases, transitions connecting the MR bands to lower-lying states were identified.

Figure 9.6: *Partial level scheme of ^{196}Pb [277].*
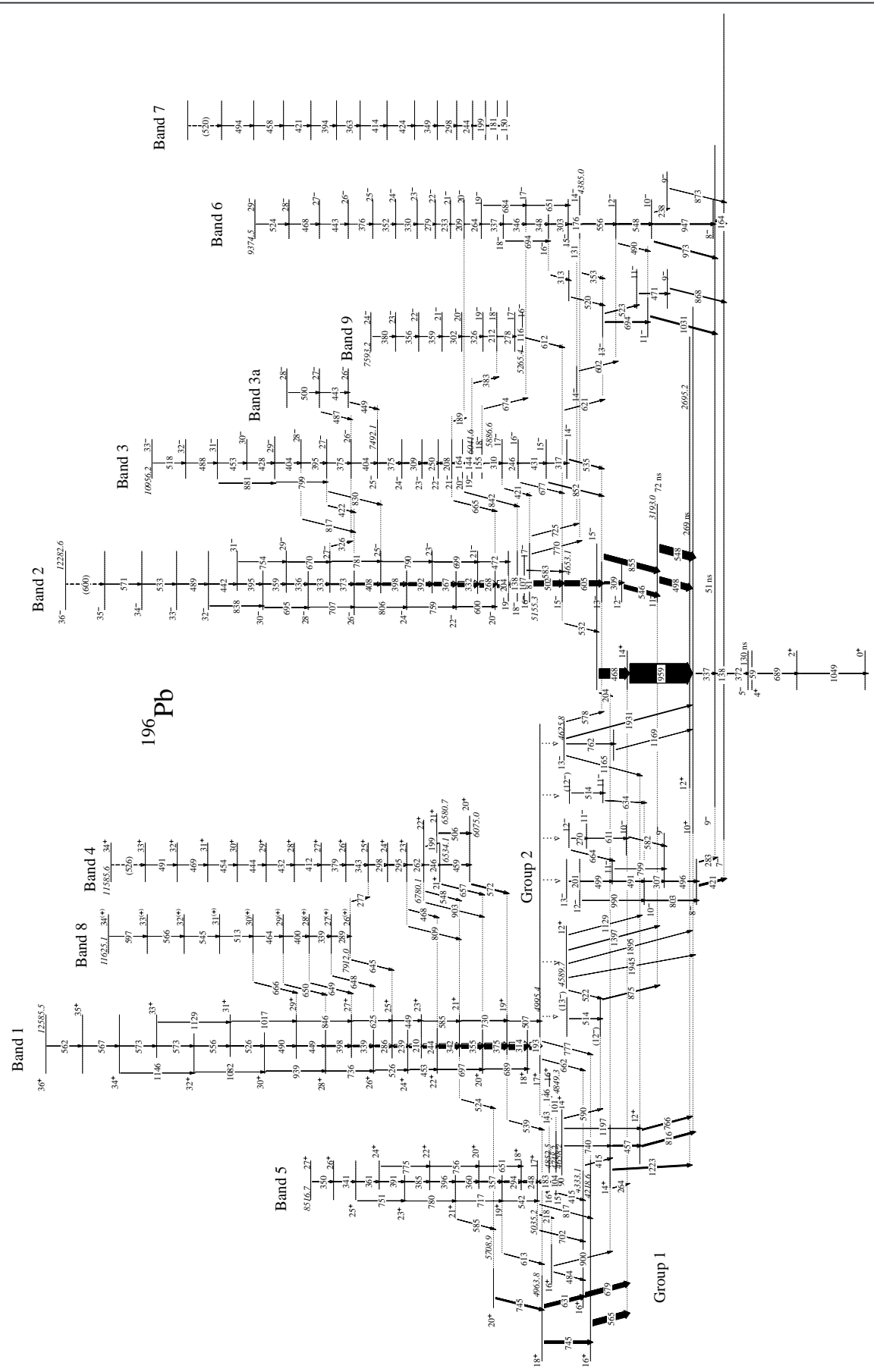
Three experiments were performed for a detailed investigation of magnetic rotation in ^{196}Pb using the EUROBALL spectrometer. One was performed with a thin target [277] aimed at extending the bands to very high spins and one with a gold-backed target optimized for a study of the decay of the bands and to determine lifetimes [278] using the Doppler-shift attenuation method (DSAM). In a third experiment, lifetimes were measured in the low-spin region of band 1 [261] using the RDM. In the first experiment, high-spin states in ^{196}Pb were populated in the ^{186}W(^{16}O,6n) reaction at a beam energy of 110 MeV at the tandem accelerator of the Legnaro National Laboratory. The second experiment was performed at the Vivitron accelerator of the Institut de Recherches Subatomiques, Strasbourg. The reaction ^{170}Er(^{30}Si,4n)^{196}Pb was used at a beam energy of 144 MeV. In the RDM experiment, the reaction ^{164}Dy(^{36}S,4n)^{196}Pb was used at a beam energy of 168 MeV and was performed at the Legnaro National Laboratory. These reactions gave the higher recoil velocities needed for the lifetime measurements. The Köln plunger device was used to measure coincidence spectra at 15 target-stopper distances [261].

The analysis of the spectroscopic data resulted in the level scheme presented in Figure 9.6; only the part that is relevant to the MR bands and their decay is shown. In addition to the previously known four bands [249], five new bands were discovered. Many new E2 crossover transitions have also been observed for the first time, which fix the ordering of the M1 transitions. All the bands, except band 7, are now connected to lower-lying states. The measurement of the DCO ratios and the linear polarisation of the transition allowed the spin assignments shown in Figure 9.6 to be made.

Lifetimes for four of the MR bands in ^{196}Pb were determined in the high-spin regions by the DSAM [278] and for band 1, lifetimes were measured at low spins by the RDM [261]. Previously, precision lifetime results were only available for band 1 at high spins [259]. The B(M1) values derived from the lifetimes are displayed in Figure 9.7. The experimental results

Figure 9.7: *Reduced M1 transition probabilities, B(M1), for states in MR bands 1, 4, 7 and 8 in ^{196}Pb [261,278]. The calculations were performed within the framework of the TAC model.*

are compared with calculations performed within the framework of the TAC model. The B(M1) values are large and show the characteristic decrease that is expected for shears bands.

The new detailed information on the MR bands in ^{196}Pb, in particular the spins, parities and excitation energies, enabled us to make configuration assignments for all bands, except for band 7. These assignments were also guided by the systematic behaviour of the bands [276,277] and by comparisons with results of TAC calculations. The MR bands may be explained by a coupling of either the two-proton $(h_{9/2}i_{13/2})_{11}^-$ or two-proton $(h_{9/2}^2)_8^+$ particle states to the high-spin neutron-hole excitations with one or more $i_{13/2}$ quasi-neutrons involved.

9.3.   Summary and outlook

The highly efficient spectrometer arrays EUROBALL and EUROGAM have allowed the detailed spectroscopy of magnetic rotational bands to be carried out in different mass regions. In the case of the M1 band in ^{124}Xe, the lifetime results revealed a smaller decrease of the B(M1) values than would be expected for a shears band. On the other hand, the bands found in ^{142}Gd show the characteristic features of magnetic rotation. However, for a final proof the knowledge of lifetimes is necessary. In the Pb isotopes reliable configuration assignments could be made to a large number of MR bands.

While a large body of information on magnetic rotation exists in the Pb region [254,276,277], it would be highly desirable to study other regions of nuclei near closed shells in similar detail. Such investigations can give information on core-polarisability effects and the influence of prolate and oblate deformation on magnetic rotation. Here, systematic investigations are lacking.

Furthermore, there are several interesting questions connected to magnetic rotation and the shears effect that need to be addressed. One of them is the possibility of antimagnetic rotation [253]. This type of excitation may occur when the current distributions of a few high-spin orbitals break the symmetry of an otherwise near-spherical nucleus, but the magnetic moments couple approximately antiparallel. In that case a band of E2 transitions with very small B(E2) values is expected. Up to now, little evidence exists for this type of excitation [253,279,280]. Another interesting question is the possibility of the opening of the shears to angles larger than 90^0. This would lead to bands with decreasing spin with increasing energy. Such bands might be populated in direct reactions rather than in heavy-ion induced compound reactions. They will probably be only populated with low intensity and new efficient spectrometers will be necessary to find them.

Acknowledgments

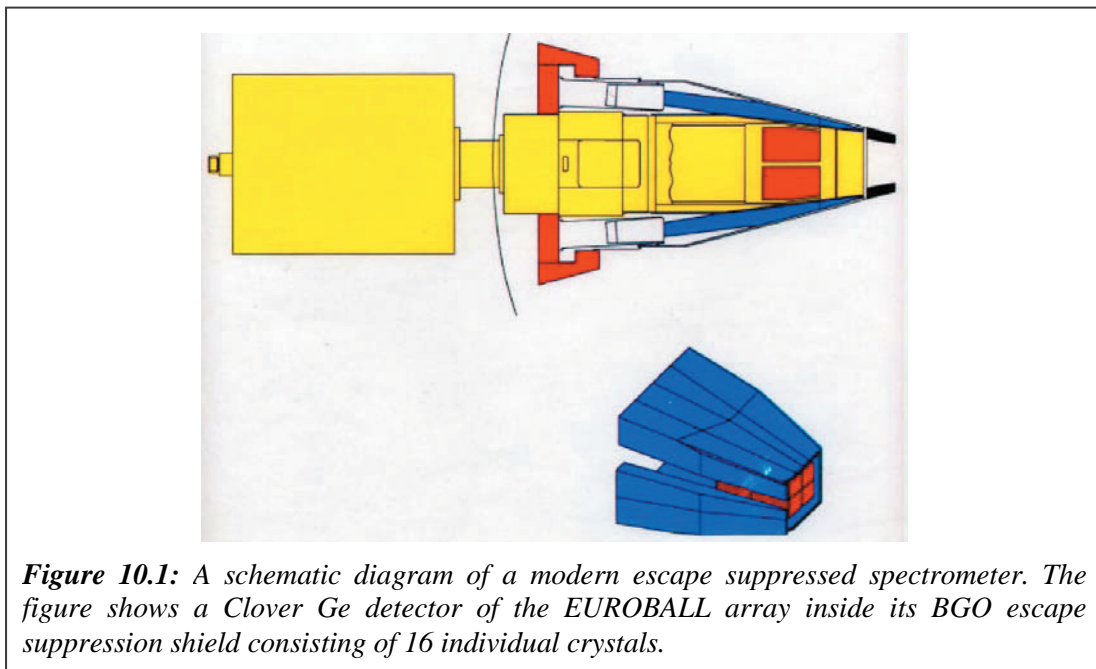# The technical merits of EUROBALL

J. Simpson

10.   The technical merits of Euroball[*]

Abstract: *The E*UROBALL *project is an outstanding scientific and technical success. This contribution summarises the technical achievements of the project. These include the development of state-of-the-art radiation detectors and associated electronics and data acquisition systems. These developments have resulted in a spectrometer with an unprecedented level of sensitivity enabling the atomic nucleus to be studied at the extremes of angular momentum, deformation, isospin and temperature.*

10.1.   Introduction

EUROBALL represented the next phase in the development of large gamma-ray arrays in Europe [1]. It was an amalgamation of all the technical developments made in several European array projects. These arrays with their very high efficiency and excellent peak to background ratio led to a revolution in the mid 1980's in nuclear spectroscopy [281] with the discovery of many new nuclear structure phenomena.

Gamma-ray detector arrays consist of as many as possible high-resolution Ge detectors around the reaction centre. A scintillation detector to detect and reject the scattered radiation from the germanium crystal surrounds each of the Ge detectors. These escape-suppressed spectrometers (ESS) improve the signal to noise of the Ge spectra, which is quantified by the peak to total ratio PT. A typical ESS is shown in Figure 10.1. For ^{60}Co the PT can increase from ~ 25% to typically 65% with suppression. This improvement in the peak-to-total ratio (PT) is crucial in high fold (F) coincidence spectroscopy since the photopeak-photopeak coincidence probability is proportional to $(PT)^F$. This results in an improvement factor of > 8 in a doubles γ^2 experiment, when compared with the background, a factor of 21 for triples γ^3, 57 for quadruples γ^4 and 157 for quintuples γ^5.
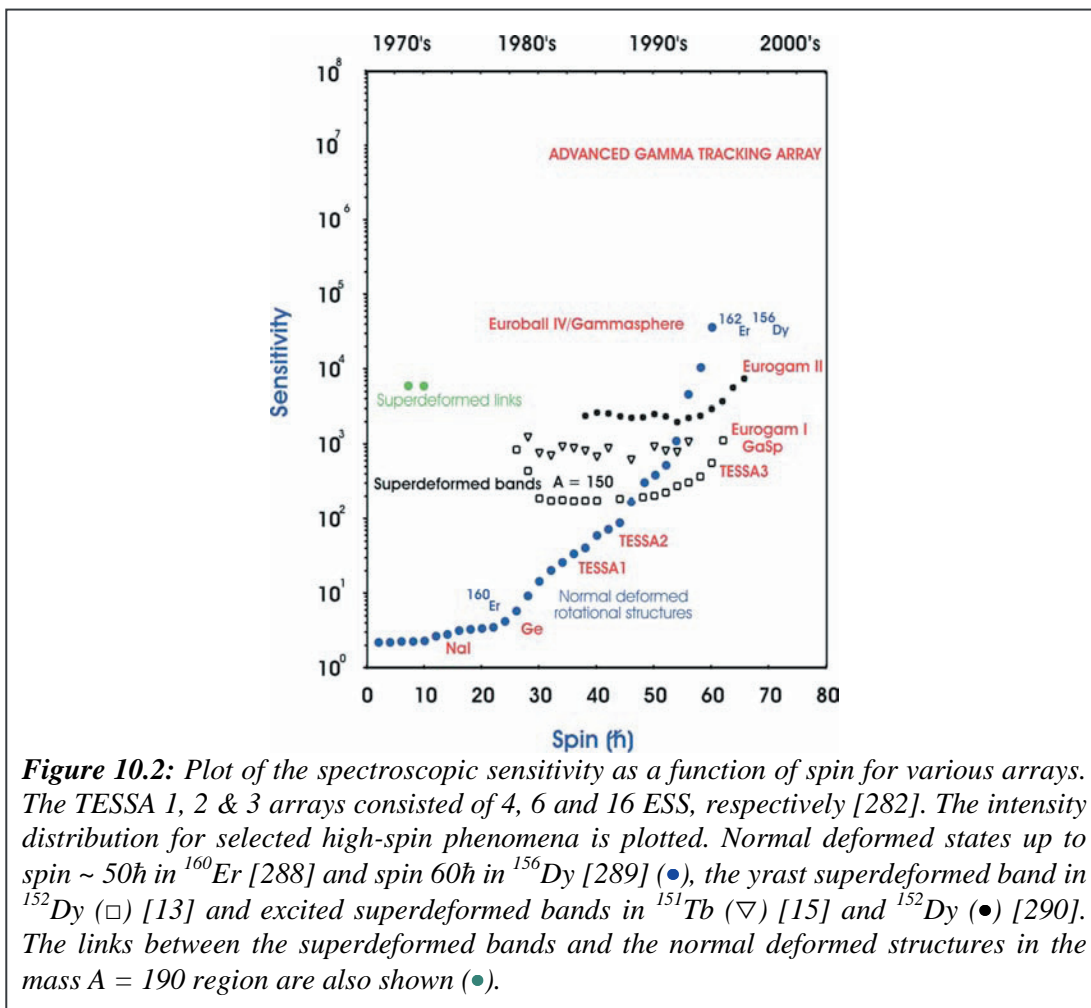

Figure 10.1: *A schematic diagram of a modern escape suppressed spectrometer. The figure shows a Clover Ge detector of the EUROBALL array inside its BGO escape suppression shield consisting of 16 individual crystals.*

[*] Contribution by J. Simpson

By the mid 1980's, arrays with ~20 ESS's having total peak efficiencies ε_p of 0.5-1.0% at 1.3 MeV were constructed. These arrays included TESSA3 (UK) [282], Chateau de Cristal (France) [283], Osiris (Germany) [284], Nordball (Denmark) [285], Hera (USA) [286], and the 8π spectrometer (Canada) [287]. These arrays enabled the study of nuclear structure features that occur at an intensity of ~ 1% of the total intensity in the nucleus, see Figure 10.2 where the intensity distribution for selected high-spin phenomena is plotted.

There then followed the construction of much bigger arrays [291, 292] using large volume Ge detectors namely EuroGam [3], GaSp [2] and Gammasphere [293] which lowered the observation limit by a further ~ 2 orders of magnitude.

The European arrays, GaSp and EuroGam were the first phase of the Euroball project. The second phase of Euroball was the development of composite Ge detectors, namely Clovers and Clusters. The third phase, Euroball III, pulled together all these developments and resulted in an array with 239 individual Ge elements with a total photopeak efficiency of ε_p of ~ 10%. This allowed the unprecedented study of the properties of the atomic nucleus with a sensitivity up to or better than 10^{-5} of the production cross-section. As an example one can take the spectrum of a normally deformed nucleus, ^{162}Er, to spin 60$\hbar$ [136] that has already been shown in Figure 5.1 (cf. Section 5). Euroball IV, which commenced operation in 1999 at IReS involved further enhancements to the project, most notably the Inner Ball spectrometer. Figure 10.2 summarises the spectroscopic sensitivity of arrays as a function of

Figure 10.2: *Plot of the spectroscopic sensitivity as a function of spin for various arrays. The TESSA 1, 2 & 3 arrays consisted of 4, 6 and 16 ESS, respectively [282]. The intensity distribution for selected high-spin phenomena is plotted. Normal deformed states up to spin ~ 50$\hbar$ in ^{160}Er [288] and spin 60$\hbar$ in ^{156}Dy [289] (●), the yrast superdeformed band in ^{152}Dy (□) [13] and excited superdeformed bands in ^{151}Tb (▽) [15] and ^{152}Dy (●) [290]. The links between the superdeformed bands and the normal deformed structures in the mass A = 190 region are also shown (●).*

spin and the approximate timescale.

In parallel with these advances in detector technology, the electronics and data acquisition systems were also revolutionised with the building of the high compact VXI electronics and associated acquisition system.

This contribution will concentrate on the developments made in detector technology, electronics and data acquisition. I will not discuss the many ancillary detectors, that have been coupled to EUROBALL for specific experiments and have contributed greatly to the spectrometers success. They are described in detail in the following chapter and in the the EUROBALL Ancillary detector handbook [294].

10.2. Large volume Germanium detectors

Throughout the period of the EUROBALL project the size and quality of hyperpure Ge crystals has increased. The drive for bigger and bigger detectors was given by the nuclear structure community because of the need for higher and higher detection efficiency. Today HPGe crystals up to with relative efficiency of up to 200% are available.

Figure 10.3: The growth of Germanium crystals;
A 15% and a 150% crystal.

EUROGAM (Figure 10.4) and GASP (Figure 10.5) were the first large detector arrays to use 65%-85% relative efficiency germanium detectors. This built on the experience gained in France where 12 similar large detectors had been used in the Chateau de Cristal [283].

Figure 10.4: The EUROGAM I spectrometer.

*Figure 10.5: The GASP spectrometer*
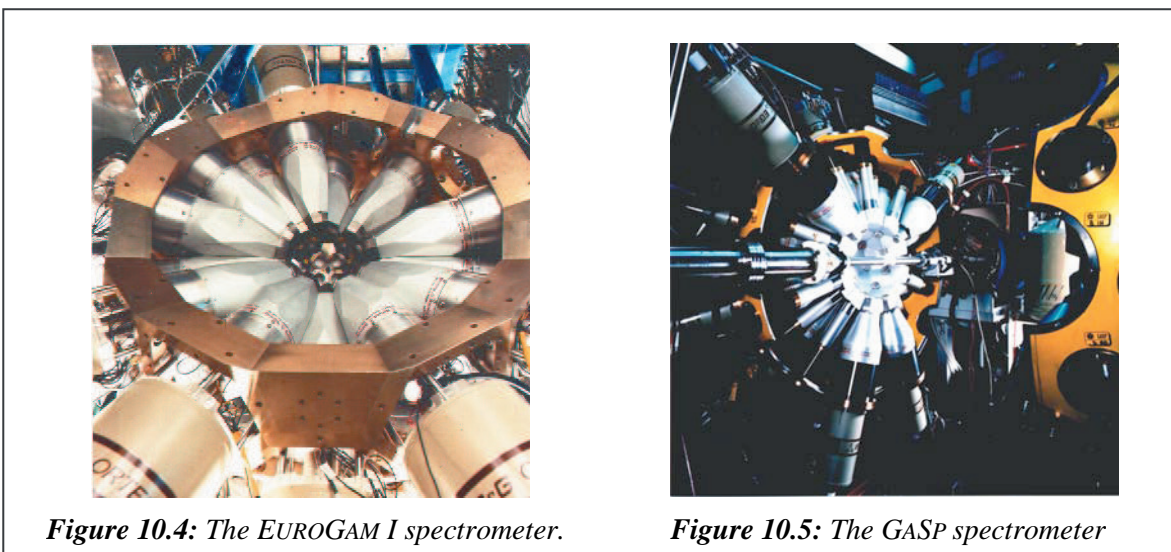
EUROGAM I used 45 detectors in bismuth germanate (BGO) suppression shields and had a total photopeak efficiency of 4.5% for 1.33 MeV gamma rays. The GASP array has 40 ESS's and can be operated in two modes, one with an efficiency of 6% and one with a lower efficiency but with the addition of an inner BGO ball. These detectors are used in the forward section of EUROBALL which contains 30 ESS's. They are arranged in three rings around the beam direction with the Ge crystals 375 mm from the target and have a total efficiency of ε_p ~1.2%.

10.3.   Composite Germanium detectors

The total photopeak efficiency that can be obtained using an array of single crystal detectors (as in EUROGAM I and GASP) is limited by the size of the crystals and by the cost. Indeed, the maximum efficiency that can be obtained using detectors of 80% relative efficiency is ~ 10% [295]. In addition, even though these large Ge detectors may be packed close to the target to give a large total photopeak efficiency, the spectrum quality is poor due to Doppler broadening. Ideally, large detectors with high granularity are needed. Developments in Ge detector technology sought to achieve this with the development of composite detectors.
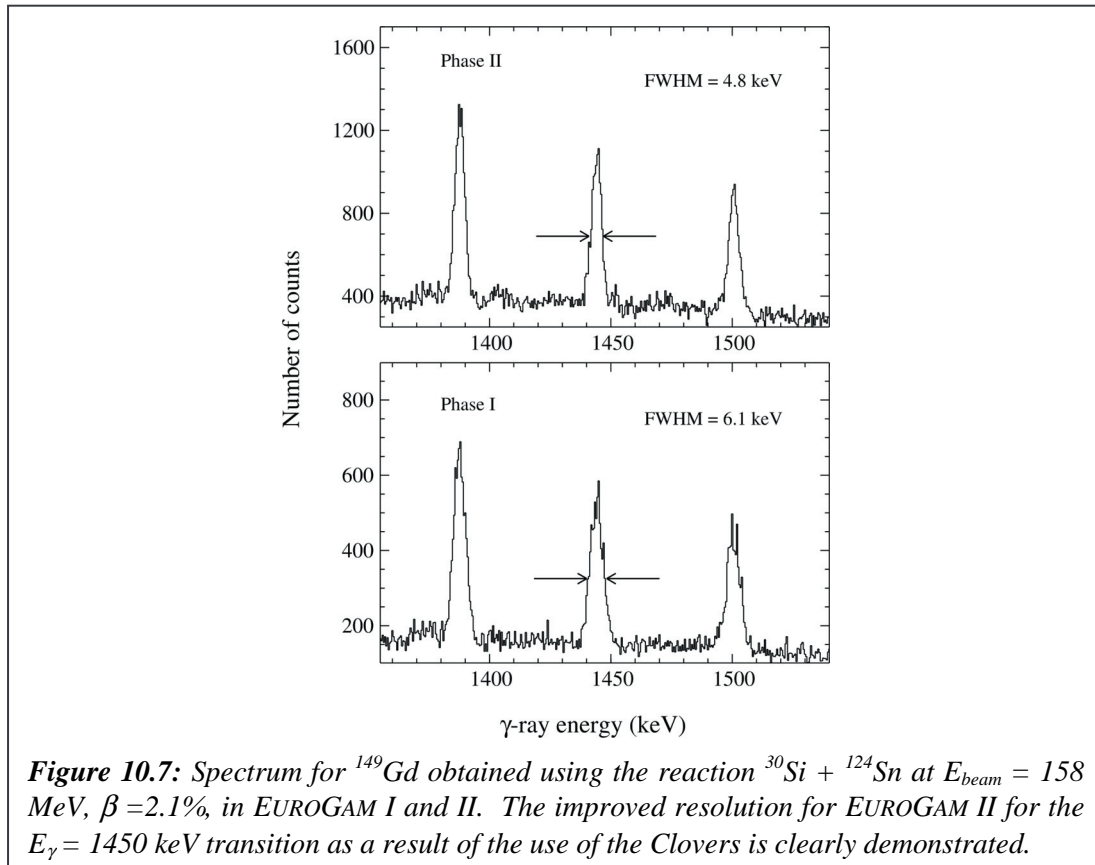
A composite detector contains several Ge crystals packed closely together in the same cryostat. The signals from each crystal are added together, including signals caused by scattering between two or more adjacent crystals. In this way a large detector can be created which has a very high photopeak efficiency and a high resolving power, since the small individual crystals minimise the effect of Doppler broadening. An array of such detectors has high granularity and high efficiency. Indeed a full 4π array of Cluster detectors, see below, can have an efficiency ε_p of over 20%.

The first composite detector to be used in a large array (EUROGAM II) was the Clover detector. This detector consists of four coaxial n-type Ge crystals arranged in the configuration of a "four-leaf Clover" and housed in the same cryostat (see Figure 10.6).
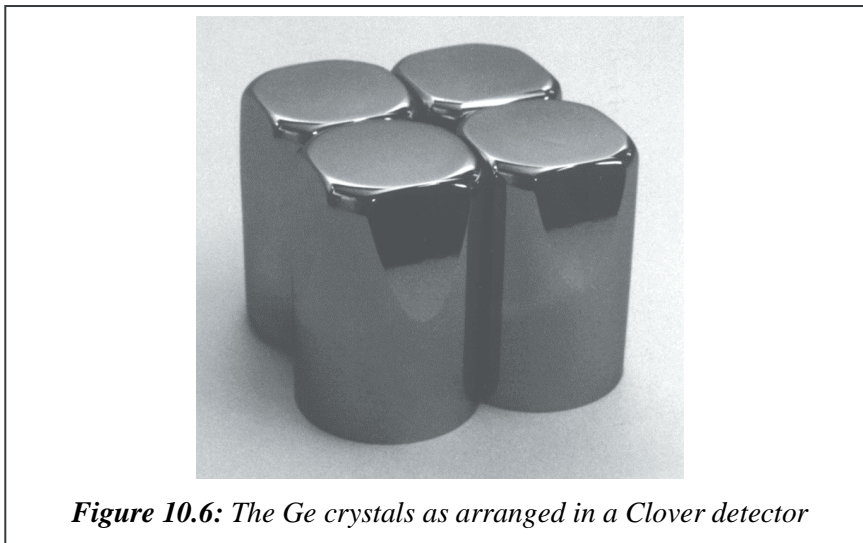
Figure 10.6: *The Ge crystals as arranged in a Clover detector*

The Clover detector [296] was developed in collaboration between IReS-Strasbourg and the company Eurysis Mesures. Each crystal is ~50 mm in diameter and ~ 70 mm long, before being shaped at the front to optimise the packing. The relative efficiency of the Clover

Figure 10.7: *Spectrum for ^{149}Gd obtained using the reaction ^{30}Si + ^{124}Sn at E_{beam} = 158 MeV, β =2.1%, in EUROGAM I and II. The improved resolution for EUROGAM II for the E_γ = 1450 keV transition as a result of the use of the Clovers is clearly demonstrated.*

detector is 140% when the scattered events are included. In EUROBALL, as in EUROGAM II, the Clover detectors are in the central section where the Doppler improvement effects are the greatest. They are arranged in two rings each with 13 detectors covering roughly 2π of solid angle. The total ε_p for the 26 Clovers is 3.8%. Figure 10.7 demonstrates this improvement in the spectroscopy of superdeformation in ^{149}Gd using the same reaction in EUROGAM I and II

The Cluster detector [297] consists of seven close packed tapered hexagonal Ge crystals (70 mm diameter and 78 mm long before shaping), each of relative efficiency 60% and resolution ~ 2 keV at 1333 keV, housed in a common cryostat (see Figs. 10.8 and 10.9). In order to achieve the very close packing required, the technique of encapsulating the crystals was developed as a collaboration between KFA Jülich, the University of Köln and the company Eurysis Mesures. Encapsulation decouples the crystal and cryostat vacuum by housing the crystal in a thin walled (0.7 mm thick), sealed aluminium capsule. The crystal is sealed for life thus avoiding the problems of surface contamination, a problem common in standard detectors. Encapsulation has proven to enhance the reliability of Ge detectors considerably. The failure rate of the 122 encapsulated EUROBALL detectors produced since 1993 is less than 4 %. After neutron damage all detectors have been annealed several times in the users lab and without any failure. Encapsulation will help to preserve the properties of the detectors over many years. In encapsulated detectors the cold parts of the preamplifiers are in a vacuum separate from that of the cryostat. It has turned out that the position of the cold electronic components, the shielding between the components and the wiring is crucial to prevent oscillation of the preamplifiers and cross talk between segments. Usually, the cryostat has to be opened several times before a perfect performance of the detector system is achieved. This procedure and also the repairs of the electronics can only be performed on systems with encapsulated detectors without running the risk of damaging the Ge detectors.

Figure 10.8: *The encapsulated Ge crystal for the EUROBALL Cluster detector.*


Figure 10.9: *Encapsulated Ge crystals arranged in the 7 detector cluster.*

The Cluster detectors are arranged in the backward end cap of EUROBALL in three rings with the Ge crystals 445 mm from the target. The 15 clusters have an efficiency ε_p of 4.4%.

Composite Ge detectors have become the standard for many applications where high-efficiency is required. Encapsulation technology has many advantages, some of which, reliability, ease of repair and handling have resulted in their use in space missions, e.g. the Mars Odyssey [298] and INTEGRAL [299] space missions.

Figure 10.10: *Mars Odyssey.*
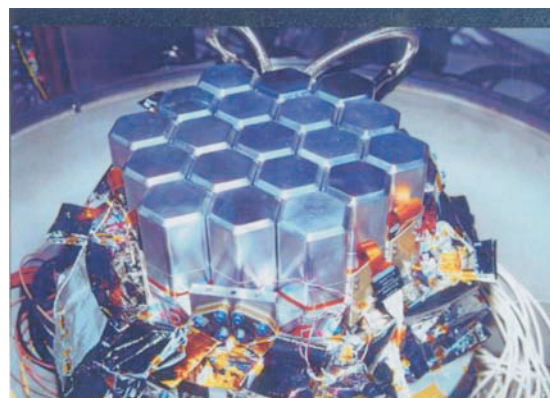
Figure 10.11: *19 encapsulated detectors to be used in the INTEGRAL mission.*

10.4. Array design

A technical achievement of EUROBALL that is often forgotten is the mechanical design itself. The array consists of three major detector types all of totally different shapes originally designed for different arrays (see Figs. 10.12 and 10.13). The design criteria included placing all the detectors together with a clearance between each adjacent suppression shield of 0.25mm, a requirement that the axis of each Ge detector looks at a common central point to an accuracy of 1mm all this with the total weight of the detectors and support structure of 9 tonnes. In addition to the support structure most of the detectors including the complex shaped suppression shields and their crystals were designed by the collaboration. In all the design complex three-dimensional computer aided design (CAD) systems and finite element analysis (FEA) was required.

Figure 10.12: A CAD generated image of EUROBALL in design.

Figure 10.13: The real thing, EUROBALL III in Legnaro, Italy.
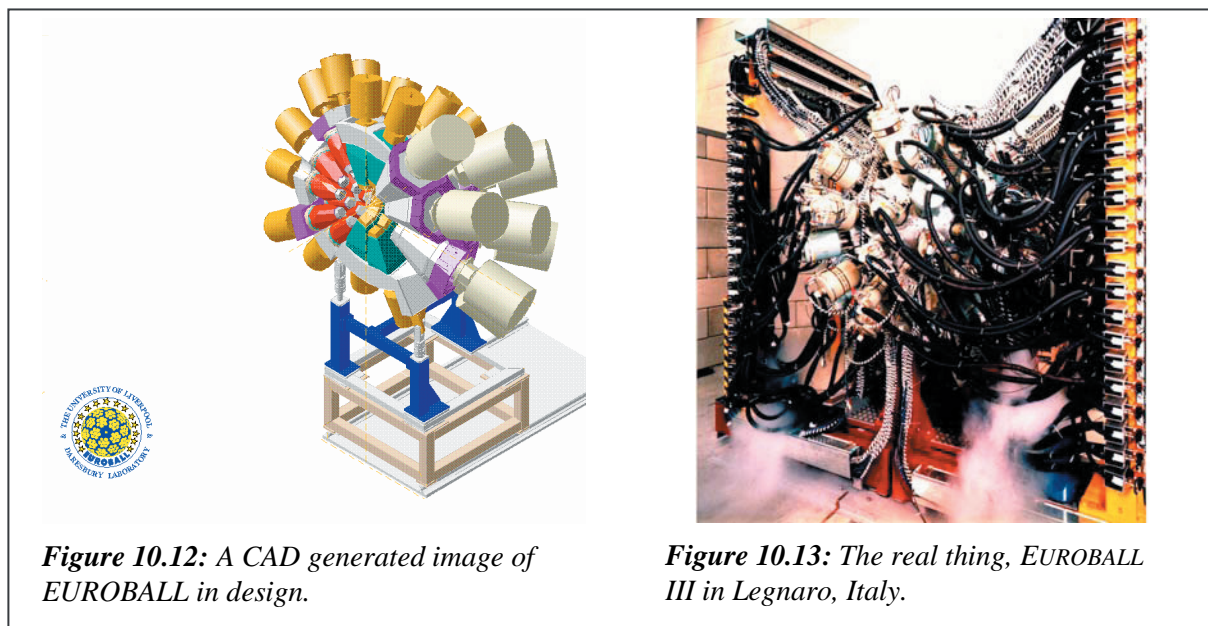
10.5. Segmented Germanium detectors

Improved granularity of an array, and hence reduced Doppler broadening, can be achieved by electrically segmenting the Ge crystals. A segmented detector is a standard n-type detector with the main high-resolution energy signal taken from the centre contact and position information taken from signals on isolated outer contacts. In EUROBALL segmented Clover detectors were designed to improve the performance of the central section (see Figure 10.14). These Clover detectors have each crystal segmented into four parts producing a single detector with 16 active elements [300]. These detectors are and have been used extensively in radioactive beam experiments at Ganil, within the EXOGAM project [301], at GSI and in the SARI array at Jyväskylä. Larger crystal segmented Clovers are now being used in EXOGAM and in the VEGA spectrometer [302].

The MINIBALL array [303], currently being assembled at ISOLDE, CERN, is a prime example of the use of encapsulated, segmented detectors. MINIBALL will consist of 40 six-fold segmented, encapsulated Ge detectors. The development is based on the encapsulation technology used for the EUROBALL Cluster detector [297]. In Figure 10.15 the 6-fold segmented MINIBALL detector is shown.
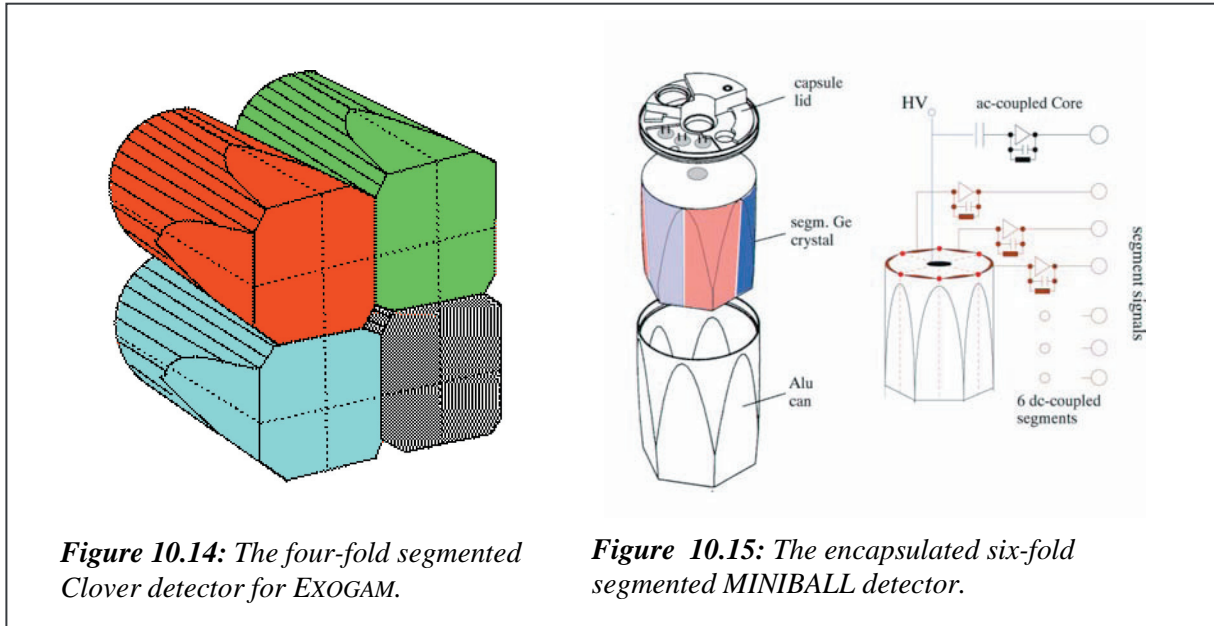
Figure 10.14: *The four-fold segmented Clover detector for EXOGAM.*

Figure 10.15: *The encapsulated six-fold segmented MINIBALL detector.*

10.6. Electronics and data acquisition

The EUROBALL project had led to significant advances in electronics and data acquisition systems. Indeed, to the user these changes are those appearing the most dramatic. The major development has been in the compression of the electronics and software monitoring and control of the parameters. In order to achieve the degree of integration needed, the VXI (VME eXtension for Instrumentation) bus standard was used for the front-end electronics. This standard allows a large card size to be used and the mixing of both high density analogue signal processing and digital circuits. VXI cards have been built for specific applications, for example, detector signal processing, digitisation and event triggering, e.g. see [304]; VXI electronics was first used for the EUROGAM I spectrometer.

The VXI electronics for EUROBALL is housed in just 9 VXI crates with additional crates for ancillary detectors. These nine crates deal with ~250 Ge channels, ~800 BGO channels and ~100 INNER BALL channels in EUROBALL IV. EUROBALL has specific VXI cards for each of its Ge and BGO suppression shield detectors. The Cluster Ge card (Fig. 10.16), for example, has 8 identical channels. Each channel has all analogue electronics for one Ge channel,
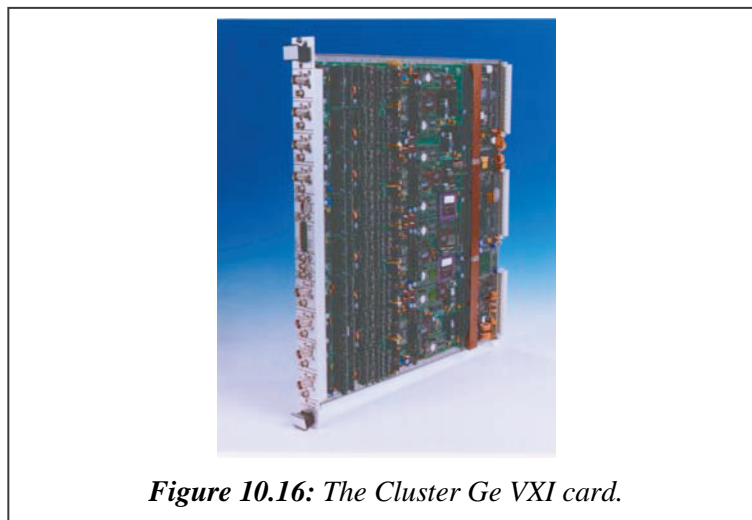
**Figure 10.16:** *The Cluster Ge VXI card.*

including shaping and timing amplifiers, constant fraction discriminators, and analogue to digital converters to provide digitized energy, and time information. One Cluster Ge card for example, when first produced, was equivalent to eight full crates of NIM electronics.

The EUROBALL data acquisition system was designed to handle data rates up to 20 Mbytes/sec. The system comprises several components. The event collector, a VME module for each DT32/FERA bus to collect event fragments for a given number of events. These sub events are then distributed via an event builder (to construct the total event) to the processor farm via a fibre channel network. The processor farm, consisting of UNIX workstations, performs the event building and any on line analysis. Event storage will be on digital linear tapes and/or exabytes. The system is required to be able to collect the data generated by event rates up to 50 - 100 kHz in order to be suitable for a wide range of experimental situations. A more thorough overview of the data acquisition system can be found in [305].
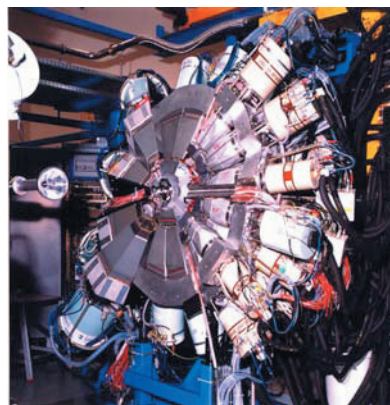
The software to control all the different electronics modules, to provide a user interface to all parts of the system, to set-up the register in all cards, to control the spectrum and tape storage system developed for EUROBALL is called MIDAS [306]. MIDAS (Multiple Instance Data Acquisition System) is now a global standard, used in many nuclear structure laboratories and also for non nuclear structure scientific experiments.

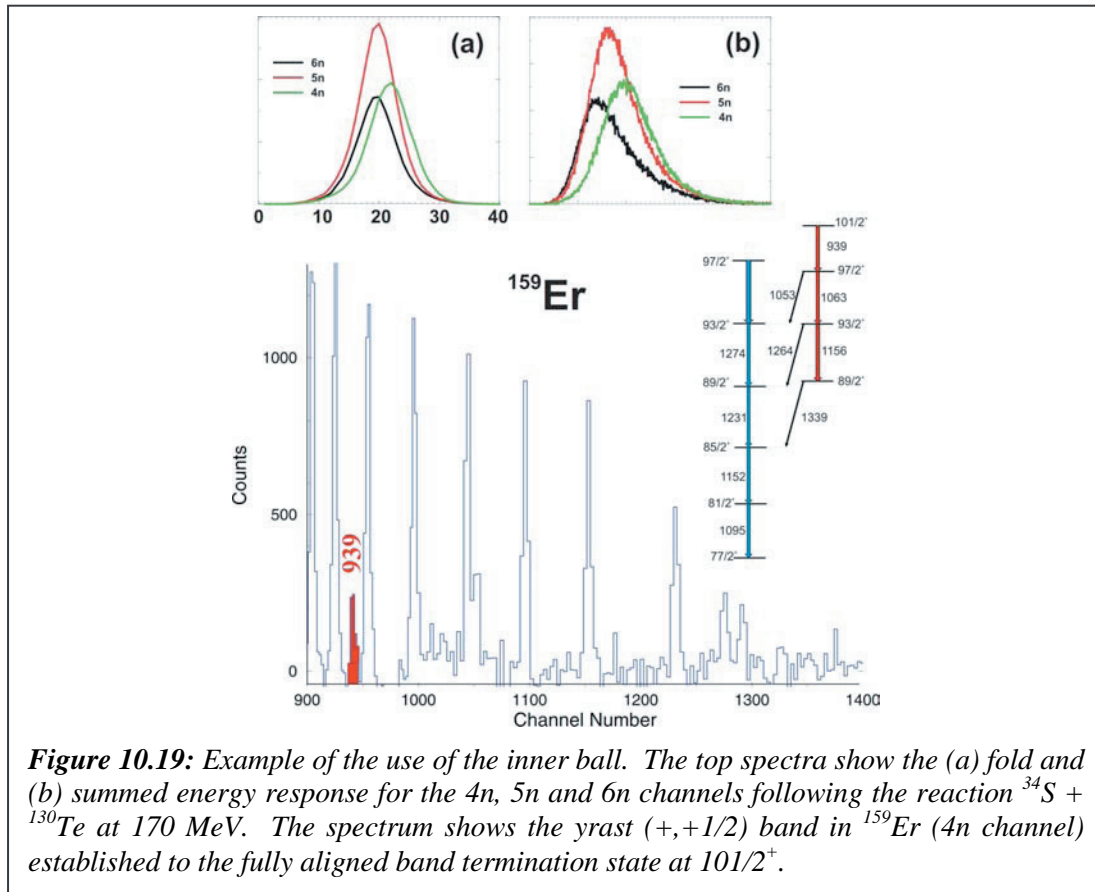## 10.7. EUROBALL IV and the inner BGO ball

The EUROBALL spectrometer was upgraded in its second phase of operation at IReS, EUROBALL IV, with the inclusion of an INNER BALL of BGO detectors. An inner scintillator ball measures the γ multiplicity and the γ-sum energy, thus probing spin and excitation energy of a nuclear reaction. This information constitutes a highly efficient filter to select specific reaction channels and to suppress unwanted background. The INNER BALL has been designed to cover almost 4π and to have good detection efficiency. This is achieved by including the Ge detectors which cover roughly 40% of the solid angle as part of the summed energy and multiplicity measurement. The design of the INNER BALL is highly complex due to the differing shapes in the three sections of the array. In the final design the cluster section comprises 80 tapered hexagonal detectors of which there are 6 types, the central section comprises 13 detectors each containing 5 different crystals and the forward section 50 trapezoidal detectors of 5 types. The full ball, shown in Figure 10.17 is operated as a 164 element device, 59 elements from the INNER BALL and 105 elements from the Ge detectors.
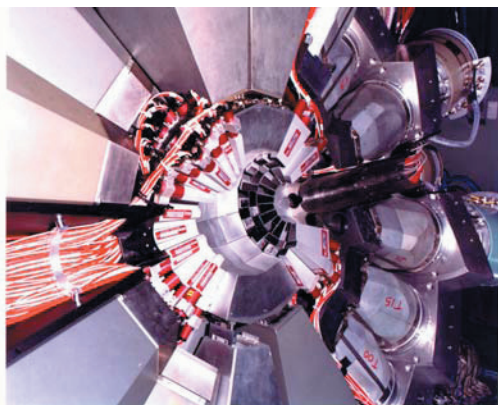
Figure 10.17: *The BGO inner-ball calorimeter of EUROBALL IV.*

Figure 10.18: *EUROBALL IV in Strasbourg, France.*

Figure 10.19: *Example of the use of the inner ball. The top spectra show the (a) fold and (b) summed energy response for the 4n, 5n and 6n channels following the reaction ^{34}S + ^{130}Te at 170 MeV. The spectrum shows the yrast (+,+1/2) band in ^{159}Er (4n channel) established to the fully aligned band termination state at $101/2^+$.*

The INNER BALL installed in EUROBALL IV (Figure 10.18) has proved to be a powerful addition to the spectrometer and several beautiful results from its use are shown in this report. Figure 10.19 shows the INNER BALL response from an experiment to study the very high spin states in Er nuclei.

10.8. Gamma-ray tracking

The developments of large volume, segmented, encapsulated detectors and high performance and compact electronics systems, mostly through EUROBALL related collaborations has made it feasible to propose the next generation gamma-ray spectrometer based on gamma-ray tracking [307]. The sensitivity and selectivity of AGATA, the proposed project to build a 4π Ge shell [308], will make it superior to any existing spectrometer by several orders of magnitude. The project will build on the strong European collaborations established during the EUROBALL years. The realisation of AGATA will ensure an exciting and interesting future for nuclear spectroscopists in their investigation of the fascinating structure of the nucleus.

Acknowledgements

Additional detectors for EUROBALL

B.M. Nyakó and J.N. Scheurer

11.   Additional detectors for EUROBALL

11.1.   DIAMANT-III: the upgraded 4π light charged-particle detector array[*]

Abstract: *DIAMANT-III is an upgraded version of the ancillary detector developed in CENBG, Bordeaux, for use in large gamma-ray spectrometers to identify the light charged particles emitted in heavy-ion induced reactions. It has 84 CsI(Tl) detectors, with improved light collection, which are equipped with preamplifiers working in vacuum. The processing of signals coming from the particle detectors is performed now entirely by VXI electronics. The newly designed VXI card is fully compatible with the existing signal processing system of EUROBALL. For each detector three types of signals are derived: the energy and the type of the particle, and a time-reference signal related to the time instance of the particle–gamma coincidence. For deriving the particle type information the zero-crossing method, the ballistic deficit method or the combination of these two, giving the best figure of merit for the particle discrimination, can be used. Data readout is managed using the G.I.R general-purpose readout interface card developed in CSNSM, Orsay. Typical result from experiments with the EUROBALL IV are used to illustrate the performance of the new ensemble.*
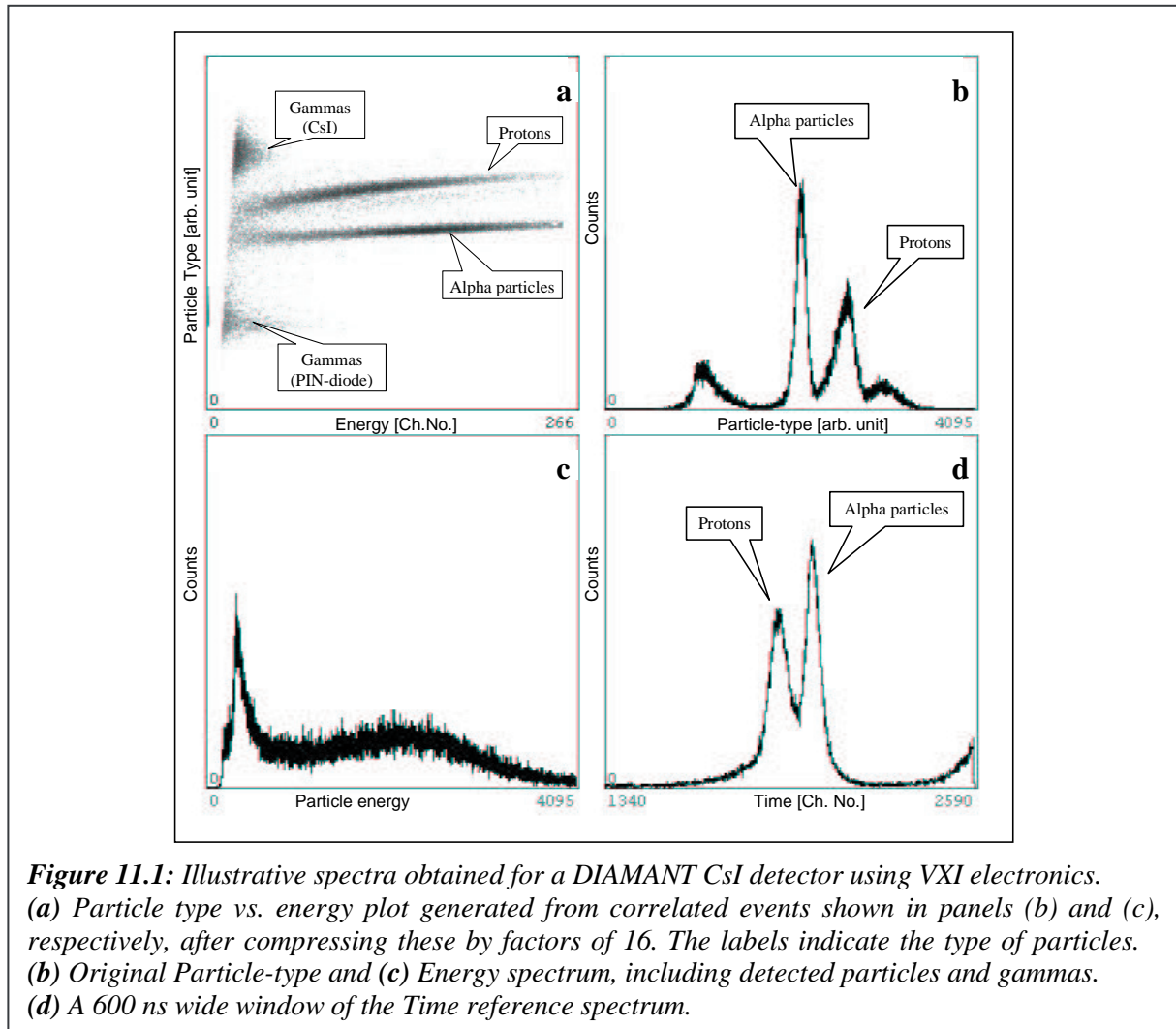
The DIAMANT array [6], serving as an ancillary detector in large gamma-ray spectrometers like EUROGAM [3] and EUROBALL [1], has recently been upgraded within a Bordeaux-Debrecen-Napoli collaboration. This system, having detectors made of CsI(Tl) scintillation crystals coupled to *pin*-photodiodes by 5 mm plexiglass light guide, is used to identify light charged particles. The detectors are arranged in a polyhedron geometry made of 18 square and 8 triangle planes which are formed by single triangle detectors (with 10mm thick light guide) and sets of 4 square detectors with maximum dimension of 14.5x14.5 mm^2. The distance of the square planes from the target is 32 mm, except the one in forward direction, which is replaced by a plane of 8 detectors arranged as a 3x3 array at a distance of 49 mm. The 3 mm thick detectors, able to fully stop protons up-to an energy of about 25 MeV, have over 70% light-collection efficiency due to our newly developed special wrapping technique.

The CsI detectors are equipped with special charge-sensitive preamplifiers [309] of low heat dissipation. They are mounted on the detectors inside the vacuum chamber. The signals from these *first-stage* preamplifiers are connected by flat ribbon cables, via vacuum feed-through, to a set of *second-stage* preamplifiers, which are used as line-drivers to send the signals through coaxial cables to the signal processing electronics.

The signal processing of DIAMANT is now done by new VXI electronics [310]. The D-size VXI card, developed in Debrecen, contains eight complete electronic channels, each of which produces three signals: energy, particle type and time reference. To reach full compatibility with the EUROBALL electronics, and to further improve the performance of DIAMANT, some new techniques have been used for signal processing. The *energy* signal is produced by a *delay-switched gated integrator* [311,312]. The integration time is adjustable from the software (3-12 μs), and it determines the signal processing time. The *time reference* for particle–gamma coincidence is derived by *non-delay-line* CFD-s [310,313] using a 600ns time window. The *particle-type* information is obtained using two pulse shape discrimination techniques: the *ballistic deficit method* [312,314] and the *zero-crossing method* [315]. Any of these or a combination of them, the *mixed method,* can be selected. The latter one gives the best figure of merit for α–proton discrimination. Although CsI detectors are slow relative to the Ge detectors, signal rise-times are 1600-2000 ns (for charged particles) and 100-200 ns, respectively, with these new solutions the readout electronics of the particle-detector array can complete the data treatment within the same time necessary for the Ge detectors, while both

---

[*] Contact persons: B.M. Nyakó (nyako@atomki.hu) and J.N. Scheurer (scheurer@cenbg.in2p3.fr)

Figure 11.1: *Illustrative spectra obtained for a DIAMANT CsI detector using VXI electronics.*
*(**a**) Particle type vs. energy plot generated from correlated events shown in panels (b) and (c),*
respectively, after compressing these by factors of 16. The labels indicate the type of particles.
*(**b**) Original Particle-type and (**c**) Energy spectrum, including detected particles and gammas.*
*(**d**) A 600 ns wide window of the Time reference spectrum.*

good *energy resolution* and *particle separation* is achieved. The short integration time enables particle detection up-to high count rates. Pile-up events are marked during data collection. The card generates also a *sumbus* signal in each channel if a particle is detected, so particle multiplicity can also be derived. For the coding of the *energy*, *particle type* and *time reference* signals three independent ADCs of the same type as used for the Ge detectors are applied. Data readout is managed using the G.I.R general-purpose readout interface card developed in CSNSM, Orsay [316].

The VXI cards are integrated into the VXI environment [304] of EUROBALL. For the synchronisation of data processing two global trigger signals, the *Fast Trigger* (FT) and the V*alidation* (VAL) generated by the Master Trigger Unit are used. On each channel a Local Trigger (LT) controls, if the signal from the CsI detector is in coincidence with a delayed FT signal. If so, the channel is involved in a particle-gamma coincidence. Data readout occurs only, if a validation signal arrives. LT can operate in slave, test or master mode, the last two mainly useful for test or stand-alone operation. The set-up and control of the VXI cards are managed using a special user interface of the MIDAS software [306].

In nuclear structure studies, data acquisition with DIAMANT can be maintained in two main operating modes: when DIAMANT alone is involved in the *validation,* or when DIAMANT is also involved in the *validation*, in which case either the Ge array or the CsI array can validate

an event. In the first case only (HI, particle-xn) channels, in the second one both (HI, particle-xn) channels and (HI, xn) channels are collected.

The measured performance of the present version is as follows: The typical energy resolution at 5 MeV measured with an alpha-source is 2%, the low-energy thresholds for proton-alpha discrimination is around 2 MeV (proton) and 4 MeV (alpha). The array's gamma absorption is to be considered only if detection of gammas below 200 keV is important (see Ref. [317]). The overall time resolution for particles has improved from 70ns to 20ns (without any correction). The measured efficiency for detecting one proton is ~70%. The presence of the CsI array does practically not affect the peak-to-total ratio of the Ge detectors, with a typical value of 0.55 for a ^{137}Cs source.

The type and quality of data, which can be obtained with DIAMANT after the upgrade, are illustrated in Figure 11.1. Putting 2-dimensional gates on spectra like the one shown in Figure 11.1a, very good enhancement can be achieved in selecting gamma-rays related to reaction channels with particle emission. Some illustrative spectra can also be seen in our contribution (B.M. Nyakó et al., A step forward in…) to the EUROBALL Booklet on the Euroball workshop held in Orsay, March 2002. With different combinations of gates put on *Time-reference vs. Energy*, *Time-reference vs. Particle-type* and/or just on the *time reference* data alone, a further cleaning of the random events is possible.

Acknowledgements

11.2. The EUCLIDES array[*]

Array description

The EUCLIDES array is a charged-particle detector array developed and built within a collaboration of the INFN laboratories in Legnaro, Padova and Firenze as well as the University of Liverpool and the Daresbury laboratory. EUCLIDES is composed of 40 ΔE-E Si telescopes (130 μm + 1000 μm thick) arranged in the same geometry as the ISIS Si-ball [4] (see Figure 11.2). The five forward elements are electrically segmented in four parts and there are plans to segment the following ten elements in two parts. The ΔE detector is mounted in a reversed configuration, enabling charged particle discrimination with pulse shape techniques [318]. The front-end electronics is composed of charge-sensitive preamplifiers and of specially designed single-unit CAMAC modules, called Silicon Shaper Analyser, which provide linear (gaussian and stretched) and logic (fast timing and crossover timing for pulse shape analysis) outputs. Data are collected through FERA ADCs and TDCs and sent to the EUROBALL data acquisition via the Fera-VXI interface.

Status

At the beginning of its operation, EUCLIDES suffered from various problems. Part of these problems is related to a faulty detector design, which has been solved by the manufacturer (Micron Semiconductors Ltd). Most of the faulty telescopes have been replaced, however this slowed down the production of segmented detectors and at the time of writing only the five forward telescopes on the array are segmented. Also the front-end electronics suffered from various bugs which took quite a long time to fix. This precluded the required development work on the pulse shape part, which remains the major missed goal of the project. The performance of EUCLIDES as a standard ΔE-E array is very satisfactory. The discrimination capability is excellent, since less than 0.01% of the detected particles are misidentified. The
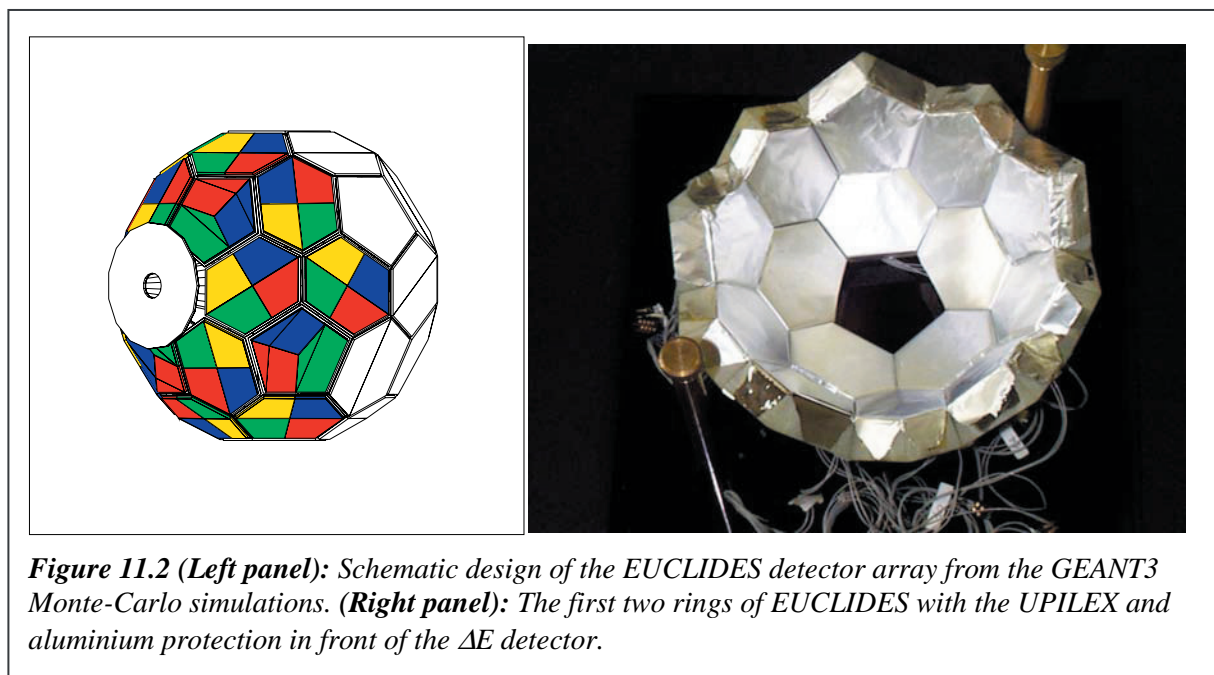
Figure 11.2 (Left panel): *Schematic design of the EUCLIDES detector array from the GEANT3 Monte-Carlo simulations.* **(Right panel):** *The first two rings of EUCLIDES with the UPILEX and aluminium protection in front of the ΔE detector.*

---

[*] Contact person: E. Farnea (farnea@pd.infn.it)

detection efficiency depends strongly on the reaction and on the absorbers used to stop the scattered beam ions; values of $\varepsilon \sim 60\%$ for protons and $\varepsilon \sim 40\%$ for α particles can be obtained.

EUROBALL experiments

EUCLIDES has been used in 24 experiments (including three commissioning runs), for a total of 141 days of beam time, in a stand-alone configuration or together with other ancillary devices:

- stand-alone: 1 experiment, 5 days
- Neutron Wall: 1 commissioning run, 10 experiments, 69 days
- Neutron Wall + Isomer tagging: 2 experiments, 16 days
- Köln plunger device: 1 commissioning run, 2 experiments, 16 days
- INNER BALL: 1 commissioning run, 4 experiments, 23 days
- HECTOR + INNER BALL: 1 experiment, 6 days
- RFD : 1 experiment, 6 days

Acknowledgements

11.3. The HECTOR array[*]

Abstract: The large volume BaF$_2$ detectors of the HECTOR array have been used in one measurement on ^{143}Eu made in the Legnaro (see references [95,134]) and more recently during spring 2002 in 3 measurements at Strasbourg. At variance from the Legnaro measurement, in Strasbourg also 3/4 of the INNER BALL was present and for one measurement also the Silicon ball EUCLIDES has been used to measure charged particles. Here below we give more details on the Strasbourg measurements whose data are presently being analysed.

EUROBALL experiments in Strasbourg with HECTOR

The part of the HECTOR array [11] used in the Strasbourg measurement consisted of 8 large volume BaF$_2$ detectors and 4 small BaF$_2$ detectors. These detectors were incorporated into the EUROBALL array, in order to measure the high-energy gamma rays from the decay of Giant Dipole resonance in coincidence with discrete lines from the residual nuclei. The large volume BaF$_2$ detectors were mounted in the forward hemisphere replacing the Phase1 detectors (detectors with green housing in Figure 11.3). As the forward part of the EUROBALL INNER BALL (consisting of BGO crystals) had to be also removed, there was room to place very close to the reaction chamber, 4 small BaF$_2$ crystals from HECTOR's multiplicity filter (detectors with yellow housing in Figure 11.3). They were used to obtain the reaction time definition.
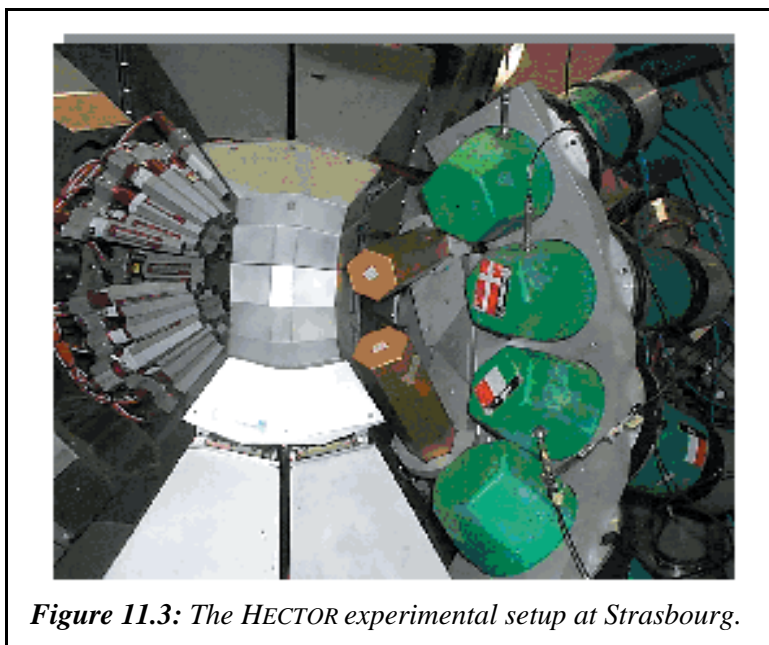
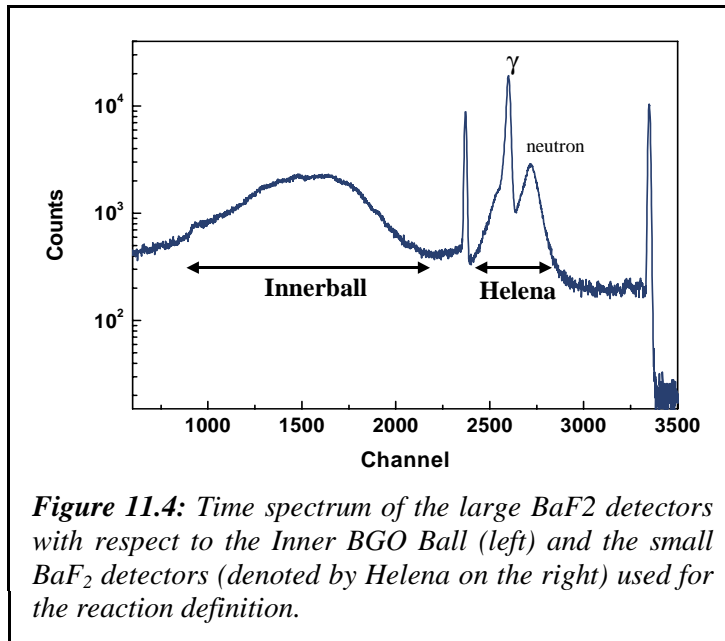
Figure 11.3: The HECTOR experimental setup at Strasbourg.

Figure 11.4 shows the time spectrum of the large BaF$_2$ detector with respect to the EUROBALL INNER BALL (left part) and the small BaF$_2$ crystals (appearing on the right part of the figure and denoted by Helena). The time resolution when the BaF$_2$ detectors fired was 1.6 ns, allowing, as can be seen in the figure, for clean separation between gamma and neutron induced events. In contrast, when the time was defined by the Inner Ball it produced a distribution with a width of 35 ns which did not allowed for gamma-neutron separation. Therefore, in the performed experiments the inner ball was used only as the multiplicity filter, while the reaction time was defined by the 4 small BaF$_2$ Helena detectors for all the events in which a high energy gamma-ray was detected.

The HECTOR electronics consisted of standard NIM modules and VME ADC and TDC (from CAEN). The coupling of the VME electronics to the VXI electronics of EUROBALL ACQ system was made using the ATTIC module from the Neutron Wall system. In the experiment in which the array of Si telescopes (EUCLIDES) was used, the coupling of its electronics was done via the FVI module.

---

[*] Contact person: A. Bracco (Angela.Bracco@mi.infn.it)

Figure 11.4: *Time spectrum of the large BaF2 detectors with respect to the Inner BGO Ball (left) and the small BaF$_2$ detectors (denoted by Helena on the right) used for the reaction definition.*

The three performed experiments were intended to address three different physical issues. One was that of the investigation of the gamma decay of the giant dipole resonance in the feeding of superdeformed structures and this experiment concerned the ^{196}Pb nucleus. An experiment aiming at searching for hyperdeformed structures in ^{126}Ba was made and there the gating with high energy gamma-rays could help in this search.

The other very interesting problem addressed in the third experiment is that of the identification of the expected Jacobi transition of nuclear shapes (namely that from oblate to very extended prolate occurring in rotating objects at very high rotational frequency). The performed experiment focused in particular on the ^{46}Ti nucleus for which such a transition is expected to be at I≈30$\hbar$ and used a 100 MeV ^{18}O beam impinging on a ^{28}Si target. The main experimental signature of this Jacobi shape change phenomenon is expected to be the large splitting of the GDR components corresponding to vibrations along the different symmetry axes. Indications of such feature in the GDR spectra in this mass region were earlier obtained both by the Seattle group [319] and by the HECTOR group [320]. However these experiments were not exclusive enough to exclude other possible explanations as for example contaminations from fission. In contrast, the GDR spectra measured by HECTOR in coincidence with the discrete lines of specific residual nuclei, measured in the germanium detectors of EUROBALL, correspond uniquely to the fusion-evaporation channel. Other indications of the Jacobi transition are the expected Giant Backbend of the E2 transitions [321] and the change of the angular distribution of the evaporated charged particles, quantities that can be simultaneously studied in the present measurement because of the presence of the EUROBALL clusters detectors and of the EUCLIDES array, respectively.
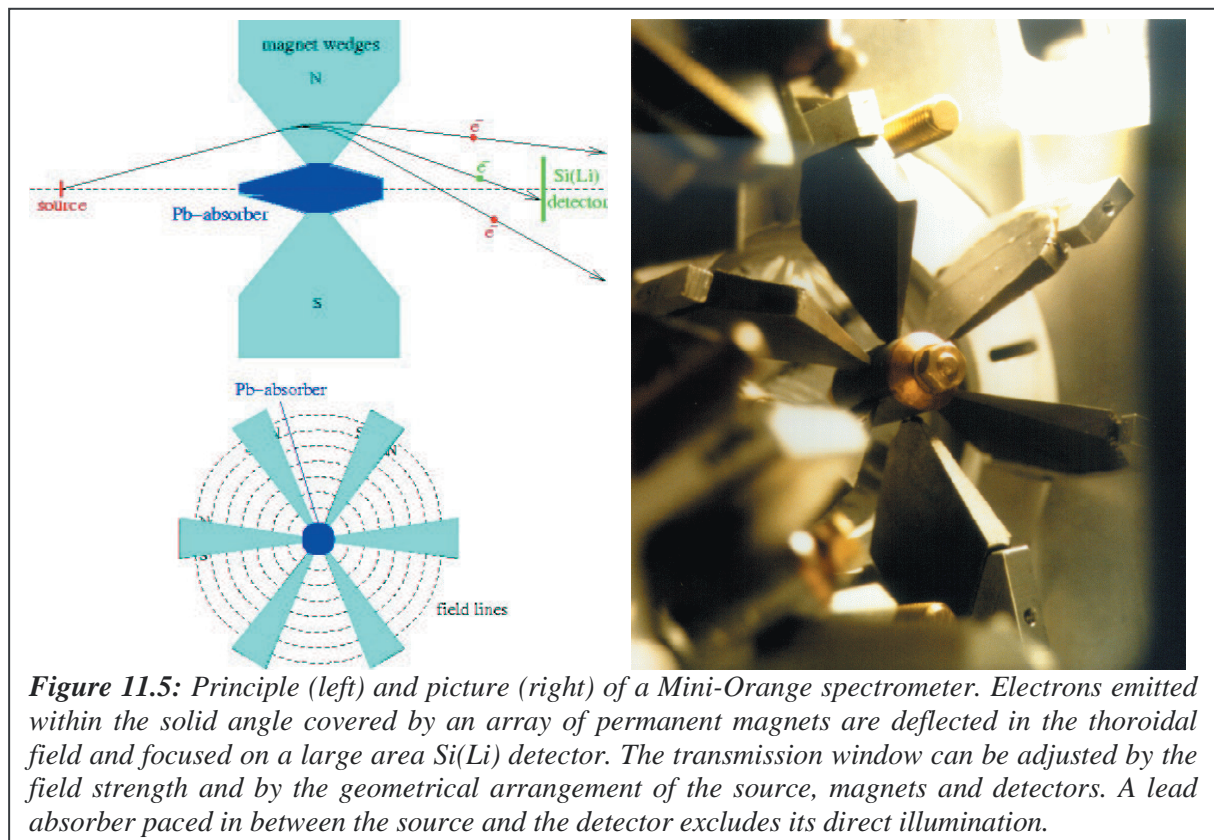
Ackowledgements

The following people are involved in the HECTOR experiments with EUROBALL : A. Maj, A. Bracco, F. Camera, S. Brambilla, J. Nyberg, and P. Bednarczyk.

11.4. The Internal Conversion Electron Mini-Orange Spectrometer (ICEMOS)[*]

Gamma-ray spectroscopy is the most powerful tool to study the structure of excited states in nuclei. But in some cases the information that is available through γ-ray detection alone is too limited in order to investigate important nuclear structure aspects. One example are electric-monopole (E0) transitions, which can not proceed via the emission of (single) γ rays, but proceed instead by internal conversion, i.e. the emission of electrons from (inner) atomic shells. Pure γ-ray spectroscopy must then be replaced by electron-gamma coincidence spectroscopy. A second important aspect of conversion-electron spectroscopy is the possibility to determine the electro-magnetic multipolarity of the emitted radiation via measurements of conversion coefficients. This method is complementary to the combined measurement of γ-ray angular distributions (sensitive to the multipole order) and of the linear polarisation (sensitive to the electromagnetic character, E or M). Finally, in heavy nuclei and/or for higher multipolarities where the conversion probabilities is large, conversion-electron spectroscopy may be the only way to identify the transitions.

In-beam conversion-electron detection is severely impaired by the atomic background of low-energy δ electrons, which are created with extremely high cross sections in heavy-ion induced reactions. In our approach, Mini-Orange spectrometers [322] are used to suppress most of this background. They consist of wedges of permanent magnets arranged to create a thoroidal field focusing electrons of a given energy on a detector placed at the focal point of this magnetic lens (see figure 11.5). Different from a large (iron-free) Orange spectrometer the radial and azimuthal variation of the magnetic field strength gives rise to a certain range of electron momenta that are transported to the detector ("transmission window"). A liquid-

Figure 11.5: *Principle (left) and picture (right) of a Mini-Orange spectrometer. Electrons emitted within the solid angle covered by an array of permanent magnets are deflected in the thoroidal field and focused on a large area Si(Li) detector. The transmission window can be adjusted by the field strength and by the geometrical arrangement of the source, magnets and detectors. A lead absorber paced in between the source and the detector excludes its direct illumination.*
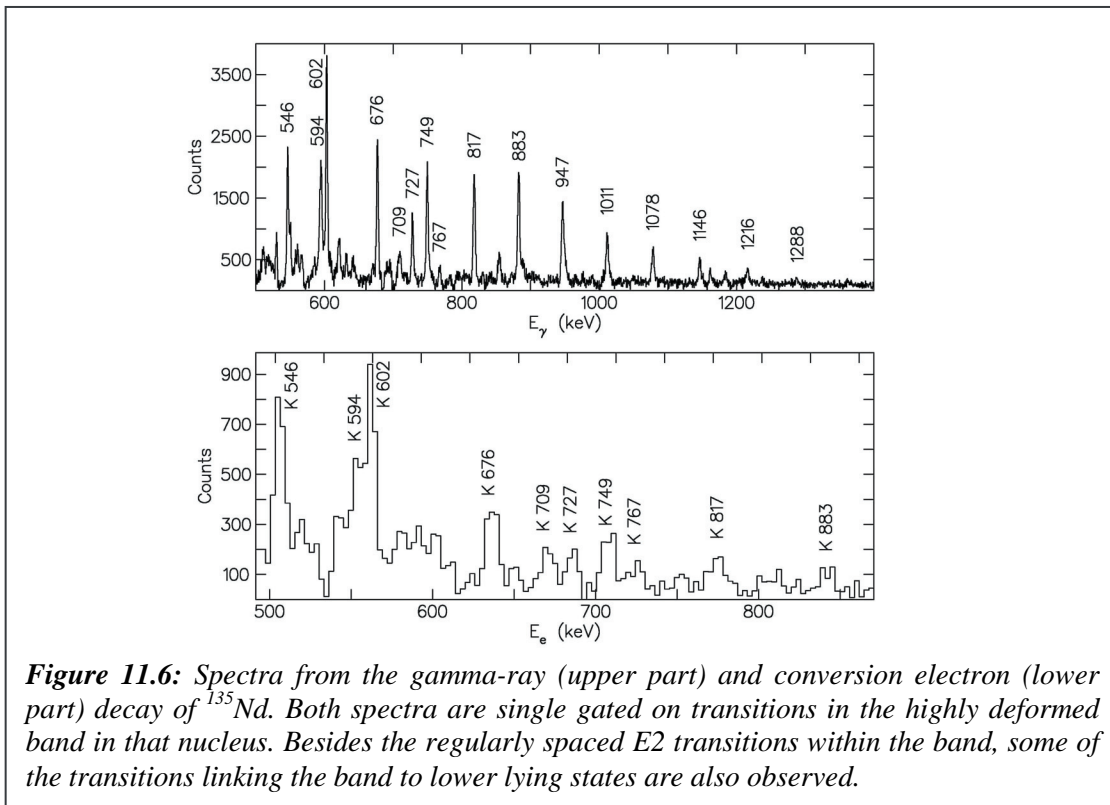
---

[*] contact persons: H. Hübel (hubel@iskp.uni-bonn.de) and W. Korten (wkorten@cea.fr)
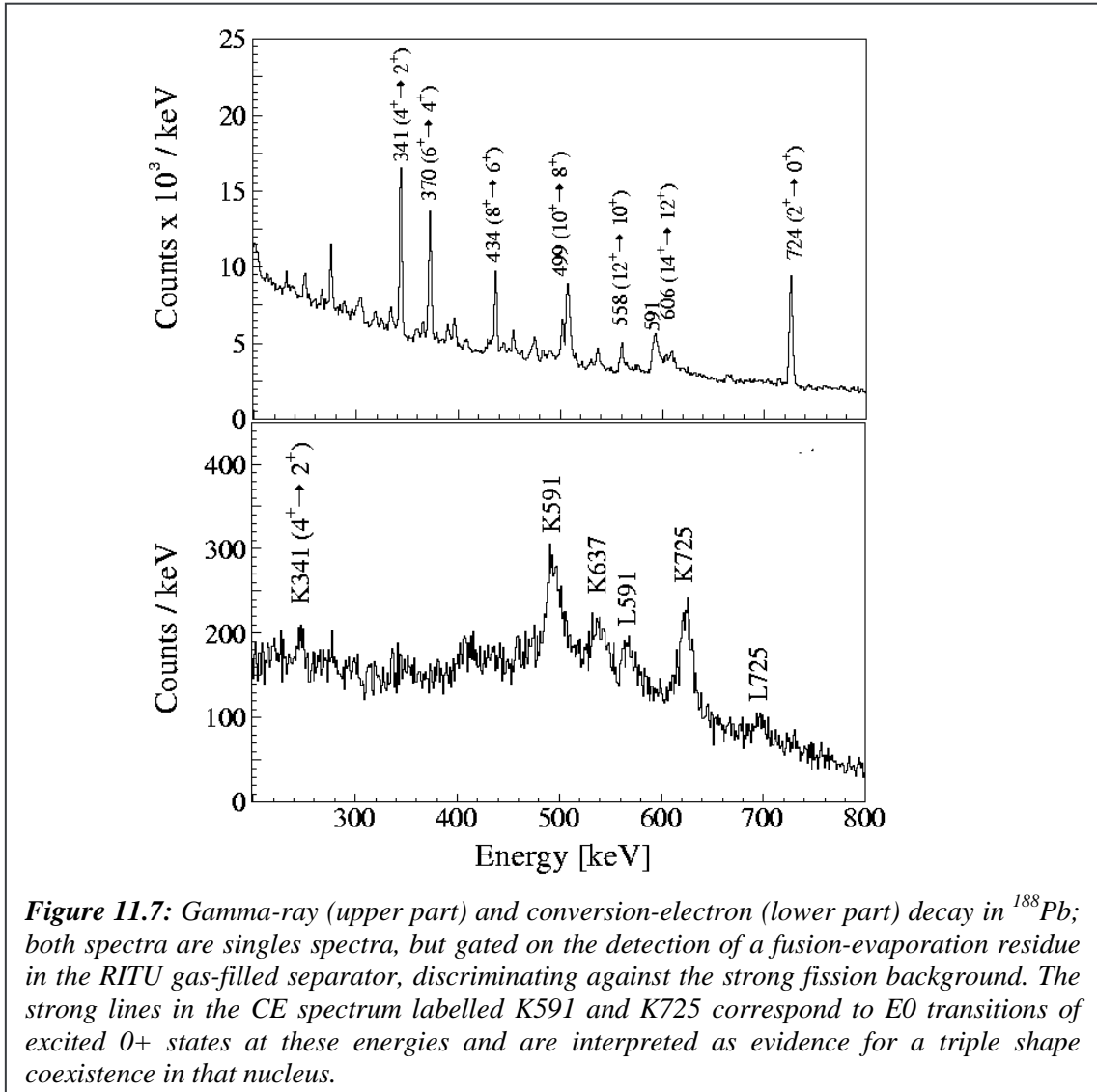
nitrogen cooled Si(Li) detector (of up to 6 mm thickness) measures the electron energy with high resolution. The setup is very compact and can be installed inside the scattering chamber of a large γ-ray spectrometer.

The transmission window of the Mini-Orange spectrometers can be adjusted through the number of magnets, their strength and by the distances between target, magnets and detector. Depending on the experimental conditions the peak position and width of the transmission curve can be changed. For a peak efficiency of ~5% at electron energies of ~600 keV the width is typically a few hundred keV. The Si(Li) detectors are located in their own vacuum chamber behind the Mini Oranges and are separated from the vacuum of the beam line by (thin) Carbon or Mylar foils, in order to protect their surfaces from contamination. The thin foil further reduces the remaining δ–electron background, especially for the very lowest energies.

Experiments to obtain spectroscopic information from *electron-gamma coincidence spectroscopy* are best done by having large, comparable efficiencies for both conversion-electron and gamma-ray detection. By replacing the forward EUROBALL sector of individual Ge detectors with a Three-Mini-Orange conversion-electron spectrometer, an efficiency of ~ 5% for electrons (in the peak of the transmission curve) can be reached, similar to the γ-ray photo-peak efficiency (at 1.3 MeV) of the remaining Clover and Cluster detectors. Experiments with ICEMOS at EUROBALL allow for the first time electron-γ coincidence spectroscopy of weakly populated nuclei.

Before being used at EUROBALL the ICEMOS spectrometer has been very successfully used in combination with several smaller Ge detector arrays. A typical in-beam spectrum from a heavy-ion reaction taken in coincidence with γ-rays from ^{135}Nd is shown in figure 11.6 and demonstrates the feasibility of the technique. In this pre-EUROBALL experiment at the MPI Heidelberg four Cluster detectors were used at a rather small distance to the target. From this

Figure 11.6: Spectra from the gamma-ray (upper part) and conversion electron (lower part) decay of ^{135}Nd. Both spectra are single gated on transitions in the highly deformed band in that nucleus. Besides the regularly spaced E2 transitions within the band, some of the transitions linking the band to lower lying states are also observed.

Figure 11.7: *Gamma-ray (upper part) and conversion-electron (lower part) decay in ^{188}Pb; both spectra are singles spectra, but gated on the detection of a fusion-evaporation residue in the RITU gas-filled separator, discriminating against the strong fission background. The strong lines in the CE spectrum labelled K591 and K725 correspond to E0 transitions of excited 0+ states at these energies and are interpreted as evidence for a triple shape coexistence in that nucleus.*
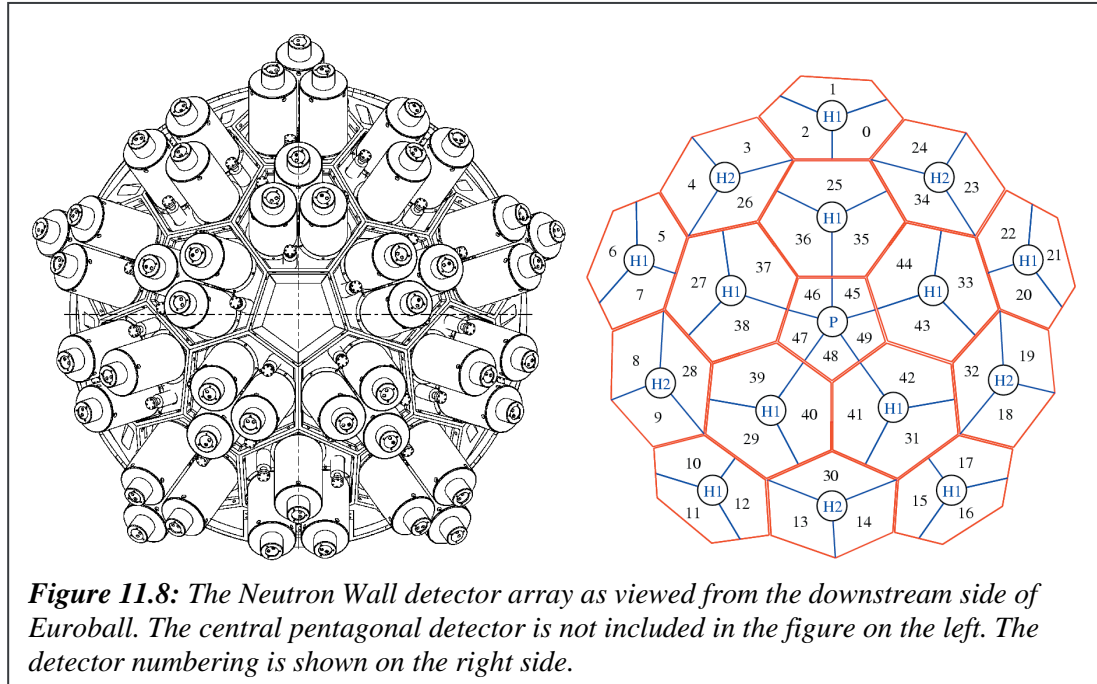
experiment the spin and parities of the yrast SD band in ^{135}Nd could be determined [323].

In an experimental campaign at the University of Jyväskylä the Mini-Oranges were combined with a γ-ray spectrometer, consisting of four segmented Clover detectors coupled to the gas-filled separator RITU. In order to maximise the gamma efficiency the Ge detectors were placed again at a relatively small distance to the target. In figure 11.7 the result from an experiment on ^{188}Pb are shown; in the electron spectra E0 decays from two new 0^+ states were observed giving evidence for a unique triple shape coexistence in this isotope [324]. In this case the production cross section is too small to measure CE-γ coincidences. This type of spectroscopy will clearly benefit from a larger Ge detector array.

In the first experimental campaign at EUROBALL we have tried to search for an E0 competition in the decay out of superdeformed bands. Unfortunately, these experiments were not successful, mainly due to experimental problems related to the electronics and DAQ system. An additional complication arose from the mounting of the Mini-Oranges at forward angles, where the δ-electron background is higher and due to scattering of the beam halo into our detectors. In the future we plan to repeat these very interesting but extremely difficult experiments with Ge detectors from the pool of EUROBALL resources.

11.5. The EUROBALL Neutron Wall detector[*]

The EUROBALL Neutron Wall detector array [7] is designed, built and managed by groups from Sweden, Germany, UK, and Poland. It is mounted in the forward hemisphere of EUROBALL, replacing the tapered Ge spectrometers and covering a solid angle of about 1π (see Figure 11.8).

Figure 11.8: *The Neutron Wall detector array as viewed from the downstream side of Euroball. The central pentagonal detector is not included in the figure on the left. The detector numbering is shown on the right side.*

The array consists of 15 pseudo-hexagonal detector units in three rings and a central pentagonal unit. Each hexagonal unit is subdivided into three hermetically separated segments, each viewed by a 130 mm diameter PMT (Philips XP4512PA). The subdivision is made in two ways, giving two types of hexagonal detector units (H1 and H2), each with a volume of 9.70 litres. The central pentagonal unit (P) has a volume of 5.37 liter and is subdivided into five hermetically separated segments, each viewed by a 75 mm diameter PMT (Philips XP4313B). This amounts to a total granularity of 50 segments and a total volume of 151 liters. The scintillation liquid used is BC501A. The distance from the focal point to the front face of the detectors is 510 mm.

Integrated front-end electronics has been designed and built for the NEUTRON WALL by SINS, Swierk, Poland. It consists of hardware for pulse shape analysis of the anode signals from the PMT's, and was implemented as a dual channel pulse-shape discriminator (PSD) unit built in NIM. Each PSD channel has a CFD, a bipolar shaping amplifier with a zero-crossover (ZCO) detector, two time-to-amplitude converters (TAC), and a charge-to-voltage Converter (QVC).

Neutron-γ discrimination is made by using a combination of the ZCO time signal and the difference in measured time of flight of neutrons and γ rays. Neutrons interact in the detectors mainly by elastic scattering against the protons of the scintillation liquid. When the recoiling protons are slowed down in the liquid, they give rise to a larger proportion of the slow

---

[*] Contact person : Johan Nyberg (johan.nyberg@tsl.uu.se)

component of the scintillation light than the recoiling electrons, which are produced by γ-ray interactions. This gives rise to a difference in the pulse shape of the anode signal, a difference which is observed as a delayed ZCO time signal for neutrons interacting in the detector compared to γ rays. In the Neutron Wall set up, neutron-γ discrimination works very well down to a recoil electron energy of at least 100 keV, which corresponds to a neutron energy of about 0.5 MeV.

One of the TAC units of the PSD is used for time of flight (TOF) measurements. It is started by the internal CFD signal and stopped by an external time reference signal. The other TAC unit is started by the internal ZCO signal and stopped either by the internal CFD (usual mode of operation) or by the external time reference signal. The charge of the anode signal from the PMT is integrated in the QVC, to give a signal whose amplitude is proportional to the energy deposited in the detector. The outputs of the two TAC units (TOF, ZCO) and of the QVC unit are sent to peak sensitive ADC for digitisation and readout.
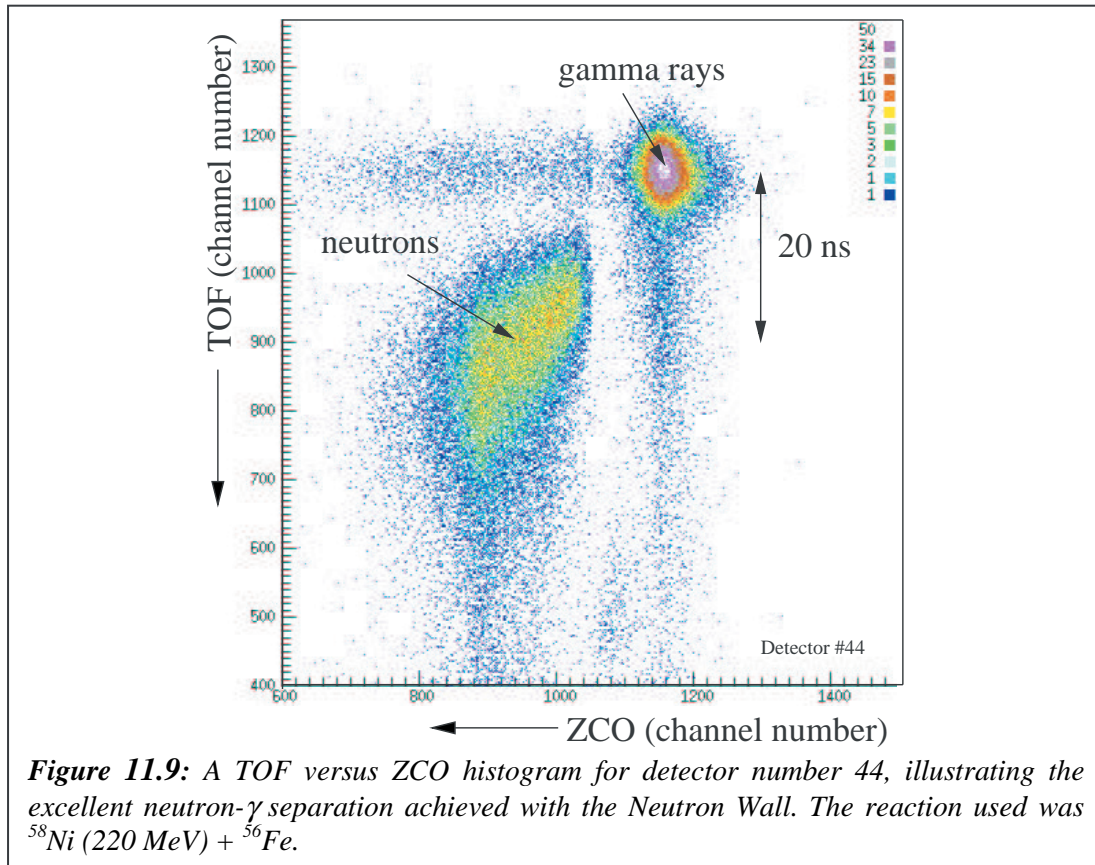
The external time reference signal, needed for the TOF measurement, is usually made as a precisely time aligned OR of all the Neutron Wall CFD signals (self-timing mode), or taken from the RF system of a pulsed beam.

Logic neutron and γ-ray signals are produced in the PSD units from the time information of the ZCO signal. These logic signals indicate if a neutron or a γ ray was detected. The neutron logic signals from all neutron detectors are OR-ed together and sent to the EUROBALL trigger system, which then can select events for readout in which at least one neutron was detected.

A completely new VME based readout system was built for the Neutron Wall. It consists of five 32 channel peak sensitive ADCs (Caen V785), a trigger and control unit (ATTIC), a VME to DT32 bus interface and readout card (V2DT), all controlled by a PowerPC (Motorola MVME2431) running LynxOS. The ATTIC and V2DT cards, as well as the software for control and readout, were developed by Daresbury Laboratory. The Neutron Wall readout system has been used also by other ancillary detectors of EUROBALL, e.g. RFD and HECTOR.

An example of the excellent neutron-γ separation achieved is shown in Figure 11.9. The data shown was obtained during the Neutron Wall commissioning run, performed at the IReS, Strasbourg in February 2001. The reaction used in this experiment was ^{58}Ni (220 MeV) + ^{56}Fe. The time reference for the TOF measurement in Figure 11.9 was the RF signal of the pulsed beam (pulsing frequency 3 MHz). The resolution of the prompt γ-ray time peak in Figure 11.9 is FWHM = 5.3 ns. Using the self-timing mode, i.e. the OR of the Neutron Wall CFD signals as time reference, a time resolution of FWHM ~ 2 ns is obtained. The disadvantage of using the CFD OR signal as a time reference is however that, for events where no prompt γ rays are detected, usually a neutron produces the time reference signal. In such events the neutron TOF signal cannot be used for neutron-γ discrimination, which then only relies on the ZCO signal and leads to a somewhat reduced discrimination.

The measured total neutron efficiency, i.e. the probability of detecting and identifying one neutron out of one emitted, in coincidence with γ rays detected by the Ge spectrometers of EUROBALL, is ~25-30% for symmetric reactions with compound nuclei in the A~100 region.

Figure 11.9: *A TOF versus ZCO histogram for detector number 44, illustrating the excellent neutron-γ separation achieved with the Neutron Wall. The reaction used was ^{58}Ni (220 MeV) + ^{56}Fe.*

For studies of the most neutron deficient nuclei, reaction channels in which more than one neutron is evaporated are most interesting. The major problem of clearly identifying such reactions, with a closely packed neutron detector array, is the scattering of neutrons. In the NEUTRON WALL the scattering probability, i.e. the probability that one neutron is detected as two or more neutrons, is about 7%. If nothing is done to identify scattered neutrons, the 2n gated γ spectra would be completely dominated by peaks from the 1n reaction channels.

A large part of the scattered neutrons can be identified by using a correlation between the distance between the two detectors that have registered a neutron and the difference in their TOF values (ΔTOF). For scattered neutrons, ΔTOF is large for large distances between the two detectors, and vice versa for short distances, while for real 2n events there is no such correlation. Extensive Monte Carlo simulations of the Neutron Wall have been done with Geant4, to study the effect of scattering [325]. The simulations were compared to data from the Neutron Wall commissioning run. It was found that using the ΔTOF-distance correlation, peaks from real 2n reactions compared to peaks from scattered 1n reactions could be enhanced by a factor of ~30, with a loss of real 2n events of about 70%. The Monte Carlo simulation also showed the importance of the neutron-γ separation when trying to identify scattered neutrons. Misinterpreted γ rays makes identification of scattered neutrons much more difficult. Further information concerning the Neutron Wall can be found at the URL http://www.nsg.tsl.uu.se/nwall.

Acknowledgements:

11.6.   A Plunger apparatus for EUROBALL[*]

A special plunger apparatus for EUROBALL III and IV has been built in Cologne following closely the design of a plunger apparatus previously built at the IKP of the University of Cologne which is described in Ref. [294]. Like the previous version also the new plunger is especially suited for coincidence recoil distance measurements (RDM). It meets the geometrical conditions defined by the different EUROBALL set-ups. Figure 11.10 shows the plunger mounted in EUROBALL IV.
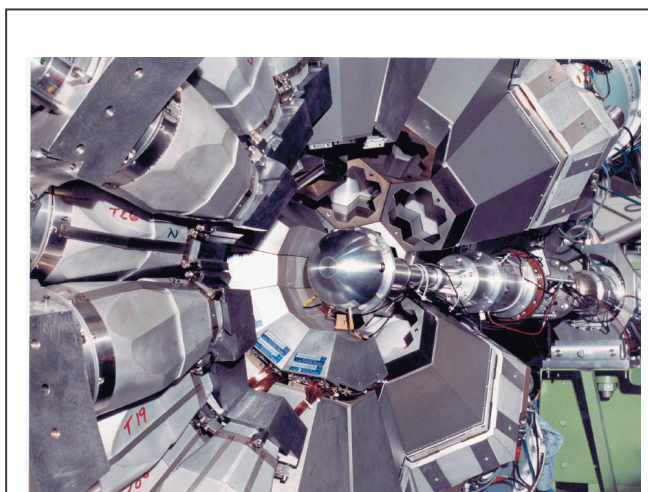
Figure 11.10: *Plunger mounted in EUROBALL IV*

It consists of a spherical target chamber and a cylindrical actuator housing. Both parts are connected by a tube which houses another tube held by bearings enabling precise axial movements. This inner tube is used to transmit the movements of a linear motor to the target.

The target chamber itself and the target and stopper frames were built such that a minimal amount of absorbing material for γ-rays is used in forward direction up to a polar angle of $\theta=60°$ with respect to the beam and in backward direction between the polar angles $\theta=300° - 343°$.

The beam axis is fixed by two lead diaphragms with a 3 mm and 10 mm hole placed at the entrance of the target chamber and the actuator housing, respectively. An inductive transducer is mounted off-axis in the target chamber measuring the target-stopper distances with an accuracy up to 0.1 μm. The target chamber consists of two hemispheres. It can be opened completely to achieve an easy mounting and adjustment of the target and stopper foils.

A piezoelectric linear motor (called Inchworm) is used as an actuator. The spindle of the motor is connected via a piezoelectric crystal with the inner tube which, is connected to the target supporting frame. This crystal allows for small variations (0-30 μm) of the target-stopper distance and is part of the automatic feedback system described below.

Piezo-feedback system

In order to compensate for slow variations of the actual target-stopper distance, e.g., when the system is heated by the beam, the plunger is equipped with a piezo-feedback system. The actual target-stopper distance is monitored permanently, in particular in-beam, by measuring the target-stopper capacitance. This signal is used to record the target-stopper displacements and to generate a DC voltage for the piezo-crystal to compensate for these displacements. Recently the software of the feedback system was renewed and is now based on the LabView system (National Instruments) under LINUX.

---

[*] Contact person : A. Dewald (dewald@ikp.uni-koeln.de)

Technical data

target-stopper separation: 0 - 8 mm
magnetic transducer range (accuracy) in [μm] : 20(0.1); 200(1); 1000(10)
Inchworm: travel distance: 25 mm,
              mechanical stability : 0.004 μm
              optical encoder, range (resolution): 25 mm (0.5 μm)

Plunger in combination with EUCLIDES

The new plunger apparatus provides the possibility of being used in combination with other ancillary detectors like the particle Si detector array EUCLIDES.
This can be achieved by removing the end cap of the plunger target chamber and mounting a special adapting ring instead, to which one half of the standard EUCLIDES vacuum chamber can be screwed on.

Experiments at Legnaro with EUROBALL III:

Investigation of magnetic rotation in ^{196}Pb:
G. Kemper, PhD thesis, University of Köln, 2000
G. Kemper et al., Eur. Phys. J. A11 (2001) 121

Decay out the SD band in ^{135}Nd:
R. Peusquens, PhD Thesis, University of Köln, 2000
Lifetime measurements with the EUROBALL spectrometer
A. Dewald et al., International Symposium on Nuclear Structure Physics; Editors: R. F. Casten, J. Jolie, U. Kneissel, K.P. Lieb, Göttingen, 2001

Experiments at IReS Strasbourg with EUROBALL IV:

Investigation of magnetic rotation in ^{124}Xe:
Investigations of nuclear structures using transition probabilities
A. Dewald, XIV International School on Nuclear Physics, Neutron Physics and Nuclear Energy, Varna, 2001
B. Saha, PhD thesis, University of Köln, in preparation

Test experiment EUCLIDES+Plunger: ^{114}Xe, ^{113}I
G. de Angelis et al., Phys. Lett. B535 (2002) 92
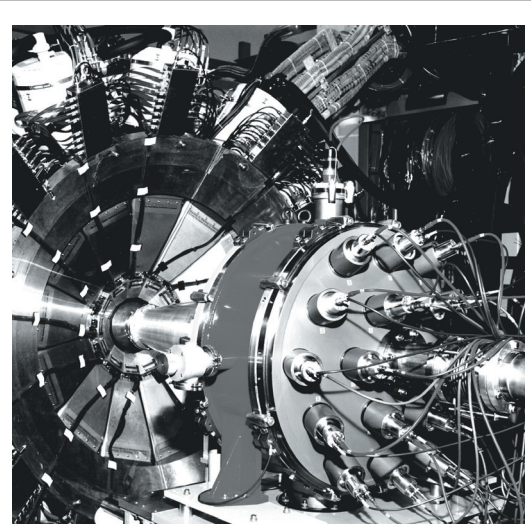
Isospin mixing in ^{46}V (EUCLIDES-Plunger)
Data analysis in progress

Isospin mixing in ^{64}Ge (EUCLIDES+Plunger)
E. Farnea et al. Phys. Lett. B551 (2003) 56

11.7. The Recoil Filter Detector for EUROBALL[*]

In-beam nuclear spectroscopy based on fusion evaporation reactions with both light and heavy ions has been one of the major tools in nuclear structure research for more than 30 years. At bombarding energies not too high above the Coulomb barrier, the fusion evaporation reactions are usually dominant, with cross sections ranging from about 0.1 barn to 1 barn. Often, it happens that, out of several reaction channels, one dominates and a single nucleus is populated preferentially. It is therefore satisfactory to perform only γ-ray measurements and usually γ-γ- double coincidences are sufficient to obtain high quality data. This is not the case, however, if one wants to study heavy nuclei, even roughly beyond Pb, where the compound nuclei mostly undergo fission and particle evaporation, which

Figure 11.11 : The Recoil Filter Detector (RFD) coupled to EUROBALL.

leads to nuclei of interest, becomes weak. When going to very heavy nuclei with *Z~100*, the situation is even worse. To perform spectroscopic studies in that region, it is necessary to make an identification and selection of γ- rays from the desired, rarely occurring evaporation residues.
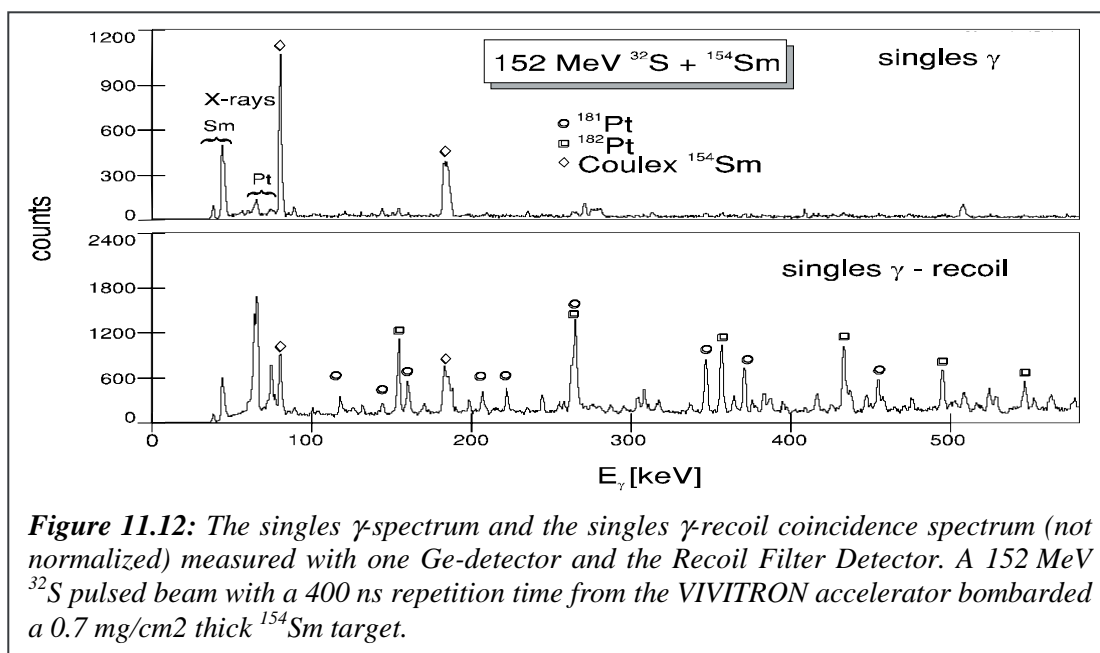
Figure 11.12: The singles γ-spectrum and the singles γ-recoil coincidence spectrum (not normalized) measured with one Ge-detector and the Recoil Filter Detector. A 152 MeV ^{32}S pulsed beam with a 400 ns repetition time from the VIVITRON accelerator bombarded a 0.7 mg/cm2 thick ^{154}Sm target.

For that purpose and to overcome the aforementioned difficulties, we have built a Recoil Filter Detector (RFD) [8]. It was intended to be used only in coincidence with γ-spectrometers (multidetector arrays) such as EUROBALL (see Figure 11.11).

---

[*] Contact person : W. Meczynski (witold.meczynski@ifj.edu.pl)

The RFD measures evaporation residues in coincidence with γ-rays detected in the Ge detector array. The recoil selection by time-of-flight techniques discriminates against other reaction channels. Therefore, the background is significantly reduced (Figure 11.12) and spectroscopic studies in reactions with low cross section become feasible.

Moreover, the granularity of the RFD system allows for "tracking" the reaction product, thus allowing for its velocity vector determination. This strongly reduces the Doppler broadening of the γ-lines emitted by the recoil in flight. This is especially important for light, or medium-light nuclei (Figure 11.13) for which the recoil velocity can be high when produced in fusion-evaporation reactions with energetic, heavy projectiles.
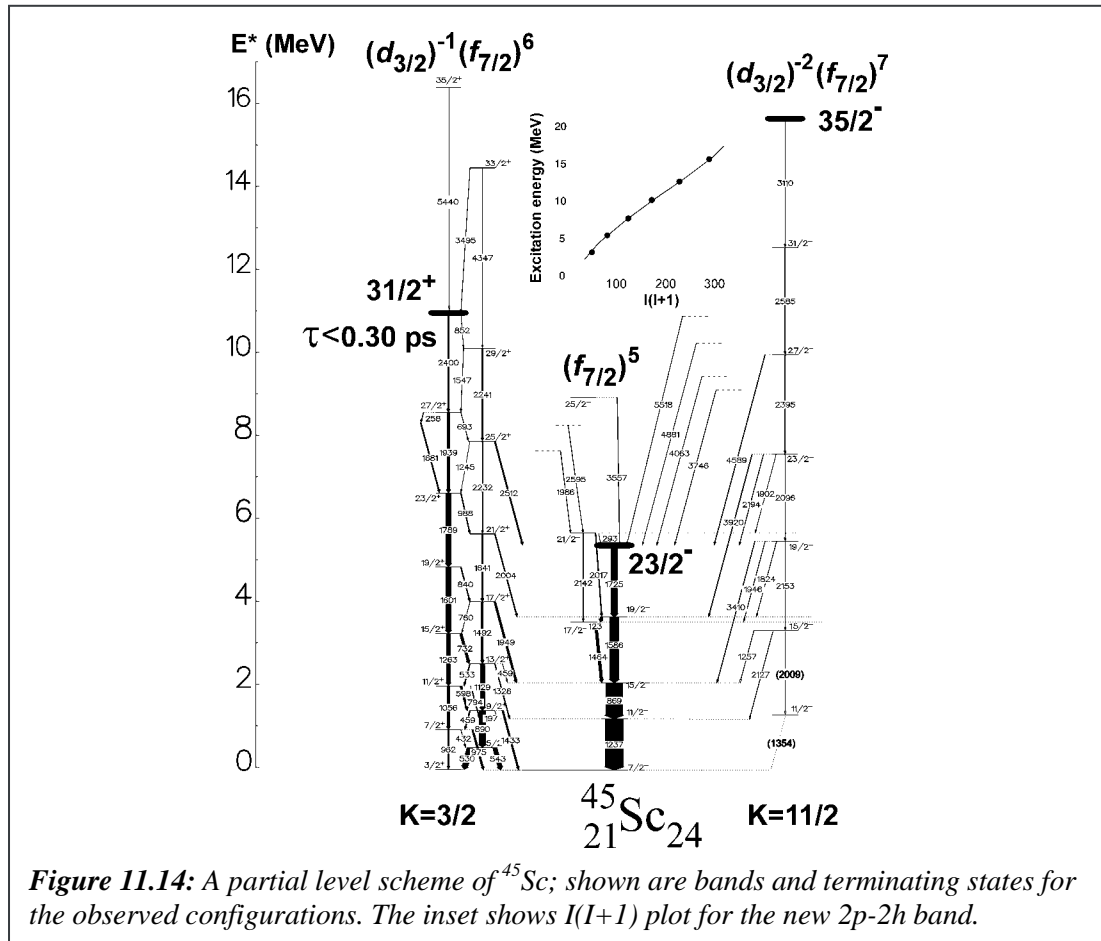
The above properties, when the RFD is coupled to the very efficient EUROBALL array equipped with the silicon ball EUCLIDES and the multiplicity filter, make such a combined system a very powerful tool for various spectroscopic studies in light, medium or in very heavy nuclei. Moreover, the use of the silicon ball and/or the multiplicity filter provides a proper information on a true reaction event having occurred in the target. This signal can then be used as a start for the RFD instead of the beam pulse. This allows working with *a continuous beam* instead of pulsed beam. This is important for studies in the region of very heavy nuclei where, because of low reaction cross sections, one needs high beam currents whereas the long flight-time of a heavy system needs slow pulsing.
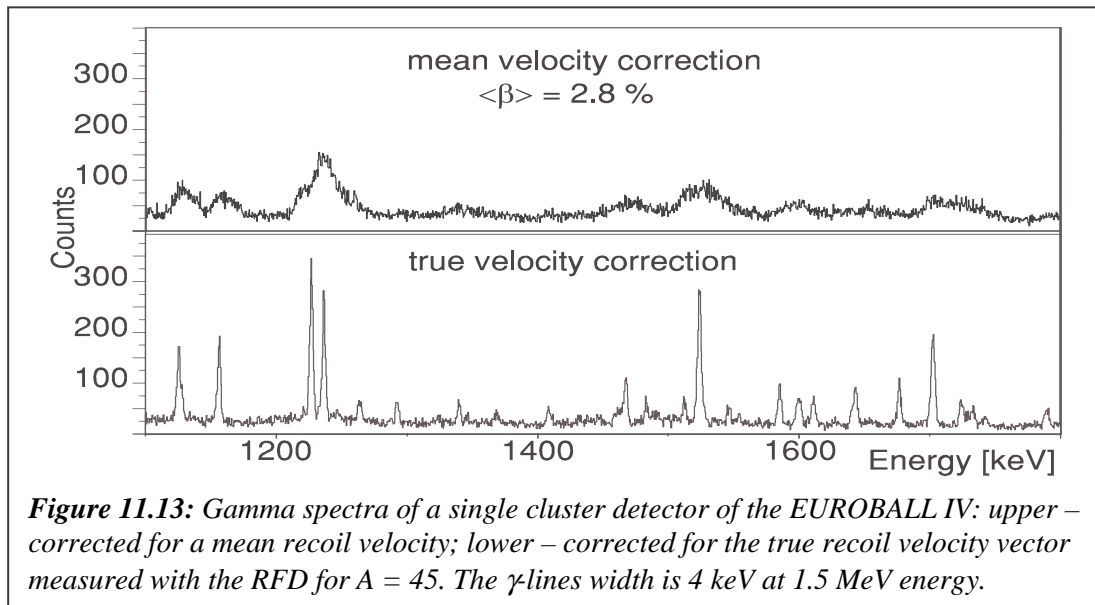
Figure 11.13: *Gamma spectra of a single cluster detector of the EUROBALL IV: upper – corrected for a mean recoil velocity; lower – corrected for the true recoil velocity vector measured with the RFD for A = 45. The γ-lines width is 4 keV at 1.5 MeV energy.*

Search for highly excited states (beyond band termination) in light nuclei: Superdeformed bands.

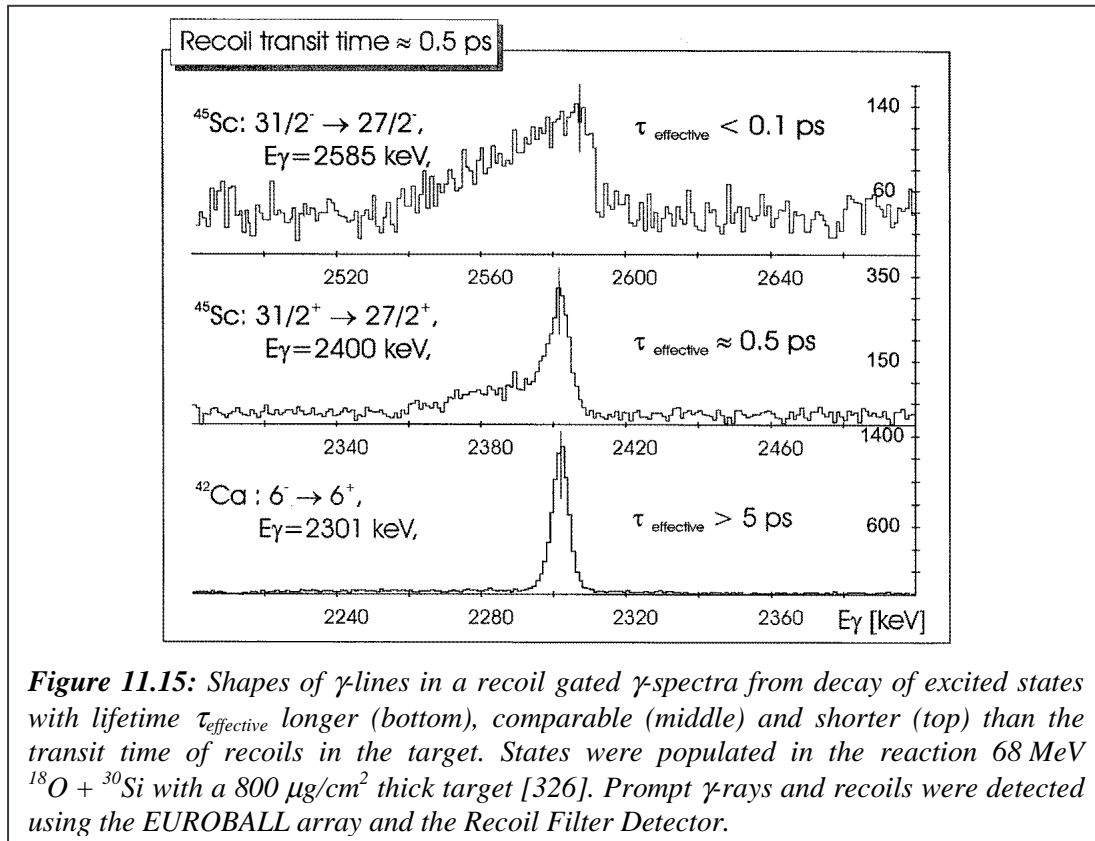Highly excited states in light nuclei commonly decay via high-energy γ-transitions (of several MeV). A huge Doppler broadening of the γ-lines severely hampered the investigations of the decay of those states (Figure 11.13). The combination of EUROBALL and the RFD allows now such studies. Two experiments have been performed to investigate nuclei close to ^{40}Ca and ^{50}Cr. The data for the latter are under evaluation. In many nuclei in the vicinity of ^{40}Ca new excited states have been observed. The new data provide valuable information on the evolution of the nuclear deformation along the observed bands. Partial data for ^{45}Sc are shown in Figure

Figure 11.14: *A partial level scheme of ^{45}Sc; shown are bands and terminating states for the observed configurations. The inset shows I(I+1) plot for the new 2p-2h band.*

11.14. The positive parity 1p-1h signature partner bands loose gradually the collectivity and terminates at spin $31/2^+$ [326]. Still higher energy transitions are observed above, likely to continue the bands. A new excited 2p-2h negative parity band has been found with a high deformation parameter $\beta \sim 0.4$. New data have also been obtained for ^{44}Ca [327] and ^{42}Ca [328]; a weak band with fast E2 transitions observed in ^{42}Ca resembles properties of the super-deformed band recently observed in ^{40}Ca.

The capability of the RFD to measure the velocity vector of the recoiling nucleus, allows for lifetime determination (or estimate lifetime limits) of excited states, as the experiments require use of thin targets (of the order of 200μg/cm^2). If the feeding time of an excited state as well as its lifetime is much longer than the transit time of the recoil through the target (typically 0.1 ps) such state decays mostly outside the target when the recoiling nucleus has already a well-defined velocity. In this case, the recoil velocity vector can be precisely measured by the RFD and the width of the γ-line can be significantly reduced (bottom panel of Figure 11.15). If, however, the lifetime of a state is comparable to or much shorter than the transit time, the recoiling nuclei in this state decay partly or entirely inside the target. Therefore, they can undergo further straggling after the γ-rays have been emitted, and consequently, the recoil velocity vector at the point of the γ-ray emission cannot be measured 'correctly' by the RFD. The application of such measured velocity vector *does not reduce* the broadening of the γ-lines, as shown in the middle and top panels of Figure 11.15.

It can be proven that the ratio of the 'uncorrected' part of the γ-line to the 'corrected' one is expressed by the ratio of the lifetime of the state to the recoil transit time through the target. In

Figure 11.15: *Shapes of γ-lines in a recoil gated γ-spectra from decay of excited states with lifetime τ_effective longer (bottom), comparable (middle) and shorter (top) than the transit time of recoils in the target. States were populated in the reaction 68 MeV $^{18}O + ^{30}Si$ with a 800 µg/cm² thick target [326]. Prompt γ-rays and recoils were detected using the EUROBALL array and the Recoil Filter Detector.*

this way, if the transit time of the recoil through the target material is known the lifetime of highly excited, short-lived states can be estimated.

Perspectives in superdeformed band decay studies in nuclei with A~150 –
Search for decay modes and linking transitions.

Superdeformation in atomic nuclei has been extensively studied during the past two decades. SD bands have been found in many nuclei throughout the nuclear chart. However, neither feeding nor decay of the SD bands has been well understood. In few cases only, the 'linking' transitions connecting the highly excited SD bands to low lying states have been observed. Much less on those transitions is known in rare earth nuclei where the SD bands have been originally discovered. Again, those transitions are of rather high energy. First, to get peaks emerging from the background corresponding to those transitions, one needs to make use of high-fold coincidence spectra. This procedure reduces severely the statistics in the high energy part of the spectra. Moreover, the linking high energy γ-transitions emitted from short-lived SD states suffer the Doppler effect and the peaks can be severely broadened. This, together with the aforementioned lowering of statistics due to high-folds coincidence requirements may hamper the search of the SD bands decay.

Still unclear remains whether the decay from SD states may (partially) occur via fission from the second well of the double-humped barrier in competition to the γ-decay via linking transitions. EUROBALL plus the RFD and the Multiplicity Filter has been employed in the reaction $^{124}Sn(^{31}P,5n)^{150}Tb$ as an efficient way to study the SD decay. The precise selection of the recoils provides very clean spectra of γ-ray in coincidence with recoils only. The obvious precise Doppler effect correction makes possible to 'narrow' the high energy peaks and facilitate their observation. The RFD measures the fusion evaporation recoils which reach the detector after several tenths of nanoseconds. If the nucleus produced in such reaction

undergoes immediate fission from the SD states, then it does not reach the RFD and will not be detected. Therefore, a careful intensity analysis of SD spectra measured with and without the RFD may provide information on the decay mode from SD states. An experiment searching for superdeformed bands in ^{209}Po in the ^{176}Yb(^{30}Si,6n) reaction may elucidate on the above question, but this data are still under analysis.

Spectroscopic studies for very heavy nuclei

Studies of very heavy and superheavy nuclei are a very challenging question of the present day's nuclear spectroscopy. However, superheavy nuclei remain so far unreachable for spectroscopic studies as they are produced with cross sections in the range of picobarns. Lower mass nuclei, however, can be produced with cross sections as high as 100nb – 10 μb and thus offer a possibility for spectroscopic studies in some special conditions. Pioneering experiments for ^{252,253,254}No [55,329,330] and ^{255}Lr [331] provided first systematic sets of in-beam spectroscopic data on very heavy, transfermium nuclei. These are only few cases which already give some hints to the importance of such studies. Therefore, new data on other heavy systems is highly desirable. An experiment with the EUROBALL plus RFD set-up provided recently encouraging results for spectroscopic studies for a lighter system, the ^{252}Fm nucleus.

Acknowledgements:

11.8. The SAPhIR detector[*]

SAPhIR (Saclay Acquitaine Photovoltaic cells for Isomer Research) is a solar-cell array used for the detection of fission fragments [9]. Since the development of large γ-ray detectors, the association of ancillary detectors is continuously growing. Impressive results on the spectroscopy of neutron-rich nuclei produced by spontaneous or induced fission have been obtained (see Section 8 of this report). The detection of fission fragments provides additional selectivity on the fragment mass, information on the fission mechanism (energy released in the fission process) and momentum for Doppler correction.

The SAPhIR array is able to measure the energy, mass, angle of the fragments and has many advantages compared to other detectors like PPAC or Si surface barrier detectors. In particular, the geometry is very versatile and can be easily adapted to the kinematics of the reaction. Moreover, the lifetime of the solar cells is long compared to surface barrier detectors.

The first experiment with SAPhIR coupled to a large γ-ray detector was performed in 1995 with EUROGAM II installed at Strasbourg. Two photovoltaic cells were used to tag isomeric states in the fragments produced by the ^{252}Cf spontaneous fission [332]. After this successful experiment, the induced fission p+^{232}Th reaction has been used with EUROGAM II coupled to an array of 10 solar cells. Soon after this, a larger array coupled to EUROBALL III and IV was considered and it became urgent to design an electronics able to handle a large number of detectors and compatible with EUROBALL .

In order to have a compact electronics, fully compatible to the EUROBALL standard, a VXI D-size card has been designed for SAPhIR handling 16 channels per card (energy and time). There is the possibility to by-pass the internal linear amplifier and to inject a (positive or negative) signal directly in the ADC. The VXI electronics could therefore also be used for other Ge and Si detectors, for example at EXOGAM during the early implementation phase (segmented clover inner and outer contacts, anti-Compton shield) and during the first SPIRAL ^{74,76}Kr Coulomb excitation experiment in 2002 instrumenting a 64 channel Si strip detector.

Two types of solar cells are being used: see Figure 11.16. They are made from a polycrystalline (type 1, left) or mono-crystalline (type 2, right) silicon p-type wafers with a thickness of 300 μm [9]. The front face of the cells consists of an Ag grid covered with a thin antireflection titanium-oxide layer. The charge collection is done through a thin Ag backing evaporated on the rear side of the wafer. The detectors are able to detect charged particles (as standard surface-barrier detectors), but a limitation arises from the large capacitance. The cells have been tested to work well for heavy particles with A > 50 and E > 30 MeV.
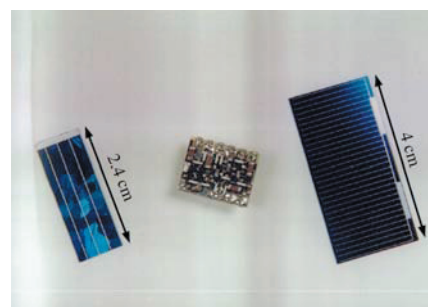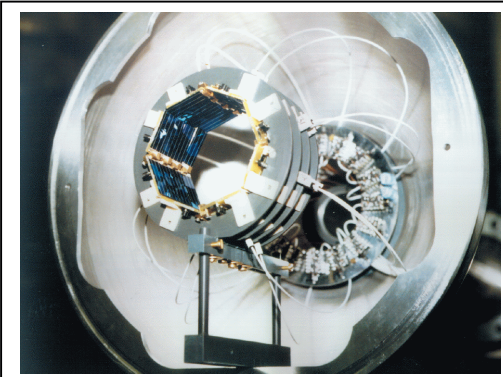

Figure 11.16: picture of two photovoltaic cells and one preamplifier.

---

[*] Contact person : Ch. Theisen (ctheisen@cea.fr)

EUROBALL experiments

Structure of neutron-rich isotopes produced by the $^{12}C+^{238}U$ induced fission


Figure 11.17: The SAPhIR array used in EUROBALL at Legnaro.

The SAPhIR setup consisted of 32 cells in a barrel geometry with a geometric efficiency of ~ 50 %: see Figure 11.17. The aim of the experiment was to study isomeric states in the range from a few ns to a few μs. Fission fragments were stopped in the array and isomeric decays occurred at rest without Doppler shift. SAPhIR provided a clear signature of the fission process as well as a time reference for lifetime measurement. From the analysis, we have identified 46 isomeric level schemes; 18 of them are new [218,222].

Lifetime measurement in fission fragments

The aim of experiments performed at EUROBALL IV was to measure lifetimes of short-lived excited states in fission fragments emitted by a ^{252}Cf source [231]. Fission fragments emanating from the source at angles less than 50° to the EUROBALL axis passed through a stretched Au foil of 3 mg cm^{-2} thickness before being detected in the SAPhIR array. The special configuration of SAPhIR used in this work consists of 48, 12 mm^{2}, solar cells arranged on a frame at a distance of 8.0 cm from the center of the EUROBALL array (Fig.11.18). The Au foil, fixed at the array center, served to degrade the fission-fragment energies by roughly a factor of two. Therefore, a fission fragment detected in SAPhIR will have associated γ-ray data corresponding to two possible Doppler shifts, namely, the full one (when emitted before the degrader foil) and the partial one (when emitted after having passed the degrader foil). In this way lifetimes in the range from 1ps to 1ns can be measured by examining the count rate in the fully and partially Doppler-shifted γ-ray peaks as a function of the gap between the source and the degrader foil. Since the first experiment performed with two cells at EUROGAM II, large progress in the development have been made. The attractive performance of SAPhIR has lead many laboratories to develop solar cells
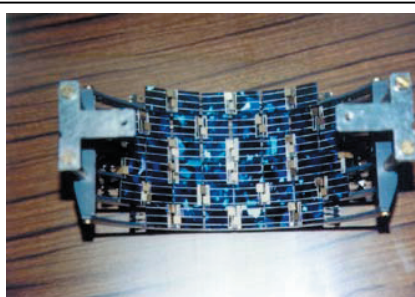
Figure 11.18: SAPhIR configuration used for the plunger experiment.

array (Cape Town, Munich, Bonn). Solar cells are also used for fission cross section measurement in the framework of the French nuclear waste management project.

The VXI electronics developed initially for the coupling with EUROBALL has been and will be intensively used at EXOGAM and with various other detectors when being integrated into a VXI system. More information can be found on the following web site: http://www-dapnia.cea.fr/ Phys/Sphn/Deformes.

11.9. The BRS Binary Reaction Trigger Spectrometer for EUROBALL IV[*]

Compared to fusion-evaporation reactions with stable projectile and target nuclei, binary reaction channels have the potential to open up new regions of the nuclear chart for γ-ray spectroscopy. For instance, nuclei on the neutron-rich side of the valley of stability can be studied by multi-nucleon transfer or deep-inelastic reactions, and high-spin states, e.g. belonging to highly deformed configurations in α-cluster nuclei, can be populated and detected very selectively by multiple α-transfer and fusion-fission exit channels. In addition, nuclear reaction studies can gain qualitatively new insights by a clean selection of a certain reaction channel, separating the γ-ray transitions from individual channels. A complete separation of the different reaction channels can be achieved, in favourable cases, by using thin targets and powerful particle trigger systems. In addition, the entry points of the γ-ray cascades and an optimal Doppler-shift correction of the resulting low background γ-ray spectra can be obtained. These are the fields of applications of the **B**inary **R**eaction Trigger **S**pectrometer (**BRS**) for EUROBALL.
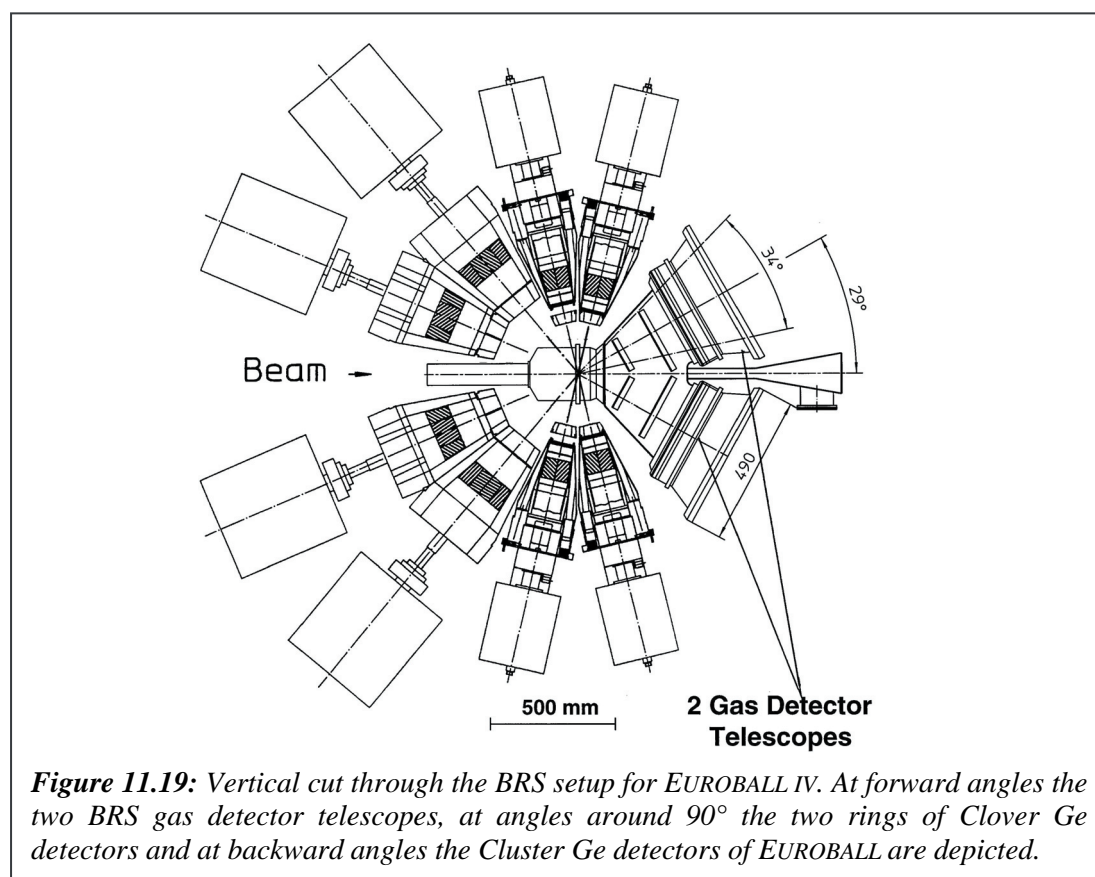
Figure 11.19: *Vertical cut through the BRS setup for EUROBALL IV. At forward angles the two BRS gas detector telescopes, at angles around 90° the two rings of Clover Ge detectors and at backward angles the Cluster Ge detectors of EUROBALL are depicted.*

By obtaining a complete reaction channel resolution in the BRS in the kinematical coincidence mode, the observational limits of EUROBALL can be considerably improved. In favorable cases a unique channel separation can already be achieved by the trigger detector and multi-fold γ-ray detection is not needed to reduce the background in the γ-ray spectra. The detection of two-fold γ-ray coincidences is, however, needed in order to identify specific γ-ray sequences.

---

[*] Contact person B. Gebauer (gebauer@hmi.de)

Features of the Trigger Spectrometer

The BRS for EUROBALL combines as essential detection elements two large-area logarithmic heavy-ion gas-detector telescopes in a kinematical coincidence setup at forward angles. In addition, six eight-fold segmented silicon detectors providing particle identification by pulse-shape discrimination, which can be integrated into the setup at forward angles, have been prepared as an option. In the EUROBALL IV setup (cf. Fig. 11.19) the two detectors are mounted symmetrically on either side of the beam axis, covering each the forward scattering angle range $12.5° < \theta < 45.5°$, i.e. $\theta = 29° \pm 16.5°$. Therefore, the 30 tapered Ge detectors of EUROBALL must be taken out, thus reducing the total photo-peak efficiency of EUROBALL by a small amount. In this geometry, the case of inverse kinematics offers best conditions, i.e. if the projectiles are heavier than the targets and/or the reaction Q-values are sufficiently negative, both ejectiles of a binary reaction can be detected in exclusive kinematical coincidence measurements.

Each gas-detector telescope comprises two consecutive gas volumes containing a two-dimensional position sensitive low-pressure multi-wire chamber (MWC) and a Bragg-curve ionization chamber (BIC), respectively. All detection planes are four-fold subdivided in order to increase the counting rate capability and the resolution. Thus the following correlations between two heavy ejectiles can be measured with high resolution:

- In the MWCs the in-plane and out-of-plane scattering angles θ and ϕ, derived from the position measurement and the time of flight (TOF) are measured with position and time resolutions of ~0.5 mm and ~200 ps, respectively. If the accelerator pulsing gives a sufficiently good time resolution (~1 ns) for non-binary exit channels the measurement of TOF versus the beam pulse for two heavy ejectiles can be used. Usually the better time resolution of the MWCs is utilized to measure the ejectile masses, more precisely the mass asymmetry in the binary channels, by measuring the time-of-flight differences between the two ejectiles detected in the two telescopes. In exclusive kinematical coincidence measurements masses and binary Q-values can be with a resolution of <1-2 MeV, which is dependent on target thickness.

- In the BICs the Bragg-Peak height (BP), Range (R) and rest Energy (E) are measured. BP delivers in BP/R and BP/E correlations a fairly mass-independent Z signal. Since the Bragg-peak width is mass dependent, whereas its height BP is not a limited mass resolution can be obtained. By measuring the Z and E correlations of two heavy ejectiles the reaction channel dynamics of binary reaction channels can be unambiguously identified and non-binary events are suppressed very effectively. These can be further suppressed using the $\phi–\phi$ correlation measured in the two MWCs, i.e. applying the co-planarity condition.

- Furthermore, if a pulsed beam of about 1 ns (FWHM) time resolution is available from the accelerator (e.g. VIVITRON post-pulsing system), kinematically complete inclusive measurements of three-body exit channels can be performed by detection of two heavy residues in the BRS. In this case the achievable resolution is limited by the time resolution of the pulsing system.

By measuring (θ/φ), TOF, E, R and Z correlations for two heavy ejectiles in the BRS gas detector telescopes alone, the reaction dynamics of quasi-elastic, deeply-inelastic and fusion-fission channels can be determined for masses, which are not too heavy and the Doppler-shifts of γ-rays emitted from the ejectiles can be corrected for. In many cases, sufficient characterization can already be achieved by measuring these quantities for one ejectile in one-arm experiments, usually for the lighter one. In this mode of operation, normal kinematics can be used, detecting the lighter nucleus in the BRS.

Dynamical Ranges

The most stringent restrictions in the dynamical ranges result from the fixed-angle settings and the limited opening angles of the detector telescopes in comparison with the kinematics. The lightest particles, which can be identified adequately in the BRS gas telescopes, are low-energy α particles (<5 MeV/u can be stopped). In the MWCs the low-energy thresholds are <0.1 MeV/u. In the BICs adequate Z resolution can only be achieved for kinetic energies at or above the Bragg-maximum. In cases where the correlation angles are too large for detection of two correlated ejectiles or the kinetic energy of one of the ejectiles is too low for detection, the measurement of the faster ejectile will often deliver a good trigger for γ-ray spectroscopy. In this case the detected ejectile must be stopped in the ionization chamber. With BICs of 125 mm active depth this is possible, for example, for 6 MeV/u ^{16}O, 7.5 MeV/u ^{28}Si, 8.5 MeV/u ^{40}Ca or 9 MeV/u ^{58}Ni with a pressure of 400 mbar of the CF_4 gas. At energies well above the Bragg maximum, ejectile nuclear charges should be separable at least up to Z=30.

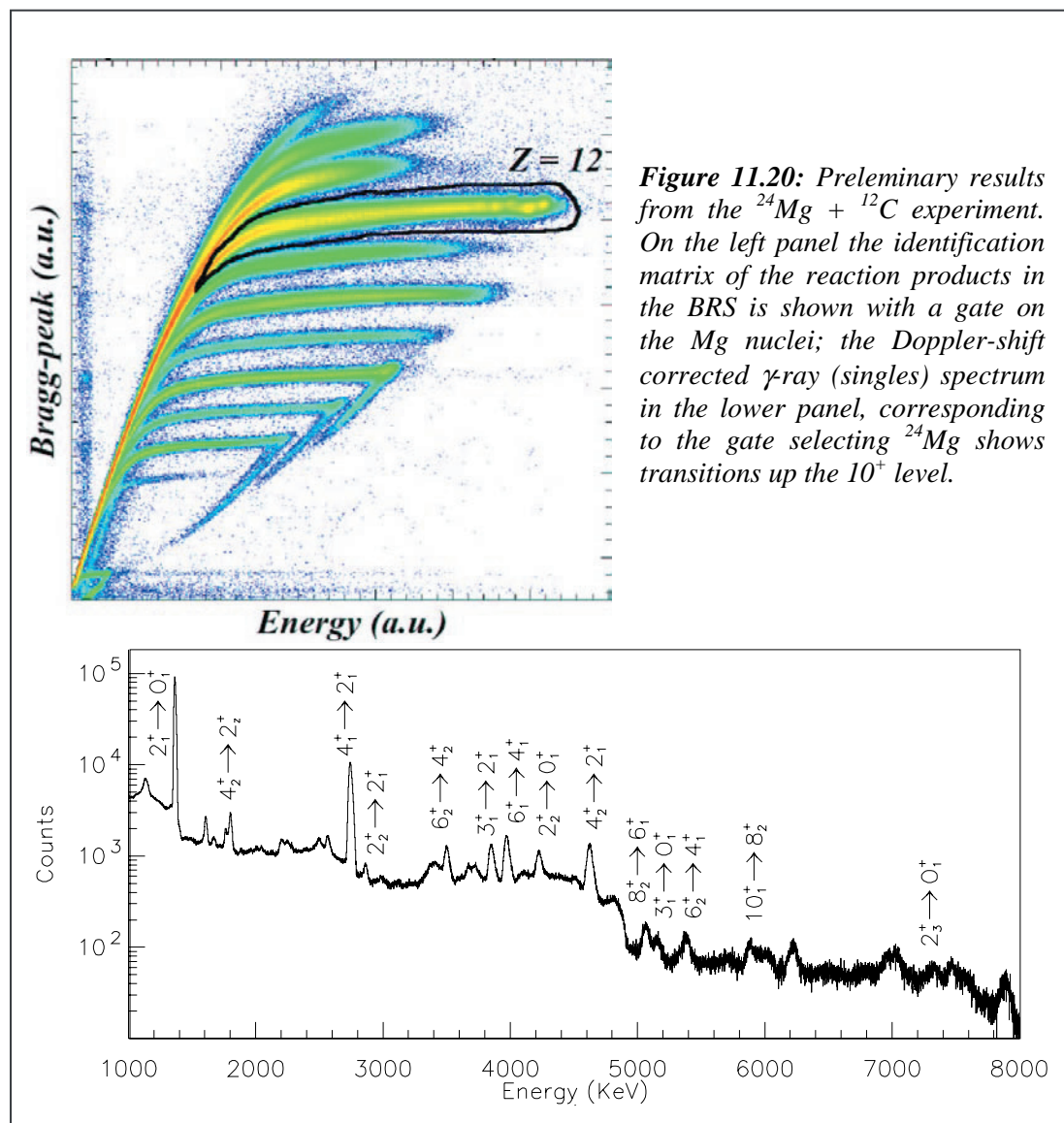**Experiments performed at EUROBALL**

In October 1998 the first experiment with the BRS and **EUROBALL III** was performed at the Legnaro National Laboratory ("*Search for γ-ray Transitions in Hyperdeformed 4N-nuclei A=36-44*") using the reaction ^{32}S + ^{24}Mg at a beam energy of 163 MeV. At this time only a one arm-experiment could be performed. However, due to the good pulsing system of the LNL accelerator the TOF could be used for the determination of the velocity vectors and for Doppler-shift corrections.

Results of previous measurements with the BRS and some results of this experiment are published in

1. S. Thummerer et al. Il Nuovo Cimento Vol.111A (1998) 1077, and
2. S. Thummerer et al. Physica Scripta T88 (2000) 114.

In September 2002 the BRS was installed for a commissioning run at EUROBALL IV at IReS Strasbourg, and later two experiments (W. von Oertzen (Berlin) et al. "Search for rare γ-decays in the strongly deformed light neutron rich isotopes $^{10-12}$Be and $^{13-16}$C" and Ch. Beck (Strasbourg), W. von Oertzen (Berlin) et al. "Search for gamma-ray transition from SD and HD states in ^{24}Mg in the ^{24}Mg on ^{12}C reaction") were successfully performed in October 2002. Lateron two further experiments (B. Gebauer (Berlin) et al. "Search for gamma-ray transition in the HD 4N-nuclei with A=36-46" and X. Liang (Paisley), F. Haas (Strasbourg) et al. "Search for excited states in the neutron-rich Na and Mg nuclei around N=20 using deep inelastic processes") had successful beam times at the VIVITRON in April 2003. The data are processed by four different groups at IReS (Strasbourg), HMI (Berlin); FLNR (Dubna) and Paisley (UK).

Figure 11.20: *Preliminary results from the ^{24}Mg + ^{12}C experiment. On the left panel the identification matrix of the reaction products in the BRS is shown with a gate on the Mg nuclei; the Doppler-shift corrected γ-ray (singles) spectrum in the lower panel, corresponding to the gate selecting ^{24}Mg shows transitions up the 10^+ level.*

In Figure 11.20 preliminary results from the ^{24}Mg + ^{12}C experiment (EB-01/5) are shown. The upper panel shows the identification of the reaction products in the BRS with a gate on the Mg nuclei, the lower panel the corresponding Doppler-shift corrected γ-ray (singles) spectrum of the gate selecting ^{24}Mg.

Acknowledgements

Annex

EUROBALL experiments and publications

Annex: EUROBALL experiments and publications

A) Scientific results in refereed journals

1999

A01) *Decay-out of the yrast superdeformed band in 136Nd: Towards an experimental extraction of the neutron pairing gap at large deformation*

S. Perries, A. Astier, L. Ducroux, M. Meyer, N. Redon, C. M. Petrache, D. Bazzacco, G. Falconi, S. Lunardi, M. Lunardon, C. Rossi Alvarez, C. A. Ur, R.Venturelli, G. Viesti, I. Deloncle, M. G. Porquet, G. de Angelis, M. de Poli, D. Foltescu, A. Gadea, D. R. Napoli, Zs. Podolyak, A. Bracco, S. Frattini, S. Leoni, B. Cederwall, A. Johnson, and R. A. Wyss
Physical Review C60 (1999) 064313

A02) *Triaxial superdeformed bands in 164Lu and enhanced E1 decay-out strength*

S. Tormanen, S.W. Ødegård, G.B. Hagemann, A. Harsmann, M. Bergstrom, R.A. Bark, B. Herskind, G. Sletten, P.O. Tjom, A. Görgen, H. Hubel, B. Aengenvoort, U.J. van Severen, C. Fahlander, D. Napoli, S.M. Lenzi, C. Petrache, C. Ur, H.J. Jensen, H. Ryde, R.Bengtsson, A. Bracco, S. Frattini, R. Chapman, D.M. Cullen, S.L. King
Physics Letters B454 (1999) 8

A03) *Measurements of g-factors of excited states in Ba and Ce nuclei using gamma-rays from secondary fission fragments*

A.G. Smith, G.S. Simpson, J. Billowes, J.L. Durell, P.J. Dagnall, S.J. Freeman, M. Leddy, A.A. Roach, J.F. Smith, A. Jungclaus, K.P. Lieb, C. Teich, B.J.P. Gall, F. Hoellinger, N. Schulz, I. Ahmad, J. Greene, A. Algora
Physics Letters B453 (1999) 206

A04) *Correlated spins of complementary fragment pairs in the spontaneous fission of 252Cf*

A. G. Smith, G. S. Simpson, J. Billowes, P. J. Dagnall, J. L. Durell, S. J. Freeman, M. Leddy, W. R. Phillips, A. A. Roach, J. F. Smith, A. Jungclaus, K. P. Lieb, C. Theich, B. J. P. Gall, F. Hoellinger, N.Schulz, I. Ahmad, J. P. Greene, A. Algora
Physical Review C60 (1999) 064611

A05) *Unresolved gamma-rays in 114Te : mass dependence of rotational damping*

S. Frattini, A. Bracco, S. Leoni, F. Camera, B. Million, N. Blasi, G. Lo Bianco, M. Pignanelli, E. Vigezzi, B. Herskind, T. Dossing, M. Bergstrom, P. Varmette, S. Tormanen, A. Maj, M. Kmiecik, D. R. Napoli, and M. Matsuo
Physical Review Letters 83 (1999) 5234

A06) *Structure of Neutron Rich Palladium Isotopes Produced in Heavy Ion Induced Fission*

M. Houry, R. Lucas, M.-G. Porquet, Ch. Theisen, M. Girod, M. Aiche, M.M. Aleonard, A. Astier, G. Barreau, F. Becker, J.F. Chemin, I. Deloncle, T.P. Doan, J.L. Durell, K. Hauschild, W. Korten, Y. Le Coz, M.J. Leddy, S. Perries, N. Redon, A.A. Roach, J.N. Scheurer, A.G. Smith, B.J. Varley
The European Physical Journal A 6 (1999) 43

A07) *Excited Superdeformed Band in 143Eu*

A. Axelsson, J. Nyberg, A. Atac, M.H. Bergstrom, B. Herskind, G. de Angelis, T. Back, D. Bazzacco, A. Bracco, F. Camera, B. Cederwall, C. Fahlander, J.H. Huijnen, S. Lunardi, B. Million, D.R. Napoli, J. Persson, M. Piiparinen, C. Rossi Alvarez, G. Sletten, P.G. Varmette, M. Weiszflog
The European Physical Journal A6 (1999) 175

A08) *Triaxial Superdeformation in 163Lu*

J. Domscheit, S. Tormanen, B. Aengenvoort, H. Hubel, R.A. Bark, M. Bergstrom, A. Bracco, R. Chapman, D.M. Cullen, C. Fahlander, S. Frattini, A. Görgen, G.B. Hagemann, A. Harsmann, B. Herskind, H.J. Jensen, S.L. King, S. Lenzi, D. Napoli, S.W. Ødegård, C.M. Petrache, H. Ryde, U.J. van Severen, G. Sletten, P.O. Tjom and C. Ur
Nuclear Physics A660 (1999) 381

2000

A09) *First evidence for smooth band termination in valence space in the mass 130 region: Spectroscopy of 127La*

C. M. Parry, R. Wadsworth, A. N. Wilson, A. J. Boston, P. J. Nolan, E.S. Paul, J. A. Sampson, A. T. Semple, C. Foin, J. Genevey, A. Gizon, J. Gizon, I. Ragnarsson, and B. G. Dong
Physical Review C61 (2000) 021303 (R)

A10) *New States in 44,46Ar Isotopes from Deep-Inelastic Heavy Ion Reactions Studies*

B. Fornal, R. Broda, W. Krolas, T. Pawłat, J. Wrzesinski, D. Bazzacco, S. Lunardi, C. Rossi Alvarez, G. Viesti,G. de Angelis, M. Cinausero, D. Napoli, J. Gerl, E. Caurier, F. Nowacki
The European Physical Journal A7 (2000) 147

A11) *The rotational gamma-continuum in the mass region A ~ 110*

A. Bracco, S. Frattini, S. Leoni, F. Camera, B. Million, N. Blasi, G. Falconi, G. Lo Bianco, M. Pignanelli, E. Vigezzi, B. Herskind, M. Bergstrom, P. Varmette, S. Tormanen, A. Maj, M. Kmiecik, D. R. Napoli, M. Matsuo
Nuclear Physics A673 (2000) 64

A12) *Search for hyperdeformed structures populated in the 37Cl+120Sn reaction*

V. Rizzi, G. Viesti, D. Bazzacco, A. Algora-Pineda, D. Appelbe, G. de Angelis, N. Belcari, M. Cinausero, M. De Poli, T. E. Drake,A. Gadea, A. Galindo Uribarri,N. Gelli, D. Fabris, E. Farnea, E. Fioretto, W. Krolas, T. Kroell, F. Lucarelli, S. Lunardi, M. Lunardon, T. Martinez, R. Menegazzo, B. K. Nayak, G. Nebbia, D. R. Napoli, B. Nyako, C. M. Petrache, Z. Podolyak, G. Prete, C. Rossi Alvarez, A. Samant, P. Spolaore, C. Ur and K. Zuber
The European Physical Journal A7 (2000) 299

A13) *High spin study of 128Ce and systematics of quasiparticle pair alignment*

E. Paul, P. Bednarczyk, A. J. Boston, C.J. Chiara, C. Foin, D.B. Fossan, J. Genevey, A. Gizon, J. Gizon, D.G. Jenkins, N. Kelsall, N. Kintz, T. Koike, D.R. LaFosse, P.J. Nolan, B.M. Nyakó, C.M. Parry, J.A. Sampson, A.T. Semple, K. Starosta, J. Timár, R. Wadsworth, A.N. Wilson, and L. Zolnai
Nuclear Physics A676 (2000) 32

A14) *Very high rotational frequencies and band termination in 73Br*

C. Plettner, H. Schnare, R. Schwengner, L. Kaubler, F. Donau, I. Ragnarsson, A. V. Afanasjev, A. Algora, G. de Angelis, A. Gadea, D. R. Napoli, J. Eberth, T. Steinhardt, O. Thelen, M. Hausmann, A. Muller, A. Jungclaus, K. P. Lieb, D. G. Jenkins, R. Wadsworth, A. N. Wilson, S. Frauendorf
Physical Review C 62 (2000) 014313

A15) *Proton and gamma-decay lifetime measurements in the second minimum of 58Cu*

D. Rudolph, C. Fahlander, A. Algora, C. Andreoiu, R. Cardona, C. Chandler, G. de Angelis, E. Farnea, A. Gadea, J. Garces Narro, J. Nyberg, M. Palacz, Zs. Podolyak, T. Steinhardt, O. Thelen
Physical Review C63 (2000) 021301 (R)

A16) *Multiple octupole excitations in 148Gd*

Z. Podolyak, P. G. Bizzeti, A. M. Bizzeti-Sona, S. Lunardi, D. Bazzacco,A. Dewald, A. Algora, G. de Angelis, M. De Poli, E. Farnea, A. Gadea, D. R. Kasemann, T. Klug, Th. Kroell, S. Lenzi, D. R. Napoli, C. M. Petrache, R. Peusquens, C. Rossi Alvarez, T. Martinez, C. A. Ur
The European Physical Journal A8 (2000) 147

A17) *Signature inversion caused by triaxiality and unpaired band crossing in 72Br*

C. Plettner, I. Ragnarsson, H. Schnare, R. Schwengner, L. Kaubler, F. Donau, A. Algora, G. de Angelis, A. Gadea, D. R. Napoli, J. Eberth, T. Steinhardt, O. Thelen, M. Hausmann, A. Mueller, A. Jungclaus, K. P. Lieb, D. G. Jenkins, R. Wadsworth, A. N. Wilson
Physical Review Letters 85 (2000) 2454

A18) *Co-existing coupling schemes at high spin in 166Hf*

D. Ringkjobing Jensen, J. Domscheit, G. B. Hagemann, M. Bergstrom, B. Herskind, B. S. Nielsen, G. Sletten, P.G. Varmette, S. Tormanen, H. Hubel, W. Ma, A. Bracco, F. Camera, F. Demaria, S. Frattini, B. Million, D. Napoli, A. Maj, B.M. Nyako, D. T. Joss, and M. Aiche
The European Physical Journal A8 (2000) 165

A19) *Discrete line γ-ray spectroscopy in the 50-60 ℏ spin domain of 161,162Er*

J. Simpson, A.P. Bagshaw, A. Pipidis, M.A. Riley, M.A. Bentley, D.M. Cullen, P.J. Dagnall, G.B. Hagemann, S.L. King, R.W. Laird, J.C. Lisle, S. Sheperd, A.G. Smith, S. Tormanen, A. Afanasjev and I. Ragnarsson
Physical Review C62 (2000) 024321

A20) *Smooth band termination in odd mass La nuclei: 127,129,131La*

R. Wadsworth, E.S. Paul, A. Astier, D. Bazzacco, A.J. Boston, N. Buforn, C. Chiara, D.B. Fossan, C. Fox, J. Gizon, D.G. Jenkins, N.S. Kelsall, T. Koike, D.R. LaFosse, S. Lunardi, P.J. Nolan, B.M. Nyako, C.M. Petrache, H. Scraggs, K. Starosta, J. Timar, A. Walker, A.N. Wilson, L. Zolnai, B.G. Dong, and I. Ragnarsson
Physical Review C62 (2000) 034315

A21) *Magnetic properties of the νj15/2 intruder orbital in the superdeformed minimum of 197Pb*

N. Buforn, A. Astier, R. Duffait, M. Meyer, S. Perriès, A. Prèvost, N. Redon, O. Stèzowski, A. Goergen, H. Hübel, E. Mergel, S. Neumann, D. Rossbach, N. Nenoff, G. Schoenwasser, A.Bauchet, I. Deloncle, M.G. Porquet, A.N. Wilson, R. Lucas, F.A. Beck, D. Curien, G. Duchêne, B.J.P. Gall, N. Kintz, J.P. Vivien, D.M. Cullen
The European Physical Journal A9 (2000) 29

2001

A22) *Excited States in 103Sn: Neutron single-particle energies with respect to 100Sn*

C. Fahlander, J. Kownacki, L.O. Norlin, J. Nyberg, M. Palacz, D. Rudolph, D. Sohler, A. Algora, C. Andreoiu, G. de Angelis, A. Atac, D. Bazzacco, L. Berglund, J. Blomqvist, T. Back, J. Cederkall, B. Cederwall, Zs. Dombradi, B. Fant, E. Farnea, A. Gadea, M. Gorska, H. Grawe, N. Hashimoto-Saitoh, A. Johnson, K. Jonsson, A. Kerek, W. Klamra, S. Lenzi, A. Likar, M. Lipoglavsek, M. Moszynski, D. Napoli, C. Rossi Alvarez, H. Roth, T. Saitoh, D. Severyniak, O. Skeppstedt, M. Weissflog, M. Wolinska
Physical Review C63 (2001) 021307 (R)

A23) *Measurement of the linear polarisation of interband transitions in superdeformed 190Hg: model-independent evidence for octupole vibrational structures*

A. Korichi, A.N. Wilson, F. Hannachi, A. Lopez-Martens, M. Rejmund, C. Schuck, C. Vieu, S. Chmel, A. Görgen, H. Hubel, D. Rossbach, G. Schönwasser, M. Bergstrom, B.M. Nyako, J. Timar, D. Bazzacco, S. Lunardi, C. Rossi Alvarez, P. Bednarczyk, N. Kintz, S. Nagulesaran, D.M. Cullen, J.F. Sharpey-Schafer, M.P. Carpenter, R.V.F. Janssens, T.L. Khoo, T. Lauritzen, and R. Wadsworth
Physical Review Letters 86 (2001) 2746

A24) *Observation of a double giant dipole resonance in fusion-evaporation reactions*

G. Viesti, V. Rizzi, M. Cinausero, N. Gelli, A. Gadea, D. Bazzacco, A. Algora-Pineda, D. Appelbe, G. de Angelis, N. Belcari, M. De Poli, T. E. Drake, D. Fabris, E. Farnea, E. Fioretto, A. Galindo-Uribarri, W. Krolas, T. Kroll, F. Lucarelli, S. Lunardi, M. Lunardon, T. Martinez, R. Menegazzo, B. K. Nayak, G. Nebbia, D. R. Napoli, B. Nyako, C. Petrache, Z. Podolyak, G. Prete, C. Rossi Alvarez, P. Spolaore, C. Ur, and K. Zuber
Physical Review C63 (2001) 034611

A25) *Quantum tunneling of the excited rotational bands in the superdeformed nucleus 143Eu*

S. Leoni, A. Bracco, F. Camera, B. Million, A. Algora, A. Axelsson, G. Benzoni, M. Bergström, N. Blasi, M. Castoldi, S. Frattini, A. Gadea, B. Herskind, M. Kmiecik, G. Lo Bianco, A. Maj, J. Nyberg, M. Pignanelli, J. Styczen, E. Vigezzi, M. Zieblinski and A. Zucchiatti
Physics Letters B498 (2001) 137

A26) *High spin states in neutron-rich Dy isotopes populated in deep-inelastic reactions*

X. Liang, R. Chapman, K. M. Spohr, M. B. Smith, P. Bednarczyk, S. Naguleswaran, F. Haas, G. de Angelis, S. M. Campbell, P. J. Dagnall, M. Davison, G. Duchene, Th. Kroell, S. Lunardi and D.J. Middleton
The European Physical Journal A10 (2001) 41

A27) *New excited superdeformed bands in heavy Pb nuclei: Clue for an octupole softness near the N = 118 gap at large deformation*

A. Prévost, N. Buforn, A. Astier, R. Duffait, M. Meyer, S. Perriès, N. Redon, O. Stézowski, A. Bauchet, I. Deloncle, M.G. Porquet, A. Görgen, H. Hübel, E. Mergel, S. Neumann, D. Roßbach, N. Nenoff, G. Schönwaßer, A.N. Wilson, R. Lucas, F.A. Beck, D. Curien, G. Duchêne, B.J.P. Gall, N. Kintz, J.P. Vivien, D.M. Cullen
The European Physical Journal A10 (2001) 13

A28) *First identification of rotational bands in 103Tc: Evolution of intrinsic proton states of the 97-105Tc isotopes*

A. Bauchet, I. Deloncle, M.-G. Porquet, A. Astier, N. Buforn, M. Meyer, S. Perriès, N. Redon, B.J.P. Gall, F. Hoellinger, N. Schulz, G. Duchêne, S. Courtin, Ts. Venkova, P.A. Butler, N. Amzal, R.D. Herzberg, A. Chewter, R. Cunningham, M. Houry, R. Lucas, W. Urban, A. Nowak, E. Piasecki, J. Duprat, C. Petrache, T. Kröll
The European Physical Journal A10 (2001) 145

A29) *Evidence for the wobbling mode in nuclei*

S.W. Ødegård, G.B. Hagemann, D. R. Jensen, M. Bergstrom, B. Herskind, G. Sletten, S. Tormanen, J. Wilson, P.O. Tjom, I. Hamamoto, K. Spohr, H. Hübel, A. Görgen, G. Schönwasser, A. Bracco, S. Leoni, A. Maj, C. M. Petrache, P. Bednarczyk and D. Curien
Physical Review Letters 86 (2001) 5866

A30) *The lifetime of the proton-decaying 8916 keV state in ^{58}Cu*

D. Rudolph, A. Gadea, G. de Angelis, C. Fahlander, A. Algora, C. Andreoiu, R. Cardona, C. Chandler, E. Farnea, J. Garces Narro, J. Nyberg, M. Palacz, Zs. Podolyak, T. Steinhardt, O. Thelen
Nuclear Physics A 694 (2001) 132

A31) *Coexistence of superdeformed shapes in 154Er*

K. Lagergren, B. Cederwall, T. Bäck, R. Wyss, E. Ideguchi, A. Johnson, A. Ataç, A. Axelsson, F. Azaiez, A. Bracco, J. Cederkäll, Zs. Dombrádi, C. Fahlander, A. Gadea, B. Million, C. M. Petrache, C. Rossi-Alvarez, J. A. Sampson, D. Sohler, and M. Weiszflog
Physical Review Letters 87 (2001) 022502

A32) *Coulomb energy difference in T=1 mirror rotational bands in 50Fe and 50Cr*

S.M. Lenzi, N. Marginean, D.R. Napoli, C.A. Ur, A.P. Zuker, G. de Angelis, A. Algora, M. Axiotis, D. Bazzacco, N. Belcari, M.A. Bentley, P.G. Bizzeti, A. Bizzeti-Sona, F. Brandolini, P. von Brentano, D. Bucurescu, J.A. Cameron, C. Chandler, M. De Poli, A. Dewald, J. Eberth, E. Farnea, A.Gadea, J. Garces-Narro, W. Gelletly, H. Grawe, R. Isocrate, D.T. Joss, C.A. Kalfas, T. Klug, T. Lampman, S. Lunardi, T. Martinez, G. Martinez-Pinedo, R. Menegazzo, J. Nyberg, Zs. Podolyak, A. Poves, R.V. Ribas, C. Rossi Alvarez, B. Rubio, J. Sanchez-Solano, P. Spolaore, T. Steinhardt, O. Thelen, D. Tonev, A. Vitturi, W. von Oertzen, M. Weiszflog
Physical Review Letters 87 (2001) 122501

A33) *Evidence for Octupole Vibration in Superdeformed 196Pb*

D. Rossbach, A. Görgen, H. Hübel, E. Mergel, G. Schönwasser, A.N. Wilson, F. Azaiez, A. Astier, D. Bazzacco, M. Bergstrom, C. Bourgeois, N. Buforn, F. Hannachi, K. Hauschild, A. Korichi, W. Korten, T. Kröll, A. Lopez-Martens, R. Lucas, H.J. Maier, N. Redon, P. Reiter, C. Rossi-Alvarez, O. Stezowski, P. Thirolf
Physics Letters 513B (2001) 9

A34) *Investigation of the Magnetic Rotation in 196Pb*

G. Kemper, A. Dewald, I. Wiedenhöver, R. Peusquens, S. Kasemann, K.O. Zell, P. von Brentano, H. Hübel, S. Chmel, A. Görgen, D. Bazzacco, R. Venturelli, S. Lunardi, D.R. Napoli, F. Hannachi, A. Lopez-Martens, R. Krücken, J.R. Cooper, R.M. Clark, M.A. Deleplanque, I.Y. Lee, A.O. Machiavelli, F.S. Stephens
The European Physical Journal A11 (2001) 121

A35) *Exploring the Emission Barriers in Hot Nuclei*

G. Viesti, V. Rizzi, D. Fabris, M. Lunardon, G. Nebbia, M. Cinausero, E. Fioretto, G. Prete, A. Brondi, G. La Rana, R. Moro, E. Vardaci, M. Aiche, M.M.Aleonard, G. Barreau, D. Boivin, J.N. Scheurer, J.F. Chemin, K. Hagel, J.B. Natowitz, R. Wada, S. Courtin, F. Haas, N. Rowley, B.M. Nyako, J. Gal, J. Molnar
Physics Letters B521 (2001) 165

A36) *Coulomb Energy Differences between Isobaric Analogue States in 70Br and 70Se Identification of Excited States of the Tz=0 Nucleus 70Br*

G. de Angelis, T. Martinez, A. Gadea, N. Marginean, E. Farnea, E. Maglione, S. Lenzi, W. Gelletly, C.A. Ur, D.R. Napoli, Th. Kroell, S. Lunardi, B. Rubio, M. Axiotis, D. Bazzacco, A.M. Bizzeti-Sona, P.G. Bizzeti, P. Bednarczyk, A. Bracco, F. Brandolini, F. Camera, D. Curien, M. De Poli, O. Dorvaux, J. Eberth, H. Grawe, R. Menegazzo, G. Nardelli, J. Nyberg, P. Pavan, B. Quintana, C. Rossi Alvarez, P. Spolaore, T. Steinhardt, I. Stefanescu, O. Thelen, R.Venturelli
The European Physical Journal A12 (2001) 51

A37) *High-spin states in 44Ca*

M. Lach, P. Bednarczyk, A. Bracco, J. Grebosz, M. Kadluczka, N. Kintz, A. Maj, J.C. Merdinger, W. Meczynski, J.L. Pedroza, N. Schulz, M.B. Smith, K.M. Spohr, J. Styczen, J.P. Vivien, M. Zieblinski
The European Physical Journal A12 (2001) 381

2002

A38) *Wobbling Phonon Excitations, Coexisting with Normal Deformed Structures in 163Lu*

D.R. Jensen, G.B. Hagemann, I. Hamamoto, S.W. Ødegård, M. Bergstrom, B. Herskind, G. Sletten, S. Tormanen, J.N. Wilson, P.O. Tjom, K. Spohr, H. Hübel, A. Görgen, G. Schönwasser, A. Bracco, S. Leoni, A. Maj, C.M. Petrache, P. Bednarczyk, D. Curien
Nuclear Physics A703 (2002) 3

A39) *Transition rates and nuclear structure changes in mirror nuclei 47Cr and 47V*

D. Tonev, P. Petkov, A. Dewald, T. Klug, P. von Brentano, W. Andrejtscheff, S. M. Lenzi, D. R. Napoli, N. Marginean, F. Brandolini, C. A. Ur, M. Axiotis, P. G. Bizzeti, and A. Bizzeti-Sona
Physical Review C65 (2002) 034314

A40) *Enhanced population of superdeformation in the mass A = 150 region*

Th. Byrski, F.A. Beck, P. Bednarczyk, N. Kintz, K. Zuber, J.P. Vivien, S. Courtin, D. Curien, G. Duchene, C. Finck, B. Gall, A. Nourreddine, A. Odahara, O. Stezowski, Ch. Theisen
Physical Review C 65 (2002) 034324

A41) *Coherent Proton-Neutron Contribution to Octupole Correlations in the Neutron-Deficient 114Xe Nucleus*

G. de Angelis, A. Gadea, E. Farnea, R. Isocrate, P. Petkov, N. Marginean, D.R. Napoli, A. Dewald, M. Bellato, A. Bracco, F. Camera, D. Curien, M. De Poli, E. Fioretto, A. Fitzler, S. Kasemann, N. Kintz, T. Klug, S. Lenzi, S. Lunardi, R. Menegazzo, P. Pavan, J.L. Pedroza, V. Pucknell, C. Ring, J. Sampson, R. Wyss
Physics Letters B 535 (2002) 93

A42) *Development of magnetic rotation in light Gd nuclei; study of 142Gd*

R.M. Lieder, T. Rzaca-Urban, H. Brands, W. Gast, H.M. Jäger, L. Mihailescu, Z. Marcinkowska, W. Urban, T. Morek, Ch. Droste, P. Szymanski, S. Chmel, D. Bazzacco, G. Falconi, R. Menegazzo, S. Lunardi, C. Rossi Alvarez, G. de Angelis, E. Farnea, A. Gadea, D.R. Napoli, Z. Podolyak, Ts. Venkova, R. Wyss,
The European Physical Journal A 13 (2002) 297

A43) *Candidate for the 6+ state in the yrast sequence of 36S*

X. Liang, R. Chapman, F. Haas, K.-M. Spohr, P. Bednarczyk, S. M. Campbell, P. J. Dagnall, M. Davison, G. de Angelis, G. Duchêne, Th. Kröll, S. Lunardi, S. Naguleswaran, and M. B. Smith
Physical Review C66 (2002) 014302

A44) *Count Fluctuation Analysis in the Triaxial Strongly Deformed Potential Well of 163Lu*

S.W. Ødegård, B. Herskind, T. Døssing, G.B. Hagemann, D.R. Jensen, G. Sletten, J.N. Wilson, S. Leoni, P.O. Tjøm, P. Bednarczyk, D. Curien
The European Physical Journal A 14 (2002) 309

A45) *Effect of E1 Decay in the Population of Superdeformed Structures*

G. Benzoni, A. Bracco, F. Camera, S. Leoni, B. Million, A. Maj, A. Algora, A. Axelsson, M. Bergstrom, N. Blasi, M. Castoldi, S. Frattini, A. Gadea, B. Herskind, M. Kmiecik, G. Lo Bianco, J. Nyberg, M. Pignanelli, J. Styczen, O. Wieland, M. Zieblinski, A. Zucchiatti
Physics Letters B 540 (2002) 199

A46) *Neutron Excitations Across the N=50 Shell Gap in 102In*

D. Sohler, M. Palacz, Zs. Dombradi, J. Blomqvist, C. Fahlander, L.-O. Norlin, J. Nyberg, T. Back, K. Lagergren, D. Rudolph, A. Algora, C. Andreoiu, G. de Angelis, A. Atac, D. Bazzacco, J. Cederkall, B. Cederwall, B. Fant, E. Farnea, A. Gadea, M. Gorska, H. Grawe, N. Hashimoto-Saitoh, A. Johnson, A. Kerek, W. Klamra, J. Kownacki, S.M. Lenzi, A. Likar, M. Lipoglavsek, M. Moszynski, D.R. Napoli, C. Rossi-Alvarez, H.A. Roth, T. Saitoh, D. Seweryniak, O. Skeppstedt, J. Timar, M. Weiszflog, M. Wolinska
Nuclear Physics A708 (2002) 181

A47) *Lifetimes in the yrast and an octupole-vibrational superdeformed band in 196Pb*

D. Rossbach, A.Görgen, H.Hubel, E.Mergel, G.Schönwasser, F.Azaiez, C.Bourgeois, F. Hannachi, A. Korichi, A. Lopez-Martens, A. Astier, N. Buforn, N. Redon, O. Stezowski, D. Bazzacco, Th. Kröll, C. Rossi-Alvarez, K. Hauschild, W. Korten, R. Lucas, H.J.Maier, P. Reiter, P.G. Thirolf
Physical Review C66 (2002) 024316

A48) *Detailed Study of Magnetic Rotation in 196Pb*

A.K. Singh, N. Nenoff, D. Rossbach, A. Görgen, S. Chmel, F. Azaiez, A. Astier, D. Bazzacco, M. Belleguic, S. Bouneau, C. Bourgeois, N. Buforn, B. Cederwall, I. Deloncle, J. Domscheit, F. Hannachi, K. Hauschild, H. Hubel, A. Korichi, W. Korten, Th. Kröll, Y. Le Coz, A. Lopez-Martens, R. Lucas, S. Lunardi, H.J. Maier, E. Mergel, M. Meyer, C.M. Petrache, N. Redon, P. Reiter, C. Rossi-Alvarez, G. Schönwasser, O. Stezowski, P.G. Thirolf, A.N. Wilson
Nuclear Physics A707 (2002) 3

A49) *Evidence for excited states in 95Ag*

K. Lagergren, B. Cederwall, A. Johnson, J. Blomqvist, D. Sohler, G. de Angelis, P. Bednarczyk, T. Back, T. Claesson, O. Dorvaux, E. Farnea, A. Gadea, M. Gorska, L. Milechina, L.O. Norlin, A. Odahara, M. Palacz, I. Stefanescu, O. Thelen, J.P. Vivien
The European Physical Journal A14 (2002) 393

A50) *Lifetimes of Yrast Rotational States of the Fission Fragments 100Zr and 104Mo Measured using a Differential Plunger*

A.G. Smith, R.M. Wall, D. Patel, G.S. Simpson, D.M. Cullen, J.L. Durell, S.J. Freeman, J.C. Lisle, J.F. Smith, B.J. Varley, G. Barreau, M. Petit, Ch. Theisen, E. Bouchez, M. Houry, R. Lucas, B. Cahan, A. Le Coguie, B.J.P. Gall, O. Dorvaux, N. Schulz
J. Phys. (London) G28 (2002) 2307

A51) *Evidence for Second-Phonon Nuclear Wobbling*

D. R. Jensen, G. B. Hagemann, I. Hamamoto, S. W. Ødegård, B. Herskind, G. Sletten, J. N. Wilson, K. Spohr, H. Hübel, P. Bringel, A. Neußer, G. Schönwaßer, A. K. Singh, W. C. Ma, H. Amro, A. Bracco, S. Leoni, G. Benzoni, A. Maj, C. M. Petrache, G. Lo Bianco, P. Bednarczyk, and D. Curien
Physical Review Letters 89 (2002) 142503

A52) *Observation of yrast states in neutron-rich 41Cl*

X. Liang, R. Chapman, F. Haas, K.-M. Spohr, P. Bednarczyk, S.M. Campbell, P.J. Dagnall, M. Davison, G. de Angelis, G. Duchêne, Th. Kröll, S. Lunardi, S. Naguleswaran, and M.B. Smith
Physical Review C66 (2002) 037301(R)

A53) *High-spin study of odd-A $_{49}$In isotopes beyond the neutron mid-shell*

R. Lucas, M.-G. Porquet, Ts. Venkova, I. Deloncle, M. Houry, Ch. Theisen, A. Astier, A. Bauchet, S. Lalkovski, G. Barreau, N. Buforn, T.P. Doan, L. Donadille, O. Dorvaux, J. Durell, Th. Ethvignot, B.P.J. Gall, D. Grimwood, W. Korten, Y. Le Coz, M. Meyer, A. Minkova, A. Prévost, N. Redon, A. Roach, N. Schultz, O. Stézowski, A.G. Smith and B.J. Varley
The European Physical Journal A15 (2002) 315

A54) *Candidates for chiral doublet bands in ^{136}Nd*

E. Mergel, C.M. Petrache, G. Lo Bianco, H. Hubel, J. Domscheit, D. Rossbach, G. Schönwasser, N. Nenoff, A. Neußer, A. Görgen, F. Becker, E. Bouchez, M. Houry, A. Hürstel, Y. Le Coz, R. Lucas, Ch. Theisen, W. Korten, A. Bracco, N. Blasi, F. Camera, S. Leoni, F. Hannachi, A. Lopez-Martens, M. Rejmund, D. Gaßmann, P. Reiter, P.G. Thirolf, A. Astier, N. Buforn, M. Meyer, N. Redon, O. Stezowski
European Physical Journal A15 (2002) 417

A55) *High-spin structure of the neutron-rich $^{109, 111, 113}$Rh isotopes*

Ts. Venkova, M.-G. Porquet, A. Astier, A. Bauchet, I. Deloncle, S. Lalkovski, N. Buforn, L. Donadille, O. Dorvaux, B.J.P. Gall, R. Lucas, M. Meyer, M. Minkova, A. Prévost, N. Redon, N. Schulz, O. Stézowski
European Physical Journal A15 (2002) 429

A56) *First triaxial superdeformed band in ^{170}Hf*

A. Neußer, H. Hübel, G.B. Hagemann, S. Bhattacharya, P. Bringel, D. Curien, O. Dorvaux, J. Domscheit, F. Hannachi, D.R. Jensen, A. Lopez-Martens, E. Mergel, N. Nenoff, A.K. Singh
European Physical Journal A15 (2002) 439

A57) *High-spin structure of the neutron-rich odd-odd $^{106, 108}$Rh and $^{110, 112}$Ag isotopes*

M.-G. Porquet, Ts. Venkova, P. Petkov, A. Bauchet, I. Deloncle, A. Astier, N. Buforn, J. Duprat, B.J.P. Gall, C. Gautherin, E. Gueorguieva, F. Hoellinger, T. Kutsarova, R. Lucas, M. Meyer, A. Minkova, N. Redon, N. Schulz, H. Sergolle, A. Wilson
European Physical Journal A15 (2002) 463

A58) *Lifetimes of magnetic-rotational bands in ^{196}Pb*

A.K. Singh, H. Hübel, D. Rossbach, S. Chmel, A. Görgen, E. Mergel, G. Schönwasser, F. Azaiez, C. Bourgeois, F. Hannachi, A. Korichi, A. Lopez-Martens, A. Astier, N. Buforn, N. Redon, O. Stezowski, D. Bazzacco, T. Kröll, C. Rossi-Alvarez, K. Hauschild, W. Korten, R. Lucas, H.J. Maier, P. Reiter, P.G. Thirolf, A.N. Wilson
Physical Review C66 (2002) 064314

A59) *Shape coexistence at high spin in the N=Z + 2 nucleus ^{70}Se*

G. Rainovski, H. Schnare, R. Schwengner, C. Plettner, L. Kaubler, F. Dönau, I. Ragnarsson, J. Eberth, T. Steinhardt, O. Thelen, M. Hausmann, A. Jungclaus, K.P. Lieb, A. Müller, G. de Angelis, A. Gadea, D.R. Napoli, A. Algora, D.G. Jenkins, R. Wadsworth, A. Wilson, W. Andrejtscheff, V.I. Dimitrov
J. Phys. (London) G28 (2002) 2617

2003

A60) *Experimental evidence for signature inversion in 132La from a revisited level scheme*

J. Timár, D. Sohler, B.M. Nyakó, L. Zolnai, R. Wyss, E.S. Paul, A.J. Boston, C. Fox, P.J. Nolan, J.A. Sampson, H.C. Scraggs, A. Walker, J. Gizon, A. Gizon, D. Bazzacco, S. Lunardi, C.M. Petrache, A. Astier, N. Buforn, P. Bednarczyk, and N. Kintz,
The European Physical Journal A16 (2003) 1

A61) *Isospin mixing in the N=Z nucleus ^{64}Ge*

E. Farnea, G. de Angelis, A. Gadea, P.G. Bizzeti, A. Dewald, J. Eberth, A. Algora, M. Axiotis, D. Bazzacco, A.M. Bizzeti-Sona, F. Brandolini, G. Colo, W. Gelletly, M.A. Kaci, N. Kintz, T. Klug, Th. Kröll, S.M. Lenzi, S. Lunardi, N. Marginean, T. Martinez, R. Menegazzo, D.R. Napoli, J. Nyberg, P. Pavan, Zs. Podolyak, C.M. Petrache, B. Quintana, B. Rubio, P. Spolaore, Th. Steinhardt, J.L. Tain, O. Thelen, C.A. Ur, R. Venturelli, M. Weiszflog
Physics Letters B551 (2003) 56

A62) *One- and two-phonon wobbling excitations in triaxial ^{165}Lu*

G. Schönwasser, H. Hübel, G.B. Hagemann, P. Bednarczyk, G. Benzoni, G. Lo Bianco, A. Bracco, P. Bringel, R. Chapman, D. Curien, J. Domscheit, B. Herskind, D.R. Jensen, S. Leoni, W.C. Ma, A. Maj, A. Neußer, S.W. Ødegård, C. Petrache, D. Roßbach, H. Ryde, K.H. Spohr, A.K. Singh
Physics Letters B552 (2003) 9

A63) *In-beam gamma-ray spectroscopy of ^{42}Ca*

M. Lach, J. Styczen, W. Meczynski, P. Bednarczyk, A. Bracco, J. Grebosz, A. Maj, J.C. Merdinger, N. Schulz, M.B. Smith, K.M. Spohr, J.P. Vivien, M. Zieblinski
The European Physical Journal A16 (2003) 309

A64) *Electromagnetic B(E2) transition strengths along the yrast negative-parity band of ^{113}I*

P. Petkov, A. Dewald, A. Fitzler, T. Klug, G. de Angelis, E. Farnea, A. Gadea, R. Isocrate, N. Marginean, D. R. Napoli, D. Curien, N. Kintz, S. Lenzi, S. Lunardi, R. Menegazzo, V. Pucknell, and C. Ring
Physical Review C67 (2003) 054306

A65) *Lifetime measurements in ^{148}Gd*

Zs. Podolyák, P.G. Bizzeti, A.M. Bizzeti-Sona, S. Lunardi, D. Bazzacco, A. Dewald, A. Algora, G. de Angelis, E. Farnea, A. Gadea, D.R. Kasemann, T. Klug, Th. Kröll, S. Lenzi, D.R. Napoli, C.M. Petrache, R. Peusquens, C. Rossi Alvarez, T. Martinez, C.A. Ur
The European Physical Journal A17 (2003) 29

A66) *Four-quasiparticle alignments in 66Ge*

E.A. Stefanova, I. Stefanescu, G. de Angelis, D. Curien, J. Eberth, E. Farnea, A. Gadea, G. Gersch, A. Jungclaus, K.P. Lieb, T. Martinez, R. Schwengner, T. Steinhardt, O. Thelen, D. Weisshaar, R. Wyss
Physical Review C67 (2003) 054319

A67) *Candidate chiral twin bands in the odd-odd nucleus 132Cs: Exploring the limits of chirality in the mass A ~130 region*

G. Rainovski, E. S. Paul, H. J. Chantler, P. J. Nolan, D. G. Jenkins, R. Wadsworth, P. Raddon, A. Simons, D. B. Fossan, T. Koike, K. Starosta, C. Vaman, E. Farnea, A. Gadea, Th. Kröll, R. Isocrate, G. de Angelis, D. Curien, and V. I. Dimitrov
Physical Review C68 (2003) 024318

A68) *Evolution of the π g9/2-ν h11/2 configuration in neutron-rich 110,112Rh and 114,116Ag isotopes*

M.-G. Porquet, Ts. Venkova, A. Astier, A. Bauchet, I. Deloncle, N. Buforn, L. Donadille, O. Dorvaux, B.J.P. Gall, S. Lalkovski, R. Lucas, M. Meyer, A. Minkova, A. Prevost, N. Redon, N. Schulz and O. Stezowski
The European Physical Journal A18 (2003) 25

A69) *Two-quasiparticle and collective excitations in transitional 108,110Pd nuclei*

S. Lalkovski, A. Minkova, M.-G. Porquet, A. Bauchet, I. Deloncle, A. Astier, N. Buforn, L. Donadille, O. Dorvaux, B.J.P. Gall,R. Lucas, M. Meyer, A. Prevost, N. Redon, N. Schulz and O. Stezowski
The European Physical Journal A, in press

A70) *Quantized Wobbling in Nuclei*

G.B. Hagemann and I. Hamamoto
Nuclear Physics News, Vol. 13 (2003) 20

A71) *Coexisting wobbling and quasiparticle excitations in the triaxial potential well of ^{163}Lu*

D.R. Jensen, G.B. Hagemann, I. Hamamoto, B. Herskind, G. Sletten, J.N. Wilson, S.W. Oedegaard, K. Spohr, H. Hubel, P. Bringel, A. Neusser, G. Schönwasser, A.K. Singh, W.C. Ma,, H. Amro, A. Bracco, S. Leoni, G. Benzoni, A. Maj, C.M. Petrache, G. Lo Bianco, P. Bednarczyk and D. Curien

B) Technical developments

B01) *Development of a Composite Ge Detector for EUROBALL,*

J. Eberth, P. von Brentano, W. Teichert, H.G. Thomas, A. von der Werth, R.M. Lieder, H. Jäger, H. Kämmerling, D. Kutchin, K.H. Maier, M. Berst, D. Gutknecht and R. Henck
Prog. Part. Nucl. Phys. 28 (1992) 495.

B02) *Encapsulated Ge Detectors: Development and first Tests*

J. Eberth, H.G. Thomas, P. von Brentano, R.M. Lieder, H.M. Jäger, H. Kämmerling, M. Berst, D. Gutknecht and R. Henck
Nucl. Instr. and Meth. in Phys. Res. A369 (1996) 135

B03) *The Response of the EUROBALL CLUSTER Detector to γ-Radiation up to 10 MeV,*

M. Wilhelm, J. Eberth, G. Pascovici, E. Radermacher, H.G. Thomas, P. von Brentano, H. Prade and R.M. Lieder
Nucl. Instr. and Meth. in Phys. Res. A381 (1996) 462

B04) *The EUROBALL Neutron Wall - Design and Performance Tests of Neutron Detectors*

O. Skeppstedt, H.A. Roth, L. Lindstrom, R. Wadsworth, I. Hibbert, N. Kelsall, D. Jenkins, H. Grawe, M. Gorska, M. Moszynski, Z. Sujkowski, D. Wolski, M. Kapusta, M. Hellstrom, S. Kalogeropoulos, D. Oner, A. Johnson, J. Cederkall, W. Klamra, J. Nyberg, M. Weiszflog, J. Kay, R. Griffiths, J. Garces Narro, C. Pearson, J. Eberth
Nucl. Instr. and Meth. in Phys. Res. A421 (1999) 531

B05) *EuroSiB - a 4π Silicon Ball for Charged-Particle Detection in EUROBALL*

G. Pausch, H. Prade, M. Sobiella, H. Schnare, R. Schwengner, L. Kaubler, C. Borcan, H.-G. Ortlepp, U. Oehmichen, H. Grawe, R. Schubart, J. Gerl, J. Cederkall, A. Johnson, A. Kerek, W. Klamra, M. Moszynski, D. Wolski, M. Kapusta, A. Axelsson, M. Weiszflog, T. Härtlein, D. Pansegrau, G. de Angelis, S. Ashrafi, A. Likar, M. Lipoglavsek
Nucl. Instr. and Meth. in Phys. Res. A443 (2000) 304

B06) *Measurements of 15 MeV γ-rays with the Ge cluster detectors of EUROBALL.*

B. Million, A. Bracco, F. Camera, S. Brambilla, A. Gadea, D. Giugni, B. Herskind, M. Kmiecik, R. Isocrate, S. Leoni, A. Maj, F. Prelz, O. Wieland
Nucl. Instrum. and Meth. in Phys. Res. A452 (2000) 422

B07) *The VXI electronics of the DIAMANT particle detector array*

J. Gál, G. Hegyesi, J. Molnár, B.M. Nyakó, G. Kalinka, J.N. Scheurer, M.M. Aléonard, J.F. Chemin, J.L. Pedroza, K. Juhász, V.R.F. Pucknell
Nucl. Instr. and Meth. in Phys. Res. A, submitted

C) PhD Theses

Kai Strähle (University of Bonn, Germany, 1993)
"Superdeformation in ^{144,145,146}Gd und Entwicklung eines gekapselten Ge-Detektors"

Stefan Utzelmann (University of Bonn, Germany, 1996)
"Superdeformation in ^{144,145}Gd und Kerngestaltsänderung in ^{180}Os"

Joakim Cederkäll (Royal Institute of Technology, Stockholm, Sweden, 1998)
"Nuclear structure close to ^{100}Sn"

Matej Lipoglavsek (University of Lund, Sweden, 1998)
"Rigidity of the doubly-magic ^{100}Sn core"

Nami Saitoh (University of Tsukuba, Japan, June 1999)
"Nuclear Structures in ^{182,183}Re and K-forbiddenness in A ~ 180 Nuclei"

Takehiko R. Saitoh (University of Copenhagen, Denmark, June 1999)
"Structures in doubly odd ^{180}Ta, proton-odd ^{181}Ta and neutron-odd ^{183}W"

1998

C.B. Aengenvoort (University of Bonn, Germany)
"Zerfall der superdeformierten Banden in den Kernen ^{135}Nd und ^{163}Lu"

Severin Thummerer (Free University of Berlin, Germany)
"Gamma-spectroscopy of deformed nuclei with binary reactions"

S. Frattini (University of Milano, Italy)
"Study of the nuclear rotational motion at high spin in the mass region A=160 and A=110"

1999

Andrew Bagshaw (University of Manchester, United Kingdom)
"High-Spin Spectroscopy of ^{161,162}Er"

Adrian Roach (University of Manchester, United Kingdom)
"Gamma-ray spectroscopy of neutron-rich Cadmium nuclei"

Stephan Perries (University of Lyon-1, France)
"Proprietes de la matiere nucleaire superdeformée dans les regions de masse A ~ 190 et A ~ 130"

2000

Anders Axelsson (University of Uppsala, Sweden)
"Studies of collective excitations in Rare Earth Nuclei"

Andreas Görgen (University of Bonn, Germany)
"Magnetische Rotation in Pb Isotopen"

Michael Houry (University of Paris XI, Orsay, France)
"Spectroscopie γ des noyaux riches en neutrons produits par fission induite ^{12}C+^{238}U. Structure nucléaire des isotopes de palladium"

Guido Kemper (University of Köln, Germany)
"Dynamische Formänderungen in ^{136}Nd und magnetische Rotation in ^{196}Pb"

Nathalie Kintz (University Louis Pasteur, Strasbourg, France)
"Etude des bifurcations Delta I = 4 dans les noyaux superdeformes de la region de masse A ~ 150"

Rüdiger Peusquens (University of Köln, Germany)
"Software für Gammaspektroskopiemessungen und Superdeformation im Kern ^{135}Nd"

Gary Simpson (University of Manchester, United Kingdom)
"Gamma-ray angular correlations in spontaneous fission"

2001

Armand Bauchet (University of Paris XI Orsay, France)
"Spectroscopie gamma de fragments de fission aupres d'EUROBALL : mise en evidence du role des orbitales de proton dans des noyaux riches en neutrons de la region de masse A ~ 100"

Nadege Buforn (University of Lyon-1, France)
"Force de Coriolis et déformation nucléaire : résultats dans les isotopes de cadmium et de plomb avec le multidetecteur-γ EUROBALL"

Jochen Domscheit (University of Bonn, Germany)
"Untersuchung verschiedener Kernformen bei hohem Drehimpuls"

Enrico Farnea (University of Surrey, United Kingdom)
"Spectroscopic studies of isospin mixing in ^{64}Ge"

Christina Plettner (Technical University of Dresden, Germany)
"Nuclear structure phenomena in the 72,73Br nuclei"

Ahmed N. Qadir (University of Manchester, United Kingdom)
"Spectroscopic study of neutron rich nuclei north-west of ^{208}Pb"

Detlef Roßbach (University of Bonn, Germany)
"Struktur angeregter superdeformierter Zustände in Pb Isotopen"

Ronan Wall (University of Manchester, United Kingdom)
"A differential Doppler-shift technique for the measurement of excited states in fission fragments"

2002

Corina Andreoiu (University of Lund, Sweden)
"The Nucleus ^{59}Cu: Complex Structure, Shape Evolution, Exotic Decay Modes"

Edgar Galindo (University of Göttingen, Germany)
"Lifetime measurements of high spin states in ^{95}Ru and ^{101}Ag"

Xiaoying Liang (University of Paisley, United Kingdom)
"Spectroscopy of neutron rich nuclei produced in deep inelastic processes"

Stein Westad Ødegaard (University of Oslo, Norway)
"Triaxiality and Wobbling in Nuclei"

Jerzy Grebosz (The Niewodniczanski Institute of Nuclear Physics, Krakow, Poland)
"Distinction of fusion reaction products with the Recoil Filter Detector; experiment control and data reduction with the use of object oriented programming"

2003 and in preparation

Tom Armstrong (University of Manchester, United Kingdom)
"Two QP Bands in Neutron-Rich Nuclei"

Mihalis Axiotis (National Technological University of Athens, Greece)
"High spin spectroscopy of ^{52}Mn and ^{52}Fe"

Giovanna Benzoni (University of Milano, Italy)
"Study of nuclear shapes in thermally excited highly rotating nuclei"

P.T.W. Choy (University of Liverpool, United Kingdom)

Karsten Jessen (University of Köln, Germany, 2003)
"Spektroskopie der Z=N Kerne ^{48}Cr und ^{46}V"

Karin Lagergren (Royal Institute of Technology, Stockholm, Sweden 2003)

Stefan Lalkovski (University of Sofia, 2003)
"Study of high-spin states of neutron-rich ^{108,110}Pd isotopes from induced fission"

Trinitario Martinez (University of Valencia, Spain)
"Structure of the nuclei close to the N=Z line ^{70,71}Br"

Edgar Mergel (University of Bonn, Germany)
"Untersuchung der Formkoexistenz in Atomkernen mit Hilfe von Gamma- und Konversionselektronenspektroskopie"

Aurelien Prevost (University of Lyon, France, 2003)
"A la recherche des grandes deformations nucleaires avec les multidétecteurs EUROBALL et EXOGAM"

Dennis Ringkjoebing Jensen (University of Copenhagen, Denmark, Feb.2003)
"Wobbling Phonon Excitations in Nuclei - Evidence for Triaxiality"

Jérôme Robin (University Louis Pasteur, Strasbourg, France, 2003)
"Transition de phases : recherche et étude de transitions de liaison entre les puits superdéformés et normalement déformés dans les noyaux ^{151,150}Tb"

Bejoy Saha (University of Köln, Germany, 2003)
"Kernstrukturuntersuchung an ^{124}Xe mit Hilfe elektromagnetischer Uebergangswahrscheinlichkeiten"

Gero Schönwasser (University of Bonn, Germany)
"Triaxiale Superdeformation in Lu Isotopen"

Andrew Simons (University of York, United Kingdom)

Talal Yousef (University of Manchester, United Kingdom)

D) Invited Talks at International Conferences and Workshops

1998

D01) *The Euroball array*
C. Rossi Alvarez
SNEC98 Conference, Padova, Italy, April 1998
Proceedings published in **Nuovo Cimento 111A (1998) 601**

D02) *Nuclear Structure Experiments with Euroball*
D.R. Napoli
33rd Holzhau Spring Meeting FZ Rossendorf Holzhau (Germany), April 1998

D03) *Nuclear shapes and the EUROBALL facility*
M. Pignanelli
International School of Physics "Enrico Fermi", Course CXXXVIII,
Proceedings published in IOS Press, Amsterdam 1998

D04) *The status of the Euroball array at LNL*
C. Rossi Alvarez
6th Int. Spring Seminar in Nuclear Physics, S. Agata sui due Golfi (Italy), May 1998,
Proceedings published in World Scientific, Singapore, 1999, p. 477.

D05) *Decay Out of the Highly-Deformed Bands in the A = 130 Mass Region and Experimental Δ_n for Nd Nuclei*
C.M. Petrache
Nuclear Structure 98, Gatlinburg (USA), 1998
Proceedings published in **AIP Conf. Proc. 481 (1999) 368**.

D06) *Double and Triple Octupole Excitations in the A=150 Region*
P.G. Bizzeti
Nuclear Structure 98, Gatlinburg (USA), 1998
Proceedings published in **AIP Conf. Proc. 481 (1999) 493**.

D07) *The Limits of Gamma-Ray Spectroscopy with Multi-Detector Arrays*
J. Simpson
Int. Nuclear Physics Conf. INPC/98, Paris (France), August 1998
Proceedings published in **Nucl. Phys. A654 (1999) 178c**.

D08) *Recent results from large γ-detector arrays (*GASP *and* EUROBALL*) at Legnaro*
S. Lunardi
XXXIII Zakopane School of Physics "Trends in Nuclear Physics", Zakopane, Poland, September 1998,
Proceedings published in **Acta Phys. Pol. B (1999)**.

1999

D09) *New Results from Euroball.*
S. Lunardi
Proceedings of the Conference Experimental Nuclear Physics in Europe, Sevilla, Spain, June 1999,
Proceedings published in **AIP Conf. Proc. 495 (1999) 165**.

D10) *Search for the GDR Built on Superdeformed Nuclei*
A.Bracco

Int. Conf. on Achievements and Perspectives in Nuclear Structure, Crete (Greece), July 1999, Proceedings published in **Physica Scripta, T88 (2000) 182**.

D11) *Search for Exotic Shapes*
G.B. Hagemann
Int. Conf. on Achievements and Perspectives in Nuclear Structure, Crete (Greece), July 1999, Proceedings published in **Physica Scripta, T88 (2000) 77**.

D12) *Prompt particle decays of deformed second minima*
D. Rudolph
Int. Conf. on Achievements and Perspectives in Nuclear Structure, Crete (Greece), July 1999, Proceedings published in **Physica Scripta T88 (2000) 21**.

D13) *EUROBALL: Present status and results*
J. Simpson
Annual Fall Meeting of the Division of the Nuclear Physics, APS, Pacific Groves, October 1999, USA

D14) *Prompt particle decays from deformed high-spin states*
D. Rudolph
First Int. Symp. on Proton Emitting Nuclei, Oak Ridge,USA, October 1999,
Proceedings published in **AIP Conf. Proc. 518 (2000) 285**.

D15) *Study of fission fragments from the $^{12}C+^{238}U$ reaction : prompt and delayed spectroscopy*
R. Lucas
Second International Conference on Fission and Neutron-Rich Nuclei,
St. Andrews (Scotland), June 28-July 2, 1999.

2000

D16) *Status and new results with Euroball IV*
G. Duchene
Int. Symp. Exotic Nuclear Structures, Debrecen, May 2000

D17) *First identification of excited states in the N=Z-2 nucleus ^{50}Fe*
S.M. Lenzi
Int. Conf. Structure of the nucleus at the dawn of the century, Bologna (Italy), June 2000

D18) *Exotic Nuclear States: the new information from Euroball*
M. Pignanelli
Int. Conf. Structure of the nucleus at the dawn of the century, Bologna (Italy), June 2000

D19) *Nuclear Structure at high spin and termal energy studied with Euroball*
A. Bracco
Int. Conf. Structure of the nucleus at the dawn of the century, Bologna (Italy), June 2000

D20) *Mass and deformation dependence of rotational damping*
S. Leoni
Int. Conf. Nuclear structure and related topics, Dubna (Russia), June 2000

D21) *Role of E1 decay in the feeding of superdeformation from very selective GDR experiments*
F. Camera
Int. Conf. on Nuclear structure and related topics, Dubna (Russia), June 2000

D22) *The Giant Dipole Resonance in the Superdeformed nuclei and the feeding of superdeformed bands*
F. Camera
GR2000, Int. Conf. on Giant Resonances, Osaka (Japan), June 2000.

D23) *Euroball: selected physics cases*
D. Curien
Nucleus Nucleus Collisions, Strasbourg (France), June 2000
Proceedings published in Nucl.Phys. A685, 198c (2001)

D24) *Gamma decay of the GDR on superdeformed configurations in ^{143}Eu*
A. Bracco
Nuclear Structure 2000, Michigan State University (USA), August 2000
Proceedings published in **Nucl. Phys. A682 (2001) 449c**.

D25) *Towards far from Stability with Euroball*
S. Lunardi
International School on Nuclear Physics, Erice (Italy), September 2000
Proceedings published in **Progress in Particle and Nuclear Physics 46 (2001) 253**.

D26) *EUROBALL Experiments at Strasbourg*
G. Duchêne
NSNA2000, Rossendorf (Germany)

D27) *Evolution of Nuclear Shapes and Exotic Decays Near ^{56}Ni*
D. Rudolph, C. Andreoiu, J. Ekman, C. Fahlander, A. Gadea, and D.G. Sarantites
Proceedings published in **Acta Phys. Pol. B 32 (2001) 703**.

D27) *High spin spectroscopy of light $f_{7/2}$ nuclei studied with EUROBALL IV and the Recoil Filter Detector: a smooth band termination in ^{45}S*
P. Bednarczyk, W. Meczynski, J. Styczen, J. Grebosz, M. Lach, A. Maj, M. Zieblinski, N. Kintz, J.C. Merdinger, N. Schulz, J.P. Vivien, A. Bracco, J.L. Pedroza, M.B. Smith, K.M. Spohr, Proceedings published in **Acta Phys. Polonica B 32 (2001) 747**.

2001

D28) *Structure of N=Z nuclei from studies with GASP and EUROBALL*
S. Lunardi
Int. Conf. High Spin Physics 2001, Warsaw (Poland), February 2001
Proceedings published in **Acta Phys. Pol. B 32 (2001) 2403**.

D29) *First evidence for the wobbling mode in a triaxial superdeformed odd-A nucleus*
Hamamoto et al.,
Int. Conf. High Spin Physics 2001, Warsaw (Poland), February 2001
Proceedings published in **Acta Phys. Pol. B 32 (2001) 2545**.

D30) *Search for Magnetic Rotation in the A ~ 140 Region*
T. Rzaca Urban,
Int. Conf. High Spin Physics 2001, Warsaw (Poland), February 2001
Proceedings published in **Acta Phys. Pol. B 32 (2001) 2645**.

D31) *Spectroscopy of Superdeformed Pb Isotopes*
H. Hübel,
Int. Conf. High Spin Physics 2001, Warsaw (Poland), February 2001
Proceedings published in **Acta Phys. Pol. B 32 (2001) 2673**.

D32) *Nuclear Structure Physics with large gamma-arrays*
S. Lunardi
International Nuclear Physics Conference, INPC2001, Berkeley (USA), July 2001

D33) *Collectivity and single particle effects in medium-light nuclei*
S. M. Lenzi
Symposium on Nuclear Structure Physics, Göttingen (Germany), March 2001

D34) *Medium heavy nuclei with N=Z and Isospin symmetry*
P. G. Bizzeti
Symposium on Nuclear Structure Physics, Göttingen (Germany), March 2001

D35) *Towards far from stability with large Ge-arrays*
G. de Angelis
7th Internationa Spring Seminar on Nuclear Physics, Maiori (Italy), May 2001

D36) *Quantum tunneling in superdeformed ^{143}Eu*
S. Leoni
7th Internationa Spring Seminar on Nuclear Physics, Maiori (Italy), May 2001

D37)
R. Chapman
3rd Int. Balkan workshop on applied physics, Targoviste (Romania), June 2001

D38)
M. Bentley
Int Conf. on Symmetires and Spins, Prague (Czech Republique), July 2001

D39) *The spectroscopy of fission fragments using fission sources at large γ-ray arrays*
J. Durell
Workshop on Nuclear Spectroscopy and Nuclear Astrophysics, Rossendorf (Germany), 2000

D40) *The structure and spectroscopy of neutron rich nuclei*
J. Durell
Int. Conf. on Exotic Nuclei and Masses, ENAM 2001, Hameenlinna (Finland), August 2001 to be published

D41) *The structure of intermediate mass neutron rich nuclei*
J. Durell
Int. Symp. on Radioactive Beam Research, Copenhagen (Denmark),

D42) *Nuclear properties and symetries in 1f$_{7/2}$ shell nuclei*
S. M. Lenzi
XIIIth Colloque Ganil, Belgodere, Corsica (France), September 2001

2002

D43)
M. Bentley
25th Int. Symp. On Nucl. Phys. Taxco, Mexico January 2002

D44) *Highlights from the physics with Euroball*
W. Korten
NS2002 Legnaro Italy, September 2002

E) EUROBALL experiments

1997/98

A. T. Semple (Liverpool) et al.
"A study of the N=72 shell gap and i$_{13/2}$ intruder orbital occupation in the superdeformed mass A=130 region."

A. G. Smith (Manchester) et al.
"Measurements of g-factors in neutron-rich fission fragments."

A. Jungclaus (Göttingen) et al.
"RDTF g-factor measurement in the dipole yrast superdeformed band in ^{192}Hg."

A. Bracco (Milano) et al.
"Lifetime measurements and collectivity in ^{114}Te: From discrete rotational bands to the chaotic regime."

A. Atac (Uppsala) et al.
"Decay out and other aspects of superdeformation in ^{143}Eu."

B. Cederwall (Stockholm) et al.
"A study of superdeformation and search for superdeformed-normaldeformed linking transitions in ^{154}Er."

S. Lunardi (Padova) et al.
"Decay-out of the yrast superdeformed band in ^{144}Gd."

I. Wiedenhöver (Köln) et al.
"Collectivity of low-lying SD states and members of the ΔI=1 bands in ^{196}Pb"

G. Hagemann (NBI Copenhagen) et al.
"Tilted rotation in a triaxial SD well and ND residual interaction."

J. Simpson (Daresbury) et al.
"Spectroscopy in the unpaired regime of ^{161,162}Er."

C. M. Petrache (Padova) et al.
"Lifetime of the quasi-continuum in the highly-deformed minimum, shell structure and polarization effects in Nd nuclei."

R. Krücken (Berkeley) et al.
"Lifetimes of the low-spin termination of the superdeformed band in ^{135}Nd."

P.H. Regan (Surrey) et al.
"Investigation of the deformed oblate minimum in ^{74}Kr."

R. Broda, B. Fornal (Cracow) et al.
"Gamma-spectroscopy in neutron-rich sdf nuclei produced in deep-inelastic heavy-ion reactions."

G. de Angelis (Legnaro) et al.
"High spin and band crossing phenomena in the ^{64}Ge nucleus."

P.J. Dagnall (Manchester), J.F. Chemin (Bordeaux) et al.
"The investigation of SD states and their population in nuclei around ^{82}Sr."

J. Durell (Manchester), C. Theisen (Saclay) et al.
"Gamma-ray studies of the fission of ^{238}U induced by ^{12}C: Spectroscopy and fission dynamics."

S. M. Lenzi (Padova) et al.
"High spin states in ^{48}Cr."

Zs. Podolyak (Legnaro) et al.
"Lifetime measurement for a three octupole-phonon state in ^{148}Gd."

J. Eberth, S. Skoda (Köln) et al.
"Investigation of prolate-oblate shape mixing in the N=Z+1 nucleus ^{73}Kr: A precise measurement of transition probabilities."

P.A. Butler (Liverpool) et al.
"Fission decay of exotic shapes in actinide nuclei."

G. Viesti (Padova) et al.
"Search for hyperdeformation in nuclei around ^{152}Dy with the ^{37}Cl+^{120}Sn reaction."

R.M. Lieder (Jülich) et al.
"Search for coexistence of highly and superdeformed shapes in ^{142}Gd."

B. Herskind (NBI Copenhagen) et al.
"Search for hyperdeformation in $^{168-170}$Hf by use of the very cold near symmetric reaction ^{76}Ge + ^{96}Zr → ^{172}Hf."

Th. Kröll (Padova) et al.
"Investigation of SD states in ^{236}U populated by a transfer reaction."

M.G. Porquet (CSNSM Orsay) et al.
"Fission induced by heavy-ions: pairing correlations in highly-deformed neutron-rich A~100 nuclei."

A. Lopez-Martens (Strasbourg) et al.
"The intensity distribution of primary SD decay-out lines in ^{194}Pb."

D. R. Page (Liverpool) et al.
"In beam spectroscopy near the neutron drip line."

D. Rudolph (Lund) et al.
"Spectroscopy of 2nd well proton emitters in the mass A~60 region."

F. Dönau (Rossendorf) et al.
"Search for proton-neutron pairing in nuclei with mass number A~70."

C. Fahlander (Lund), L. O. Norlin (Stockolm) et al.
"Search for excited states in ^{103}Sn."

A. Bracco (Milano) et al.
"Search for gamma decay of the giant dipole resonance in superdeformed nuclei."

J. Nyberg (Uppsala) et al.
"High spin studies of nuclei around doubly magic ^{40}Ca."

S. Skoda, J. Eberth (Köln) et al.
"Investigation of T=0 coupling in the N=Z nuclei ^{62}Ga, ^{66}As and ^{68}Se – a survey of the deformation dependence."

160

B. Gebauer (Berlin) et al.
 "Search for gamma-ray transitions in hyperdeformed 4N-nuclei with A=36-44."

S.M. Lenzi (Padova) et al.
 "High spin states in neutron deficient f $_{7/2}$ nuclei."

P.H. Regan (Surrey), R. Wadsworth (York)
 "Investigation of pairing correlations and collectivity in the N=Z nucleus ^{80}Zr."

1999

G. Duchêne (Strasbourg) et al.
 "Decay-out mechanism of superdeformed bands in ^{151}Tb."

J.P. Vivien (Strasbourg) et al.
 "Staggering effects in N=85 isotones : the ^{150}Tb case."

P. Nolan (Liverpool) et al.
"Superdeformation in ^{131,132}Ce : a search for discrete decay paths."

R. Wadsworth (York) et al.
"Competition between strongly deformed and smoothly terminating band structure in ^{127}La."

A. Astier (IPN Lyon) et al.
"Neutron quenching factor g_{eff} / g_{free} measurement in the SD ^{197}Pb nucleus."

A.G. Smith (Manchester) et al.
"Lifetime measurement in neutron rich fission fragments using a differential Plunger."

G.B. Hagemann (NBI Copenhagen) et al.
"Search for the wobbling mode built on triaxial superdeformed shapes."

A. Korichi (CSNSM Orsay) et al.
"Study of the superdeformed octupole vibrational structures in ^{190}Hg."

J. Simpson (Daresbury) et al.
"Nuclear Spectroscopy at the high spin limit in 'normal-deformed nuclei': Observation of discrete states in ^{159,160}Er at I > 60h and E_x > 30 MeV."

P. Twin (Liverpool) et al.
"Superdeformed ^{152}Dy: collective excitations and decay-out."

R. Chapman (Paisley) et al.
"A study of neutron-rich nuclei using deep-inelastic reactions."

H. Hübel (Bonn), F. Azaiez (IPN Orsay) et al.
"The level scheme of superdeformed ^{196}Pb - Search for linking transitions."

P. Bednarczyk (Cracow - Strasbourg) et al.
"A search for a band termination in the deformed odd-A $f_{7/2}$ nuclei: ^{45}Sc and ^{45}Ti."

P.A. Butler (Liverpool) et al.
"Octupole structure of ^{224}U."

2000

J. Styczen (Cracow) et al.
"Gamma-ray spectroscopy of the transactinide nucleus ^{252}Fm."

B. Gall (Strasbourg) et al.
"Octupole deformation studies : a step towards spectroscopy of high-Z nuclei."

E. Mergel (Bonn) et al.
"Conversion-electron spectroscopy in the decay of superdeformed ^{194}Pb."

G. Lo Bianco (Camerino) et al.
"Conversion electron spectroscopy in the decay-out region of ^{136}Nd."

A. Dewald (Köln) et al.
"Investigation of isospin forbidden E1 transitions in ^{46}V."

M.G. Porquet (CSNSM Orsay) et al.
"High-spin structures of neutron-rich nuclei around the closed shells, Z=40, Z=50, N=50 and N=82 from heavy-ion induced fission."

A. Bracco (Milano) et al.
"Do K-selection rule persist in thermally excited nuclei?"

A.G. Smith (Manchester) et al.
"Lifetime measurements in neutron-rich fission fragments using a differential plunger."

G. Viesti (Padova) et al.
"Exploring the emission barrier in excited nuclei."

E. Farnea (Valencia), A. Dewald (Köln) et al.
"Isospin mixing and forbidden E1 decays in the ^{64}Ge nucleus."

A.Dewald (Köln) et al.
"Investigation of magnetic rotation and study of anomalous collective effects in the quasi gamma-bands of transitional nuclei around A=130."

2001

R. Wadsworth (York) et al.
"Study of band structure, alignments and pairing correlations in the N=Z nucleus ^{76}Sr."

B. Cederwall (Stockholm) et al.
"Superdeformation, shell structure and neutron-proton correlations at A=90, N=Z."

C.D. O'Leary (Liverpool), M.A. Bentley (Staffordshire) et al.
"A=46 isobaric analogue states: Mirror symmetry and cross-conjugate symmetry in light $f_{7/2}$ proton rich nuclei."

M. Weiszflog (Uppsala) et al.
"Excitations and E2 polarizations of the ^{100}Sn core studied through the excited states of ^{97}Ag."

S.M. Lenzi (Padova) et al.
"High spin structure, exotic shapes and isospin symmetry in sd-shell nuclei near ^{32}S."

J. Eberth (Köln) et al.
"Study of the oblate deformed $g_{9/2}$ band in the N=Z+1 nucleus ^{69}Se : Absence of blocking effect in odd-odd N=Z nuclei."

G. de Angelis (Legnaro) et al.
"Search for an experimental signature of the pn correlations."

M. Gorska (GSI Darmstadt) et al.
"Prompt and delayed spectroscopy in ^{98}Cd."

J. Nyberg (Uppsala) et al.
"Excited states above the 6^+ isomer in ^{102}Sn."

G. Sletten (NBI Copenhagen) et al.
"Erosion of the K-quantum number in ^{180}Ta via intermediate states."

R. Schwengner (Rossendorf) et al.
"Search for magnetic dipole bands in ^{134}Pr."

H. Hübel (Bonn) et al.
"Triaxial superdeformation and hyperdeformation in Hf isotopes populated in a cold fusion reaction."

B. Herskind (NBI Copenhagen) et al.
"Search for hyperdeformation and Jacobi shapes and a study of fission limits in heavy Xe nuclei."

G.B. Hagemann (NBI Copenhagen) et al.
"Search for the wobbling mode built on triaxial superdeformed shapes."

J.F. Smith (Manchester) et al.
"High spin study of ^{222}Th: evolution of octupole deformation and a search for highly-deformed structures approaching 30$\hbar$."

R. Wadsworth (York) et al.
"Investigation of chiral effects in ^{134}Pr."

R.M. Lieder (Jülich) et al.
"Investigation of lifetimes of dipole bands in ^{142}Gd with EUROBALL using DSAM."

P.A. Butler (Liverpool) et al.
"Search for hyperdeformation in U isotopes."

B.M. Nyako (Debrecen) et al.
"Search for hyperdeformation in ^{168}Hf."

A. Astier (IPN Lyon), H.Hübel (Bonn) et al.
"Search for excited superdeformed bands in ^{197}Bi and probe of quenching of g$_{eff}$ in the second well."

G. Duchêne (Strasbourg), P. Twin (Liverpool) et al.
"Decay-out mechanism of superdeformed bands in ^{151}Tb; comparison to ^{152}Dy identical band decay-out. Triaxial bands at high-spin."

2002

G.B. Hagemann (NBI Copenhagen) et al.
"Triaxial superdeformation and the wobbling mode in ^{164,165}Lu."

A. Maj (Cracow), A. Bracco (Milano) et al.
"Search for the Jacobi transition and fission limits in light nuclei."

A. Maj (Cracow), S. Leoni (Milano) et al.
"Gamma-ray continuum in ^{196}Pb : E1 feeding of SD bands, GDR gamma-decay and rotational damping."

B. Herskind (NBI Copenhagen), B. Million (Milano) et al.
"A study of hyperdeformation and Jacobi shapes in ^{126}Ba."

S. Lenzi (Padova) et al.
"Beyond band termination in ^{48}Cr looking for T=0 correlations."

G. Rainowski (Liverpool) et al.
"Search for magnetic dipole bands and chiral twin bands."

G.B. Hagemann (NBI Copenhagen) et al.
"Triaxial superdeformation, the wobbling mode and very high spin states in ^{161,162}Lu."

H. Hübel (Bonn), B. Herskind (NBI Copenhagen) et al.
"Nuclear shapes at the highest spins in Nd nuclei."

P. Fallon (Berkeley), K. Lagergren (Stockholm) et al.
"A study of SD and search for SD and ND linking transitions in ^{154}Er."

A. Lopez-Martens (CSNSM Orsay), T. Dossing (NBI Copenhagen) et al.
"Complete spectroscopy in the second well of ^{192}Hg."

P. Nolan (Liverpool) et al.
"SD in ^{131,132}Ce, search for band termination and discrete decay paths."

J. Simpson (Daresbury) et al.
"The role of pairing correlations and shape competition at the highest spins :
Spectroscopy of the odd Z,N=90 ^{159}Tm."

G. Smith (Manchester) et al.
"Differential plunger lifetime measurement in neutron rich fission fragment using a gas-filled detector."

W. von Oertzen (Berlin) et al.
"Search for rare γ-decays in the strongly deformed light neutron rich isotopes $^{10\text{-}12}$Be and $^{13\text{-}16}$C."

Ch. Beck (Strasbourg), W. von Oertzen (Berlin) et al.
"Search for gamma-ray transition from SD and HD states in ^{24}Mg in the ^{24}Mg on ^{12}C reaction."

J. Dobacewski (Warsaw), J.P. Vivien (Strasbourg) et al.
"Band termination, band crossing and position of the $\nu h_{11/2}$ orbital in the SD bands in ^{66}Ga."

W. Meczynski (Cracow) et al.
"Gamma ray spectroscopy of the transactinide nucleus ^{252}Fm."

O. Stezowski (Lyon), J. Styczen (Cracow) et al.
"Search for Superdeformation beyond Z=82."

O. Dorvaux (Strasbourg), M.G. Porquet (CSNSM Orsay) et al.
"Bimodal Fission of Th isotopes."

B. Herskind (NBI Copenhagen) et al.
"An extensive search of hyperdeformed bands in ^{126}Ba."

2003

P. Joshi (York) et al.
"Search for chirality in ^{106}Rh."

G. de Angelis (Legnaro) et al.
"Check for chirality of nuclear rotation in ^{134}Pr via lifetime measurements."

C. Ur (Padova) et al.
"Competing T=1 and T=0 pairing correlations in the odd-odd N=Z ^{78}Y nucleus."

A. Gadea (Legnaro) et al.
"In beam spectroscopy of the T_z=-1 ^{54}Ni nucleus."

B. Cederwall (Stockholm) et al.
"Search for a new coupling scheme in ^{96}Cd."

M. Palacz (Warsaw), J. Nyberg (Uppsala) et al.
"Direct measurement of proton neutron matrix element with respect to ^{100}Sn by studying excited states in ^{100}In."

B. Gebauer (Berlin) et al.
"Search for gamma-ray transition in the HD 4N-nuclei with A=36-46"

X. Liang (Paisley), F. Haas (Strasbourg) et al.
"Search for excited states in the neutron-rich Na and Mg nuclei around N=20 using deep inelastic processes."

References

References

In the list of references below those related to data from experiments carried out using the EUROBALL array are marked with an asterisk (*).

[1]*   J. Simpson, Z. Phys. A358 (1997) 139

[2]   GASP Collaboration Report, INFN/BE-90/11 (1990)

C. Rossi-Alvarez, Nucl. Phys. News 3 (1993) 10; D. Bazzacco, Proc. Workshop on Large γ-ray Detector Arrays, Chalk River, Canada 1992, AECL-10613, p. 376

[3]   C.W. Beausang, S. A. Forbes, P. Fallon, P. J. Nolan, P. J. Twin, J. N. Mo J. C. Lisle, M.A. Bentley, J. Simpson, F. A. Beck, D. Curien, G. deFrance, G. Duchêne, D. Popescu, Nucl. Instr. Meth. in Phys. Res. A313 (1992) 37;

F.A. Beck, Prog. Part. Nucl. Phys. 28 (1992) 443;

P.J. Nolan, Nucl. Phys. A520 (1990) 657c;

G. de France and J. Simpson, Nuclear Physics News 7 (1997) 12

[4]   E. Farnea, G. de Angelis, M. De Poli, D. De Acuna, A. Gadea, D.R. Napoli, P. Spolaore, A. Buscemi, R. Zanon, R. Isocrate, D. Bazzacco, C. Rossi Alvarez, P. Pavan, A.M. Bizzeti-Sona, P.G. Bizzeti, Nucl. Inst. and Meth. in Phys. Res. A400 (1997) 87

[5]*   A. Gadea, E.Farnea, G.de Angelis, R. Isocrate, A. Buscemi, P. Pavan, A. Algora, N. Marginean, T. Martinez, D. R. Napoli, M.De Poli, P.Spolaore, D.Bazzacco, F. Brandolini, S.M. Lenzi, S. Lunardi, R. Menegazzo, C.Rossi Alvarez, P. G. Bizzeti, A.M.Bizzeti-Sona, LNL Annual Report 1999, p. 151, INFN (REP) 160/00.

[6]*   J.N. Scheurer, M. Aiche, M.M. Aleonard, G. Barreau, F. Bourgine, D. Boivin, D. Cabaussel, J.F. Chemin, T.P. Doan, J.P. Goudour, M. Harston, A. Brondi, G. La Rana, R. Moro, E. Vardaci, D. Curien, Nucl. Instr. and Meth. in Phys. Res. A385 (1997) 501;

M. Aiche, M. M. Aléonard, B. Balauge, G. Barreau, F. Bourgine, D. Cabaussel, J. F. Chemin, C. Diarra, J.P. Goudour, M.Harston, H. Rasolofo, J. N. Scheurer, A. Brondi, G. La Rana, R. Moro, E. Vardaci and D. Curien, Nucl. Instr. and Meth. in Phys. Res. A391 (1997) 329

[7]*   Ö. Skeppstedt, H.A. Roth, L. Lindström, R. Wadsworth, I. Hibbert, N. Kelsall, D. Jenkins, H. Grawe, M. Górska, M. Moszyński, Z. Sujkowski, D. Wolski, M. Kapusta, M. Hellström, S. Kalogeropoulos, D. Oner, A. Johnson, J. Cederkäll, W. Klamra, J. Nyberg, M. Weiszflog, J. Kay, R. Griffiths, J. Garcés Narro, C. Pearson, J. Eberth,

Nucl. Inst. and Meth. in Phys. Res. A421 (1999) 531; see also http://www.nsg.tsl.uu.se/nwall/

[8]   K. Spohr, W. Meczynski, J.B. Fitzgerald, D.B. Fossan, M. Gorska, H. Grawe, J. Grebosz, J. Heese, M. Janicki, M. Lach, K.H. Maier, A. Maj, J.C. Merdinger, M. Palacz, M. Rejmund, R. Schubart, J. Styczen, Acta Phys. Pol. B26 (1995) 297

[9]*   Ch.Theisen C. Gautherin, M. Houry, W. Korten, Y. Le Coz, R. Lucas, G. Barreau, T.P. Doan, G. Belier, V. Meot, Th. Ethvignot, B. Cahan, A. Le Cougie, X. Coppalani, B. Delaitre, Ph. Le Bourlout, Ph. Legou, O. Maillard, G. Durand, A. Bouillac, G. Carles, N. Karkour, D. Linget, I. Merlin, V.F.E. Pucknell, G. Smith, Conference Proceedings of the Second International Workshop on Nuclear Fission and Fission-Product Spectroscopy, AIP Conference Proceedings 447 (1998) 143

[10]   S. Thummerer, B. Gebauer, W. Von Oertzen, M. Wilpert, Nuovo Cim. 111A (1998) 1077

[11]   A. Maj, J.J. Gaardhoje, A. Atac, S. Mitarai, J. Nyberg, A. Virtanen, A. Bracco, F. Camera, B. Million, M. Pignanelli, Nucl. Phys. A571 (1994) 185

[12]   P.J. Nolan, A. Kirwan, D.L.G. Love, A.H. Nelson, D.J. Unwin, and P.J. Twin, J. Phys. G11 (1985) L17

[13]   P.J. Twin, B.M. Nyako, A.H. Nelson, J. Simpson, M.A. Bentley, H.W. Cranmer-Gordon, P.D. Forsyth, D. Howe, A.R. Mokhtar, J.D. Morrison, J.F. Sharpey-Schafer and G. Sletten, Phys. Rev. Lett. 57 (1986) 811

[14] Table of Superdeformed Nuclear bands and Fission Isomers - Second Edition - By P.B. Singh, R.B. Firestone, and S.Y.F. Chu, Nucl.Data Sheets 97 (2002) 241

[15] Th. Byrski, F.A. Beck, D. Curien, C. Schuck, P. Fallon, A. Alderson, I. Ali, M.A. Bentley, A.M. Bruce, P.D. Forsyth, D. Howe, J.W. Roberts, J.F. Sharpey-Schafer, G. Smith and P.J. Twin, Phys. Rev. Lett. 64 (1990) 1650

[16] S. Flibotte, H.R. Andrews, G.C. Ball, C.W. Beausang, F.A. Beck, G. Belier, T. Byrski, D. Curien, P.J. Dagnall, G. de France, D. Disdier, G. Duchene, Ch. Finck, B. Haas, G. Hackman, D.S. Haslip, V.P. Janzen, B. Kharraja, J.C. Lisle, J.C. Merdinger, S.M. Mullins, W. Nazarewicz, D.C. Radford, V. Rauch, H. Savajols, J. Styczen, Ch. Theisen, P.J. Twin, J.P. Vivien, J.C. Waddington, D. Ward, K. Zuber and S. Aberg,

Phys. Rev. Lett. 71 (1993) 4299

[17] A. Lopez-Martens, F. Hannachi, A. Korichi, C. Schuck, E. Gueorguieva, Ch. Vieu, B. Haas, R. Lucas, A. Astier, G. Baldsiefen, M. Carpenter, G. de France, R. Duffait, L. Ducroux, Y. Le Coz, Ch. Finck, A. Görgen, H. Hübel, T.L. Khoo, T. Lauritsen, M. Meyer, D. Prevost, N. Redon, C. Rigollet, H. Savajols, J.F. Sharpey-Schafer, O. Stezowski, Ch. Theisen, U. van Severen, J.P. Vivien and A.N. Wilson, Phys. Lett. B380 (1996) 18

[18] A. Bohr and B. Mottelson, Nuclear Structure (Benjamin, New York, 1975), Vol. 2.

[19] I. Ragnarsson and S. Åberg, Phys. Lett. B180 (1986) 191

[20]* K. Lagergren, B. Cederwall, T. Bäck, R. Wyss, E. Ideguchi, A. Johnson, A. Atac, A. Axelsson, F. Azaiez, A. Bracco, J. Cederkäll, Zs. Dombradi, C. Fahlander, A. Gadea, B. Million, C.M. Petrache, C. Rossi-Alvarez, J.A. Sampson, D. Sohlar and M. Weiszflog, Phys. Rev. Lett. 87 (2001) 022502

[21] D.G. Sarantites, D.R. La Fosse, M. Devlin, F. Lerma, V.Q. Wood, J.X. Saladin, D.F. Winchell, C. Baktash, C.-H. Yu, P. Fallon, I.Y. Lee, A.O. Macchiavelli, R.W. MacLeod, A.V. Afanasjev and I. Ragnarsson, Phys. Rev. C57 (1998) R1

[22] R. Wadsworth and P. Nolan, Rep. Prog. Phys. 65 (2002) 1079

[23] I. Ragnarsson, Nucl. Phys. A610 (1990) 67c

[24]* A. Axelsson, J. Nyberg, A. Atac, M.H. Bergstrom, B. Herskind, G. de Angelis, T. Back, D. Bazzacco, A. Bracco, F. Camera, B. Cederwall, C. Fahlander, J.H. Huijnen, S. Lunardi, B. Million, D.R. Napoli, J. Persson, M. Piiparinen, C. Rossi Alvarez, G. Sletten, P.G. Varmette and M.Weiszflog, Eur. Phys. J. A6 (1999) 175

[25] G. Hackman, T.L. Khoo, M.P. Carpenter, T. Lauritsen, A. Lopez-Martens, I.J. Calderin, R.V.F. Janssens, D. Ackermann, I. Ahmad, S. Agarwala, D.J. Blumenthal, S.M. Fischer, D. Nisius, P. Reiter, J. Young, H. Amro, E.F. Moore, F. Hannachi, A. Korichi, I.Y. Lee, A.O. Macchiavelli, T. Døssing, and T. Nakatsukasa, Phys. Rev. Lett. 79 (1997) 4100.

[26] H. Savajols, A. Korichi, D. Ward, D. Appelbe, G.C. Ball, C.W. Beausang, F.A. Beck, T. Byrski, D. Curien, P. Dagnall, G. de France, D. Disdier, G. Duchene, S. Erturk, Ch. Finck, S. Flibotte, B. Gall, A. Galindo-Uribarri, B. Haas, G. Hackman, V.P. Janzen, B. Kharraja, J.C. Lisle, J.C. Merdinger, S.M. Mullins, S. Pilotte, D. Prevost, D.C. Radford, V. Rauch, C. Rigollet, D. Smalley, M.B. Smith, O. Stezowski, J. Styczen, Ch. Theisen, P.J. Twin, J.P. Vivien, J.C. Waddington, K. Zuber and I. Ragnarsson, Phys. Rev. Lett. 76 (1996) 4480

[27] E.F. Jones, P.M. Gore, J.H. Hamilton, A.V. Ramayya, A.P. deLima, R.S. Dodder, J.Kormicki, J.K. Hwang, C.J. Beyer, X.Q. Zhang, S.J. Zhu, G.M. Ter-Akopian, Yu.Ts. Oganessian, A.V. Daniel, J.O. Rasmussen, I.Y. Lee, J.D. Cole, M.W. Drigert, W.-C. Ma and GANDS95 Collaboration, Nucl. Phys. A682 (2001) 79c

[28]* N. Kintz, Ph.D Thesis, University of Strasbourg, IReS 00-09, N. 3555, 2000

[29] I. Hamamoto and B.R. Mottelson, Phys. Lett. B333 (1994) 294

[30] L.A. Bernstein, J.R. Hughes, J.A. Becker, L.P. Farris, E.A. Henry, S.J. Asztalos, B.Cederwall, R.M. Clark, M.A. Deleplanque, R.M. Diamond, P. Fallon, I.Y. Lee, A.O. Macchiavelli, F.S. Stephens, J.A. Cizewski and W. Younes, Phys. Rev. C52 (1995) R1171

[31] A. Afanasjev and P. Ring, Nucl. Phys. A 654 (1999) 647c

[32] J. Meyer, P. Bonche, M.S. Weiss, J. Dobaczewski, H. Flocard and P.-H.Heenen, Nucl. Phys. A588 (1995) 597

[33]* A. Korichi, A.N. Wilson, F. Hannachi, A. Lopez-Martens, M. Rejmund, C. Schuck, Ch. Vieu, S. Chmel, A. Görgen, H. Hübel, D. Rossbach, G. Schönwasser, M. Bergstrom, B.M. Nyako, J. Timar, D. Bazzacco, S. Lunardi, C. Rossi-Alvarez, P. Bednarczyk, N. Kintz, S. Naguleswaran, A. Astier, D.M. Cullen, J.F. Sharpey-Schafer, T. Lauritsen and R. Wadsworth, Phys. Rev. Lett. 86 (2001) 2746

[34]* D. Rossbach, A. Görgen, H. Hübel, E. Mergel, G. Schönwasser, A.N. Wilson, F. Azaiez, A. Astier, D. Bazzacco, M. Bergstrom, C. Bourgeois, N. Buforn, F. Hannachi, K. Hauschild, A. Korichi, W. Korten, T. Kröll, A. Lopez-Martens, R. Lucas, H.J. Maier, N. Redon, P. Reiter, C. Rossi-Alvarez, O. Stezowski and P. Thirolf, Phys. Lett. B513 (2001) 9

[35]* D. Rossbach, A. Görgen, H. Hübel, E. Mergel, G. Schönwasser, F. Azaiez, C. Bourgeois, F. Hannachi, A. Korichi, A. Lopez-Martens, A. Astier, N. Buforn, N. Redon, O. Stezowski, D. Bazzacco, T. Kröll, C. Rossi-Alvarez, K. Hauschild, W. Korten, R. Lucas, H.J. Maier, P. Reiter, P.G. Thirolf, Phys. Rev. C66 (2002) 024316

[36]* A. Prevost, N. Buforn, A. Astier, R. Duffait, M. Meyer, S. Perries, N. Redon, O. Stezowski, A. Bauchet, I. Deloncle, M.G. Porquet, A. Görgen, H. Hübel, E. Mergel, S. Neumann, D. Rossbach, N. Nenoff, G. Schönwasser, A.N. Wilson, R. Lucas, F.A. Beck, D. Curien, G. Duchene, B.J.P. Gall, N. Kintz, J.P. Vivien and D.M. Cullen, Eur. Phys. J. A10 (2001) 13

[37] B.Gall, P.Bonche, J.Dobaczewski, H.Flocard and P.-H.Heenen, Z. Phys. A348 (1994) 183 and private communication

[38]* N. Buforn, A. Astier, R. Duffait, M. Meyer, S. Perries, A. Prevost, N. Redon, O. Stezowski, A. Görgen, H. Hübel, E. Mergel, S. Neumann, D. Rossbach, N. Nenoff, G. Schönwasser, A. Bauchet, I. Deloncle, M.G. Porquet, A.N. Wilson, R. Lucas, F.A. Beck, D. Curien, G. Duchene, B.J.P. Gall, N. Kintz, J.P. Vivien and D.M. Cullen, Eur. Phys. J. A9 (2000) 29

N. Buforn, Ph.D Thesis, University of Lyon, LYCEN – T 2001-15, N 15-2001, 2001

[39] S. Perries, D. Samsoen, J. Meyer, M. Meyer and P. Quentin, Phys. Rev. C55 (1997) 1797

[40] J.N. Wilson, P.J. Nolan, C.W. Beausang, R.M. Clark, S.A. Forbes, A. Gizon, J. Gizon, K. Hauschild, I.M. Hibbert, E.S. Paul, D. Santos, A.T. Semple, J. Simpson, R. Wadsworth, Phys. Rev. Lett. 74 (1995) 1950

[41] J. Dudek, T. Werner and L.L. Riedinger, Phys. Lett. B211 (1988) 252

[42] R.R. Chasman, Phys. Lett. B302 (1993) 134

[43] T.R. Werner and J. Dudek, At. Data and Nucl. Data Tables 50 (1992) 179

[44] S. Åberg, Nucl. Phys. A557 (1993) 17c

[45] R.R. Chasman, Phys. Lett. B364 (1995) 137

[46] A. Fitzpatrick, S.Y. Araddad, R. Chapman, J. Copnell, F. Liden, J.C. Lisle, A.G. Smith, J.P. Sweeney, D.M. Thompson, W. Urban, S.J. Warburton, J. Simpson, C.W. Beausang, J.F. Sharpey-Schafer, S.J. Freeman, S. Leoni, J. Wrzesinski, Nucl. Phys. A582 (1995) 335

[47] A. Galindo-Uribarri, H.R. Andrews, G.C. Ball, T.E. Drake, V.P. Janzen, J.A. Kuehner, S.M. Mullins, L. Persson, D. Prevost, D.C. Radford, J.C. Waddington, D. Ward, R. Wyss, Phys. Rev. Lett. 71 (1993) 231

[48] G. Viesti, M. Lunardon, D. Bazzacco, R. Burch, D. Fabris, S. Lunardi, N. Medina, G. Nebbia, C. Rossi Alvarez, G. de Angelis, M. De Poli, E. Fioretto, G. Prete, J. Rico, P. Spolaore, G. Vedovato, A. Brondi, G. La Rana, R. Moro, E. Vardaci,

Phys. Rev. C51 (1995) 2385 ;

M. Lunardon, N.H. Medina, G. Viesti, D. Bazzacco, D. Fabris, S. Lunardi, G. Nebbia, C. Rossi Alvarez, G. de Angelis, M. Cinausero, D. De Acuna, M. De Poli, E. Farnea, E. Fioretto, G. Prete, G. Maron, D.R. Napoli, Phys. Rev. C56 (1997) 257

[49] D. R. LaFosse, D.G. Sarantites, C. Baktash, P.-F. Hua, B. Cederwall, P. Fallon, C.J. Gross, H.-Q. Jin, M. Korolija, I.Y. Lee, A.O. Macchiavelli, M.R. Maier, W. Rathbun, D.W. Stracener, T.R.Werner, Phys. Rev. Lett. 74 (1995) 5186

[50] D. R. LaFosse, D.G. Sarantites, C. Baktash, S. Asztalos, M.J. Brinkman, B. Cederwall, R.M. Clark, M. Devlin, P. Fallon, C.J. Gross, H.-Q. Jin, I.Y. Lee, F. Lerma, A.O. Macchiavelli, R. MacLeod, D. Rudolph, D.W. Stracener, C.-H. Yu,

Phys. Rev. C54 (1996) 1585

[51] J.N. Wilson, S.J. Asztalos, R.A. Austin, B. Busse, R.M. Clark, M.A. Deleplanque, R.M. Diamond, P. Fallon, S. Flibotte, G. Gervais, D.S. Haslip, I.Y. Lee, R. Kruecken, A.O. Macchiavelli, R.W. MacLeod, J.M. Nieminen, G.J. Schmid, F.S. Stephens, O. Stezowski, C.E. Svensson, K. Vetter, J.C. Waddington, Phys. Rev. C56 (1997) 2502

[52]* V. Rizzi, G. Viesti, D. Bazzacco, A. Algora-Pineda, D. Appelbe, G. de Angelis, N. Belcari, M. Cinausero, M. De Poli, T.E. Drake, A. Gadea, A. Galindo-Uribarri, N. Gelli, D .Fabris, E. Farnea, E. Fioretto, W. Krolas, T. Kroll, F. Lucarelli, S. Lunardi, M. Lunardon, T. Martinez, R. Menegazzo, B.K. Nayak, G. Nebbia, D.R. Napoli, B. Nyako, C. Petrache, Zs. Podolyak, G. Prete, C. Rossi Alvarez, A. Samant, P. Spolaore, C. Ur, K. Zuber, Eur. Phys. J. A7 (2000) 299

[53] A.J. Sierk, Phys. Rev. C33 (1986) 2039

[54] J.M. Nieminen, S. Flibotte, G. Gervais, D.S. Haslip, I.Y. Lee, A.O. Macchiavelli, R.W. MacLeod, O. Stezowski, C.E. Svensson, J.C. Waddington, J.N. Wilson,

Phys. Rev. C58 (1998) R1

[55] P. Reiter, T.L. Khoo, C.J. Lister, D. Seweryniak, I. Ahmad, M. Alcorta, M.P. Carpenter, J.A. Cizewski, C.N. Davids, G. Gervais, J.P. Greene, W.F. Henning, R.V.F. Janssens, T. Lauritsen, S. Siem, A.A. Sonzogni, D. Sullivan, J. Uusitalo, I. Wiedenhöver, N. Amzal, P.A. Butler, A.J. Chewter, K.Y. Ding, N. Fotiades, J.D. Fox, P.T. Greenlees, R.-D. Herzberg, G.D. Jones, W. Korten, M. Leino, K. Vetter, Phys. Rev. Lett. 82 (1999) 509

[56] J.N. Wilson, B. Herskind, Nucl. Inst. Meth. in Phys. Res. A455 (2000) 612

[57] F. Frauendorf and J. Meng, Nucl. Phys. A617 (1997) 131

[58]* S.W. Ødegård, G.B. Hagemann, D.R. Jensen, M.Bergström, B. Herskind, G. Sletten, S. Törmänen, J.N. Wilson, P.O. Tjøm, I. Hamamoto, K. Spohr, H. Hübel, A. Görgen, G. Schönwasser, A. Bracco, S. Leoni, A. Maj, C.M. Petrache, P. Bednarczyk and D. Curien, Phys. Rev. Lett. 86 (2001) 5866

[59]* D.R. Jensen, G.B. Hagemann, I. Hamamoto, S.W. Ødegård, M. Bergström, B. Herskind, G. Sletten, S. Törmänen, J.N. Wilson, P.O. Tjøm, K. Spohr, H. Hübel, A. Görgen, G. Schönwasser, A. Bracco, S. Leoni, A. Maj, C.M. Petrache, P. Bednarczyk, D. Curien, Nucl. Phys. A703 (2002) 3

[60]* D.R. Jensen, G.B. Hagemann, I. Hamamoto, S.W. Ødegård, B. Herskind, G. Sletten, J.N. Wilson, K. Spohr, H. Hübel, P. Bringel, A. Neußer, G. Schönwasser, A.K. Singh, W.C. Ma, H. Amro, A. Bracco, S. Leoni, G. Benzoni, A. Maj, C.M. Petrache, G. Lo Bianco, P. Bednarczyk, D. Curien, Phys. Rev. Lett. 89 (2002) 142503

[61] I. Hamamoto, Phys. Rev. C65 (2002) 044305

[62] S. Åberg, Nucl. Phys. A520 (1990) 35c and references therein

[63] I. Ragnarsson, Phys. Rev. Lett. 62 (1989) 2084

[64] H. Schnack-Petersen, R. Bengtsson, R.A. Bark, P. Bosetti, A. Brockstedt, H. Carlsson, L.P. Ekström, G.B. Hagemann, B. Herskind, F. Ingebretsen, H.J. Jensen, S. Leoni, A. Nordlund, H. Ryde, P.O. Tjøm, and C.X. Yang, Nucl. Phys. A594 (1995) 175

[65] W. Schmitz, C.X. Yang, H. Hübel, A.P. Byrne, R. Müsseler, N. Singh, K.H. Maier, A. Kuhnert and R. Wyss, Nucl. Phys. A539 (1992) 112

[66] W. Schmitz, H. Hübel, C.X. Yang, G. Baldsiefen, U. Birkental, G. Fröhlingsdorf, D. Mehta, R. Müsseler, M. Neffgen, P. Willsau, J. Gascon, G.B. Hagemann, A. Maj, D. Müller, J. Nyberg, M. Piiparinen, A. Virtanen and R. Wyss, Phys. Lett. B303 (1993) 230

[67] T. Bengtsson, Nucl. Phys. A496 (1989) 56 and A512 (1990) 124

[68] R. Bengtsson, www.matfys.lth.se/˜ragnar/ultimate.html

[69] R. Bengtsson and H. Ryde, to be published

[70] H. Amro, P.G. Varmette. W.C. Ma, B. Herskind, G.B. Hagemann, R.V.F. Janssens, M. Bergström, A. Bracco, M. Carpenter, J. Domscheit, S. Frattini, D.J. Hartley, H. Hübel, T.L. Khoo, F. Kondev, T. Lauritsen, C.J. Lister, B. Million, S.W. Ødegård, R.B. Piercey, L.L. Riedinger, K.A. Schmidt, S. Siem, L. Wiedenhöver, J. N. Wilson and J.A. Winger, Phys. Lett. B506 (2001) 39

[71] P. Bringel, H. Hübel, H. Amro, M. Axiotis, D. Bazzacco, S. Bhattacharya, R. Bhownik, J. Domscheit, G.B. Hagemann, D.R. Jensen, Th. Kröll, S. Lunardi, D.R. Napoli, A. Neußer, S.C. Pancholi, C.M. Petrache, G. Schönwasser, A.K. Singh and C. Ur, Abstract to FNS2002 Berkeley July-August 2002, and Eur. Phys. J. A16 (2003) 155

[72]* J. Domscheit, B. Angenvoort, S. Törmänen, R.A. Bark, M. Bergström, A. Bracco, R. Chapman, D.M. Cullen, C. Fahlander, S. Frattini, A. Görgen, G.B. Hagemann, A. Harsmann, B. Herskind, H. Hübel, H.J. Jensen, S.L. King, S. Lenzi, D.R. Napoli, S.W. Ødegård, C. Petrache, H. Ryde, U.J. van Severen, G. Sletten, P.O. Tjøm, and C. Ur, Nucl. Phys. A660 (1999) 381

[73]* S. Törmänen, S.W. Ødegård, G.B. Hagemann, A. Harsmann, M. Bergström, R.A. Bark, B. Herskind, G. Sletten, P.O. Tjøm, A. Görgen, H. Hübel, B. Aengenvoort, U.J. van Severen, H. Ryde, C. Fahlander, D. Napoli, S. Lenzi, C. Petrache, C. Ur, H.J. Jensen, A. Bracco, S. Frattini, R. Chapman, D.M. Cullen, and S.L. King, Phys. Lett. B454 (1999) 8

[74]* G. Schönwasser, H. Hübel, G.B. Hagemann, P. Bednarczyk, G. Benzoni, G. Lo Bianco, A. Bracco, P. Bringel, R. Chapman, D. Curien, J. Domscheit, B. Herskind, D.R. Jensen, S. Leoni, W,C, Ma, A. Maj, A. Neußer, S.W. Ødegård, C. Petrache, D. Roßbach, H. Ryde, K.H. Spohr, A.K. Singh, Phys. Lett. B552 (2003) 9

[75] C.X. Yang, X.G. Wu, H. Zheng, X.A. Liu, Y.S. Chen, C.W. Shen, Y.J. Ma, J.B. Lu, S. Wen, G.S. Li, S.G. Li, G.J. Yuan, P.K. Weng, Y.Z. Liu, Eur. Phys. J. A1 (1998) 237

[76] H. Amro, W.C. Ma, G.B. Hagemann, B. Herskind, J.A. Winger, Y. Li, J. Thompson, G. Sletten, J.N. Wilson, D.R. Jensen, P. Fallon, D. Ward, R.M. Diamond, A. Görgen, A. Machiavelli, H. Hübel, J. Domscheit and I. Wiedenhöwer, Abstract to FNS2002 Berkeley July-August 2002, and Phys. Lett. B553 (2003) 197

[77] Y. Li, D.G. Roux, G.B. Hagemann, W.C. Ma, H. Amro, R.M. Diamond, J. Domscheit, P. Fallon, A. Görgen, B. Herskind, H. Hübel, D.R. Jensen, A.O. Macchiavelli, G. Sletten, J. Thompson, D. Ward, I. Wiedenhöver, J.N. Wilson, J.A. Winger, to be published

[78]* D. Ringkjøbing Jensen, J. Domscheit, G.B. Hagemann, M. Bergström, B. Herskind, B.S. Nielsen, G. Sletten, P.G. Varmette, S. Törmänen, H. Hübel, W.C. Ma, A. Bracco, F. Camera, F. Demaria, S. Frattini, B. Million, D. Napoli, A. Maj, B.M. Nyako, D.T. Joss and M. Aiche, Eur. Phys. J. A8 (2000) 165

[79]* A. Neußer, S.Bhattacharya, P. Bringel, D. Curien, O. Dorvaux, J. Domscheit, G.B. Hagemann, F. Hannachi, H. Hübel, D.R. Jensen, A. Lopez-Martens, E. Mergel, N. Nenoff, A.K. Singh, Abstract to FNS2002 Berkeley July-August 2002, and Eur. Phys. J. A13 (2002) 439

[80] G. Schönwasser, H. Hübel, G.B. Hagemann, J. Domscheit, A. Görgen, B. Herskind, G. Sletten, J.N. Wilson, D.R. Napoli, C. Rossi-Alvarez, D. Bazzacco, R. Bengtsson, H. Ryde, P.O. Tjøm, and S.W. Ødegård, Eur. Phys. J. A13 (2002) 291

[81] G. Schönwasser, H. Hübel, G.B. Hagemann, H. Amro, R. Clark, R.M. Diamond, P. Fallon, B. Herskind, G. Lane, W.C. Ma, A. Machiavelli, S.W. Ødegård, G. Sletten, D. Ward and J.N. Wilson, Eur. Phys. J. A15 (2002) 435

[82]* S.W. Ødegård, Ph. D. Thesis, University of Oslo, 2002

[83] K. Starosta, T. Koike, C.J. Chiara, D.B. Fossan, D.R. LaFosse, Nucl. Phys. A682 (2001) 375c

[84] K. Starosta, T. Koike, C.J. Chiara, D.B. Fossan, D.R. LaFosse, A.A. Hecht, C.W. Beausang, M.A. Caprio, J.R. Cooper, R. Krucken, J.R. Novak, N.V. Zamfir, K.E. Zyromski, D.J. Hartley, D.L. Balabanski, J.-Y. Zhang, S. Frauendorf, V.I. Dimitrov, Phys. Rev. Lett. 86 (2001) 971

[85]* E. Mergel, C.M. Petrache, G. Lo Bianco, J. Domscheit, D. Roßbach, G. Schönwasser, N. Nenoff, A Neußer, A. Görgen, F. Becker, E. Bouchez, M. Houry, A. Hürstel, Y. Le Coz, R. Lucas, Ch. Theisen, W. Korten, A. Bracco, N. Blasi, F. Camera, S. Leoni, F. Hannachi, A. Lopez-Martens, M. Rejmund, D. Gassmann, P. Reiter, P.G. Thirolf, A. Astier, N. Buforn, M. Meyer, N. Redon, O. Stezowski, Eur. Phys. J. A15 (2002) 417

[86]* G. Rainovski, E. S. Paul, H. J. Chantler, P. J. Nolan, D. G. Jenkins, R. Wadsworth, P. Raddon, A. Simons, D. B. Fossan, T. Koike, K. Starosta, C. Vaman, E. Farnea, A. Gadea, Th. Kröll, R. Isocrate, G. de Angelis, D. Curien, and V. I. Dimitrov, Physical Review C68 (2003) 024318

[87] T. Koike, K. Starosta, C.J. Chiara, D.B. Fossan, D.R. LaFosse, Phys. Rev. C63 (2001) 061304(R)

[88] T. Koike, K. Starosta, C. Vaman, T. Ahn, D.B. Fossan, R.M. Clark, M. Cromaz, I.Y. Lee, A.O.Machiavelli, Proc. Conf. on Frontiers of Nuclear Structure, Berkeley 2002, AIP Conference Proceedings 656 (2003) 160

[89]* J. Timar, P. Joshi et al., private communication (2003)

[90]* S.W. Ødegård, B. Herskind, T. Døssing, G.B. Hagemann, D.R. Jensen, G. Sletten, J.N. Wilson, S. Leoni, P.O. Tjøm, P. Bednarczyk, and D. Curien, Eur. Phys. J. A14 (2002) 3

[91] M. Matsuzaki, Y.R. Shimizu and K. Matsuyanagi, Phys. Rev. C65 (2002) 041303

[92] K. Schiffer, B.Herskind, J.Gascon, Z. Phys. A332 (1989) 17

[93] B. Herskind, B.Lauritzen, K.Schiffer, R.A.Broglia, F.Barranco, M.Gallardo, J.Dudek, E.Vigezzi, Phys. Rev. Lett. 59 (1987) 2416

[94] F. Camera, A. Bracco, S. Leoni, B. Million, A. Maj, M. Kmiecik, Acta Physica Polonica B32 (2001) 807

[95]* A. Bracco, F. Camera and S. Leoni, Nucl. Phys. A682 (2001) 449c

[96] S. Leoni, B. Herskind, T. Døssing , A. Ataç, M. Piiparinen, Phys. Rev. Lett. 76 (1996) 3281

[97]* S. Leoni, A. Bracco, F. Camera, B. Million, A. Algora, A. Axelsson, G. Benzoni, M. Bergström, N. Blasi, M. Castaldi, S. Frattini, A. Gadea, B. Herskind, M. Kmiecik, G. Lo Bianco, A. Maj, J. Nyberg, M. Pignanelli, J. Styczen, E. Vigezzi, M. Zieblinski, A. Zucchiatti, Phys. Lett. B498 (2001) 137

[98] Y. R. Shimizu, M. Matsuo, K. Yoshida, Nucl. Phys. A682 (2001) 464c

[99] K. Yoshida and M. Matsuo, Nucl. Phys. A636 (1998) 169

[100] B. R. Mottelson, Nucl. Phys. A557 (1993) 717c

[101] T. Lauritsen, M.P. Carpenter, T. Døssing, P. Fallon, B. Herskind, R.V.F. Janssens, D.G. Jenkins, T.L. Khoo, F.G. Kondev, A. Lopez-Martens, A.O. Macchiavelli, D. Ward, K.S. Abu Saleem, I. Ahmad, R. Clark, M. Cromaz, J.P. Greene, F. Hannachi, A.M. Heinz, A. Korichi, G. Lane, C.J. Lister, P. Reiter, D. Seweryniak, S. Siem, R.C. Vondrasek, I. Wiedenhöver, Phys. Rev. Lett. 88 (2002) 042501

[102] P. Bonche, J. Dobaczewski, H. Flocard, P.H. Heenen, S.J. Krieger, J. Meyer, M.S. Weiss, Nucl. Phys. A519 (1990) 509 ; J. Meyer, P. Bonche, J. Dobaczewski, H. Flocard, P.H. Heenen, Nucl. Phys. A533 (1991) 307

[103] E. Vigezzi, R.A. Broglia, T. Døssing, Phys. Lett B249 (1990) 163 Y.R. Shimizu, F. Barranco, R.A. Broglia, T. Døssing, E. Vigezzi, Phys. Lett. B274 (1992) 253

[104] C.M. Petrache, D. Bazzacco, P. Bednarczyk, G. de Angelis, M. De Poli, C. Fahlander, G. Falconi, E. Farnea, A. Gadea, M. Lunardon, S. Lunardi, N. Marginean, R. Menegazzo, P. Pavan, Zs. Podolyak, C. Rossi Alvarez, C.A. Ur, R. Venturelli, L.H. Zhu, R. Wyss, Phys. Lett. B415 (1997) 223

[105] D. Bazzacco, F. Brandolini, R. Burch, S. Lunardi, E. Maglione, N.H. Medina, P. Pavan, C. Rossi-Alvarez, G. de Angelis, D. De Acuna, M. De Poli, J. Rico, D. Bucurescu, C. Ur, Phys. Rev. C49 (1994) R2281

[106] C.M. Petrache, D. Bazzacco, S. Lunardi, C. Rossi Alvarez, R. Venturelli, P. Pavan, N.H. Medina, M.N. Rao, R. Burch, G. de Angelis, A. Gadea, G. Maron, D.R. Napoli, L. Zhu, R. Wyss, Phys. Rev. Lett. 77 (1996) 239

[107] M. Deleplanque, S. Frauendorf, R.M. Clark, R.M. Diamond, F.S. Stephens, J.A. Becker, M.J. Brinkman, B. Cederwall, P. Fallon, L.P. Farris, E.A. Henry, H. Hübel, J.R. Hughes, W. Korten, I.Y. Lee, A.O. Macchiavelli, M.A. Stoyer, P. Willsau, J.E. Draper, C. Duyar, E. Rubel, Phys. Rev. C52 (1995) R2302

[108]   S. Lunardi, R. Venturelli, D. Bazzacco, C.M. Petrache, C. Rossi-Alvarez, G. de Angelis, G. Vedovato, D. Bucurescu, C. Ur, Phys. Rev. C52 (1995) R6

[109]* S. Perries, A. Astier, L. Ducroux, M.Meyer, N. Redon, C.M. Petrache, D. Bazzacco, G. Falconi, S. Lunardi, M. Lunardon, C. Rossi Alvarez, C.A. Ur, R. Venturelli, G. Viesti, I. Deloncle, M.G. Porquet, G. de Angelis, M. de Poli, C. Fahlander, E. Farnea, D. Foltescu, A. Gadea, D.R. Napoli, Zs. Podolyak, A. Bracco, S. Frattini, S. Leoni, B. Cederwall, A. Johnson, R.A. Wyss, Phys. Rev. C60 (1999) 064313

[110]* S. Perries, Ph.D Thesis, University of Lyon, LYCEN – T 9901, N 002-99, 1999

[111]* D. Rudolph, C. Fahlander, A. Algora, C. Andreoiu, R. Cardona, C. Chandler, G. de Angelis, E. Farnea, A. Gadea, J. Garcés Narro, J. Nyberg, M. Palacz, Zs. Podolyak, T. Steinhardt, O. Thelen, Phys. Rev. C63 (2001) 021301(R)

[112]   H.E. Jackson, J. Julien, C. Samour, A. Bloch, C. Lopata, J. Morgenstern, H. Mann, G.E. Thomas, Phys. Rev. Lett. 17 (1966) 656

[113]   C.E. Porter and R.G. Thomas, Phys. Rev. 104 (1956) 483

[114]   T.L. Khoo, M.P. Carpenter, T. Lauritsen, D. Ackermann, I. Ahmad, D.J. Blumenthal, S.M. Fischer, R.V.F. Janssens, D. Nisius, E.F. Moore, A. Lopez-Martens, T.Døssing, R. Krücken, S.J. Asztalos, J.A. Becker, L. Bernstein, R.M. Clark, M.A. Deleplanque, R.M. Diamond, P. Fallon, L.P. Farris, F. Hannachi, E.A. Henry, A. Korichi, I.Y. Lee, A.O. Macchiavelli, F.S. Stephens, Phys. Rev. Lett. 76 (1996) 1583

[115]   A. Lopez-Martens, T. Døssing, T.L. Khoo, A. Korichi, F. Hannachi, I.J. Calderin, T. Lauritsen, I. Ahmad, M.P. Carpenter, S.M. Fischer, G. Hackman, R.V.F. Janssens, D. Nisius, P. Reiter, H. Amro, E.F. Moore, Nucl. Phys. A647 (1999) 217

[116]   S. Åberg, Phys. Rev. Lett. 82 (1999) 299

[117]   B. Lauritzen, T. Døssing, R. A. Broglia, Nucl. Phys. A457 (1986) 61

[118]   M. Matsuo, T. Døssing, E. Vigezzi, R.A. Broglia, K. Yoshida, Nucl. Phys. A617 (1997) 1

[119]   T. Døssing, B. Herskind, S. Leoni, A. Bracco, R.A. Broglia, M. Matsuo, E. Vigezzi, Phys. Rep. 268 (1996) 1

[120]   B. Herskind, A. Bracco, R.A. Broglia, A. Ikeda, S. Leoni, J. Lisle, M. Matsuo, E. Vigezzi, Phys. Rev. Lett. 68 (1992) 3008

[121]   J.C. Bacelar, G.B. Hagemann, B. Herskind, B. Lauritzen, A. Holm, J.C. Lisle, P.O. Tjøm, Phys. Rev. Lett. 55 (1985) 1858

[122]   S. Leoni, A. Bracco, T. Døssing, B. Herskind, M. Matsuo, E. Vigezzi, J. Wrzesinski, Eur. Phys. J. A4 (1999) 229

[123]   P. Bosetti, S. Leoni, A. Bracco, B. Herskind, T. Døssing, G.B. Hagemann, R. Bark, A. Brocksted, P. Ekström, H. Carlsson, A. Nordlund, H. Ryde, F. Camera, S. Frattini, M. Mattiuzzi, B. Million, D. Bazzacco, R. Burch, G. de Angelis, D. De Acuna, M. de Poli, P. Pavan, Phys. Rev. Lett. 76 (1996) 1204

[124]* A. Bracco and S. Leoni, Rep. Prog. Phys. 65 (2002) 299

[125]   M. Matsuo, T. Døssing, B. Herskind, S. Leoni, E. Vigezzi, R.A. Broglia,
Phys. Lett. B465 (1999) 1

[126]* S. Frattini, A. Bracco, S. Leoni, F. Camera, B. Million, N. Blasi, G. Lo Bianco, M. Pignanelli, E. Vigezzi, B. Herskind, T. Døssing, M. Bergström, P. Varmette, S. Tormanen, A. Maj, M. Kmiecik, D.R. Napoli, M. Matsuo, Phys. Rev. Lett. 83 (1999) 5234

[127]* A. Bracco, S. Frattini, S. Leoni, F. Camera, B. Million, N. Blasi, G. Falconi, G. Lo Bianco, M. Pignanelli, E. Vigezzi, B. Herskind, M. Bergström, P. Varmette, S. Törmanen, A. Maj, M. Kmiecik, D.R. Napoli, M. Matsuo, Nucl. Phys. A673 (2000) 64

[128]   A. Bracco, P. Bosetti, S. Frattini, E. Vigezzi, S. Leoni, T. Døssing, B. Herskind, M. Matsuo, Phys. Rev. Lett. 76 (1996) 4484

[129] S. Leoni B. Herskind, T. Døssing, A. Ataç, I.G. Bearden, M. Bergström, C. Fahlander, G.B. Hagemann, A. Holm, D.T. Joss, M. Lipoglavsek, A. Maj, P.J. Nolan, J. Nyberg, M. Palacz, E.S. Paul, J. Persson, M.J. Piiparinen, N. Redon, A.T. Semple, G. Sletten, J.P. Vivien, Phys. Lett. B409 (1997) 71

[130] K. Yoshida and M. Matsuo, Nucl. Phys. A612 (1997) 26

[131] K. Yoshida, M. Matsuo and Y.R. Shimizu, Nucl.Phys. A696 (2001) 85

[132] S. Leoni, T. Døssing, A. Bracco, S. Frattini, G. Montingelli, E. Vigezzi, M. Bergström, G.B. Hagemann, B. Herskind, M. Matsuo, Nucl. Phys. A671 (2000) 71

[133] M. Gallardo, M. Diebel, T. Døssing, R.A. Broglia, Nucl. Phys. A443 (1985) 415

[134]* G. Benzoni, A. Bracco, F. Camera, S. Leoni, B. Million, A. Maj, A. Algora, A. Axelsson, M. Bergström, N. Blasi, M. Castaldi, S. Frattini, A. Gadea, B. Herskind, M. Kmiecik, G. Lo Bianco, J. Nyberg, M. Pignanelli, J. Styczen, O. Wieland, M. Zieblinski, A. Zucchiatti, Phys. Lett. B540 (2002) 199

[135]* G. Viesti, V. Rizzi, M. Cinausero, N. Gelli, A. Gadea, D. Bazzacco, A. Algora-Pineda, D. Appelbe, G. de Angelis, N. Belcari, M. De Poli, T. E. Drake, D. Fabris, E. Farnea, E. Fioretto, A. Galindo-Uribarri, W. Krolas, T. Kroll, F. Lucarelli, S. Lunardi, M. Lunardon, T. Martinez, R. Menegazzo, B. K. Nayak, G. Nebbia, D. R. Napoli, B. Nyako, C. Petrache, Z. Podolyak, G. Prete, C. Rossi Alvarez, P. Spolaore, C. Ur, and K. Zuber, Phys. Rev. C63 (2001) 034611

[136]* J. Simpson, A.P. Bagshaw, A. Pipidis, M.A. Riley, M.A. Bentley, D.M. Cullen, P.J. Dagnall, G.B. Hagemann, S.L. King, R.W. Laird, J.C. Lisle, S. Shepherd, A.G. Smith, S. Tormanen, A.V. Afanasjev, I. Ragnarsson, Phys. Rev. C62 (2000) 024321

[137] M.A. Riley, J.D. Garrett, J. Simpson, J.F. Sharpey-Schafer, Phys. Rev. Lett. 60 (1988) 553

[138] A.V. Afanasjev, D.B. Fossan, G.J. Lane, I. Ragnarsson, Phys. Rep. 322 (1999) 1

[139] I. Ragnarsson, Z.Xing, F.Bengtsson, M.A.Riley, Phys. Scr. 34 (1986) 651

[140] J. Simpson, M.A. Riley, S.J. Gale, J.F. Sharpey-Schafer, M.A. Bentley, A.M. Bruce, R. Chapman, R.M. Clark, S. Clarke, J. Copnell, D.M. Cullen, P. Fallon, A. Fitzpatrick, P.D. Forsyth, S.J. Freeman, P.M. Jones, M.J. Joyce, F. Linden, J.C. Lisle, A.O. Macchiavelli, A.G. Smith, J.F. Smith, J. Sweeney, D.M. Thompson, S. Warburton, J.N. Wilson, T. Bengtsson, I. Ragnarsson, Phys. Lett. B327 (1994) 187

[141]* C. Plettner, H. Schnare, R. Schwengner, L. Käubler, F. Dönau, I. Ragnarsson, A.V. Afanasjev, A. Algora, G. de Angelis, A. Gadea, D.R. Napoli, J. Eberth, T. Steinhardt, O. Thelen, M. Hausmann, A. Müller, A. Jungclaus, K.P. Lieb, D.G. Jenkins, R. Wadsworth, A.N. Wilson, S. Frauendorf, Phys. Rev. C62 (2000) 014313

[142] A.V. Afanasjev and I. Ragnarsson, Nucl. Phys. A608 (1996) 176

[143]* E.S. Paul et al., to be submitted to Phys. Rev. Lett. (2003)

[144]* C.M. Parry, R. Wadsworth, A.N. Wilson, A.J. Boston, P.J. Nolan, E.S. Paul, J.A. Sampson, A.T. Semple, J. Gizon, A. Gizon, C. Foin, J. Genevey, I. Ragnarsson, and B.G. Dong, Phys. Rev. C61 (2000) 021303

[145]* R. Wadsworth, E.S. Paul, A. Astier, D. Bazzacco, A.J. Boston, N. Buforn, C.J. Chiara, D.B. Fossan, C. Fox, J. Gizon, D.G. Jenkins, N.S. Kelsall, T. Koike, D.R. LaFosse, S. Lunardi, P.J. Nolan, B.M. Nyakó, C.M. Petrache, H.C. Scraggs, K. Starosta, J. Timár, A. Walker, A.N. Wilson, L. Zolnai, B.G. Dong, and I. Ragnarsson, Phys. Rev. C62 (2000) 034315

[146] G. Colo, M.A. Nagarajan, P. van Isacker, and A. Vitturi, Phys. Rev. C52 (1995) R1175

[147] J. Dobaczewski and I. Hamamoto, Phys. Lett. B345 (1995) 181

[148] Particle Data Group, Eur. Phys. J. C15 (2000) 110

[149] see, e.g.: N. Auerbach, Phys. Reports 98 (1983) 274 and papers quoted therein

[150] J. Jänecke, in Isospin in Nuclear Physics, Ed. D.H. Wilkinson (North Holland, Amsterdam,1969), p.298

[151] L. Radicati, Phys. Rev. 87 (1952) 521

[152] P.J. Ennis, C.J. Lister, W. Gelletly, H.G. Price, B.J. Varley, P.A. Butler, T. Hoare, S. Cwiok, W. Nazarewicz, Nucl. Phys. A535 (1991) 392; Nucl. Phys. A560 (1993) 1079, erratum

[153]* E. Farnea G. de Angelis, A. Gadea, P.G. Bizzeti, A. Dewald, J. Eberth, A. Algora, M. Axiotis, D. Bazzacco, A.M. Bizzeti-Sona, F. Brandolini, G. Colo, W. Gelletly, M.A. Kaci, N. Kintz, T. Klug, Th. Kroll, S.M. Lenzi, S. Lunardi, N. Margineăn , T. Martinez, R. Menegazzo, D.R. Napoli, J. Nyberg, P. Pavan, Zs. Podolyak, C.M. Petrache, B. Quintana, B. Rubio, P. Spolaore, Th. Steinhardt, J.L. Tain, O. Thelen, C.A. Ur, R. Venturelli, M. Weiszflog,

Phys. Lett. B551 (2003) 56

[154]* A. Gadea, E. Farnea, G. de Angelis, N. Belcari, T. Martinez, B. Rubio, J.L. Tain, D.R. Napoli, M. De Poli, P. Spolaore, G. Prete, E. Fioretto, D. Bazzacco, F. Brandolini, S. M. Lenzi, S. Lunardi, P. Pavan, C. Rossi Alvarez, P.G. Bizzeti, A.M. Bizzeti-Sona, J. Eberth, T. Steinhardt, O. Thelen, R. Wyss, C. Fahlander, D. Rudolph, A. Atac, A. Axelsson, J. Nyberg, J. Persson, M. Weiszflog, W. Gelletly, P. Regan, Zs. Podolyak, J. Garces Narro, Proc. Conference on Experimental Nuclear Physics in Europe, Sevilla, Spain, June 1999, Eds. B. Rubio, M. Lozano and W. Gelletly, AIP Conf. Proc. 495 (1999) 195

[155] P.G. Bizzeti, A.M. Bizzeti-Sona, T. Fazzini, N. Taccetti, and F. Velatini, LNL - INFN (Rep) 047/91(1991) p.152

[156] L.M. García-Raffi, J. L. Tain, J. Bea, A. Gadea, J. Rico, B. Rubio, Nucl. Instr. and Meth. in Phys. Res. A391 (1997) 461

[157] A. Dewald, P. Sala, R. Wrzal, G. Bohm, D. Lieberz, G. Siems, R. Wirowski, K.O. Zell, A. Gelberg, P. von Brentano, P. Nolan, A.J. Kirwan, P.J. Bishop, R. Julin, A. Lampinen, J. Hattula, Nucl. Phys. A545 (1992) 822

[158] U. Hermkens, F. Becker, J. Eberth, S. Freund, T. Mylaeus, S. Skoda, W. Teichert, A. von der Werth, Z. Phys. A343 (1992) 371

[159] T.W. Burrows, Nucl.Data Sheets 68 (1993) 1

[160] F. Brandolini, S.M. Lenzi, D.R. Napoli, R.V. Ribas, H. Somacal, C.A. Ur, D. Bazzacco, J.A. Cameron, G. de Angelis, M. de Poli, C. Fahlander, A. Gadea, S. Lunardi, G. Martinez Pinedo, N.H. Medina, C. Rossi Alvarez, J. Sanchez Solano, C.E. Svensson, Nucl. Phys. A642 (1998) 387

[161] P. Schuurmans, J. Camps, T. Phalet, N. Severijns, B. Vereecke, S. Versyck, Nucl. Phys. A672 (2000) 89

[162] S.M. Lenzi, D.R. Napoli, A. Gadea, M.A. Cardona, D. Hojman, M.A. Nagarajan, C. Rossi Alvarez, N.H. Medina, G. de Angelis, D. Bazzacco, M.E. Debray, M. De Poli, S. Lunardi, D. de Acuna, Z. Phys. A354 (1996) 117

[163] S.M. Lenzi, C.A. Ur, D.R. Napoli, M.A. Nagarajan, D. Bazzacco, D.M. Brink, M.A. Cardona, G. de Angelis, M. De Poli, A. Gadea, D. Hojman, S. Lunardi, N.H. Medina, C. Rossi Alvarez, Phys. Rev.C56 (1997) 1313

[164] J.A. Cameron, M.A. Bentley, A.M. Bruce, R.A. Cunningham, H.G. Price, J. Simpson, D.D. Warner, A.N. James, W. Gelletly, P. Van Isacker, Phys. Lett. B319 (1993) 58

[165] M.A. Bentley, C.D. O'Leary, A. Poves, G. Martinez-Pinedo, D.E. Appelbe, R.A. Bark, D.M. Cullen, S. Erturk, A. Maj, Phys. Lett. B437 (1998) 243

[166] C.D. O'Leary, M.A. Bentley, D.E. Appelbe, D.M. Cullen, S. Erturk, R.A. Bark, A. Maj, T. Saitoh, Phys. Rev. Lett. 79 (1997) 4349

[167]* D. Tonev, P. Petkov, A. Dewald, T. Klug, P. von Brentano, W. Andrejtscheff, S.M. Lenzi, D.R. Napoli, N. Marginean, F. Brandolini, C.A. Ur, M. Axiotis, P.G. Bizzeti, A. Bizzeti-Sona, Phys. Rev. C65 (2002) 034314

[168] E. Caurier, ANTOINE code, Strasbourg (1989-2001)

[169]* S.M. Lenzi, N. Margineăn, D.R. Napoli, C.A. Ur, A.P. Zuker, G. de Angelis, A. Algora, M. Axiotis, D. Bazzacco, N. Belcari, M.A. Bentley, P.G. Bizzeti, A. Bizzeti-Sona, F. Brandolini, P. von Brentano, D. Bucurescu, J.A. Cameron, C. Chandler, M. De Poli, A. Dewald, H. Eberth, E. Farnea, A. Gadea, J. Garces-Narro, W. Gelletly, H. Grawe, R. Isocrate, D.T. Joss, C.A. Kalfas, T. Klug, T. Lampman, S. Lunardi, T. Martinez, G. Martinez-Pinedo, R. Menegazzo, J. Nyberg, Zs. Podolyak, A. Poves, R.V. Ribas, C. Rossi Alvarez, B. Rubio, J. Sanchez-Solano, P. Spolaore, T. Steinhardt, O. Thelen, D. Tonev, A. Vitturi, W. von Oertzen, M. Weiszflog, Phys. Rev. Lett. 87 (2001) 122501; in [177], p. 240

[170] J.A. Sheikh, P. Van Isacker, D.D. Warner, and J.A. Cameron, Phys. Lett. B252 (1990) 314

[171] M.A. Bentley, S.J. Williams, D.T. Joss, C.D. O'Leary, A.M. Bruce, J.A. Cameron, M.P. Carpenter, P. Fallon, L. Frankland, W. Gelletly, C.J. Lister, G. Martinez-Pinedo, A. Poves, P.H. Regan, P. Reiter, B. Rubio, J. Sanchez Solano, D. Seweryniak, C.E. Svensson, S.M. Vincent, D.D. Warner, Phys. Rev. C62 (2000) 051303(R)

[172] J.A. Sheikh, D.D. Warner, and P. Van Isacker, Phys. Lett. B443 (1998) 16

[173] A.P. Zuker J. Duflo, S. Lenzi, G. Martinez-Pinedo, A. Poves and J. Sanchez-Solano, nucl-th/0104048.

[174] A.P. Zuker, S.M. Lenzi, G. Martínez-Pinedo, and A. Poves, Phys. Rev. Lett. 89 (2002) 142502

[175] C.D. O'Leary, M.A. Bentley, S.M. Lenzi, G. Martinez-Pinedo, D.D. Warner, A.M. Bruce, J.A. Cameron, M.P. Carpenter, C.N. Davids, P. Fallon, L. Frankland, W. Gelletly, R.V.F. Janssens, D.T. Joss, C.J. Lister, P.H. Regan, P. Reiter, B. Rubio, D. Seweryniak, C.E. Svensson, S.M. Vincent, S.J. Williams, Phys. Lett. B525 (2002) 49

[176]* G. de Angelis, Proc. Conference on Frontiers of Nuclear Structure, Berkeley 2002, AIP Conference Proceedings 656 (2003) 253

[177]* Proceedings International Workshop PINGST 2000 - Selected Topics on N=Z Nuclei, Lund, Sweden, June 2000, Eds. D. Rudolph and M. Hellström (Blooms i Lund AB, 2000) and http://pingst2000.kosufy.lu.se/proceedings.asp

[178] H. Schatz, A. Aprahamian, J. Görres, M. Wiescher, T. Rauscher, J.F. Rembges, F.K. Thielemann, B. Pfeiffer, P. Möller, K.-L. Kratz, H. Herndl, B.A. Brown, H. Rebel, Phys. Rep. 294 (1998) 167

[179] C.E. Svensson, C. Baktash, J.A. Cameron, M. Devlin, J. Eberth, S. Flibotte, D.S. Haslip, D.R. LaFosse, I.Y. Lee, A.O. Macchiavelli, R.W. MacLeod, J.M. Nieminen, S.D. Paul, L.L. Riedinger, D. Rudolph, D.G. Sarantites, H.G. Thomas, J.C. Waddington, W. Weintraub, J.N. Wilson, A.V. Afanasjev, I. Ragnarsson, Phys. Rev. Lett. 79 (1997) 1233

[180] D. Rudolph, C. Baktash, W. Nazarewicz, W. Satula, M.J. Brinkman, M. Devlin, H.-Q. Jin, D.R. LaFosse, L.L. Riedinger, D.G. Sarantites, C.H. Yu, Phys. Rev. Lett. 80 (1998) 3018

[181] D. Rudolph, C. Baktash, M. J. Brinkman, E. Caurier, D.J. Dean, M. Devlin, J. Dobaczewski, P.-H. Heenen, H.-Q. Jin, D.R. LaFosse, W. Nazarewicz, F. Nowacki, A. Poves, L.L. Riedinger, D.G. Sarantites, W. Satula, C.H. Yu, Phys. Rev. Lett. 82 (1999) 3763

[182] C. Andreoiu, D. Rudolph, C. Fahlander, A. Gadea, D.G. Sarantites, C.E. Svensson, in [177], p. 21 C. Andreoiou, PhD thesis, University of Lund

[183] D. Rudolph, C. Baktash, M. Devlin, D.R. LaFosse, L.L. Riedinger, D.G. Sarantites, C.-H. Yu, Phys. Rev. Lett. 86 (2001) 1450

[184] D. Rudolph, C. Andreoiu, C. Fahlander, R.J. Charity, M. Devlin, D.G. Sarantites, L.G. Sobotka, D.P. Balamuth, J. Eberth, A. Galindo-Uribarri, P.A. Hausladen, D. Seweryniak, Th. Steinhardt, Phys. Rev. Lett. 89 (2002) 022501

[185] D. Rudolph, D. Weisshaar, F. Cristancho, J. Eberth, C. Fahlander, O. Iordanov, S. Skoda, Ch. Teich, O. Thelen, H.G. Thomas, Eur. Phys. J. A6 (1999) 377; D. Rudolph, Proc. International Conference on Achievements and Perspectives in Nuclear Structure, Crete, Greece, July 1999, Eds. S. Åberg and C. Kalfas, Phys. Scr. T88 (2000) 21

[186]* D. Rudolph, A. Gadea, G. de Angelis, C. Fahlander, A. Algora, C. Andreoiu, R. Cardona, C. Chandler, E. Farnea, J. Garcés Narro, J. Nyberg, M. Palacz, Zs. Podolyak, T. Steinhardt, O. Thelen, Nucl. Phys. A694 (2001) 132

[187] D. Rudolph, D.G. Sarantites, C. Andreoiu, C. Fahlander, D.P. Balamuth, R.J. Charity, M. Devlin, J. Eberth, A. Galindo-Uribarri, P.A. Hausladen, D. Seweryniak, L.G. Sobotka, Th. Steinhardt, Eur. Phys. J. A14 (2002) 137

[188] C.E. Svensson, D. Rudolph, C. Baktash, M.A. Bentley, J.A. Cameron, M.P. Carpenter, M. Devlin, J. Eberth, S. Flibotte, A. Galindo-Uribarri, G. Hackman, D.S. Haslip, R.V.F. Janssens, D.R. LaFosse, T.J. Lampman, T. Lauritsen, I.Y. Lee, F. Lerma, C.J. Lister, A.O. Macchiavelli, J.M. Nieminen, S.D. Paul, D.C. Radford, L.L. Riedinger, D.G. Sarantites, B. Schaly, D. Seweryniak, O. Thelen, H.G. Thomas, J.C. Waddington, D. Ward, W. Weintraub, J.N. Wilson, C.H. Yu, A.V. Afanasjev, I. Ragnarsson, Phys. Rev. Lett. 82 (1999) 3400

[189] S.M. Fischer, C.J. Lister, D.P. Balamuth, R. Bauer, J.A. Becker, L.A. Bernstein, M.P. Carpenter, J. Durell, N. Fotiades, S.J. Freeman, P.E. Garrett, P.A. Hausladen, R.V.F. Janssens, D. Jenkins, M. Leddy, J. Ressler, J. Schwartz, D. Svelnys, D.G. Sarantites, D. Seweryniak, B.J. Varley, R. Wyss, Phys. Rev. Lett. 87 (2001) 132501

[190] N.S. Kelsall, R. Wadsworth, A.N. Wilson, P. Fallon, A.O. Macchiavelli, R.M. Clark, D.G. Sarantites, D. Seweryniak, C.E. Svensson, S.M. Vincent, S. Frauendorf, J.A. Sheikh, G.C. Ball, Phys. Rev. C64 (2001) 024309

[191] G. de Angelis, C. Fahlander, A. Gadea, E. Farnea, W. Gelletly, A. Aprahamian, D. Bazzacco, F. Becker, P.G. Bizzeti, A. Bizzeti-Sona, F. Brandolini, D. de Acuna, M. De Poli, J. Eberth, D. Foltescu, S.M. Lenzi, S. Lunardi, T. Martinez, D.R. Napoli, P. Pavan, C.M. Petrache, C. Rossi Alvarez, D. Rudolph, B. Rubio, W. Satula, S. Skoda, P. Spolaore, H.G. Thomas, C.A. Ur, R. Wyss, Phys. Lett. B415 (1997) 217

[192] N. Marginean D. Bucurescu, C. Rossi Alvarez, C.A. Ur, Y. Sun, D. Bazzacco, S. Lunardi, G. de Angelis, M. Axiotis, E. Farnea, A. Gadea, M. Ionescu-Bujor, A. Iordachescu, W. Krolas, Th. Kröll, S.M. Lenzi, T. Martinez, R. Menegazzo, D.R. Napoli, P. Pavan, Zs. Podolyàk, M. De Poli, B. Quintana, P. Spolaore, Phys. Rev. C65 (2002) 051303(R)

[193]* T. Steinhardt, priv. comm.

[194] N.S. Kelsall, S.M. Fischer, D.P. Balamuth, G.C. Ball, M.P. Carpenter, R.M. Clark, J. Durell, P. Fallon, S.J. Freeman, P.A. Hausladen, R.V.F. Janssens, D.G. Jenkins, M.J. Leddy, C.J. Lister, A.O. Macchiavelli, D.G. Sarantites, D.C. Schmidt, D. Seweryniak, C.E. Svensson, B.J. Varley, S. Vincent, R. Wadsworth, A.N. Wilson, A.V. Afanasjev, S. Frauendorf, I. Ragnarsson, R. Wyss, Phys. Rev. C65 (2002) 044331

[195] D. Rudolph, W. Satula, C. Baktash, I. Birriel, M. Devlin, C.J. Gross, H.-Q. Jin, D.R. LaFosse, F. Lerma, J.X. Saladin, D.G. Sarantites, G. Sylvan, S.L. Tabor, D.F. Winchell, V.Q. Wood, R. Wyss, C.H. Yu, Phys. Rev. C56 (1997) 98

[196] N.S. Kelsall, C.E. Svensson, S. Fischer, D.E. Appelbe, R.A.E. Austin, D.P. Balamuth, G.C. Ball, J.A. Cameron, M.P. Carpenter, R.M. Clark, M. Cromaz, M.A. Deleplanque, R.M. Diamond, J.L. Durell, P. Fallon, S.J. Freeman, P.A. Hausladen, D.F. Hodgson, R.V.F. Janssens, D.G. Jenkins, G.J. Lane, M.J. Leddy, C.J. Lister, A.O. Macchiavelli, C.D. O'Leary, D.G. Sarantites, F.S. Stephens, D.C. Schmidt, D. Seweryniak, B.J. Varley, S. Vincent, K. Vetter, J.C. Waddington, R. Wadsworth, D. Ward, A.N. Wilson, A.V. Afanasjev, S. Frauendorf, I. Ragnarsson, R. Wyss, Proc. Conference on Frontiers of Nuclear Structure, Berkeley 2002, AIP Conference Proceedings 656 (2003) 261

[197] D.G. Jenkins, D.P. Balamuth, M.P. Carpenter, C.J. Lister, D. Seweryniak, S.M. Fischer, R.M. Clark, P. Fallon, A.O. Macchiavelli, C.E. Svensson, D.G. Sarantites, N.S. Kelsall, R. Wadsworth, in [177], p. 53

[198]* I. Stefanescu, priv. comm.

[199] S.M. Fischer, D.P. Balamuth, P.A. Hausladen, C.J. Lister, M.P. Carpenter, D. Seweryniak, J. Schwartz, Phys. Rev. Lett. 84 (2000) 4064

[200]* C. Plettner, I. Ragnarsson, H. Schnare, R. Schwengner, L. Käubler, F. Dönau, A. Algora, G. de Angelis, D.R. Napoli, A. Gadea, J. Eberth, T. Steinhardt, O. Thelen, M. Hausmann, A. Müller, A. Jungclaus, K.P. Lieb, D.G. Jenkins, R. Wadsworth, A.N. Wilson,

Phys. Rev. Lett. 85 (2000) 2454

[201]* T. Martinez, priv. comm.

[202]* G. de Angelis, T. Martinez, A. Gadea, N. Marginean, E. Farnea, E. Maglione, S. Lenzi, W. Gelletly, C.A. Ur, D.R. Napoli, Th. Kroell, S. Lunardi, B. Rubio, M. Axiotis, D. Bazzacco, A.M. Bizzeti Sona, P.G. Bizzeti, P. Bednarczyk, A. Bracco, F. Brandolini, F. Camera, D. Curien, M. De Poli, O. Dorvaux, J. Eberth, H. Grawe, R. Menegazzo, G. Nardelli, J. Nyberg, P. Pavan, B. Quintana, C. Rossi Alvarez, P. Spolaore, T. Steinhardt, I. Stefanescu, O. Thelen, R. Venturelli, Eur. Phys. J. A12 (2001) 51

[203]* C. Fahlander, M. Palacz, D. Rudolph, D. Sohler, J. Blomqvist, J. Kownacki, L.O. Norlin, J. Nyberg, A. Algora, C. Andreoiu, G. de Angelis, A. Ataç, D. Bazzacco, L. Berglund, T. Bäck, J. Cederkäll, B. Cederwall, Zs. Dombradi, B. Fant, E. Farnea, A. Gadea, M. Górska, H. Grawe, N. Hashimoto-Saitoh, A. Johnson, A. Kerek, W. Klamra, K. Lagergren, S.M. Lenzi, A. Likar, M. Lipoglavsek, M. Moszyński, D.R. Napoli, C. Rossi-Alvarez, H.A. Roth, T. Saitoh, D. Seweryniak, Ö. Skeppstedt, M. Weiszflog, M. Wolinska,

Phys. Rev. C63 (2001) 021307(R)

[204]* K. Lagergren, B. Cederwall, A. Johnson, J. Blomqvist, D. Sohler, G. de Angelis, P. Bednarczyk, T. Bäck, T. Claesson, O. Dorvaux, E.Farnea, A. Gadea, M. Górska, L. Milechina, L.O. Norlin, A. Odahara, M. Palacz, I. Stefanescu, O. Thelen, J.P. Vivien, Eur. Phys. J. A14 (2002) 393

[205]* D. Sohler, M. Palacz, Zs. Dombradi, J. Blomqvist, C. Fahlander, L.O. Norlin, J. Nyberg, T. Bäck, K. Lagergren, D. Rudolph, A. Algora, C. Andreoiu, G. de Angelis, A. Atac, D. Bazzacco, J. Cederkäll, B. Cederwall, B. Fant, E. Farnea, A. Gadea, M. Górska, H. Grawe, N. Hashimoto-Saitoh, A. Johnson, A. Kerek, W. Klamra, J. Kownacki, S.M. Lenzi, A. Likar, M. Lipoglavsek, M. Moszyński, D.R. Napoli, C. Rossi-Alvarez, H.A. Roth, T. Saitoh, D. Seweryniak, Ö. Skeppstedt, M. Weiszflog, M. Wolinska, Nucl. Phys. A708 (2002) 181

[206] M. Lipoglavšek, C. Baktash, M.P. Carpenter, D.J. Dean, T. Engeland, C. Fahlander, M. Hjorth-Jensen, R.V.F. Janssens, A. Likar, J. Nyberg, E. Osnes, S.D. Paul, A. Piechaczek, D.C. Radford, D. Rudolph, D. Seweryniak, D.G. Sarantites, M. Vencelj, C.H. Yu, Phys. Rev. C65 (2002) 021302(R)

[207] M. Górska, M. Lipoglavšek, H. Grawe, J. Nyberg, A. Ataç, A. Axelsson, R. Bark, J. Blomqvist, J. Cederkäll, B. Cederwall, G. de Angelis, C. Fahlander, A. Johnson, S. Leoni, A. Likar, M. Matiuzzi, S. Mitarai, L.-O.Norlin, M. Palacz, J. Persson, H.A. Roth, R. Schubart, D. Seweryniak, T. Shizuma, Ö. Skeppstedt, G. Sletten, W.B. Walters, M.Weiszflog, Phys. Rev. Lett. 79 (1997) 2415

[208] M. Lipoglavšek, M. Górska, J. Nyberg, A. Ataç, A. Axelsson, R.A. Bark, J. Blomqvist, J. Cederkäll, B. Cederwall, G. de Angelis, C. Fahlander, H. Grawe, A. Johnson, S. Leoni, A. Likar, M. Matiuzzi, S. Mitarai, L.-O. Norlin, M. Palacz, J. Persson, H.A. Roth, R. Schubart, D. Seweryniak, T. Shizuma, Ö. Skeppstedt, D. Sohler, G. Sletten, W.B. Walters, M. Weiszflog, Z. Phys. A356 (1996) 239

M. Lipoglavšek, D. Seweryniak, C.N. Davids, C. Fahlander, M. Górska, R.V.F. Janssens, J. Nyberg, J. Uusitalo, W.B. Walters, I. Ahmad, J. Blomqvist, M.P. Carpenter, J.A. Cizewski, S.M. Fischer, H. Grawe, G. Hackman, M. Huhta,, C.J. Lister, D. Nisius, G. Poli, P. Reiter, J. Ressler, J. Schwartz, A. Sonzogni, Phys. Lett. B440 (1998) 246

[209] H. Grawe and M. Lewitowicz, Nucl. Phys. A693 (2001) 116

[210] W. Urban, M.A. Jones, C.J. Pearson, I. Ahmad, M. Bentaleb, J.L. Durell, M.J. Leddy, E. Lubkiewicz, L.R. Morss, W.R. Phillips, N. Schulz, A.G. Smith, B.J. Varley, Nucl. Instr. Meth. in Phys. Res. A365 (1995) 596

[211] A.G. Smith, W.R. Phillips, J.L. Durell, W. Urban, B.J. Varley, C.J. Pearson, J.A. Shannon, I. Ahmad, C.J. Lister, L.R. Morss, K.L. Nash, C.W. Williams, M. Bentaleb, E. Lubkiewicz, N. Schulz, Phys. Rev. Lett. 73 (1994) 2540

[212] A. Guessous, N. Schulz, W.R. Phillips, I. Ahmad, M. Bentaleb, J.L. Durell, M.A. Jones, M. Leddy, E. Lubkiewicz, L.R. Morss, R. Piepenbring, A.G. Smith, W. Urban, B.J. Varley, Phys. Rev. Lett. 75 (1995) 2280

[213] J.A. Shannon, W.R. Phillips, J.L. Durell, B.J. Varley, W. Urban, C.J. Pearson, I. Ahmad, C.J. Lister, L.R. Morss, K.L. Nash, C.W. Williams, N. Schulz, E. Lubkiewicz, M. Bentaleb, Phys. Lett. B336 (1994) 136

[214]* I. Deloncle, A. Bauchet, M.-G. Porquet, M. Girod, S. Peru, J.-P. Delaroche, A. Wilson, B.J.P. Gall, F. Hoellinger, N. Schulz, E. Gueorguieva, A. Minkova, T. Kutsarova, Ts. Venkova, J. Duprat, H. Sergolle, C. Gautherin, R. Lucas, A. Astier, N. Buforn, M. Meyer, S. Perries, N. Redon, Eur. Phys. J. A8 (2000) 177

[215]* Ts. Venkova, M.-G. Porquet, I. Deloncle, B.J.P. Gall, H. De Witte, P. Petkov, A. Bauchet, T. Kutsarova, E. Gueorguieva, J. Duprat, C. Gautherin, F. Hoellinger, R. Lucas, A. Minkova, N. Schulz, H. Sergolle, E.A. Stefanova, A. Wilson, Eur. Phys. J. A6 (1999) 405

[216]* Ts. Venkova, M.-G. Porquet, A. Astier, A. Bauchet, I. Deloncle, S. Lalkovski, N. Buforn, L. Donadille, O. Dorvaux, B.J.P. Gall, R. Lucas, M. Meyer, M. Minkova, A. Prévost, N. Redon, N. Schulz, O. Stézowski, Eur. Phys. J. A15 (2002) 429

[217]* A. Bauchet, I. Deloncle, M.-G. Porquet, A. Astier, N. Buforn, M. Meyer, S. Perries, N. Redon, B.J.P. Gall, F. Hoellinger, N. Schulz, G. Duchene, S. Courtin, Ts. Venkova, P.A. Butler, N. Amzal, R.D. Herzberg, A. Chewter, R. Cunningham, M. Houry, R. Lucas, W. Urban, A. Nowak, E. Piasecki, J. Duprat, C. Petrache, T. Kröll, Eur. Phys. J. A10 (2001) 145

A. Bauchet, Ph.D Thesis, University of Orsay, 2001

[218]* M. Houry, R. Lucas, M.-G. Porquet, Ch. Theisen, M. Girod, M. Aiche, M.M. Aleonard, A. Astier, G. Barreau, F. Becker, J.F. Chemin, I. Deloncle, T.P. Doan, J.L. Durell, K. Hauschild, W. Korten, Y. Le Coz, M.J. Leddy, S. Perries, N. Redon, A.A. Roach, J.N. Scheurer, A.G. Smith, B.J. Varley, Eur. Phys. J. A6 (1999) 43

M. Houry, PhD Thesis, University of Paris XI, 2000

[219] T. Kutsarova, A. Minkova, M.-G. Porquet, I. Deloncle, E. Gueorguieva, F. Azaiez, S. Bouneau, C. Bourgeois, J. Duprat, B.J.P. Gall, C. Gautherin, F. Hoellinger, R. Lucas, N. Schulz, H. Sergolle, Ts. Venkova, A. Wilson, Phys. Rev. C58 (1998) 1966

[220]* N. Buforn, A. Astier, J. Meyer, M. Meyer, S. Perries, N. Redon, O. Stezowski, M.G. Porquet, I. Deloncle, A. Bauchet, J. Duprat, B.J.P. Gall, C. Gautherin, E. Gueorguieva, F. Hoellinger, T. Kutsarova, R. Lucas, A. Minkova, N. Schulz, H. Sergolle, Ts. Venkova, A.N. Wilson, Eur. Phys. J. A7 (2000) 347

N. Buforn, Ph.D Thesis, University of Lyon, 2001

[221] J.L.Durell, Proc. Int. Conf. on Spectroscopy of Heavy Nuclei, 1989, Crete, Greece, (1990) p.307

[222]* R. Lucas, M.-G. Porquet, Ts. Venkova, I. Deloncle, M. Houry, Ch. Theisen, A. Astier, A. Bauchet, S. Lalkovski, G. Barreau, N. Buforn, T.P. Doan, L. Donadille, O. Dorvaux, J. Durell, Th. Ethvignot, B.P.J. Gall, D. Grimwood, W. Korten, Y. Le Coz, M. Meyer, A. Minkova, A. Prévost, N. Redon, A. Roach, N. Schulz, A.G. Smith, O. Stézowski, B.J. Varley, Eur. Phys. J. A15 (2002) 315

[223] W. Urban, W. Kurcewicz, A. Korgul, P.J. Daly, P. Bhattacharyya, C.T. Zhang, J.L. Durell, M.J. Leddy, M.A. Jones, W.R. Phillips, A.G. Smith, B.J. Varley, M. Bentaleb, E. Lubkiewicz, N. Schulz, I. Ahmad, L.R. Morss, J. Blomqvist, Phys. Rev. C62 (2000) 027301

[224] W. Urban, W.R. Phillips, N. Schulz, B.J.P. Gall, I. Ahmad, M. Bentaleb, J.L. Durell, M.A. Jones, M.J. Leddy, E. Lubkiewicz, L.R. Morss, A.G. Smith, B.J. Varley, Phys. Rev. C62 (2000) 044315

[225] W. Urban, N. Schulz, M. Bentaleb, E. Lubkiewicz, J.L. Durell, M.J. Leddy, M.A. Jones, W.R. Phillips, A.G. Smith, B.J. Varley, I. Ahmad, L.R. Morss, Eur. Phys. J. A8 (2000) 5

[226]* A.G. Smith, G.S. Simpson, J. Billowes, J.L. Durell, P.J. Dagnall, S.J. Freeman, M. Leddy, A.A. Roach, J.F. Smith, A. Jungclaus, K.P. Lieb, C. Teich, B.J.P. Gall, F. Hoellinger, N. Schulz, I. Ahmad, J. Greene, A. Algora, Phys. Lett. B435 (1999) 206

[227] K. Skarsvåg, Phys. Rev. C22 (1980) 638

[228] J.B. Wilhelmy, E. Cheifetz, R.C. Jared, S.G. Thompson, H.R. Bowman, J.O. Rasmussen, Phys. Rev. C5 (1972) 2041

[229] A.G. Smith, J.L. Durell, W.R. Phillips, M.A. Jones, M. Leddy, W. Urban, B.J. Varley, I. Ahmad, L.R. Morss, M. Bentaleb, A. Guessous, E. Lubkiewicz, N. Schulz, R. Wyss, Phys. Rev. Lett. 77 (1996) 1711

[230] W. Urban, J.L. Durell, A.G. Smith, W.R. Phillips, M.A. Jones, B.J. Varley, T. Rzaca-Urban, I. Ahmad, L.R. Morss, M. Bentaleb, N. Schulz, Nucl. Phys. A689 (2001) 605

[231]* A.G. Smith, R.M. Wall, D. Patel, G.S. Simpson, D.M. Cullen, J.L. Durell, S.J. Freeman, J.C. Lisle, J.F. Smith, B.J. Varley, G. Barreau, M. Petit, C. Theisen, E. Bouchez, M. Houry, R. Lucas, B. Cahan, A.L. Coguie, B.J.P. Gall, O. Dorvaux and N. Schulz,

J. Phys. G28 (2002) 2307

[232] R.Broda, Il Nuovo Cimento A111 (1998) 621

[233] B. Fornal, R.H. Mayer, I.G. Bearden, Ph. Benet, R. Broda, P.J. Daly, Z.W. Grabowski, I. Ahmad, M.P. Carpenter, P.B. Fernandez, R.V.F. Janssens, T.L. Khoo, T. Lauritsen, E.F. Moore, M. Drigert, Phys. Rev. C49 (1994) 2413

[234] B. Fornal, R. Broda, K.H. Maier, J. Wrzesinski, G.J. Lane, M. Cromaz, A.O. Macchiavelli, R.M. Clark, K. Vetter, A.P. Byrne, G.D. Dracoulis, M.P. Carpenter, R.V.F. Janssens, I. Wiedenhöver, M. Rejmund, J. Blomqvist, Phys. Rev.Lett. 87 (2001) 212501

[235] T. Pawlat, R. Broda, W. Krolas, A. Maj, M. Zieblinski, H. Grawe, R. Schubart, K.H. Maier, J. Heese, H. Kluge, M. Schramm, Nucl.Phys. A574 (1994) 623

[236] R. Broda, B. Fornal, W. Krolas, T. Pawlat, D. Bazzacco, S. Lunardi, C. Rossi Alvarez, R. Menegazzo, G. de Angelis, P. Bednarczyk, J. Rico, D. De Acuna, P.J. Daly, R.H. Mayer, M. Sferrazza, H. Grawe, K.H. Maier, R. Schubart, Phys. Rev. Lett. 74 (1995) 868

[237] J. Wrzesiński, K.H. Maier, R. Broda, B. Fornal, W. Krolas, T. Pawlat, D. Bazzacco, S. Lunardi, C. Rossi Alvarez, G. de Angelis, A. Gadea, J. Gerl, M. Rejmund,

Eur. Phys. J. A10 (2001) 259

[238] R. Broda, B. Fornal, J. Wrzesiński, W. Krolas, T. Pawlat, K-H. Maier, D. Bazzacco, S. Lunardi, N. Marginean, C. Ur, G. Viesti, G. de Angelis, M. Carpenter, R.V.F. Janssens, D. Seweryniak, I. Wiedenhöver, P.J. Daly, P. Bhattacharyya, Z.W. Grabowski, M. Rejmund, J. Gerl, Proc. of the 7th Int. Spring Seminar on Nuclear Physics, Maiori, Italy, May 2001, World Scientific p.195, ed.by Aldo Covello

[239]* B. Fornal, R. Broda, W. Krolas, T. Pawlat, J. Wrzesinski, D. Bazzacco, S. Lunardi, C. Rossi Alvarez, G. Viesti, G. de Angelis, M. Cinausero, D. Napoli, J. Gerl, E. Caurier, F. Nowacki, Eur. Phys. J. A7 (2000) 147

[240]* X. Liang, R. Chapman, K.-M. Spohr, M.B. Smith, P. Bednarczyk, S. Naguleswaran, F. Haas, G. de Angelis, S.M. Campbell, P.J. Dagnall, M. Davison, G. Duchene, Th. Kröll, S. Lunardi, D.J. Middleton, Eur. Phys. J. A10 (2001) 41

[241]* X. Liang, R. Chapman, F. Haas, K.-M. Spohr, P. Bednarczyk, S. M. Campbell, P. J. Dagnall, M. Davison, G. de Angelis, G. Duchêne, Th. Kröll, S. Lunardi, S. Naguleswaran, and M.B. Smith, Phys. Rev. C66 (2002) 014302

[242]* X. Liang, R. Chapman, F. Haas, K.-M. Spohr, P. Bednarczyk, S. M. Campbell, P. J. Dagnall, M. Davison, G. de Angelis, G. Duchêne, Th. Kröll, S. Lunardi, S. Naguleswaran, and M.B. Smith, Phys. Rev. C. 66 (2002) 037301(R)

[243] G. Baldsiefen et al., Proc. X. Internat. School on Nucl. Phys., Neutron Phys. and Nucl. Energy, eds. W. Andreitscheff and D. Elenkov, Varna (1991)

[244] R.M. Clark, R. Wadsworth, E.S. Paul, C.W. Beausang, I. Ali, A. Astier, D.M. Cullen, P.J. Dagnall, P. Fallon, M.J. Joyce, M. Meyer, N. Redon, P.H. Regan, W. Nazarewicz, R. Wyss, Phys. Lett. B275 (1992) 247

[245] G. Baldsiefen, H. Hübel, D. Mehta, B.V.T. Rao, U. Birkental, G. Frohlingsdorf, M. Neffgen, N. Nenoff, S.C. Pancholi, N. Singh, W. Schmitz, K. Theine, P. Willsau, H. Grawe, J. Heese, H. Kluge, K.H. Maier, M. Schramm, R. Schubart, H.J. Maier, Phys. Lett. B275 (1992) 252

[246] A. Kuhnert, M.A. Stoyer, J.A. Becker, E.A. Henry, M.J. Brinkman, S.W. Yates, T.F. Wang, J.A. Cizewski, F.S. Stephens, M.A. Deleplanque, R.M. Diamond, A.O. Macchiavelli, J.E. Draper, F. Azaiez, W.H. Kelly, W. Korten, Phys. Rev. C46 (1992) 133

[247] R.M. Clark, R. Wadsworth, E.S. Paul, C.W. Beausang, I. Ali, A. Astier, D.M. Cullen, P.J. Dagnall, P. Fallon, M.J. Joyce, M. Meyer, N. Redon, P.H. Regan, J.F. Sharpey-Schafer, W. Nazarewicz, R. Wyss, Z. Phys. A342 (1992) 371

[248] J.R. Hughes, Y. Liang, R.V.F. Janssens, A. Kuhnert, J.A. Becker, I. Ahmad, I.G. Bearden, M.J. Brinkman, J. Burde, M.P. Carpenter, J.A. Cizewski, P.J. Daly, M.A. Deleplanque, R.M. Diamond, J.E. Draper, C. Duyar, B. Fornal, U. Garg, Z.W. Grabowski, E.A. Henry, R.G. Henry, W. Hesselink, N. Kalantar-Nayestanaki, W.H. Kelly, T.L. Khoo, T. Lauritsen, R.H. Mayer, D. Nisius, J.R.B. Oliveira, A.J.M. Plompen, W. Reviol, E. Rubel, F. Soramel, F.S. Stephens, M.A. Stoyer, D. Vo, T.F. Wang, Phys. Rev. C47 (1993) R1337

[249] E.F. Moore, M.P. Carpenter, Y. Liang, R.V.F. Janssens, I. Ahmad, I.G. Bearden, P.J. Daly, M.W. Drigert, B. Fornal, U. Garg, Z.W. Grabowski, H.L. Harrington, R.G. Henry, T.L. Khoo, T. Lauritsen, R.H. Mayer, D. Nisius, W. Reviol, M. Sferrazza, Phys. Rev. C51 (1995) 115

[250] G. Baldsiefen, H. Hübel, W. Korten, U.J. van Severen, J.A. Cizewski, N.H. Medina, D.R. Napoli, C. Rossi Alvarez, G. Lo Bianco, S. Signorelli, Z. Phys. A355 (1996) 337

[251] R.B. Firestone, Table of Isotopes, eighth edition, Wiley (1996)

[252] S. Frauendorf, Z. Phys. A358 (1997) 163

[253] S. Frauendorf, Rev. Mod. Phys. 73 (2001) 463

[254] A. Amita, A.K. Jain, B. Singh, At. Data and Nucl. Data Tables 74 (2000) 283

[255] S. Chmel, F. Brandolini, R.V. Ribas, G. Baldsiefen, A. Gorgen, M. De Poli, P. Pavan, H. Hübel, Phys. Rev. Lett. 79 (1997) 2002

[256] G. Baldsiefen, H. Hübel, W. Korten, D. Mehta, N. Nenoff, B.V.T. Rao, P. Willsau, H. Grawe, J. Heese, H. Kluge, K.H. Maier, R. Schubart, S. Frauendorf, H.J.Maier,

Nucl. Phys. A574 (1994) 521

[257] M. Neffgen, G. Baldsiefen, S. Frauendorf, H. Grawe, J. Heese, H. Hübel, H. Kluge, A. Korichi, W. Korten, K.H. Maier, D. Mehta, J. Meng, N. Nenoff, M. Piiparinen, M. Schonhofer, R. Schubart, U.J. van Severen, N. Singh, G. Sletten, B.V.T. Rao, P. Willsau, Nucl. Phys. A595 (1995) 499

[258] R.M. Clark, S.J. Asztalos, G. Baldsiefen, J.A. Becker, L. Bernstein, M.A. Deleplanque, R.M. Diamond, P. Fallon, I.M. Hibbert, H. Hübel, R. Krucken, I.Y. Lee, A.O. Macchiavelli, R.W. MacLeod, G. Schmid, F.S. Stephens, K. Vetter, R. Wadsworth, S. Frauendorf, Phys. Rev. Lett. 78 (1997) 1868

[259] R.M. Clark, R. Krucken, S.J. Asztalos, J.A. Becker, B. Busse, S. Chmel, M.A. Deleplanque, R.M. Diamond, P. Fallon, D. Jenkins, K. Hauschild, I.M. Hibbert, H. Hübel, I.Y. Lee, A.O. Macchiavelli, R.W. MacLeod, G. Schmid, F.S. Stephens, U.J. van Severen, K. Vetter, R. Wadsworth, S. Wan, Phys. Lett. B440 (1998) 251

[260] R. Krücken, R.M. Clark, A. Dewald, M.A. Deleplanque, R.M. Diamond, P. Fallon, K. Hauschild, I.Y. Lee, A.O. Macchiavelli, R. Peusquens, G.J. Schmid, F.S. Stephens, K. Vetter, P. von Brentano, Phys. Rev. C58 (1998) R1876

[261]* G. Kemper, A. Dewald, I. Wiedenhöver, R. Peusquens, S. Kasemann, K.O. Zell, P. von Brentano, H. Hübel, S. Chmel, A. Gorgen, D. Bazzacco, R. Venturelli, S. Lunardi, D.R. Napoli, F. Hannachi, A. Lopez-Martens, R. Krucken, J.R. Cooper, R.M. Clark, M.A. Deleplanque, I.Y. Lee, A.O. Machiavelli, F.S. Stephens, Eur. Phys. J. A11 (2001) 121

[262] R.M. Clark, S.J. Asztalos, B. Busse, C.J. Chiara, M. Cromaz, M.A. Deleplanque, R.M. Diamond, P. Fallon, D.B. Fossan, D.G. Jenkins, S. Juutinen, N. Kelsall, R. Krucken, G.J. Lane, I.Y. Lee, A.O. Macchiavelli, R.W. MacLeod, G. Schmid, J.M. Sears, J.F. Smith, F.S. Stephens, K. Vetter, R. Wadsworth, S. Frauendorf, Phys. Rev. Lett. 82 (1999) 3220

[263] D.G. Jenkins, R. Wadsworth, J.A. Cameron, R.M. Clark, D.B. Fossan, I.M. Hibbert, V.P. Janzen, R. Krucken, G.J. Lane, I.Y. Lee, A.O. Macchiavelli, C.M. Parry, J.M. Sears, J.F. Smith, S. Frauendorf, Phys. Rev. Lett. 83 (1999) 500

[264] N.S. Kelsall, R. Wadsworth, S.J. Asztalos, B. Busse, C.J. Chiara, R.M. Clark, M.A. Deleplanque, R.M. Diamond, P. Fallon, D.B. Fossan, D.G. Jenkins, S. Juutinen, R. Krücken, G.J. Lane, I.Y. Lee, A.O. Macchiavelli, C.M. Parry, G.J. Schmid, J.M. Sears, J.F. Smith, F.S. Stephens, K. Vetter, S.G. Frauendorf, Phys. Rev. C61 (2000) 011301

[265] C.J. Chiara, S.J. Asztalos, B. Busse, R.M. Clark, M. Cromaz, M.A. Deleplanque, R.M. Diamond, P. Fallon, D.B. Fossan, D.G. Jenkins, S. Juutinen, N.S. Kelsall, R. Krucken, G.J. Lane, I.Y. Lee, A.O. Macchiavelli, R.W. MacLeod, G. Schmid, J.M. Sears, J.F. Smith, F.S. Stephens, K. Vetter, R. Wadsworth, S. Frauendorf, Phys. Rev. C61 (2000) 034318

[266] F. Brandolini, M. Ionescu-Bujor, N.H. Medina, R.V. Ribas, D. Bazzacco, M. De Poli, P. Pavan, C. Rossi Alvarez, G. de Angelis, S. Lunardi, D. De Acuna, D.R. Napoli, S. Frauendorf, Phys. Lett. B388 (1996) 468

[267] H. Hübel, G. Baldsiefen, R.M. Clark, S.J.Asztalos, J.A. Becker, L. Bernstein, M.A. Deleplanque, R.M. Diamond, P. Fallon, I.M. Hibbert, R. Krucken, I.Y. Lee, A.O. Macchiavelli, R.W. MacLeod, G. Schmid, F.S. Stephens, K. Vetter, R. Wadsworth, Z. Phys. A358 (1997) 237

[268] S. Frauendorf, Nucl. Phys. A557 (1993) 259c

[269] R.M. Clark and A.O. Macchiavelli, Annu. Rev. Nucl. Part. Sci. 50 (2000) 1

[270] I. Schneider, R.S. Chakrawarthy, I. Wiedenhöver, A. Schmidt, H. Meise, P. Petkov, A. Dewald, P. von Brentano, O. Stuch, K. Jessen, D. Weisshaar, C. Schumacher, O. Vogel, G. Sletten, B. Herskind, M. Bergstrom, J. Wrzesinski, Phys. Rev. C60 (1999) 014312

[271]* A. Dewald, O. Moller, R. Peusquens, A. Fitzler, B. Saha, T. Klug, I. Schneider, D. Tonev, P. von Brentano, B. J. P. Gall, contribution to the symposium on Nuclear Structure Physics with Euroball, Orsay, March 2002

[272] P. Petkov, A. Dewald, R. Kuhn, R. Peusquens, D. Tonev, S. Kasemann, K.O. Zell, P. von Brentano, D. Bazzacco, C. Rossi-Alvarez, G. de Angelis, S. Lunardi, P. Pavan, D.R. Napoli, Phys. Rev. C62 (2000) 014314

[273] F. Dönau, Nucl. Phys. A471 (1987) 469

[274]* R.M. Lieder, T. Rzaca-Urban, H. Brands, W. Gast, H.M. Jager, L. Mihailescu, Z. Marcinkowska, W. Urban, T. Morek, Ch. Droste, P. Szymanski, S. Chmel, D. Bazzacco, G. Falconi, R. Menegazzo, S. Lunardi, C. Rossi Alvarez, G. de Angelis, E. Farnea, A. Gadea, D.R. Napoli, Z. Podolyak, Ts. Venkova, Eur. Phys. J. A13 (2002) 297

[275]* R.M. Lieder, W.Gast, H.M. Jager, L. Mihailescu, T. Rzaca-Urban, Z. Marcinkowska, W. Urban, T. Morek, Ch. Droste, S. Chmel, D. Bazzacco, R. Menegazzo, S. Lunardi, C. Rossi-Alvarez, G. de Angelis, E. Farnea, A. Gadea, D.R.Napoli, Z. Podolyak, Ts. Venkova, contribution to the symposium on Nuclear Structure Physics with Euroball, Orsay, March 2002

[276] A. Görgen, N. Nenoff, H. Hübel, G. Baldsiefen, J.A. Becker, A.P. Byrne, S. Chmel, R.M. Clark, M.A. Deleplanque, R.M. Diamond, P. Fallon, K. Hauschild, I.M. Hibbert, W. Korten, R. Krücken, I. Y. Lee, A.O. Macchiavelli, E.S. Paul, U.J. van Severen, F.S. Stephens, K. Vetter, R. Wadsworth, A.N. Wilson, J.N. Wilson,

Nucl. Phys. A683 (2001) 108

[277]* A.K. Singh, N. Nenoff, D. Rossbach, A. Gorgen, S. Chmel, F. Azaiez, A. Astier, D. Bazzacco, M. Belleguic, S. Bouneau, C. Bourgeois, N. Buforn, B. Cederwall, I. Deloncle, J. Domscheit, F. Hannachi, K. Hauschild, H. Hübel, A. Korichi, W. Korten, T. Kroll, Y. LeCoz, A. Lopez-Martens, R. Lucas, S. Lunardi, H.J. Maier, E. Mergel, M. Meyer, C.M. Petrache, N. Redon, P. Reiter, C. Rossi-Alvarez, G. Schonwasser, O. Stezowski, P.G. Thirolf, A.N. Wilson, Nucl. Phys. A707 (2002) 3

[278]* A.K. Singh, H. Hübel, D. Rossbach, S. Chmel, A. Gorgen, E. Mergel, G. Schonwasser, F. Azaiez, C. Bourgeois, F. Hannachi, A. Korichi, A. Lopez-Martens, A. Astier, N. Buforn, N. Redon, O. Stezowski, D. Bazzacco, T. Kroll, C. Rossi-Alvarez, K. Hauschild, W. Korten, R. Lucas, H.J. Maier, P. Reiter, P.G. Thirolf, A.N. Wilson, Phys. Rev. C66 (2002) 064314

[279] S. Juutinen, R. Julin, M. Piiparinen, P. Ahonen, B. Cederwall, C. Fahlander, A. Lampinen, T. Lonnroth, A. Maj, S. Mitarai, D. Muller, J. Nyberg, P. Simecek, M. Sugawara, I. Thorslund, S. Tormanen, A. Virtanen, R. Wyss, Nucl. Phys. A573 (1994) 306

[280] S. Zhu, U. Garg, A.V. Afanasjev, S. Frauendorf, B. Kharraja, S.S. Ghugre, S.N. Chintalapudi, R.V.F. Janssens, M.P. Carpenter, F.G. Kondev, T. Lauritsen, Phys. Rev. C64 (2001) 041302(R)

[281] J.F. Sharpey-Schafer and J.Simpson, Prog. Part. Nucl. Phys. 21 (1988) 293

[282] P.J. Nolan, D.W. Gifford and P.J.Twin, Nucl. Inst. Meth. in Phys. Res. A236 (1985) 95

        P.J.Twin, P. J. Nolan, R. Aryaeinejad, D. J. G. Love, A. H. Nelson and A. Kirwan, Nucl. Phys. A409 (1983) 343c

[283] F.A. Beck, Proc. Conf. on Instrumentation for Heavy Ion Nuclear Research, ed. D. Shapira: Vol. 7 in the Nucl. Sci. Research Conf. Series (Harwood, New York) 1984, p. 129

[284] R.M. Lieder, H. Jäger, A. Neskakis, T. Venkova, C. Michel, Nucl. Instr. Meth. in Phys. Res. 220 (1984) 363

[285] B. Herskind, Proc. Second Int. Conf. on Nucl. Nucl. collisions, Visby, Sweden, June 1985 and Nucl. Phys. A447 (1986) 395c

[286] R.M. Diamond and F.S. Stephens, Proc. Conf. on Instrumentation for Heavy Ion Nuclear Research, ed. D. Shapira: Vol. 7 in the Nucl. Sci. Research Conf. Series (Harwood, New York) 1984, p. 259

[287] P. Taras et al., 'The 8π Proposal' October 1983;

        J.P. Martin, D. C. Radford, M. Beaulieu, P. Taras, D. Ward, H. R. Andrews, G. Ayotte, F. J. Sharp, J. C. Waddington, O. Häusser and J. Gascon, Nucl. Instr. and Meth. in Phys. Res. A257 (1987) 301

[288] J. Simpson, M.A. Riley, A.N.James, A.R.Mokhtar, H.W. Cranmer-Gordon, P.D. Forsyth, A.J. Kirwan, D. Howe, J.D. Morrison, J.F. Sharpey-Schafer,

        J. Phys. (London) G13 (1987) L235

[289] G. Kondev, M. A.Riley, R.V.F. Janssens, J. Simpson, A.V. Afanasjev, I. Ragnarsson, I. Ahmad, D.J. Blumenthal, T.B. Brown, M.P. Carpenter, P. Fallon, S.M. Fischer, G. Hackman, D.J. Hartley, C.A. Kalfas, T.L. Khoo, T. Lauritsen, W.C. Ma, D. Nisius, J.F. Sharpey-Schafer, P.G. Varmette, Phys. Lett. B437 (1998) 35

[290] P.J. Dagnall, C.W. Beausang, P.J. Twin, M.A. Bentley, F.A. Beck, Th. Byrski, S. Clarke, D. Curien, G. Duchene, G. de France, P.D. Forsyth, B. Haas, J.C. Lisle, E.S. Paul, J. Simpson, J. Styczen, J.P. Vivien, J.N. Wilson, K. Zuber, Phys. Lett. B335 (1994) 313

[291] C.W. Beausang and J. Simpson, J. Phys. (London) G22 (1996) 527

[292] P.J. Nolan, F.A. Beck and D.B. Fossan, Annu. Rev. Nucl. Part. Sci. 45 (1994) 561

[293] Gammasphere Proposal 'A National Gamma-ray Facility', ed. by M.A. Deleplanque and R.M. Diamond, March 1988, LBL;

        I.Y. Lee, Nucl. Phys. A520 (1990) 641c

[294] Ancillary Detectors and Devices for EUROBALL, GSI, Darmstadt, March 1998, Germany, edited by H. Grawe

[295] J. Gerl and R.M. Lieder, EUROBALL III, GSI Darmstadt report (1992)

        R.M. Lieder, in Experimental techniques in Nuclear Physics, Eds. D.N. Poenaru and W.Greiner, (Walter de Gruyter, Berlin 1995) p. 137

[296] F.A. Beck, D. Curien, G. Duchene, G. de France, L. Wei, Proc. Workshop on Large γ-ray Detector Arrays, Chalk River, Canada, (1992), AECL-10613, p. 359

        F.A. Beck, Proc. conference on physics from large γ–ray detector arrays, Berkeley 1994, LBL35687, CONF 940888, UC 413, p. 154

        G. Duchene, F. A. Beck, P. J. Twin, G. de France, D. Curien, L. Han, C. W. Beausang, M. A. Bentley, P. J. Nolan and J. Simpson, Nucl. Instr. Meth. in Phys. Res. A432 (1999) 90

[297] J. Eberth, H. G. Thomas, P. von Brentano, R. M. Lieder, H. M. Jäger, H. Kämmerling, M. Berst, D. Gutknecht and R. Henck, Nucl. Instr. Meth. in Phys. Res. A369 (1996) 135

[298] http://mars.jpl.nasa.gov/odyssey/index.html

[299] http://astro.estec.esa.nl/SA-general/Projects/Integral/integral.html

[300] S.L. Shepherd, P. J. Nolan, D. M. Cullen, D. E. Appelbe, J. Simpson, J. Gerl, M. Kaspar, A. Kleinböhl, I. Peter, M. Rejmund, H. Schaffner, C. Schlegel and G. de France, Nucl. Instr. Meth. in Phys. Res. A434 (1999) 373

[301] J. Simpson, F.Azaiez, G.de France, J.Fouan, J.Gerl, R.Julin, W.Korten, P.J.Nolan, B.M.Nyako, G.Sletten, P.M.Walker, and the EXOGAM Collaboration, Acta Phys.Hung.N.S. 11 (2000) 159

[302] J. Gerl et al., VEGA-Proposal, GSI report (1998)

[303] J. Eberth, H. G. Thomas, D. Weisshaar, F. Becker, B. Fiedler, S. Skoda, P. von Brentano, C. Gund, L. Palafox, P. Reiter, D. Schwalm, D. Habs, T. Servene, R. Schwengner, H. Schnare, W. Schulze, H. Prade, G. Winter, A. Jungclaus, C. Lingk, C. Teich and K.P. Lieb, Prog. Part. Nucl. Phys. 38 (1997) 29;

J. Eberth, G. Pascovici, H. G. Thomas, N. Warr, D. Weisshaar, D. Habs, P. Reiter, P. Thirolf, D. Schwalm, C. Gund, H. Scheit, M. Lauer, P.Van Duppen, S. Franchoo, M. Huyse, R.M. Lieder, W. Gast, J. Gerl, K. P. Lieb and MINIBALL COLLABORATION, Prog. Part. Nucl. Phys. 46 (2001) 389

[304] I. Lazarus, P. Coleman-Smith, N. Karkour, G.M. McPherson, A. Richard, C. Ring, IEEE Transactions on Nuclear Science 39 (1992) 1352

I. Lazarus and P.J. Coleman-Smith, IEEE Transactions on Nuclear Science 42 (1995) 891

I. Lazarus, P. Coleman-Smith, J. Thornhill, G. Bosson, N. Karkour, A. Richard, Z. Zojceski, C. Ring, IEEE Transactions on Nuclear Science 42 (1995) 2288

M.M. Aleonard, J. Alexander, J. Cresswell, J.C.Gouillaud, N. Karkour, I. Lazarus, G. McPherson, J.L. Pedroza, V. Pucknell, A. Rebii, A. Richard, C. Ring, J. Thornhill, L. Wilkinson, IEEE Transactions on Nuclear Science 39 (1992) 892

J. Alexander, F.A. Beck, C. Ender, I. Lazarus, G.M. McPherson, E.C.G. Owen, J. Pauxe, A. Richard, C. Ring, IEEE Transactions on Nuclear Science 39 (1992) 886

[305] G. Maron and V. Pucknell, A data acquisition system for EUROBALL III, EDOC306. http://npg.dl.ac.uk/documents/edoc306/

[306] V.F.E. Pucknell, The MIDAS Multi Instance Data Acquisition System, see also http://npg.dl.ac.uk/MIDAS

[307] R.M. Lieder, W. Gast, H.M. Jager, L. Mihailescu, M. Rossewij, J. Eberth, G. Pascovici, H.G. Thomas, D. Weisshaar, F. Beck, D. Curien, G. Duchene, E. Pachoud, I. Piqueras, C. Rossi Alvarez, D. Bazzacco, M. Bellato, Th. Kroell, Ch. Manea, B. Quintana, R. Venturelli, D.R. Napoli, D. Rosso, P. Spolaore, A. Geraci, A. Pullia, G. Ripamonti, F. Camera, B. Million, O. Wieland, J. Lisle, A.G. Smith, R. Well, P. Nolan, A. Boston, D. Cullen, M. Descovich, T. Enqvist, B. Cederwall, E. Ideguchi, J. van der Marel, J. Nyberg, B. Herskind, G. Sletten, J. Wilson, R. Henck, D. Gutknecht, K. Jaaskelainen, Nucl. Phys. A682 (2001) 279c

[308] AGATA Technical Proposal, Edited by J. Gerl and W. Korten, 2001

[309] J. Gál, Gy. Hegyesi, G. Kalinka, B.M. Nyakó, G.E. Perez, A. Kerek, A. Johnson, Nucl. Instr. and Meth. in Phys. Res. A366 (1995)145

[310] J. Gál, G. Hegyesi, J. Molnár, B.M. Nyakó, G. Kalinka, J.N. Scheurer, M.M. Aléonard, J.F. Chemin, J.L. Pedroza, K. Juhász, V.R.F. Pucknell submitted to Nucl. Instr. and Meth. in Phys. Res. A

[311] J. Gál, Gy. Hegyesi, G. Kalinka, B. M. Nyakó, A. Kerek, Nucl. Instr. and Meth. in Phys. Res. A397 (1997) 399

[312] J. Gál, Gy. Hegyesi, G. Kalinka, B. M. Nyakó, G. E. Perez, A. Kerek, A. Johnson, Nucl. Instr. and Meth. in Phys. Res. A399 (1997) 407

[313] J. Gál, G. Bíbok, K. Juhász, Scientific Instrumentation 3 (1988) 85

[314] J. Gál, G. Kalinka, B.M. Nyakó, G.E. Perez, Z. Máté, Gy. Hegyesi, T. Vass, A. Kerek, A. Johnson, Nucl. Instr. and Meth. in Phys. Res. A366 (1995) 120

[315] T.K. Alexander, F.S. Goulding, Nucl. Instr. and Meth. 13 (1961) 244

[316] N. Karkour and D. Linget, "GIR: General Interface Readout" CSNSM, Orsay, unpublished; EUROBALL Document EDOC308, http://npg.dl.ac.uk/documents/edoc308/

[317] M. Aiche, M. M. Aleonard, G. Barreau, D. Boivin, F. Bourgine, J.F. Chemin, T.P. Doan, J.N. Scheurer, A. Brondi, G. La Rana, R. Moro, E. Vardaci, J. Gal, G. Kalinka, B. Nyako, in Ancillary Detectors and Devices for EUROBALL, Ed. H. Grawe, GSI, Darmstadt, March 1998, Germany, p. 5

[318] G. Pausch, M. Moszynski, D. Wolski, W. Bohne, H. Grawe, D. Hilscher, R. Schubart, G. de Angelis and M. de Poli, Nucl. Inst. and Meth. in Phys. Res. A365 (1995) 176

[319] M. Kicińska-Habior, K.A. Snover, J.A. Behr, C.A. Gossett, Y. Alhassid, N. Whelan, Phys. Lett. B308 (1993) 225

[320] A. Maj, M. Kmiecik, W. Krolas, W. Meczynski, J. Styczen, M. Zieblinski, B. Million, A. Bracco, F. Camera, S. Leoni, O. Wieland, B. Herskind, M. Kicinska-Habior, Nucl. Phys. A687 (2001) 192c

[321] W.D. Myers, W.J. Świątecki, Acta. Phys. Pol. B32 (2001) 1033

[322] J. van Klinken and K. Wisshak, Nucl. Instr. and Meth. A98 (1972) 1

[323] B. Aengenvoort, W. Korten, H. Hübel, S. Chmel, A. Görgen, U.J. van Severen, W. Pohler, R. Zinken, T. Härtlein, C. Ender, F. Köck, P. Reiter, D. Schwalm, F. Schindler, J. Gerl, R. Schubart, F. Azaiez, S. Bouneau, J. Duprat, I. Deloncle, Eur. Phys. J. A1 (1998) 359

[324] Y. Le Coz, F. Becker, H. Kankaanpää, W. Korten, E. Mergel, P.A. Butler, J.F.C. Cocks, O. Dorveaux, D. Hawcroft, K. Helariutta, R.D. Herzberg, M. Houry, H. Hübel, P. Jones, R. Julin, S. Juutinen, H. Kettunen, P. Kuusiniemi, M. Leino, R. Lucas, M. Muikku, P. Nieminen, P. Rahkila, D. Rossbach, Eur. Phys. J. direct A3 (1999) 1

[325] J. Ljungvall, J. Nyberg, et al., to be published

[326]* P. Bednarczyk, W. Meczynski, J. Styczen, J. Grebosz, M. Lach, A. Maj, M. Zieblinski, N. Kintz, J.C. Merdinger, N. Schulz, J.P. Vivien, A. Bracco, J.L. Pedroza, M.B. Smith, K.M. Spohr, Acta Phys. Pol. B32 (2001) 747

[327]* M. Lach, P. Bednarczyk, A. Bracco, J. Grebosz, M. Kadluczka, N. Kintz, A. Maj, J.C. Merdinger, W. Meczynski, J.L. Pedroza, N. Schulz, M.B. Smith, K.M. Spohr, J. Styczen, J.P. Vivien, M. Zieblinski, Eur. Phys. J. A12 (2001) 381

[328]* M. Lach, J. Styczen, W. Meczynski, P. Bednarczyk, A. Bracco, J. Grebosz, A. Maj, J.C. Merdinger, N. Schulz, M.B. Smith, K.M. Spohr, J.P. Vivien, M. Zieblinski, Eur. Phys. J. A16 (2003) 381

[329] M. Leino, H. Kankaanpaa, R.-D. Herzberg, A.J. Chewter, F.P. Hessberger, Y. Le Coz, F. Becker, P.A. Butler, J.F.C. Cocks, O. Dorvaux, K. Eskola, J. Gerl, P.T. Greenlees, K. Helariutta, M. Houry, G.D. Jones, P. Jones, R. Julin, S. Juutinen, H. Kettunen, T.L. Khoo, A. Kleinbohl, W. Korten, P. Kuusiniemi, R. Lucas, M. Muikku, P. Nieminen, R.D. Page, P. Rahkila, P. Reiter, A. Savelius, Ch. Schlegel, Ch. Theisen, W.H. Trzaska, H.J. Wollersheim, Eur. Phys. J. A6 (1999) 1

[330] R.-D. Herzberg, N. Amzal, F. Becker, P.A. Butler, A.J.C. Chewter, J.F.C. Cocks, O. Dorvaux, K. Eskola, J. Gerl, P. Greenlees, N. Hammond, K. Hauschild, K. Helariutta, F.-P. Heßberger, M. Houry, G.D. Jones, P.M. Jones, R. Julin, S. Juutinen, H. Kankaanpää, H. Kettunen, T.L. Khoo, W. Korten, P. Kuusiniemi, Y. Le Coz, M. Leino, C.J. Lister, R. Lucas, M. Muikku, P. Nieminen, R.D. Page, P. Rahkila, P. Reiter, Ch. Schlegel, C.S. Scholey, O. Stezowski, Ch. Theisen, W.H. Trzaska, J. Uusitalo, H.J. Wollersheim, Phys. Rev. C65 (2002) 014303

[331] M.Leino, private communication

[332] C. Gautherin, M. Houry, W. Korten, Y. Le Coz, R. Lucas, X.H. Phan, Ch. Theisen, Ch. Badimon, G. Barreau, T.P. Doan, G. Pedemey, G. Belier, M. Girod, V. Meot, S. Peru, A. Astier, L. Ducroux, M. Meyer, N. Redon, Eur. Phys. J. A1 (1998) 391